Electrokinetic Treatment Technique for the Improvement of Soft Clayey Soils

Abiola Ayopo Abiodun

Submitted to the
Institute of Graduate Studies and Research
in partial fulfillment of the requirements for the degree of

Doctor of Philosophy
in
Civil Engineering

Eastern Mediterranean University
September 2020
Gazimağusa, North Cyprus

Approval of the Institute of Graduate Studies and Research

Prof. Dr. Ali Hakan Ulusoy
Director

I certify that this thesis satisfies the requirements as a thesis for the degree of Master of Science in Mechanical Engineering.

Prof. Dr. Umut Türker
Chair, Department of Civil Engineering

We certify that we have read this thesis and that in our opinion, it is fully adequate in scope and quality as a thesis for the degree of Master of Science in Civil Engineering.

Prof. Dr. Zalihe Nalbantoğlu Sezai
Supervisor

Examining Committee

1. Prof. Dr. Suat Akbulut _____
2. Prof. Dr. Selim Altun _____
3. Prof. Dr. Huriye Bilsel _____
4. Prof. Dr. Zalihe Nalbantoğlu Sezai _____
5. Asst. Prof. Dr. Eriş Uygar _____

ABSTRACT

This study evaluates the effect of ionic solutions on the performance of electrokinetic (EK) treatment to improve the index and engineering properties of soft soils. The use of rare combinations of ionic solutions of calcium chloride ($CaCl_2$) and sodium carbonate (Na_2CO_3), and conductive electrodes to stabilize the soft soil samples were introduced in the form of the laboratory model test tank. Atterberg limits, unconfined compression, one-dimensional swell and one-dimensional consolidation, wetting-drying, electrochemical, thermal, and microscopic tests were performed in terms of treatment duration, points of extraction in the soil from anode to cathode distances ($d_{A\leftrightarrow E}$), and different combinations of ionic solutions such as calcium chloride-distilled water ($CaCl_2$-DW), sodium carbonate-distilled water (Na_2CO_3-DW), and calcium chloride-sodium carbonate ($CaCl_2$-Na_2CO_3). Electrokinetic, EK treatment caused a significant reduction in the cation exchange capacity (CEC), specific surface area (S_a), plasticity index (PI), and volume change behavior of the treated soils using the rare combinations of ionic solutions of calcium chloride ($CaCl_2$) and sodium carbonate (Na_2CO_3). The formation of the new compounds, calcium aluminosilicate hydrates (CASH), which were detected by differential thermal analysis (DTA), resulted in the strength gain of the electrokinetic, EK treated soils due to their newly formed aggregated and flocculated structure of the treated soil particles. The effect of changing electrode length (l_e), on the performance of the electrokinetic, EK treatment on the engineering properties of soft soils were considered at different soil depths (d_s), and lengthwise anode to cathode distances ($d_{A\leftrightarrow E}$). The tests were performed using changing electrode length ratios of $0.25l_{ce}$, $0.50l_{ce}$, $0.75l_{ce}$, and $1.0l_{ce}$. The study analyzed the test data obtained from the Atterberg limit and one-dimensional swelling

tests at different extraction points in the test tank along with the anode to cathode distances ($d_{A\leftrightarrow E}$), and vertical soil depth (d_s), within the treated soils. The design of experiments, DOE software program, was used to examine the effect of the electrochemical properties on the behavior of the treated soils and to determine the significant input factors for the electrokinetic, EK treatment of the soft soils. The analysis and optimization of the data obtained produced the threshold values to provide better soil strengthening using the design-expert software. The results of the design of experiment (DOE) model analysis revealed that the effect of changing electrode lengths, l_e on the plasticity index (PI) and swelling potential (SP) of the electrokinetic, EK treated soils, was significant. For a specific soil depth (d_s), the electrode length ratios (l_{ce}) of $0.50l_{ce}$, and $0.75l_{ce}$ were significantly effective in reducing the plasticity index (PI) and the swelling potential (SP) of the electrokinetic, EK treated soils. Unlike other studies in the literature, the use of DOE analysis in the present study enabled the detection of the significant controlling factors in the electrokinetic, EK treatment and their interactive effects on the unconfined compressive strength (q_u), plasticity index (PI), and the swelling potential (SP), enabling the practicing geotechnical engineers to compute precise engineering design models for large in situ geotechnical applications.

Keywords: compressibility, electrodes, electrokinetic remediation, ionic solutions, numerical analyses, plasticity, strengthening, sodium carbonate, soft soils, swelling.

ÖZ

Bu çalışma, yumuşak zeminlerin indeks ve mühendislik özelliklerini iyileştirmek için iyonik çözeltilerin elektrokinetik (EK) işleminin performansı üzerindeki etkisini değerlendirmektedir. Yumuşak toprak numunelerini stabilize etmek için kalsiyum klorür ($CaCl_2$) ve sodyum karbonat (Na_2CO_3) iyonik çözeltilerinin nadir kombinasyonlarının ve iletken elektrotların kullanımı laboratuar modeli test tankı formunda tanıtıldı. Uygulama süresi, anottan katoda kadar topraktaki ekstraksiyon noktaları ($d_{A\leftrightarrow E}$), ve kalsiyum klorür-damıtılmış su ($CaCl_2$-DW), sodyum karbonat-damıtılmış su (Na_2CO_3-DW) ve kalsiyum klorür-sodyum karbonat ($CaCl_2$-Na_2CO_3) gibi farklı iyonik çözelti kombinasyonları açısından Atterberg limitleri, serbest basınç, tek boyutlu şişme ve tek boyutlu konsolidasyon, ıslatma-kurutma, elektrokimyasal, termal ve mikroskobik testler yapılmıştır. Elektrokinetik, EK işlemi, kalsiyum klorür ($CaCl_2$) ve sodyum karbonat (Na_2CO_3) gibi nadir iyonik çözelti kombinasyonları kullanarak işlenmiş toprakların katyon değişim kapasitesi (CEC), spesifik yüzey alanı (S_a), plastisite indeksi (PI) ve hacim değişim davranışında önemli bir azalmaya neden oldu. Diferansiyel termal analiz (DTA) ile tespit edilen yeni bileşiklerin, kalsiyum alüminosilikat hidratların (CASH) oluşumu, elektrokinetik, EK ile muamele edilmiş toprakların, yeni oluşan kümelenmiş ve topaklanmış yapısı nedeni ile kuvvet kazanımı ile sonuçlanmıştır. Değişen elektrot uzunluğunun (l_e), elektrokinetik performans üzerindeki etkisi, EK işleminin yumuşak zeminlerin mühendislik özellikleri üzerindeki etkisi, farklı toprak derinliklerinde (d_s) ve uzunlamasına anot-katot mesafelerinde ($d_{A\leftrightarrow E}$) dikkate alınmıştır. Testler, $0.25l_{ce}$, $0.50l_{ce}$, $0.75l_{ce}$ ve $1.0l_{ce}$ 'lik değişen elektrot uzunluk oranları kullanılarak gerçekleştirildi. Çalışma, test tankında farklı ekstraksiyon noktalarında ve farklı anot katod mesafeleri ($d_{A\leftrightarrow E}$) ve dikey toprak

derinliklerinde (d_s) işlenmiş toprakda, Atterberg limiti ve tek boyutlu şişme testlerinden elde edilen test verilerini analiz etti. Deney tasarım, DOE yazılım programı, elektrokimyasal özelliklerin işlenmiş toprakların davranışı üzerindeki etkisini incelemek ve yumuşak toprakların elektrokinetik, EK işlemi için önemli girdi faktörlerini belirlemek için kullanılmıştır. Elde edilen verilerin analizi ve optimizasyonu, design-expert yazılımı kullanılarak daha iyi zemin güçlendirmesi sağlamak için eşik değerleri üretti. Deney tasarımı (DOE) model analizinin sonuçları, elektrot uzunluğu le'nin elektrokinetik, EK ile muamele edilmiş toprakların plastisite indeksi (PI) ve şişme potansiyeli (SP) üzerindeki etkisinin önemli olduğunu ortaya koymuştur. Spesifik bir toprak derinliği (d_s) için, $0.50l_{ce}$ ve $0.75l_{ce}$ elektrot uzunluğu oranları (l_{ce}), elektrokinetik, EK ile muamele edilmiş toprakların plastisite indeksini (PI) ve şişme potansiyelini (SP) azaltmada önemli ölçüde etkiliydi. Literatürdeki diğer çalışmalardan farklı olarak, mevcut çalışmada DOE analizinin kullanılması, elektrokinetik EK tedavisinde önemli kontrol faktörleri ve bunların serbest basınç mukavemeti, q_u, plastisite indeksi (PI) ve şişme potansiyeli (SP) üzerindeki etkileşimli etkilerinin tesbiti uygulamadaki geoteknik mühendislerinin büyük arazi geoteknik uygulamalarında hassas mühendislik tasarım modellerini hesaplamasına olanak tanır.

Anahtar kelimeler: sıkıştırılabilirlik, elektrotlar, elektrokinetik iyileştirme, iyonik çözeltiler, sayısal analizler, plastisite, güçlendirme, sodyum karbonat, yumuşak zeminler, şişme.

DEDICATION

To my personal Lord and Savior: Jesus Christ and to my beloved family.

ACKNOWLEDGMENT

My sincere appreciation goes to every academic and non-academic staff of the Civil Engineering Department, Eastern Mediterranean University for their immeasurable outstanding academic values and skills added to my life in the course of my studies.

My sincere gratitude to my dear supervisor, Prof. Dr. Zalihe Nalbantoğlu Sezai for her inexhaustible supervision from the beginning to the end of this study. It was with her consistent, invaluable, and diligent supervision that made this study to be successful.

I appreciate families, friends, and colleagues for their kind roles during my studies.

I am grateful to the body of Christ for her love, prayers, and support during my studies.

My heartfelt gratitude to my beloved sister: a worthy mother: Mrs. Mosjiola Bintu (Abiodun) Olubamiro for her unwavering support in all my years of academic pursuits.

I am so thankful to God for my adorable wife: Adepeju Modupeolu Abiodun and my lovable daughter: Zion Miracle Abiodun in making this study an excellent success.

I love you all.

TABLE OF CONTENTS

LIST OF TABLES

LIST OF FIGURES

LIST OF SYMBOLS AND ABBREVIATIONS

A	Cross-sectional Area
C_c	Compression Index
C_r	Rebound Index
C_u	Undrained Shear Strength
C_v	Coefficient of Consolidation
^oC	Degree Celsius
D	Dielectric Constant
$d_{A \leftrightarrow E}$	Anode to Cathode Distance
$d_{E \leftrightarrow A}$	Cathode to Anode Distance
E_m	Electromigration
E_{os}	Electroosmosis
d	Diameter
e	Void Ratio
G_s	Specific Gravity
H	Vertical Height
H	Height
ΔH	Change in Height
I	Electrical Flow
I_s	Ionic Strength
i	Hydraulic Gradient
K_h	Saturated Hydraulic Conductivity
k_t	Thermal Conductivity
i_e	Electrical Gradient

i_h	Hydraulic Gradient
i_t	Thermal Gradient
J_w	Water Flux
k	Hydraulic Gradient
kg	Kilogram
K_{eo}	Electroosmotic Permeability
kPa	Kilopascal
1/K	Diffuse Double Layer Thickness
L	Vertical Distance
l	Sample Length
LL	Liquid Limit
LI	Liquidity Index
ΔL	Change in Length
m_v	Coefficient of Compressibility
m	Meters
N_{MB}	Normality of the Methylene Blue
n	Porosity
η	Viscosity
pH	Degree of Acidity or Alkalinity
ρ_b	In Situ Bulk Density
ρ_d	In Situ Dry Density
$\rho_{d\ (max)}$	Maximum Dry Density
$\sigma p'$	Preconsolidation Pressure
ρ	Electrical Resistivity
Q_e	Electrical Conductivity

Q_h	Discharge Rate
Q_t	Thermal Flow
σ_p'	Preconsolidation Pressure
q_{eo}	Electroosmotic Flow
σ	Electrical Conductivity
q_u	Unconfined Compressive Strength
R	Resistance
s	Solubility in Water
S_a	Specific Surface Area
T_{ds}	Total Dissolved Solids
ΔT	Change in Temperature
t_{90}	Average Degree of Consolidation
μ	Electrophoretic Mobility
μ	Micro Particles Size
V	Sedimentation Potential
V_{MB}	Methylene Blue Adsorption
ΔV	Potential Difference
v_h	Fluid flow Velocity
σ	Electrical Conductivity
w	In Situ Water Content
w_{opt}	Optimum Moisture Content
ε	Shear Displacement
ζ	Zeta Potential
σ'	Effective Stress
ASTM	American Society for Testing and Materials

CEC	Cation Exchange Capacity
DC	Direct Current
DDL	Diffuse Double Layer
EK	Electrokinetic
MB	Methylene Blue
PI	Plasticity Index
PL	Plastic Limit
XRD	X-ray Diffraction

Chapter 1

INTRODUCTION

1.1 Background and problem statement

Construction on soft soils poses a challenge to construction activities in the geotechnical engineering field (Chew *et al*., 2004; Nordin, 2015; Azhar *et al*., 2017). Soft soil may be water-saturated, fine-grained low permeable soil that makes the drainage of pore water from its voids difficult. The stability of structures on soft soils depends on the volume and strength properties of the soft soils on which it is built. The soft soils possess high compressibility, high plasticity, excessive settlement, and low shear strength (Shang *et al*., 2004; Jayasekera, 2007). Soft soils can trigger geotechnical hazards such as structural collapse, slope failure, and landslides. A potential site of soft soils is not suitable for use without the improvement of their engineering properties (Ou *et al*., 2009; Islam *et al*., 2012). The numerous soft soil stabilization methods depend on the soil, material, and environmental factors employed to enhance the soil stability with the consideration of the cost, time, installation setup, and applicability to in-situ and ex-situ soils. To remediate the deficient properties of soft soils, effective soil stabilization methods using suitable stabilizing materials and methodology are required (Yeung, 2006; Ivliev, 2008). The electrokinetic, EK stabilization technique is a newly emerging method to mitigate the deficiencies associated with low permeable, not quickly drained problematic soft soils.

Soft soils are characterized by excessive compression, frost susceptibility, high swell potential, and low shear strength (Abdullah and Al-Abadi, 2010; Nordin, 2015). In recent years, the collapse, expansion, heave, instability, landslides, shrinkage, settling, and tilting problems attributed to the deficient soils have caused tremendous damages to the civil engineering structures built-in, on or through them, and many attempts have been made to mitigate these soils (Abdullah and Al-Abadi, 2010; Gingine *et al*., 2013; Ranjitha and Blessing, 2017). The geotechnical hazards in problematic soft soils have caused instability of dams, landslides in slope regions, pipeline failure, and settling or tilting of buildings (Askin and Turer, 2016; Wahab *et al*., 2018). Thus, the deficient soft grounds are not suitable without improving their index and engineering properties either before or after the construction activities (Nordin, 2015; Azhar *et al*., 2017).

Until now, the challenges attributed to deficient soft soils that affect the construction or performance of foundations or other sub-structures seem unsustainable at low cost (Virkutyte *et al*., 2002; Mohamedelhassan *et al*., 2012; Azhar *et al*., 2017). There appear to be unending lasting solutions to standardize the mitigation methods to combat the challenges posed by these deficient soft soils. Their hazardous effect on the foundation structures invariably transfers the distress to structures such as dams, embankment, light buildings, levees, pavements, roads, rails, pipelines, walls, and natural geology formations or artifacts (Nordin, 2015; Ranjitha and Blessing, 2017).

There is a need for collective efforts by the geotechnical community to find sustainable, effective, efficient, and comprehensive solutions to the defective properties of existing problematic soils. Geotechnical engineers need to define in clear terms the precisely standardized index, physicochemical, and engineering properties required for the underlying or adjacent soil deposits to attain, during the application of

any ground stabilization or the improvement method. This approach will guide in applying the suitable soil enhancement method(s), thus, reducing the testing and trial procedures, which consume enormous funding, technical skills, workforce, and time duration (Jayasekera, 2004; Badv and Mohammedzadeh, 2015; James *et al*., 2019).

For many decades, several attempts have been made to mitigate the problematic properties of soft soils to avoid their associated damages and make them suitable for construction purposes before, during, or after the construction of structures on these soils (Kaniraj and Yee, 2011; James *et al*., 2019). The demarcated land for urban building development and construction activities is spreading to the Tuzla region of Famagusta city in North Cyprus. The Tuzla area is made up of highly compressible, blue, soft marine clayey soil deposits. The challenges associated with the differential settlements in this region during or after construction activities need adequate control, prevention, and mitigation. It is crucial to improve the existing soft soil conditions before a construction activity begins. According to Gingine *et al*. (2013), the objective of stabilizing soft soils as building and foundation materials are categorized below as:

- To increase: the densification, bearing capacity, stiffness, stability, and strength;
- To reduce: the compressibility, distortion under stress, natural variability of borrow materials, susceptibility to liquefaction, volume-change properties, water pressure;
- To control: expansion, permeability, settlement, shrinking and swelling behaviors;
- To prevent detrimental biochemical changes due to environmental conditions.

In this regard, it is appropriate to find an alternative soil improvement technique, which offers economical and technical advantages for geotechnical applications. The wide range of improvement methods is grouped into chemical, mechanical, physical, bioremediation, tension-resistant foundation methods (Barker *et al*., 2004; Azhar *et al*., 2017). The choice of soil improvement depends on many factors. These factors can be grouped into soil-related, materials-related, and operational-related factors (Choi and Lui, 1995; Wang *et al*., 2011; Ou *et al*., 2015). The soil-related factors are seepage conditions, type of soil, toxicity, or corrosivity (Li *et al*., 2012; Yan *et al*., 2015). The material-related factors include the availability of materials. The operational-related involve cost, construction duration, the degree of improvement required, durability, the feasibility of building control and performance, type, and reversibility or irreversibility of the overall processes to achieve desired results (Kaniraj *et al*., 2011; Mosavat *et al*., 2013; Arutselvam, 2014; Zhang *et al*., 2017).

Preloading causes the soil to attain a significant proportion of its final settlement before construction. Unfortunately, it often takes about 5-10 months' duration or more to achieve this. (Charles and Watts, 2002). The more cost-effective way of reducing the chemical improvement of low permeability, fine-grained clay soil using calcium-based stabilizing agents, such as cement and lime, is a common practice for both shallow and deep stabilization in the last few decades (Shang *et al*., 2004; Liu and Shang, 2014; Zhang *et al*., 2014; Abiodun and Nalbantoglu, 2015). Its overall advantages can be summarized as an increase in bearing capacity, soil durability, stiffness and strength, and a substantial reduction in the soil compressibility, soil plasticity, shrinkage, and swelling potential or swelling pressure of the soils (Morefield *et al*., 2006; Mandal *et al*., 2013; Zhou *et al*., 2015; Abiodun and Nalbantoglu, 2017; James *et al*., 2019).

However, the chemical stabilization methods are not applicable to improve problematic soil conditions under existing structures. Nevertheless, there are other stabilizing methods suitable for fine-grained soils under existing structures. Examples of such ground improvement methods are electroosmotic consolidation, soil freezing, and hydrofracture grouting (Alshawabkeh and Sheahan 2003; Kaniraj and Yee, 2011).

Deep ground improvement methods include blasting, compaction piles, dewatering, dynamic compaction, grouting, lime piles, preloading, pre-wetting, thermal treatment, vertical drains, vibro-compaction, and many other methods (Kaniraj *et al*., 2011; Moayedi *et al*., 2013; Wahab *et al*., 2018). These methods have been known to be successful in minimizing severe damages. However, they are costly, result in observable movements of ground that are potentially detrimental to overlying and adjacent structures, and can be challenging to implement in some existing structures (Alshawabkeh and Sheahan, 2003; Nordin, 2015; Shin *et al*., 2017; Wang *et al*., 2018).

The electrochemical stabilization method, which is a chemical treatment under the influence of an electrical gradient, is applied to overcome the significant limitations attributed to other types of stabilization methods. This technique draws chemical ions between bespoke electrodes inserted at both ends into the treated soil (Rogers *et al*., 2003; Alshawabkeh and Sheahan, 2003; Barker *et al*., 2004). The EK technique is advantageous in that it is applicable both in ex-situ and insitu, cost-effective, easy to operate, rapid, timely, and straightforward installation (Fourie *et al*., 2007; Mosavat *et al*., 2013; Pérez *et al*., 2013; Zhang *et al*., 2014). It is energy-efficient by using direct current (DC) or low AC with differential voltage gradient specifications in the range of 12 to 80 V/m primarily, to produce a considerable electric field across a moist soil media through a pair of conductive electrodes (anodes and cathodes) (Asavadorndeja

and Glawe, 2005; Jayasekera, 2015). Also, it is sustainable, repeatable, flexible in operation, technically simple, and it is adaptable to various in situ ground conditions.

EK technique is a non-noise operation, without excavation, drilling or boring, soil removal or replacement, vibration, no subsurface or underground site disturbance, and relatively short treatment duration with very efficient results (Rogers *et al*., 2003; Moayedi *et al*., 2014a; Azhar *et al*., 2017). EK technique is also applicable to remediate deficient soils under existing structures such as light buildings, pipelines, roads, and railways (Liaki *et al*., 2010; Gingine *et al*., 2013; Ranjitha and Blessing, 2017). There are minimal health and safety risks involved. It has the potential to mitigate large ground both in areas and in-depth (Shang *et al*., 2004; Yeung, 2006). It is useful in reducing geotechnical hazards such as liquefaction, preventing slope failures, settling, tilting, or sliding (Jones *et al*., 2011; Mosavat *et al*., 2013; Malekzadeh *et al*., 2016).

However, the EK technique has still not been commonly used as a standard field application in geotechnical engineering. This drawback is a result of a lack of understanding of the controlling factors, electrochemical effects, and physicochemical phenomena when chemical stabilizers are introduced concurrently with the passage of the current through a soil-pore water-electrode system (Ou *et al*., 2009; Li *et al*., 2012).

1.2 Rationale and background of the study

This study is a continuous research development in the Civil Engineering Department, Eastern Mediterranean University, to establish significant controlling factors, to validate the phenomena, concepts, and processes of EK improvement of problematic soils. This study is to develop the practical applications of improving the in-situ deficient soft soil condition by using specific ionic solutions during EK treatment

techniques. A quite number of studies are available on the use of the EK treatment method, as a viable and promising alternative to the conventional in situ ground improvement and treatment technique (Rogers *et al*., 2002, 2003; Liaki 2006). The use of this creative technique will provide viable solutions for the enhancement of soft soils, and eventually, it could be used in geotechnical engineering field applications.

The first stage of this study examines the determination of the index and engineering properties of the insitu natural soft soils. The second phase of this study involves a detailed laboratory study that would evaluate the efficacy of the use of the paired and unpaired calcium chloride, $CaCl_2$, and sodium carbonate, Na_2CO_3 combinations, which were continuously supplied at the anode and cathode, respectively. This process was designed to stimulate the movement of desired ions through the soil media, enhancing the EK's ability to facilitate the precipitation of cementitious hydrates, leading to soil cementation in the soil mass. In this section of the study, all the response data in the form of physicochemical and engineering properties were collected. The experimental data were carefully measured using the testing apparatus, recorded and analyzed in detail over different EK treatment durations during laboratory testing.

Moreover, most of the studies investigating the performance of EK treatment of problematic soils (Lefebvre and Burnotte, 2002; Thuy *et al*., 2013; Arutselvam, 2014) have been conducted using the conventional methods of applying initial measurements through which further process is estimated to examine the performance of the results.

The third phase of the present study comprises the numerical model analysis method employed to establish the efficacy of the input factors at different environmental conditions and to test the quality of the desired output data and properties. Obtaining

the maximum rate and amount of electrokinetic diffusion of stabilizing ions within the soil system and the subsequent calcium carbonate precipitation is the primary concern of almost all the EK stabilization studies in the literature (Keykha *et al*., 2014; Ng *et al*., 2014), despite the input parameters and the obtained results. An initial differential cell concentration measurement such as pH, total dissolved solids, salinity, and electrical conductivity was carried out in the current study to evaluate the variation of the peak rate of diffusion of ions and the efficacy of precipitates and cementitious gels.

Most studies have been conducted on EK stabilization of soft soils by using different conventional methods (Jayasekera, 2015; Askin and Turer, 2016; Suied *et al*., 2017). However, only a few studies have used advanced statistical methods for optimization of the rate of diffusion of the stabilizing ions and cementitious gels precipitation rate (Rittirong *et al*., 2008; Sondi *et al*., 2009; Keykha *et al*., 2014). The conventional trial and error method is only able to provide a solution by interpreting the effect of an individual factor of the final product after rigorous repeated, varied attempts, which are continued until the desired result is obtained. Also, these traditional methods do not usually consider the possible interactions of an individual factor with other influencing factors. Also, the methods are costly, time-consuming, and error bound.

To overcome the drawbacks of the conventional soil improvement methods, response surface methodology (RSM), which is an efficient statistical method was employed in this study. The Central Composite Face-centered (CCF) design is one of the models used for describing the response surface method (RSM), which was used to fit in a second-order model relating to each response such as the effect of applied voltage, initial cell concentration, and temperature. The responses were the physicochemical and engineering properties obtained after the EK stabilization of the treated soil. The

optimal condition at which the combination of the diffusion rate and potential of calcium carbonate precipitation was also received. This study presents the findings of such a multiresponse EK study using RSM, which was rarely studied in the literature.

1.3 Research aim and objectives

This study aims to investigate the use of EK treatment as an effective, innovative method to improve the overall physicochemical and engineering properties of soft clay soil. The soil properties considered in this study include unconfined compressive strength, compressibility, swelling, shrinkage, and plasticity. To achieve the desired objectives, the following research work has been carried out within the context of:

- Extracting the undisturbed soft soil block samples with the retained insitu conditions.
- Determining the effectiveness of the electrokinetic treatment technique on soft soils.
- Studying the significance of the determinant input factors during the EK treatment.
- Studying EK effects on the physicochemical and engineering behavior of soft soils.
- Examining the changing electrode length ratios on the vertical depth of soft soils.

1.4 Contribution to knowledge

The outcomes of the experimental investigations presented in this study have increased the understanding of the EK treatment used to improve the physicochemical and engineering properties of problematic soils. The results of the findings indicate that the EK technique has the possible potential to be implemented in the field with success recorded from the laboratory scale experiment. The result is an indication that the EK treatment is not only suitable to improve the soil properties before the construction of the project, but it is also applicable to problematic soils under existing foundations and structures. The findings of this current study, which are using suitable combinations of ionic solutions and common metallic electrodes with suitable experimental setups in the laboratory have indicated a high potential to be adopted in the field application.

1.5 Outline of the thesis

Chapter 1 of this thesis presents the introduction of the EK treatment technique, its background, the problem statement, and the rationale of the study. Also, it discusses the aims and objectives of the study and its contribution to the existing knowledge.

Chapter 2 presents the detailed literature reviews of electrokinetic phenomena to understand the theoretical and fundamental background required for EK treatment. The understanding of electrokinetic requires comprehensive research literature on the clay mineralogy, clay water-electrolyte system, flow theories, EK phenomena, EK setups, EK controlling factors, properties of EK treated soils, and gaps in the literature.

Chapter 3 presents the electrokinetic, EK materials used in the present study and the test methodology used to determine the effectiveness of electrokinetic, EK treatment with different combinations of ionic solutions, different treatment durations, as well as the lengthwise anode to cathode distances, vertical electrode lengths, and soil depths.

Chapter 4 presents the numerical analysis of the recorded data obtained from the physicochemical, engineering, and index properties of the electrokinetic, EK treated soils in order to establish their significant controlling factors and the threshold values.

Chapter 5 presents the results of the preliminary laboratory works on the untreated and treated soil block samples. The laboratory tests were conducted for the assessment and determination of the physicochemical and engineering properties of natural soft soil used in this study. Also, detailed laboratory tests were conducted for the assessment and evaluation of the results of the physicochemical, index, engineering, thermal, and microscopic analysis of the EK treated soils and then compared with the natural soil.

Chapter 6 presents the conclusion of the findings of the EK treatment of the soil. This section summarizes the test results of the chemical analysis, index, and engineering properties, thermal and microscopic properties for EK treatment of soft soil using different combinations of ionic solutions, and other selected determinant factors. Also, the section provides recommendations for future research studies of EK soil treatment.

Chapter 2

LITERATURE REVIEW

2.1 Introduction

This overview is a part of significant ongoing efforts to examine the efficacy of the electrokinetic, EK treatment methods using different combinations of ionic solutions for improving the physicochemical, physical, and engineering properties of soft soils.

2.2 Background

In the field of geotechnical engineering, building structures on soft soils is a great challenge. In recent years, the consideration to improve the deficient properties of soft soils such as high plasticity, high compressibility, excessive settlement, and low shear strength is a continuous subject under intensive researches (Zhang *et al*., 2014; Nordin, 2015). The geotechnical damages caused by these properties of soft soils reflect as the bulging of roads, cracks in walls, instability or failure of bridges, dams, retaining walls and slopes; settling and tilting of foundations, misalignment of structures, leakages in pipelines, and damage of natural earth artifacts (Glendinning *et al*., 2007; Ahmad *et al*., 2011; Mosavat *et al*., 2012; Schmidt *et al*., 2015; Hassan *et al*., 2016). The geotechnical engineers' keen interest to improve soft ground conditions stems from the increasing demand for construction activities (Zhang *et al*., 2014; Moayedi *et al*., 2014a). To mitigate the properties of soft soils, innovative soil stabilization methods are required using the suitable stabilizing materials such as non-traditional materials or ionic solutions (Yeung, 2006; Ivliev, 2008; Moayedi and Mosallanezhad, 2017).

Several methods of soft soil stabilization depend on the type of soil, material, and environmental factors employed to aid their improvement with regards to cost, time, mode of setup and operation, and suitability for insitu and exsitu soils. The quest for innovative methods to stabilize soft soils to attain desired results at efficient and low-cost value when building structures on soft ground is vital (Ranjitha and Blessing, 2017). The preloading of soft soils, for example, reduces settlement and increases in strength. Still, it takes a long time to achieve the anticipated consolidation results in soft soils (Charles and Watts, 2002). A weighty preload decreases the time during the consolidation of soft soils to attain final settlement but can cause a premature ground failure (Liaki *et al*., 2010). The use of preloading with vertical drains, jet grouting, soil freezing, and electroosmotic consolidation methods on soft soils can reduce the total time of installation and operation (Gaafer *et al*., 2015; Cai *et al*., 2017; Fu *et al*., 2018).

However, these methods may trigger observable ground movement that poses a threat to the surrounding or adjacent structures (Shin *et al*., 2017; Wang *et al*., 2018). Ca-based chemicals such as lime, cement, fly ash, and geopolymers are used in chemical treatment methods (Nalbantoglu and Gucbilmez, 2001; 2002; Nalbantoğlu, 2004; Tran *et al*., 2018; Liu *et al*., 2019) to stabilize soft soils in a short time, and do not cause ground movement. However, these stabilizers are not suitable to provide stabilization for soft soils under established structures due to the constraints in reaching subsurface regions beneath the foundation structures (Mosavat *et al*., 2014). In the literature, the use of an innovative EK treatment technique is one of the most cost-time effective, non-disruptive, no disturbance on the ground or adjacent structure, and stabilizes low permeable fine-grained, insitu, or exsitu soft soils under existing structures (Gingine *et al*., 2013; Ranjitha and Blessing, 2017; Estabragh *et al*., 2019; Abiodun and

Nalbantoglu, 2020). EK treatment technique has noiseless setup operations; thus, it causes no environmental pollution as it requires no drilling or excavation of soils.

It can cover a large ground area and depth. It requires less highly skilled expertise and heavy machinery. It reduces carbon emissions and lowers construction sites' health and safety risk factors (Moayedi *et al*., 2014b). The method has rapid and simple setup procedures. It finds practical application in slope stabilization. It can be applied easily to mitigate a wide range of problematic soils (Wahab *et al*., 2018). Its setup is portable, easy to fabricate, and often available (Schmidt *et al*., 2015; Askin and Turer, 2016).

However, the EK treatment of soils has been faced with many challenges or limitations based on the design system, soil conditions, and environmental factors (Claudio *et al*., 2013; Ranjitha and Blessing, 2017). The coupling of the laboratory-scale model system for the EK treatment setup has some challenges. On a laboratory scale, the preparation of soil samples for EK treatment requires lots of effort (Ahmad *et al*., 2011; Wang *et al*., 2016; Azhar *et al*., 2017). Often, the time and energy put in the remolded slurry sample to replicate the soft soil on the field are huge. The rigorous process involves oven drying, then pulverization, to produce a dry soil solid, or ready-made synthetic clayey soil is utilized (Shang, 1997; Hamir *et al*., 2001; Arutselvam, 2014).

Until now, the EK treatment technique does not have standardized procedures in geotechnical applications. Its complexity is due to the selection of the appropriate materials, controlling factors, and limited understanding of the electrochemical, hydrochemical, and physicochemical effects, and soil-ionic liquid interactions. There are limited or no empirical and theoretical formulations to define the critical processes during the geotechnical applications of EK treatment of soils (Mosavat *et al*., 2012).

Also, in the literature, EK soil treatment has many other challenges attributed to its complex test setup, inappropriate selection of ionic solutions, electrode type, power supply, and soil conditions (Yuan *et al*., 2012). The use of a low-cost, easily available, and suitable materials, especially different mixture of ionic solutions, should be utilized to achieve the desired results in the EK treated soils (Kaniraj and Yee, 2011).

Other primary drawbacks to consider for the EK treatment technique are the trial and error approaches, uncertainty in energy usage, loss of energy efficiency with time, costs irregularities, and corrosion of electrodes (Abiodun and Nalbantoglu, 2018). There is a possibility of intoxication, salinization, detrimental effects to plants and organisms, and contamination of underground water and adjacent water bodies (Kim *et al*., 2011b; Mohamedelhassan, 2011). Also, the irregular flow path, seepage, leaching, and leakage related issues are few other reasons why the EK technique is considered as a last resort for large scale geotechnical in situ applications (Kim *et al*., 2011a; Fourie *et al*., 2007; Gingine *et al*., 2013). The on-site limitations that hinder the EK process are irregular topography, slopes, underground structures, buried metals, and complexity in a broad range of soil deposits (Zhang *et al*., 2013; Deriszadeh and Wong, 2014; Jayasekera, 2015; Abiodun and Nalbantoglu, 2016; James *et al*., 2019).

In the literature, many geotechnical researchers have used several combinations of ionic solutions for EK treatment (Schmidt *et al*., 2007; Liu and Shang, 2014; Jayasekera, 2015). However, studies on the use of the combination of calcium chloride, $CaCl_2$, and sodium carbonate, Na_2CO_3 ionic solutions, are relatively rare in EK treatment to stabilize soft soils. Thus, this study focuses on the use and effects of the combinations of these ionic solutions using a small-scale laboratory model of the EK treatment technique to improve and examine the engineering properties of soft soils.

This chapter discusses the basic principles of EK treatment technique, EK phenomena, EK flow types, EK setups, EK materials, and their effects on EK treatment. It also discusses the proposed test setup models of the EK treatment technique used in the present study, EK controlling factors, and the previous studies on the EK treatment of soft soils. It provides a detailed overview of EK experimental input factors, output results, and the engineering properties assessment for the several EK treated soft soils.

2.3 Basic principles of electrokinetic technique

The principles of the EK technique uses electrical energy supplied from a power source via conductive electrodes to drive charged species towards the oppositely charged electrode in porous soil media to initiate combined effects of a chemical, hydraulic, and thermal gradients under an applied electric field (Alshawabkeh, 2001). As a result, several geochemical reactions, EK phenomena, and exchange of ions, cementation, flocculation, and aggregation exist during the EK treatment of soil (Jayasekera, 2015).

2.3.1 Geochemical reactions

The transport of fluids and solute initiate several geochemical reactions such as the oxidation-reduction (redox) reaction, sorption, desorption, dissolution, and precipitation within the soil porous media during the EK soil treatment (Paz-Garcia *et al*., 2012; Rojo *et al*., 2014). This section discusses detailed geochemical reactions.

2.3.1.1 Oxidation and reduction (redox) reactions

The exchange of electrons between reactive materials causes oxidation-reduction (redox) reactions. The species that gain electrons are reduced, and the species that loses electrons is oxidized. The redox reactions are pH-dependent; thus, a suitable pH level is needed to limit their detrimental effects during the EK treatment (Jayasekera, 2008).

2.3.1.2 Sorption and desorption reactions

Sorption is the separation of chemical ions from the solution to a solid surface or solid-phase through mechanisms of adsorption or ion exchange. The negatively charged clay surfaces attract and absorb heavy metals and cations during EK treatment of soils. Metals and cations possess different sorption capacity and depend on the size and valence of the cations, and type of clay minerals (Acar and Alshawabkeh, 1993).

Whereas, desorption is the process responsible for the release of ions from the soil surface. Such processes are controlled by changes in soil pH due to the migration of H^+ and OH^- ions aided by the electrolytic reaction. Acar and Alshawabkeh (1993) reported that the desorption of cations from the clay surface is more effective as the H^+ ion concentration increases, a function of surface charge density of clay minerals, cations concentration, and the presence of organic matter and CO_3^{2-} ions in the soil.

2.3.1.3 Precipitation and dissolution reactions

Precipitation defines a separation of a substance from a solution as a solid, and dissolution defines the process by which a solid solute forms a solution in a solvent. The transport of fluid and solute via porous soil media depends on these two processes and is a function of soil pore fluid pH and concentration. Acar and Alshawabkeh (1993) reported that the highly alkaline environment aids heavy metals to precipitate, blocks the soil pores, and slows down or hinders the electrokinetic soil treatment mechanisms, whereas due to the highly acidic environment, the newly formed precipitates during the electrokinetic soil treatment are often subjected to dissolution.

2.3.2 Electrochemical gradients

The chemical, hydraulic, electrical, and thermal (CHET) gradients play vital roles as driving forces in EK treatment of soils. The electrical gradient is the primary driving force that aids chemical and hydraulic gradients to drive fluid via soil pores and also results in thermal gradient in the electrokinetic, EK system (Yeung and Datla, 1995).

The combination of these gradients has various effects on the EK system (Iyer, 2001):

- It results in a redox reaction: oxidation is the loss of electrons to generate an acid front at the anode, and reduction is the gain of electrons to produce a base front at the cathode. The species that loses or gains electrons is oxidized or reduced, respectively.
- It causes complex EK phenomena such as electroosmosis, electromigration, and electrophoresis. Electroosmosis defines the migration of fluid, electromigration is the migration of charged ionic species, and electrophoresis represents the movement of charged fine particles through the porous soil media under an applied electric field.

2.3.3 Particle size association (clay structure)

The attraction and repulsion forces between clay fines cause non-identical kinds of clay structures. The groups of clay structures are: aggregated, deflocculated, dispersed, and flocculated (Figure 2.1). The clay structure dictates the properties of soil, such as the compressibility, hydraulic conductivity, and shear strength due to the shape, size, and fabric of soil particles and electrical forces among them (Thuy *et al*., 2013; Azhar *et al*., 2017). The flocculated and aggregated soil structures make soils to exhibit lower compressibility, higher permeability, and higher strength when compared to soils with a dispersed structure (Lambe and Whitman, 1969; Cameselle *et al*., 2013). The changes in the engineering properties of soils are linked to changes in the structure of the diffuse double layer of clay fines (Meegoda and Ratnaweera, 1994; Nordin, 2015).

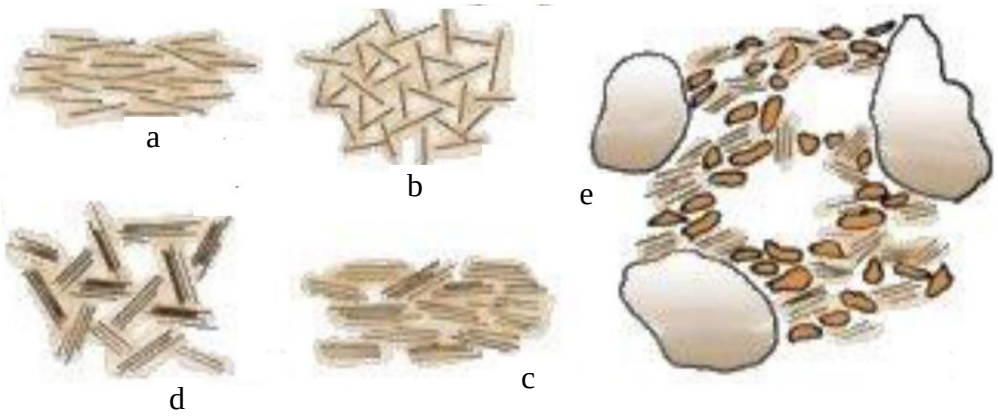

Figure 2.1: Clay structures: (a) dispersed structure, (b) flocculated structure, (c) aggregated structure, (d) flocculated and aggregated structures, and (e) the natural structure of clay, after (Olphen, 1963).

2.3.4 Diffuse double layer, DDL

Negative charges are held on the surfaces of clay-sized minerals due to isomorphous substitution and deficient bonding of the locations accessible for cations, thus releasing protons from hydroxides (Mitchell, 1993). The region of negatively charged surface of clay particles that attract cations is called the diffuse double layer (Mitchell, 1993).

The diffuse double layer, DDL, is a boundary interface between the clay particle surface and the soil ionic solution (Figure 2.2a). The concentration of cations decreases along with the distance from the clay's surface (Figure 2.2b). The clay minerals and ionic solution contact causes the cations reaction, causes the collapse of the DDL structure, and hence reduce the hydration ability of the clay mineral, which causes flocculation of the clay particles, to form flocs (Mitchell, 1993; Alshawabkeh, 2001; Iyer, 2001; Abdullah and Al-Abadi, 2010; Wang *et al*., 2011; Arutselvam, 2014).

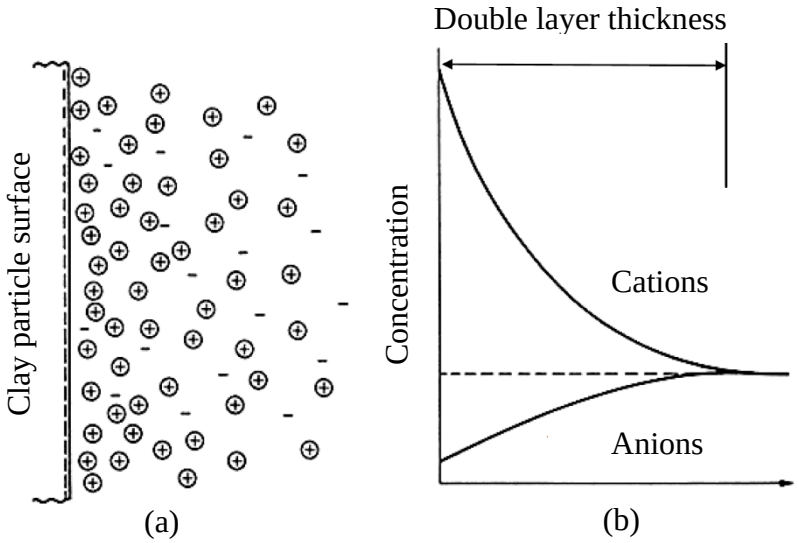

Figure 2.2: (a) Structure of electrical DDL adjacent to a clay surface, and (b) potential positions of cations and anions away from the clay surface, after (Alshawabkeh, 2001).

The flocculated structure is as a result of depression or collapse of DDL, whereas dispersed structure comes from enlarging DDL. Thus, the higher swelling pressure in expansive soils and the less affinity of the particles in suspension to flocculate depend on the thickness of the DDL (Moayedi *et al*., 2014c; Arutselvam, 2014; Nordin, 2015).

2.3.5 Electrokinetic, EK phenomena

The EK phenomena are influenced by driving forces to create the tangential motion of either continuous fluid or dispersed phase to an adjacent soil charged surfaces (Nordin, 2015; Kollannur and Arnepalli, 2019). The driving forces exist as chemical, hydraulic, electrical, pressure, or thermal gradient. EK treatment of soils induces several changes in the pore fluid chemistry of soil pores, diffuse double layer (DDL), and soil-water structure interaction (Alshawabkeh, 2001; Wang *et al*., 2011; Arutselvam, 2014).

The tangential fluid flow via the DDL interfaces of the chemically and electrically active low permeable, fine-grained soils produces several intertwined EK phenomena (Jayasekera, 2008). The EK phenomena comprise of electrolysis, electroosmosis, electrophoresis, electromigration, streaming potential, and sedimentation potential

(Figure 2.3) (Iyer, 2001). Their combined effects can cause several changes in the physicochemical, hydrological, mineralogical, and engineering properties of the EK treated soils under an electric field (Mitchell, 1993; Ahmad *et al*., 2006; Yeung, 2006).

EK phenomena have gained more attention in geotechnical engineering research due to their practical suitability for driving fluids, charged ions, and solutes in the fine-grained, low permeable soft soils (Li *et al*., 2012; Kollannur and Arnepalli, 2019).

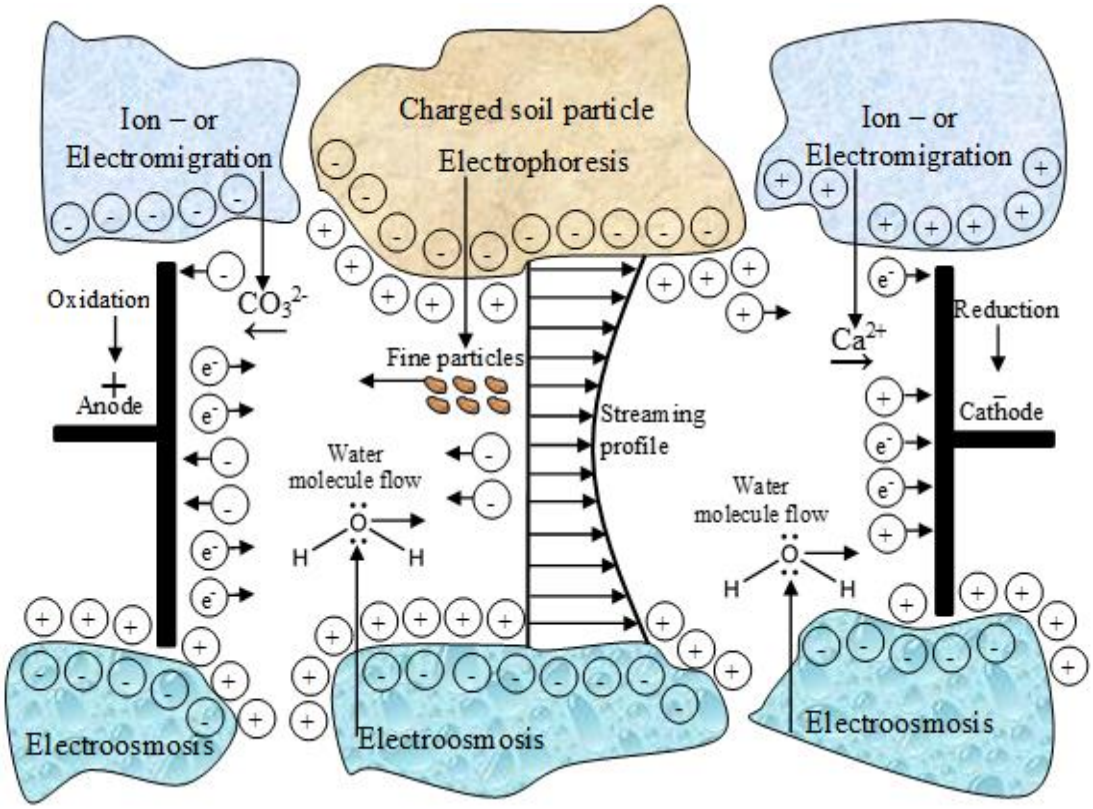

Figure 2.3: Schematic diagram of EK phenomena during the EK treatment of soil (Iyer, 2001: modified).

2.3.5.1 Electrolysis

Electrolysis is a redox reaction that converts electrical energy into chemical potential energy under an electric field during the EK treatment of soils (Samidurai *et al*., 2017). It initiates the gain of electrons, causes reduction, generates H_2 and OH^- ions, produces basic fonts, and increases pH to ≥ 7 to ≥ 10 at the cathode. Also, electrolysis causes loss of electrons, aids oxidation, generates O_2 and H^+ ions, yields acidic font, and decreases pH to ≤ 7 to ≤ 2 at the anode (Malekzadeh *et al*., 2017). It occurs due to electron(s) transfer from the anode(s) to the cathode(s) that are inserted in the soil and caused anode to corrode. The acidity font controls the mobility of ions and the electroosmotic flow rate during the EK treatment of soils (Paz-Garcia *et al*., 2012).

The redox reactions of ionic solutions attributed to electrolysis generate H_2 and OH^- ions at the cathode, and as well as O_2 and H^+ ions at the anode, given in Equations 2.1 and 2.2 (Barker *et al*., 2004; Cameselle *et al*., 2013; Kollannur and Arnepalli, 2019):

Anode: $2H_2O - 4e^- \rightarrow O_2 + 4H^+$ (oxidation: electron loss) $E_o = 1.229$ V (2.1)

Cathode: $2H_2O + 2e^- \rightarrow H_2 + 2OH^-$ (reduction: electrons gain) $E_o = 0.828$ V (2.2)

The generation of H_2 gas at the anode via electroosmosis and diffusion of acidic font towards the cathode lowered the pH in the anode region (Reddy *et al*., 2006). The formation of OH^- ions in porous soil media at the cathode via diffusion of alkaline font towards the anode increased the pH in the cathode region. At a certain point during the EK treatment, the acidic and alkaline fonts migrate to a certain meeting point and become neutral in effect within the porous soil media (Figure 2.4) (Azhar *et al*., 2017).

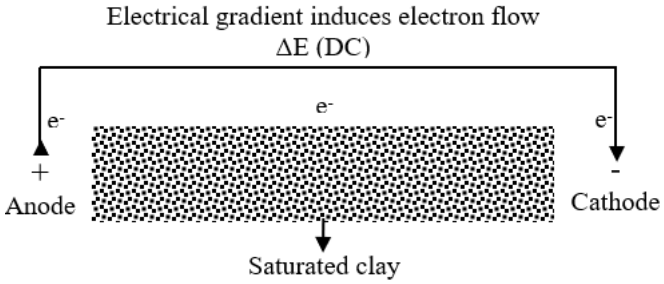

Figure 2.4: Electrolysis phenomenon (Mitchell and Soga, 2005).

2.3.5.2 Electroosmosis, E_{os}

Electroosmosis, E_{os} is a primary EK phenomenon that aids fluid flow in the stationary porous soil media from the anode to the cathode in response to the electrical gradient applied to soil media. It is a driving force that distributes cationic-stabilizing agents to the soil porous media (Tajudin *et al*., 2015; Mosavat *et al*., 2013; Ramadan *et al*., 2018). Liaki *et al*. (2010) stated that soil place in between electrodes placed in ionic solutions under an electric field aided fluid flow from one end to another (Figure 2.5).

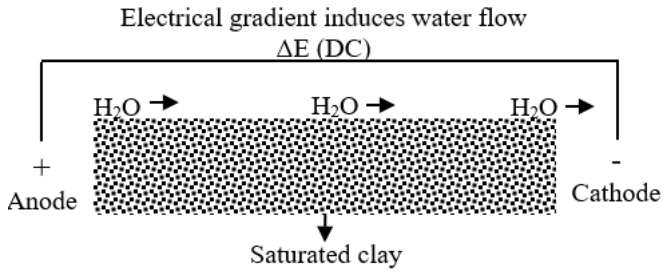

Figure 2.5: Electroosmotic phenomenon (Mitchell and Soga, 2005).

Under an electric potential to a saturated clay, electroosmosis causes pore fluid to flow from anode to cathode ends, respectively (Kim *et al*., 2011b; Yeung, 2011). Also, the mobile layer of the DDL moves towards the cathode and exerts a viscous drag on the free water in the porous medium to advance the mobility of water in the soil (Mosavat *et al*., 2013; Jayasekera, 2015). E_{os} does not occur in granular soils unless a high number of clay-sized particles is present (Ng *et al*., 2014; Yuan and Hicks, 2016).

2.3.5.3 Electroosmotic flow, q_{eo}

The electroosmotic flow rate (q_{eo}) is a function of the coefficient of electroosmotic permeability (K_{eo}) in soil media, which measures the volume rate of fluid flowing via a unit cross-sectional area due to a unit electric gradient under constant conditions during EK testing duration (Shang *et al*., 2004; Esmaeily *et al*., 2006). The K_{eo} is given in Equations 2.3 and 2.4, where ζ, n, η, and D, are the zeta potential, porosity, viscosity, and dielectric constant, respectively, and are the controlling factors of K_{eo}.

$$K_{eo} = \frac{D\zeta}{\eta} n \tag{2.3}$$

$$K_{eo} = \frac{q_{eo}}{\left(\frac{\Delta V}{\Delta L}\right) A} \tag{2.4}$$

The H-S model theory defines q_{eo} as a function of porosity and flow via the media (Yeung, 2011; Yuan and Hicks, 2016), and given in Equation 2.5 and Figure 2.6 as:

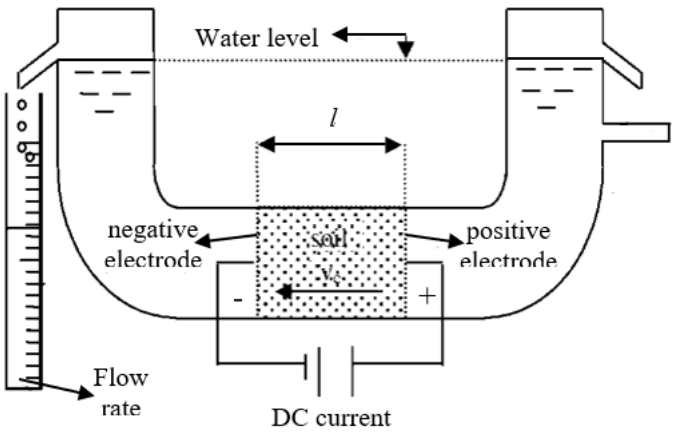

Figure 2.6: Test set up for the evaluation of the q_{eo} (Azzam and Ozey, 2001).

According to this formula, the value of K_{eo} is assumed to be a function of the soil-pore fluid interface, porosity, permittivity, and the viscosity of the soil pore fluid. During the EK treatment of soil, the change in the ion concentration or pH level of pore fluid alters the K_{eo} values of the treated soils. Thus, low pH values decrease the

K_{eo}values, and as a result, the q_{eo} decreases or stops at some later stages of the EK treatment of soil (Alshawabkeh, 2001). Based on the H-S model, the q_{eo} is given as:

$$q_{eo} = K_{eo}\, i_e\, A = K_{eo} \left(\frac{\Delta V}{\Delta L}\right) A \quad (2.5)$$

where q_{eo} defines the volume flow rate of pore fluid via a cross-sectional area of (A) of soil media under an applied potential gradient of, i_e, = ΔV/ΔL. The ΔV is the electric potential difference, and ΔL is the unit length of the soil (Casagrande, 1952). In this regard, the cumulative flow rate, q_{eo}, the cross-sectional area, A, and the sample height are used to determine the K_{eo} value (Yeung, 2011; Wu *et al*., 2013; Harris *et al*., 2018).

2.3.5.4 Electrophoresis, E_P

Electrophoresis, E_P is the transport of charged particles and solids, usually micelles or colloids, relative to a stationary liquid under an applied voltage gradient (Figure 2.7).

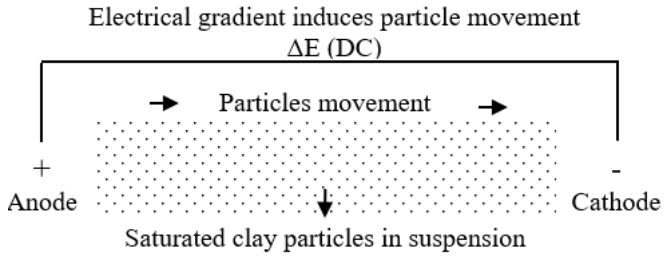

Figure 2.7: Electrophoretic phenomenon (Mitchell and Soga, 2005).

In a given solution, the particle velocity divided by the electric field magnitude defines the electrophoretic mobility, μ. The μ depends on the electrical gradient and magnitude of the charge(s) on the particle and is inversely proportional to the particle sizes, concentration, and fluid viscosity, which influence the media viscosity (Shang, 1997).

2.3.5.5 Electromigration, E_m

Electromigration, E_m is a flow of charged ions in the soil pores towards the electrode of opposite charge under the electric field influence (Figure 2.8) (Rojo *et al*., 2014).

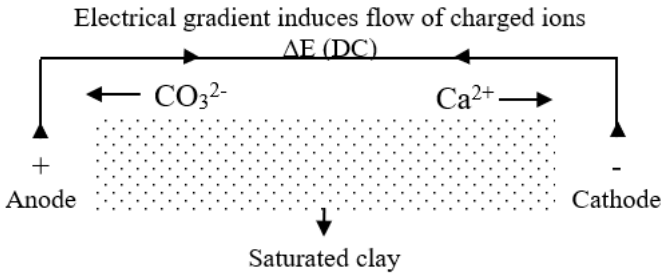

Figure 2.8: Electromigration phenomenon (Mitchell and Soga, 2005).

The ions include the existing ions in the soil, ionic solutions (added to the electrodes), and electrodes as they degrade (Liaki *et al*., 2010). Due to ion charge, E_m causes the ions to flow towards either the anode or cathode. The effective ionic mobility is the migration rate of charged ions under a unit electric field and accounts for soil porosity and tortuosity (Yeung and Datla, 1995; Micic *et al*., 2001; Rojo *et al*., 2014).

The relative use of electroosmosis and ion migration to the total mass transported under the electric field depends on soil type, water content, types of ion species, pore fluid concentration (chemistry), EK processing, and EK setup (boundary) conditions (Micic *et al*., 2001; Alshawabkeh, 2001; Alshawabkeh, 2009; Rojo *et al*., 2014).

2.3.5.6 Sedimentation potential, V

Sedimentation potential, V is the potential difference sensed by porous soil media placed in between two identical electrodes at a vertical distance, L apart in a suspension in which soil particles or soil sediments are under the influence of gravity (Figure 2.9).

It speeds up the velocity and porosity of clay suspensions to form soil sediments. It depends on the changes in the ionic strength, dielectric constant, and viscosity of soil media (Reddy *et al*., 2006; Masi and Losito, 2015; Asadollahfardi and Rezaee, 2018).

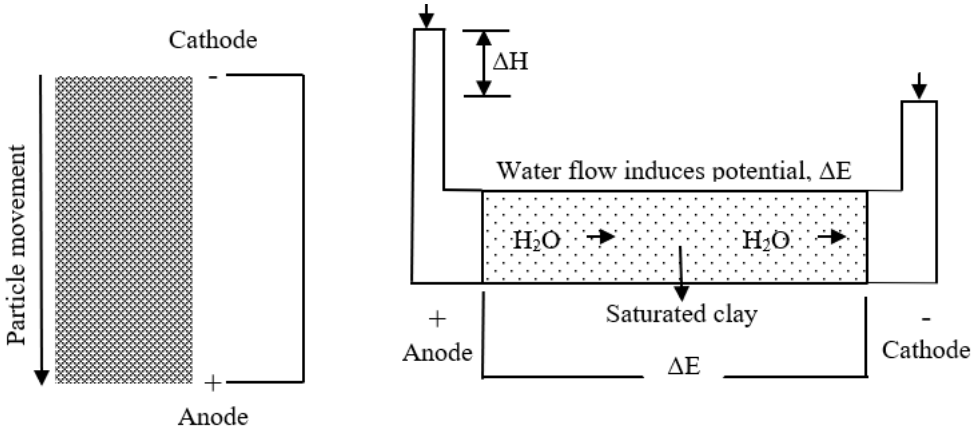

(a) (b)

Figure 2.9: (a) Sedimentation potential, (b) streaming potential (Mitchell and Soga, 2005).

2.4 Conductance flow phenomena in porous soil medium

The porous media of clay particles have distinctive physicochemical properties that define the chemical, electrical, hydraulic, and thermal flow (Thuy *et al*., 2013), which are complex and play a vital role in the response of soil to volume change, and stability. The extensive study of fluid flow via the pores of rocks and soils is due to their vital role in the geotechnical problems, designs, and applications of consolidation, seepage, settlement, strength, and stability of soils (Jayasekara, 2008; Sumbarda-Ramos, 2010).

2.4.1 Chemical flow

Chemical flow is the flow of a chemical species due to the chemical gradient such as advection, diffusion, dissolution, precipitation, and sorption (Paz-Garcia *et al*., 2012). It occurs in a non-active sand porous medium by advection, while the suspended species are driven by flowing fluid. Whereas, it exists in fine-grained soils of very low hydraulic conductivity through diffusion, sorption, and dissolution (Nordin, 2013).

Fick (1885) reported the Fick's law of diffusion to be a net chemical flow in a free porous medium. It depends on its chemical gradient that occurs from an area of high

to that of low concentration due to Brownian molecular motion, given in Figure 2.10 (Shackelford and Daniel 1991; Jayasekera, 2015; Kollannur and Arnepalli, 2019).

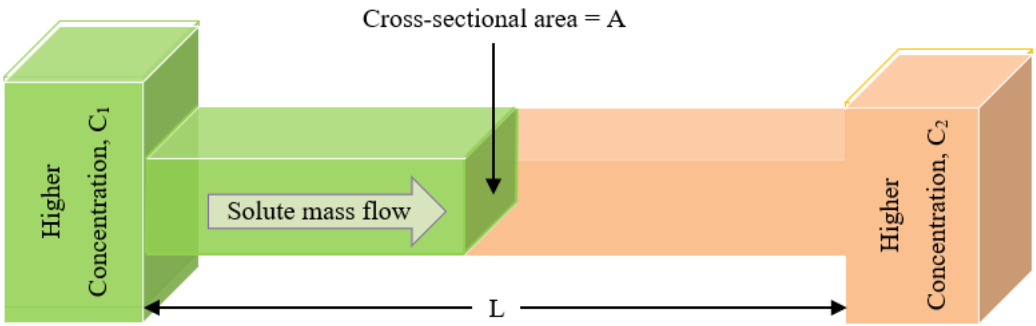

Figure 2.10: Fick's law of diffusion (Shackelford and Daniel, 1991).

2.4.2 Hydraulic flow

Henry Darcy (1856) described the quantitative transport of fluid flow via a porous sand porous medium due to a hydraulic gradient or head difference beds within a defined lateral distance and expressed his findings, as in Equation 2.6 (Gingine *et al.*, 2013):

$$J_w = \frac{Q_h}{A} = K_h \frac{\Delta H}{L} \quad (2.6)$$

where J_w is the water flux, Q_h $\left(Q = \frac{V}{t}\right)$ is the discharge rate flowing through a cross-sectional area A, V is the flow volume, within a time duration, t. K_h is a proportionality constant known as the saturated hydraulic conductivity, ΔH is the difference in potential hydraulic gradient between two points separated by a longitudinal distance, L across which water flows. The hydraulic flow is given in Equations 2.7 and 2.8:

$$Q_h = v_h A \quad (2.7)$$

$$Q_h = K_h i_h A \quad (2.8)$$

where Q_h is the hydraulic flow, v_h is the fluid flow velocity, i_h $\left(\frac{\Delta H}{L}\right)$ is the hydraulic gradient, and A is the cross-sectional area perpendicular to the direction of flow.

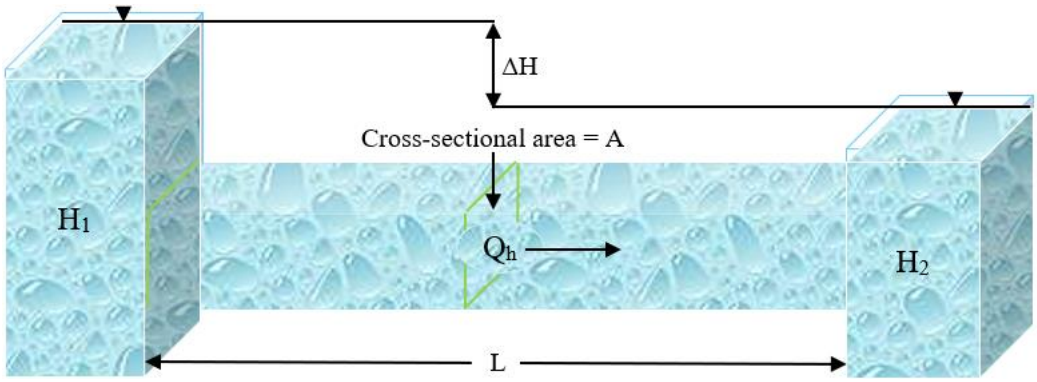

Figure 2.11: Darcy's law of hydraulic flow (Yeung, 2011).

2.4.3 Electrical flow

Electrical flow is the flow of charged ions due to an electrical potential applied via a medium (Yeung and Datla, 1995). It occurs via the fluid in porous soil media and particle interface via the DDL, since soil solids are poor electrical conductors (Arutselvam, 2014; Azhar *et al*., 2017). The creation of an electric field in a soil media aids electrons, e^- to gain kinetic energy, KE, and collides e^- with atoms to transfer KE, given by Ohm's Law in Equation 2.9, Figure 2.12 (Mitchell and Soga, 2005) stated:

$$I = \sigma_e \, i_e \, A \tag{2.9}$$

where I is the electrical flow, σ_e is the electrical conductivity, i_e is the electrical gradient, and A is the cross-section area perpendicular to the flow direction. The σ_e applies to soil-ionic solutions, which equates the inverse of the electrical resistivity:

$$\sigma_e = \frac{1}{R}\frac{L}{A}\left(\frac{\text{Siemens}}{\text{meter}} = \frac{S}{m}\right) \tag{2.10}$$

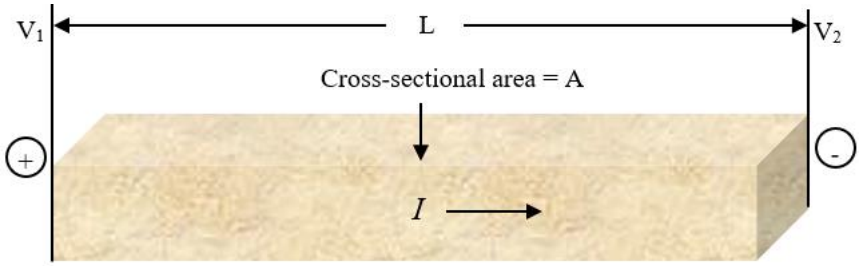

Figure 2.12: Ohm's law of electrical flow (Yuan and Hicks, 2016).

where R is the resistance (Ω), l is the sample length (m), and A for cross-sectional area (m^2). The σ_e value for a saturated fine-grained soil has a range of 0.01 to 1.0 s/m.

The σ_e depends on several soil properties: the degree of saturation, pore fluid, geometry, mineralogy, soil structure, temperature, tortuosity, and interlinks, which controls fluid flow pathways and hydraulic conductivity in the soil (Jayasekera, 2008).

2.4.4 Thermal flow

Fourier's law explains the thermal flow as the transfer of internal energy due to a thermal gradient via conduction, convection, or radiation, given in Equation 2.11:

$$Q_t = k_t\, i_t\, A \qquad (2.11)$$

where Q_t is the thermal flow, k_t is the thermal conductivity; i_t is the thermal gradient, $\frac{\Delta T}{L}$ and A is the cross-sectional area proportional to the flow direction (Figure 2.13).

The heat energy defines the energy possessed by atoms as they collide and oscillate around their steady equilibrium position (Kim *et al*., 2011b; Cameselle *et al*., 2013). The resistance to conduction of heat is a function of the freedom possessed by atoms when colliding and oscillating at their steady equilibrium position (Barker *et al*., 2004).

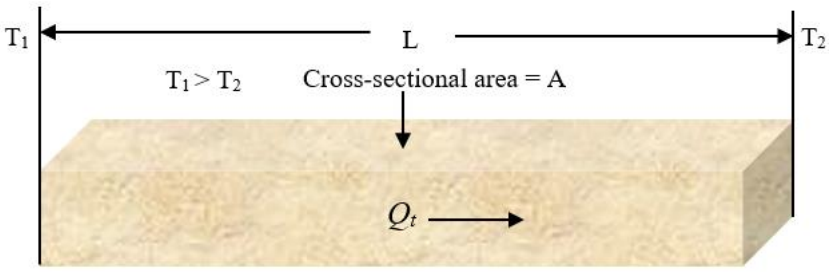

Figure 2.13: Fourier's law of thermal flow (Malekzadeh *et al*. 2016)

2.5 Electrokinetic treatment technique setup

The laboratory-scale model setup for EK treatment of soils comprises a test tank, an array of electrode materials, a combination of ionic solutions, and a power supply device. Figure 2.14 presents a simple setup for the electrokinetic, EK treatment of soil.

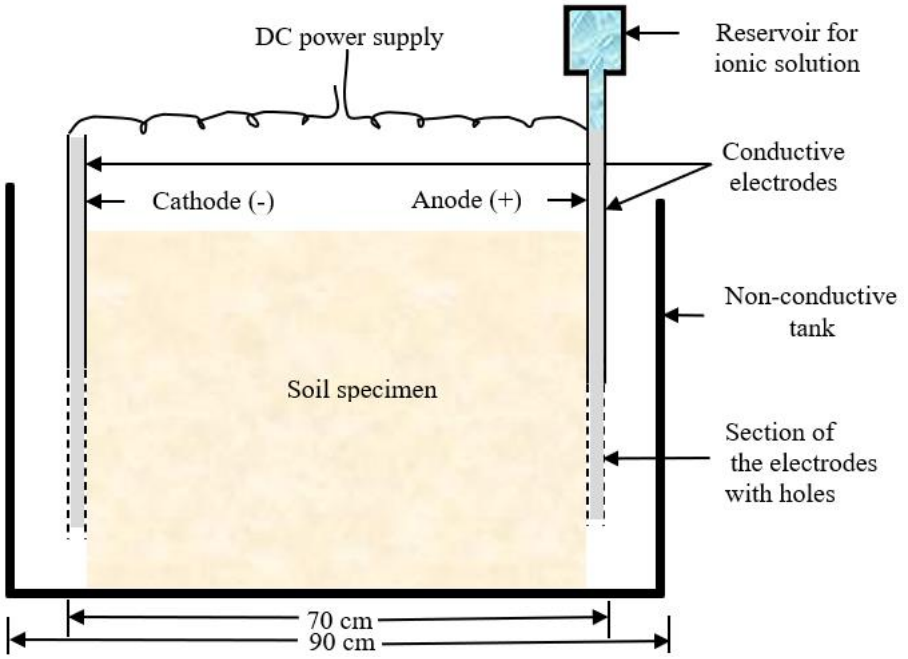

Figure 2.14: Schematic diagram for a laboratory set up for electrokinetic treatment (Jayasekera, 2007).

The EK treatment setup uses electric current from the power supply device to drive charged ions from ionic solutions within the porous soil media by using conductive electrodes inserted into the deficient soft soil, in order to achieve the desired engineering properties (Sumbarda-Ramos, 2010; Ou *et al*., 2013; Azhar *et al*., 2017).

2.5.1 Test tank materials of EK technique

The EK test tank is often a non-conductive, non-reactive, transparent plexiglass, perspex, or PVC-U sheet material (Ahmad *et al*., 2015). The non-conductive property prevents short-circuiting, electric shock, and corrosion, while its transparency enables easy monitoring of the changes in the EK treated soil and the electrolytes during testing

(Wahab *et al*., 2018). The most common test tank dimensions are of 2:1:1 and 2:1:2 ratios for the length, width and height, respectively (Micic *et al*., 2001; Nordin, 2015).

2.5.2 Electrode materials of EK technique

In the literature, the electrode used were inert metals (graphite), non-inert metals (gold, silver, platinum, aluminum, copper, zinc carbon-based (graphite), and geosynthetic materials (Kaniraj *et al*., 2011). The electrodes have different shapes (rectangular, circular, or mesh-like) and setups (paired or an array of electrodes) (Pérez *et al*., 2013). Several electrodes are costly, difficult to fabricate, corrode rapidly, contaminate and toxify soils, aid loss of soil-electrode contact, and loss of energy, time, and efficiency (Jones *et al*., 2006; Malekzadeh *et al*., 2016). The use of alloy or geosynthetic material has been reported to overcome many limitations and to attain optimal efficiency during EK treatment of soils (Glendinning *et al*., 2007; Shrestha, 2014; Azhar *et al*., 2017).

2.5.3 Ionic solutions of EK technique

The usual ionic solutions used for the EK mitigation of soils by notable geotechnical researchers are using of $CaCl_2$, $AlCl_3$, H_3PO_4 for EK soil treatment (Ahmad *et al*., 2011), citric, and acetic acids for decontamination of polluted dredged sediments (Rozas and Castellotem, 2012), modification of salt affected soils (Jayasekera and Hall, 2007), and $CaCl_2$ and Na_2SiO_3 for soil strengthening (Nordin *et al*., 2013). These ionic solutions are used as anolyte and catholyte solutions based on their position in the EK test setup and their contributory ions (Ozkan *et al*., 1999; Loch *et al*., 2010; Masi and Losito, 2015). Malekzadeh *et al*. (2016) reported that the usual range of molar concentration of ionic solutions used for EK treatment of soil is from 0.5-1.5 M.

2.5.4 Power supply device EK technique

In the existing studies, a constant voltage gradient between 20 V/m to 100 V/m was deemed acceptable for a wide range of problematic soils (Mitchell and Soga 2005).

DC is often used over AC, because the electrical conductivity, σ of natural soil is low, the current and voltage required for driving soil pore fluids and ions during the EK treatment, are often low (Micic *et al*., 2001; Glendinning *et al*., 2008). DC is cost-effective, reduce electrocution risk, reduce corrosion of electrode, and gives superior efficiency in EK treatment of soils (Mohamedelhassan *et al*., 2012; Suied *et al*., 2017).

2.6 Effect of EK materials on EK treatment of soils

Liaki *et al*., (2010) stated that EK materials have different effects on the results of the EK treatment of soils and could play a vital role in the efficacy of the EK technique. Therefore, a careful selection of EK materials based on the soil type, soil properties, and the methods of preparation, as indicated in Section 2.5.1, is highly recommended.

2.6.1 Effect of electrode materials on EK treatment of soils

Mohamedelhassan and Sang (2001) indicated that gold, platinum, silver, titanium are good conductors, non-corrosive, but are costly electrodes, and carbon-based graphite is cheap, but are less efficient and caused a huge power loss during EK treatment of soils. Segall and Bruell (1992) reported that metal electrodes provided a higher electrical flow rate and power generation than the carbon-based graphite. The copper, (Cu), aluminum, (Al), and stainless steel are cheap, available, easy to fabricate, and a good conductor of electricity. Jayasekera and Hall (2007) stated that Cu has the ability for oxygen consumption around electrodes, and its conductive oxide reduced the voltage loss at the anode. In contrast, the copper metal often caused the loss of voltage near the cathode and reduced the overall efficiency of the EK treatment of soils.

Stainless steel is a better alternative due to its high resistance to heat generation and corrosion and thus allows soil hardening (Liaki *et al*., 2010). However, Lefebvre and Burnotte (2002) and Jayasekera and Hall (2007) indicated that stainless steel corrosion

released iron ions precipitate, caused the loss of soil-electrode contact, and caused the power loss at electrodes and reduced the efficiency of the method. Also, the aluminum electrode reacts with H^+ to form $Al(OH)_3$ and could contaminate the EK treated soils.

2.6.2 Effect of ionic solutions on EK treatment of soils

In the literature, several commonly used combinations of ionic solutions for EK soil treatment are $CaCl_2$ and NaCl (Chien *et al*., 2009), $CaCl_2$, $AlCl_3$, and H_3PO_4 (Ahmad *et al*., 2011), $CaCl_2$ and $NaSiO_3$ (Nordin *et al*., 2013), saturated hydrated lime or saline solutions (Mosavat *et al*., 2013) and acidic solutions (Ozkan *et al*., 1999; Rozas and Castellote, 2012). Rogers *et al*. (2002) reported the criteria for the selection of ionic solutions for EK soil treatment to be highly soluble in solution and electron-transport ability, low-cost, non-toxic, non-corrosive, environmentally safe, readily available.

Jensen (2003) stated that the anolyte solutions of high solubility tend to replace Na^+ ions within the DDL of clay platelets with its charged cations, and cause a reduction in the size of DDL, reducing the plasticity and increasing the strength of treated soils. Barker *et al*. (2004) stated that the dissolution of the alumina, Al_2O_3, and silica, SiO_2 clay minerals is caused by an alkaline font formed at the cathode and reacted with cations such as Ca^{2+}, Al^{3+}, or Fe^{2+} ions, and precipitated to form silicate or aluminate gels. These cementitious agents caused an increase in the soil shear strength (Moayedi *et al*., 2013). Also, using the lime enhanced solution in EK soil treatment can dissolve the SiO_2 and Al_2O_3 in the clay minerals to form calcium aluminum hydrate (CAH) and calcium silicate hydrate (CSH) gels (Zhang *et al*., 2014; Askin and Turer, 2016).

2.7 Proposed test setup models for the EK treatment

The EK treatment setup model for a specific soil depends on the properties of the soil, soil preparation methods, EK materials, and the desired results (James *et al*., 2019).

Rittirong *et al*. (2008) adopted a complex EK test setup to aid a surface charge loading to achieve an initial consolidation of soft soil during the EK treatment of soil for the electroosmotic dewatering and therefore to increase in the shear strength of the soil. Nordin *et al*. (2015) reported a complete EK treatment test setup for the stabilization of soft soils, which comprises the test tank, soil chamber, electrode cells, ionic solution reservoirs, electric wire connectors, power supply device, and measuring cylinders.

Whereas, Liaki *et al*. (2010) adopted a simple EK test setup to study the physicochemical changes in a pure kaolinite sample using stainless steel electrodes and deionized water, to replicate electrokinetic treatment with no electrolytes added. Mosavat *et al*. (2013) applied the EK treatment on kaolinite and bentonite clay soils.

Badv and Mohammadzadeh (2015) used the setup given in Figure 2.19 to study the laboratory assessment of the electroosmotic consolidation technique for sediments.

2.8 Previous laboratories studies on EK treatment

In the early 1900s, the EK treatment technique applies for electroosmotic consolidation, stabilizing, dewatering, and improvement of the engineering properties of soils (Yeung, 2011; Samidurai *et al*., 2017; Wahab *et al*., 2018; James *et al*., 2019). Casagrande (1952) reported that electroosmosis could drive fine-grained soil pore fluid much efficiently than gravity as a result of which compressible soils can be consolidated, and aided the EK technique for many geotechnical in situ applications.

The use of EK treatment of soils by many geotechnical researchers was to mitigate the physical properties of soils of low hydraulic conductivity (Tajudin *et al*., 2015; Azhar *et al*., 2017), slope stabilization or strengthening of backfilling (Jones *et al*., 2011; Lamont-Black *et al*., 2013; Wahab *et al*., 2018), stabilization of embankments and excavations (Lamont-Black *et al*., 2012; Azhar *et al*., 2017), ground water lowering and soil drainage (Wang *et al*., 2011; Badv and Mohamedelhassan, 2011), stabilization of soils by consolidation (Kaniraj *et al*., 2011; Kaniraj and Yee, 2011), detoxification, decontamination and desalination of soils (Yeung, 2011; Paz-Garcia *et al*., 2012; Zhang *et al*., 2013), dewatering of tailings and sludge (Reddy *et al*., 2006; Glendinning *et al*., 2007; Jones *et al*., 2011), pile driving (Milligan 1994; Kaniraj *et al*., 2011; Yuan and Hicks, 2016), soil stabilization of a wide range of deficient or problematic soils: liquefied, dispersive, compressible, expansive and collapsible soils (Jayasekera *et al*., 2004; Abdullah and Al-Abadi, 2010; Megur and Rakaraddi, 2014; James *et al*., 2019).

As a result, the EK soil treatment has attracted much interest as an innovative and alternative ground improvement technique, primarily for dewatering, consolidation, strengthening, and stabilization of fine-grained soils. Several laboratory scale model experiments and insitu pilot studies have shown that the EK soil treatment applies to a broad range of geotechnical applications for remediation of many deficient soils.

In geotechnical applications, the EK treatment methods have been reported by several researchers, with particular attention to the selection of materials, importantly, using laboratory scale-model of complex setup systems and different combinations of EK materials, especially the electrodes and the ionic solutions to achieve a significant increase in the engineering properties of deficient soils. However, this study intends to

introduce the rare combinations of two different kinds of ionic solutions for strengthening soft soils to achieve satisfactory results using a laboratory scale-model.

2.9 Controlling factors affecting EK treatment and applications

The efficacy of the EK soil treatment depends on its controlling factors such as the pH, ions concentration, salinity, total dissolved solids, electrical conductivity, and resistivity, water content, zeta potential, soil index and EK material properties, and environmental conditions as well (Mohamedelhassan, 2011; Malekzadeh *et al*., 2016).

2.9.1 Soil type

Nordin *et al*. (2015) reported that the use of EK treatment techniques gave satisfactory results in different soils due to their properties and preparation. Therefore, soil types and properties, and methods of soil preparation can be determinant factors for the selection of materials, design, and set up for the specific EK soil treatment (Azhar *et al*., 2017; da Silva *et al*., 2017). EK soil treatment is effective on clay soils with particle size less than 2 μm or silty clays with moderate plasticity due to kaolinite rather than illite and montmorillonite (Jayasekera, 2004; Mosavat *et al*., 2013; Yan *et al*., 2015).

The EK technique is not effective in soils (in bentonite and illite) with high cation exchange capacity, and buffering capacity (Sumbarda-Ramos, 2010). It is effective in remolded soil slurry samples, whereas it is less effective in compacted or densified soil samples due to low soil porosity (Micic *et al*., 2001; Nordin 2013; Zhang *et al*., 2017).

2.9.2 pH

Li *et al*. (2012) and Cameselle *et al*. (2013) reported that the EK processes depend on the pH variations resulting from the interactions of soil-ionic solutions during the EK soil treatment. Therefore, to maximize the efficacy of the technique, it is required to adjust to the suitable pH level in the soil, often less than 7. A more basic environment

is preferred over an acidic type in the soil, to increase the ion precipitation, electrical conductivity, and soil strength, to reduce soil buffering capacity, and plasticity (Airoldi *et al*., 2009; Liaki *et al*., 2010; Askin and Turer, 2016; Malekzadeh *et al*., 2016).

Since a low pH value (< 7) favors an increase in the corrosion rate of an anode, it is desirable to have a high pH value (> 7) in order to reduce this effect. To attain a suitable pH value (range of 8 to 12), the water electrolysis must form acidic and alkaline fonts to ease mass transport phenomena via the porous soil media (da Silva *et al*., 2017).

2.9.3 Salinity and total dissolved solids, T_{ds}

The amount of salt content in the soil affects its pH and electroosmotic flow (Mitchell and Soga 2005). When the soil salinity and total dissolved solids, T_{ds} increased, this can reduce the electroosmotic flow, and therefore, EK consolidation is unlikely to be successful in highly saline soils (Malekzadeh *et al*., 2016). Jayasekera and Hall (2007) classified certain soils with a salinity value of ≥ 9.521 ppt (9.5 g/L) as extremely saline.

Bergado *et al*. (2003) defined the T_{ds} limit to be 6.0 ppt, and Mitchell (1991) stated that soil with salinity above 1.264 ppt (1.264 g/L) might not give a good response or effective performance for the electrokinetic, EK soil stabilization or soil remediation.

Mohamedelhassan and Shang (2002) reported that K_{eo} is mainly controlled by porosity when the pore fluid salinities are smaller than a particular value (8 g NaCl/L or 8.0 ppt) in their paper, and increases in magnitude with an increase in the soil porosity. Micic *et al*. (2001) stated that all of the successful applications of electrokinetic treatment reported in the literature involved soils of low salinity, that is, the salt content in the pore water of the soil media is less than < 2.0 g NaCl/liter or the equivalent, 2.0 ppt.

2.9.4 Electrical conductivity, σ

Yan *et al*. (2012) stated that electrical conductivity, σ depends on temperature, water content, porosity, resistivity, composition, salinity, fabric, and the structure of the soil. According to Malekzadeh *et al*. (2016), the threshold range of σ values between 0.005 to 0.5 S/m is suitable to attain cost-effective results in electrokinetic, EK soil treatment.

Loch *et al*. (2010) reported the σ of fine grained soils with a minimum value of 0.01 S/m for EK soil treatment to be effective. Mitchell (1991) stated that soil with σ above 2.5 mS/cm might not give a good performance for EK treatment for soil stabilization.

2.9.5 Moisture content, *w*

Mosavat *et al*. (2013) suggested that for effective EK technique, soil moisture should be conductive enough with a moderate soil hydraulic conductivity to permit fluid flow, but the soil pores should not be fully saturated to avoid the side effects of tortuosity.

2.9.6 Voltage and current

The electrical gradient variation depends on the soil electrochemical properties, such as electrical conductivity, σ. Higher σ soils require more charged ions and higher currents than lower electrical σ soils. However, different researchers have reported suitable energy consumption to be 0.07-0.9 kWh/m^3 (Karunaratne *et al*., 2004; Fourie *et al*., 2007), and as 3.43 to 26.54 kWh/m^3 (Kalumba *et al*., 2009; Jones *et al*., 2011).

2.9.7 Cost and time

The processing duration of EK soil treatment is a function of the current and voltage levels, rate of transport, electrode configuration, and spacing (Gingine *et al*., 2013). The cost depends on the type and depth of the ionic solution, the σ of the soil and pore water, spacing of electrodes, type and process designed employed, site preparation requirements, electricity, and labor costs (Pérez *et al*., 2013; Moayedi *et al*., 2014b).

2.10 Geotechnical properties of EK treated soils

This section provides a concise detailed overview of the physical, engineering, microscopy, and thermal properties of the EK treated soils in the previous studies.

2.10.1 Index and Atterberg limits properties of EK treated soils

EK effect can modify the chemistry of the porous media and thus influences various index properties of the soils (Jayasekera, 2015). EK soil treatment after 15 days, Mosavat *et al*. (2013) reported that there was a remarkable reduction in Atterberg limits of treated soils using an electrokinetic treatment. As such, Atterberg limit measurements appeared to be suitable, sensitive parameters to examine electrochemical and physicochemical changes of EK treated soils. It is a good indicator that pozzolanic reactions have taken place in the EK treated soils (Asavadorndeja and Glawe, 2005). In the EK assessment of phosphoric acid injection into the soil, Ozkan *et al*. (1999) stated that the changes in the Atterberg limit of the treated soils are related to the changes caused by EK processing, and are also a reflection of the changes in shear strength of the treated soils (Abdullah and Al-Abadi, 2010; James *et al*., 2019).

Gingine *et al*. (2013) reported that K^+ caused a substantial reduction in the values of the plasticity index, PI, and percent free swell of EK treated soils. Liaki *et al*. (2010) presented the results of the alteration in index properties as a function of varying pH during the EK process. James *et al*. (2019) reported PI reduction from the initial value of 39.9% to 32.2% and 15.1% due to a decrease in the liquid limit of EK treated soils.

Abdullah and Al-Abadi (2010) reported that Ca^{2+} and K^+ ions from ionic solutions decreased the PI values of the EK treated soils. James *et al*. (2019) reported 6% and 20% reduction of liquid limit in EK treated soils using calcium hydroxide and calcium

chloride ionic solutions, and various researchers reported some increment in the liquid limit, LL and plastic limit, PL of the EK treated soils using different ionic solutions (Liaki *et al*., 2010; Kaniraj and Yee, 2011; Thuy *et al*., 2013; Wahab *et al*., 2018).

2.10.2 Shear strength of EK treated soils

Several geotechnical researchers have reported a drastic increase in the compressive strength in the EK treated soils within anode to cathode distances of the EK test setup (Ozkan *et al*., 1999; Chien *et al*., 2010; Gingine *et al*., 2013; Zhang *et al*., 2017). Wang *et al*. (2011) reported that the mean tensile strength of treated soils increased by 17% to 116% after the EK treatment of the soils. In most EK treatment, the soil strength increased near to the electrode regions more than the middle section of the test setup.

Asavadorndeja and Glawe (2005) reported that it is precipitation, which provides the most significant contribution to the increase in soil strength. They also added that the decrease in water content during EK soil treatment could provide some contribution to the increase in soil strength. Glendinning *et al*. (2005) indicated that soil-ionic solutions reaction and EK processing duration played vital roles in the improvement in shear strength of EK treated soils. Jayasekera (2015) and Jones *et al*. (2011) reported that the EK processing under a voltage gradient of 2 V/cm, increased the shear strength of the EK treated soils by 65.8% and 263%, respectively. Also, Micic *et al*. (2000) reported a fourfold increase in the average undrained shear strength of EK treated soils.

The increase in the unconfined compressive strength of the treated soils was as a result of electroosmotic cementation of their soil particles due to the intense precipitation of binding agents. The ion exchange and reduction in soil plasticity aided the strength gain of the treated soil (Hamir *et al*., 2001; Micic *et al*., 2001; Zhang *et al*., 2017).

2.10.3 Morphology of EK treated soils

The mineralogical properties of the active clay minerals in the soil can be altered during EK treatment due to soil-ionic solution reactions. The alteration of the mineralogical properties of soils invariably alters its index and engineering behaviors. Asavadorndeja and Glawe (2005) used X-ray diffraction (XRD) analysis to compare the mineralogical compositions of the untreated soils, and EK treated soils.

Yuan and Hicks (2016) stated that electrical conductivity is a function of the soil mineralogy and pore fluid contents of EK treated soils. Wang *et al*. (2011) reported the mineralogical composition of the EK treated soils at the anode and cathode regions, in the electrochemical modification of tensile strength and pore structure in mudstone.

As reported in the literature (Lav and Lav, 2000; Cristelo *et al*., 2012), the presence of charged cations from ionic solutions reacted with silicate, and aluminate clay minerals caused cementation and bonding of the soil fines, resulted in a more flocculated and aggregated structure and caused a reduction in the plasticity and an increase in strength of the EK treated soils (Jeyakanthan and Gnanendran, 2011; Malekzadeh *et al*., 2016).

2.10.4 Electroosmotic flow of EK treated soils

Several complex electrochemical processes initiate electroosmotic flow, q_{eo} during the EK soil treatment (Gingine *et al*., 2013; Mosavat *et al*., 2013; Jayasekera, 2015). The coupling chemical, electrical, hydraulic, and thermal gradient caused the fluid flow within the soil, which invariably affects the hydraulic conductivity and the volume change behavior of the EK treated soils (Yeung, 2011; Malekzadeh *et al*., 2016).

The EK technique uses ionic solutions and conductive electrodes to promote q_{eo} in the EK treated soils (Schmidt *et al*., 2007). Shang *et al*. (2004) noted that a 15% $CaCl_2$ solution enhanced the q_{eo} in the calcareous soil. Keykha *et al*. (2014) reported that soil fluid flow increased from the anode to the cathode by the q_{eo} from 73% to 77%. Virkutyte *et al*. (2002) observed in their study that flow rate, q_{eo}, from the anode to the cathode could cause the formation of a low-pH environment in the EK treated soils.

2.11 Gaps in the literature and recommendations

The overview of the previous studies on the EK soil treatment of laboratory model and insitu pilot tests have proven their efficacy in geotechnical applications. However, there are still lots of gaps to be covered in the EK treatment techniques, such as the:

- Most previous studies did not focus on the leaching effects in the EK treated soils.
- There is a seldom evaluation of the spatial and depth effects of EK soil treatment.
- Most previous studies did not use non-toxic liquid wastes in EK soil treatment.
- Most previous studies did not study anti-corrosion techniques for EK electrodes.
- There is still a gap in the standardization of the EK materials, methods, and setups.
- There are a few statistical or numerical model contributions for EK soil treatment.

Based on the overview of the EK soil treatment, this study discussed the use of rare combinations of the calcium chloride, $CaCl_2$ and sodium carbonate, Na_2CO_3 ionic solutions for soft soil stabilization. The study also discussed the wet-dry cycle of the EK treated soil, the effect of electrode length, thermal differential analyses, and the effect of EK treatment of soil on the morphological changes of the treated soils. Also, numerical modeling has been applied to the experimental data using advanced statistical design and analysis of experiments to analyze and interpret the test results.

Chapter 3

MATERIALS AND METHODS

3.1 Introduction

This chapter presents the research materials and methods used in the investigation of the electrokinetic, EK treatment of soft soil using different combinations of ionic solutions. The laboratory tests such as the index and engineering properties determined by the American Standard of Testing Materials, electrochemical, microscopic, and thermal analyses were performed in terms of EK treatment duration of 28 days, anode to cathode distances and at different electrode lengths, l_e to soil depths, d_s ratios.

3.2 Research materials

The materials used in this study were soil blocks, conductive electrodes, electric wires, power devices, test tanks, ionic solutions, measuring devices, and dial gauges.

3.2.1 Soil

The soft soil used in this study was taken from the Tuzla region on the coastline of the Mediterranean Sea, Famagusta North Cyprus at latitude 35.1614° N and longitude 33.8802° E, given in Figure 1. According to the Unified Soil Classification System, the soil was highly plastic inorganic clay, CH with a plastic limit, PL of 33%, liquid limit, LL of 60%, and the plasticity index, PI of 27%. Table 3.1 gives the index and the physical properties, and Table 3.2 presents the chemical composition of the soil.

Figure 3.1: Geographical site of soft soil (Google maps, 2020).

Table 3.1: Physical and index properties of the Tuzla soft clay soil.

Soil properties	Quantities
In situ dry density, ρ_d (g/cm^3)	1.31
In situ water content, w (%)[a]	48
Clay size fraction, < 2 μm (%)[b]	61
Silt size fraction, 2–74 μm (%)[b]	36
Sand size fraction, > 74 μm (%)[b]	3
Specific gravity, Gs[c]	2.75
Maximum dry density, $\rho_{d(max)}$ (g/cm^3)[d]	1.61
Optimum moisture content, w_{opt} (%)[d]	20
Liquid limit, LL (%)[e]	60
Plastic limit, PL (%)[e]	33
Plasticity Index, PI (%)[e]	27
Liquidity index, LI[e]	0.88
Activity[e]	0.51
USCS Classification[f]	CH

[a]According to ASTM (2005) D2216.
[b]According to ASTM (2007) D422.
[c]According to ASTM (2006) D854.
[d]According to ASTM (2007) D698.
[e]According to ASTM (2000a) D4318.
[f]According to ASTM (2000b) D2487-00 Unified Soil Classification System.

The chemical composition of the soil was determined using a sequential wavelength dispersive X-Ray fluorescence spectrometer (Rigaku instrument: ZSX Primus model).

Table 3.2: Chemical composition of the natural soft soil.

Oxides	SiO_2	CaO	Na_2O	Cl	Fe_2O_3	Al_2O_3	MgO	K_2O	others
Mass, %	28.85	20.60	12.70	11.98	9.78	9.06	3.26	2.18	1.59

3.2.2 Ionic solutions

The selection of the ionic solutions was dependent on specific criteria such as: highly soluble in water, inexpensive, readily available, non-toxic, non-corrosive, and environmentally safe. Besides satisfying the requirements mentioned above, the ionic solutions selected for this study were a rare combination of calcium chloride ($CaCl_2$) (anolyte solution) and sodium carbonate (Na_2CO_3) (catholyte solution) due to their high calcium (Ca^{2+}) and carbonate (CO_3^{2-}) ions content, respectively. This research study focuses on the use of sodium carbonate ionic solution as a substitute for sodium silicate, Na_2SiO_3, which is one of the most often used ionic solutions in the previous studies (Chien *et al*., 2010; Ou *et al*., 2013; Arutselvam, 2014; Azhar *et al*., 2018).

Also, distilled water, DW, was used to provide different combinations of unpaired ionic solutions such as calcium chloride-distilled water, $CaCl_2$-DW, and sodium carbonate-distilled water, Na_2CO_3-DW in order to study the effects of individual ionic solution on the EK treated soils. Also, the paired calcium chloride and sodium carbonate, $CaCl_2$-Na_2CO_3 ionic solutions were used in this study to evaluate the benefits of combining calcium cations, Ca^{2+}, and carbonate anions, CO_3^{2-} in improving the electrochemical, index, and engineering properties of the EK treated soils. Table 3.3 shows the chemical and physical properties of the ionic solutions used in this study.

Table 3.3: Chemical and physical properties of the ionic solutions.

Properties	$CaCl_2$ 1.0M	Na_2CO_3 1.0M	Distilled Water
Molecular formula	$CaCl_2.2H_2O$	Na_2CO_3	H_2O
Molecular weight, M (g/mol)	110.98	105.99	18.02
Specific gravity, G_s at 20°C	1.85	2.15	1.00
Appearance	White pellets	White powder	Pure
Electrical conductivity, σ (mS/cm)	10.87	18.58	0.055
Ionic strength, I_s (mol/mL)	1.37	2.33	---
pH	8.65	11.75	7.00
Solubility in water, s (g/L) at 20°C	147.10	105.99	---
Total dissolved solids, T_{ds} (g/L)	5.46	9.33	---
Salinity (ppt)	5.46	9.33	---
Toxicity	Non	Non	Non

3.2.3 Electrodes

In this study, aluminum and stainless-steel metallic plates were used as the anode and cathode, respectively. The selection of these metal electrodes was because they were easy to fabricate, good electrical conductivity, electrical flow rate, less susceptibility to corrosion effect, and can be sourced at low cost. The electrode plates used in this study were perforated with holes, each having a diameter of 0.2 cm and a spacing of 1.5 cm center to center. Figure 3.2 shows the perforated anode and cathode electrodes.

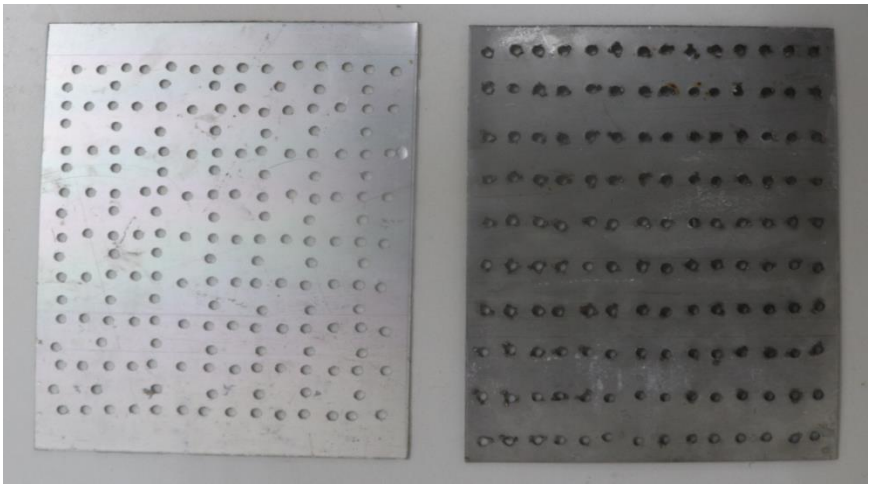

(a) (b)

Figure 3.2: Perforated (a) aluminum plate and (b) stainless steel plate electrodes.

3.2.4 Power supply device

The Thurlby Thandar Instruments (model TS3022S) supplied adjustable DC with a peak capacity of 100 V and 2 A was used to provide adequate power to the electrodes.

3.2.5 Test tanks

In this study, the laboratory EK soil treatment was conducted in a transparent glass test tank. Two different test tanks having different dimensions were used to study the performance of the combinations of ionic solutions in terms of the anode to cathode distances and electrode length to soil depth. Figure 3.3 shows the test tank setup for EK treatment. More information about the test tank setup will be given in Section 3.4.

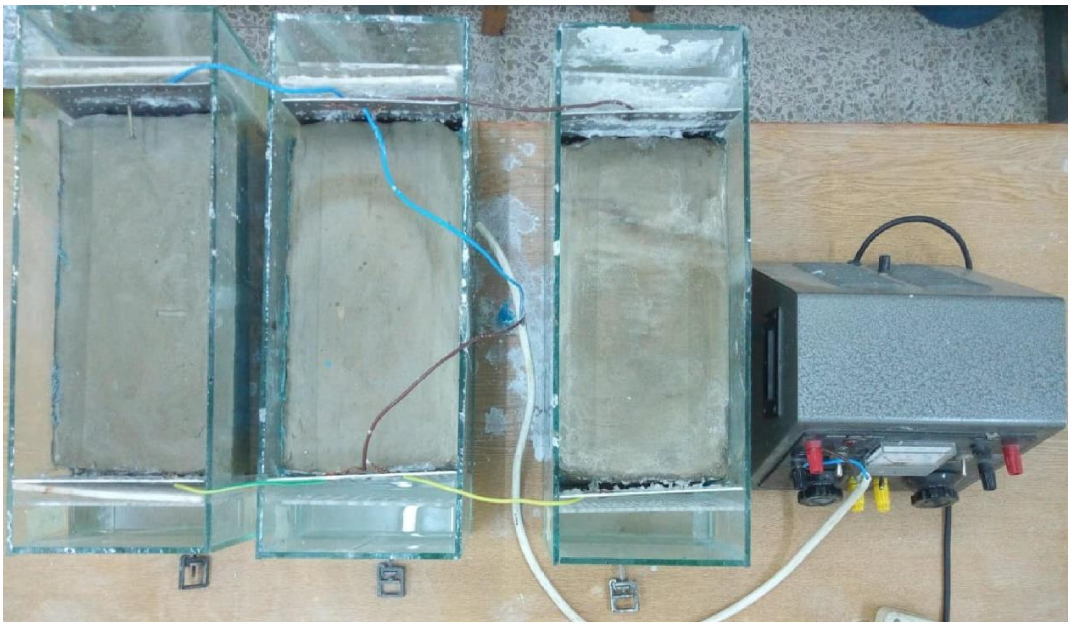

Figure 3.3: Glass rectangular test tank test setup.

3.3 Electrochemical technique procedures

3.3.1 Preparation of soil blocks

In the present study, to retain the insitu soil conditions, soil blocks were extracted from the in situ soft soil deposit existing at a depth of about 4 m. An excavator was used to facilitate the opening of a large soil pit to work comfortably and obtain the soil blocks without difficulty. The insitu moisture content, *w* of the soft soil, was around 48%, which facilitated the ease for the extraction of the soil block samples from the excavated pit and prevented the soil from collapsing during the pit excavation process.

Two types of hollow rectangular stainless-steel boxes with sharp ends, with the first sets having dimensions of 30 cm x 15 cm x 20 cm, and the second sets having dimensions of 30 cm x 15 cm x 30 cm, and both sets with a thickness of 0.05 cm were used for the extraction of the soil blocks. Before the extraction of insitu soil, the inner and outer parts of the steel boxes were lubricated with nonreactive and nonflammable oil.

The idea was to prevent the friction and the disturbance of the soil blocks inside the boxes. The boxes were gently pushed into the excavated soil pit, and then a sharp steel plate was introduced into the lower base of the boxes to separate the soil blocks formed inside the boxes from the ground repeatedly. The excess soil in the boxes was trimmed so that the soil block samples in the boxes were maintained at equal dimensions with the internal dimensions of the hollow steel boxes, as given in Table 3.4 and Table 3.5.

The soil blocks having different dimensions presented in Table 3.4 and Table 3.5 were used for the first batch testing setups and the second batch testing setups, respectively.

Table 3.4: Physical properties of the soil blocks for the first batch testing setups.

Properties	Values
Initial water content, *w* (%)	48
Dimension of the soil blocks in the test tanks (cm)	L = 30, B = 15, H = 20
Volume of the soil blocks in the test tanks (cm^3)	9000.00±0.05
Mass of soil blocks in the test tanks, *m* (g)	17474.50±0.05
Bulk density achieved, ρ_b (g/cm^3)	1.94±0.01
Dry density achieved, ρ_d (g/cm^3)	1.31±0.01
Mass of dry soil, m_{ds} (g)	11807.10
Mass of water, m_w (g)	5667.41
Volume of dry solid, V_{ds} (cm^3)	4293.49
Volume of voids, V_v (cm^3)	4706.51
Volume of water, V_w (cm^3)	5667.41

Note: L, length; H, height; D, diameter

Table 3.5: Physical properties of the soil blocks for the second batch testing setups.

Properties	Values
Initial water content, *w* (%)	48
Dimension of the soil blocks in the test tanks (cm)	L = 30, B = 15, H = 30
Volume of the soil blocks in the test tanks (cm^3)	13500.00±0.05
Mass of soil blocks in the test tanks, *m* (g)	26211.75±0.05
Bulk density achieved, ρ_b (g/cm^3)	1.94±0.01
Dry density achieved, ρ_d (g/cm^3)	1.31±0.01
Mass of dry soil, m_{ds} (g)	17710.64
Mass of water, m_w (g)	8501.11
Volume of dry solid, V_{ds} (cm^3)	6440.23
Volume of voids, V_v (cm^3)	7059.77
Volume of water, V_w (cm^3)	8501.11

Note: L, length; H, height; D, diameter

Then the soil blocks were carefully extruded from the steel boxes, kept in airtight polythene bags to prevent their moisture loss. The same process was repeated for all soil blocks needed for the laboratory EK treatment studies. The saturation of the soil blocks was conducted in the test tanks for three days to allow the soil blocks to attain their initial insitu water content before the EK treatment. Tables 3.4 and 3.5 show the water content and void ratio values obtained for the soft clay soil after their saturation.

3.3.2 Procedures for preparation of ionic solutions

Since the concentration of the ionic solutions range commonly used in the previous studies (Baker *et al*., 2004; Malekzadeh *et al*., 2016), was between 0.5 M to 1.5 M, in the present study, the concentration of 1.0 M for the ionic solutions have been selected for the EK treatment. The ionic solutions were prepared by dissolving known molar mass of solute salt of $CaCl_2$ and Na_2CO_3 in one liter of distilled water inside a volumetric flask. The ionic solution admixtures were carefully mixed using a portable electric stirrer device to attain a uniform solution. The ionic solutions were calibrated for their electrochemical properties using a Multiparameter (Bante 900 model) device.

Figure 3.4 presents the measured and calibrated linear curves for the pH, total dissolved solids, T_{ds}, electrical conductivity, σ, salinity, and ionic strength, I_s properties of the $CaCl_2$ and Na_2CO_3 ionic solutions using different molar concentrations of the ionic solutions. The R^2 values and curve equations of the parameters were provided to examine the consistency and validity of the data taken during the EK treatment of the soft soils. In ionic chemical selection, the primary precaution was to select suitable chemical stabilizers that pose no detrimental health and safety hazards. Also, heat build-up was avoided during the preparation of ionic solutions under controlled room temperature. The ionic solutions were prepared and stored carefully in tightly covered, non-reactive glass bottles to prevent contamination.

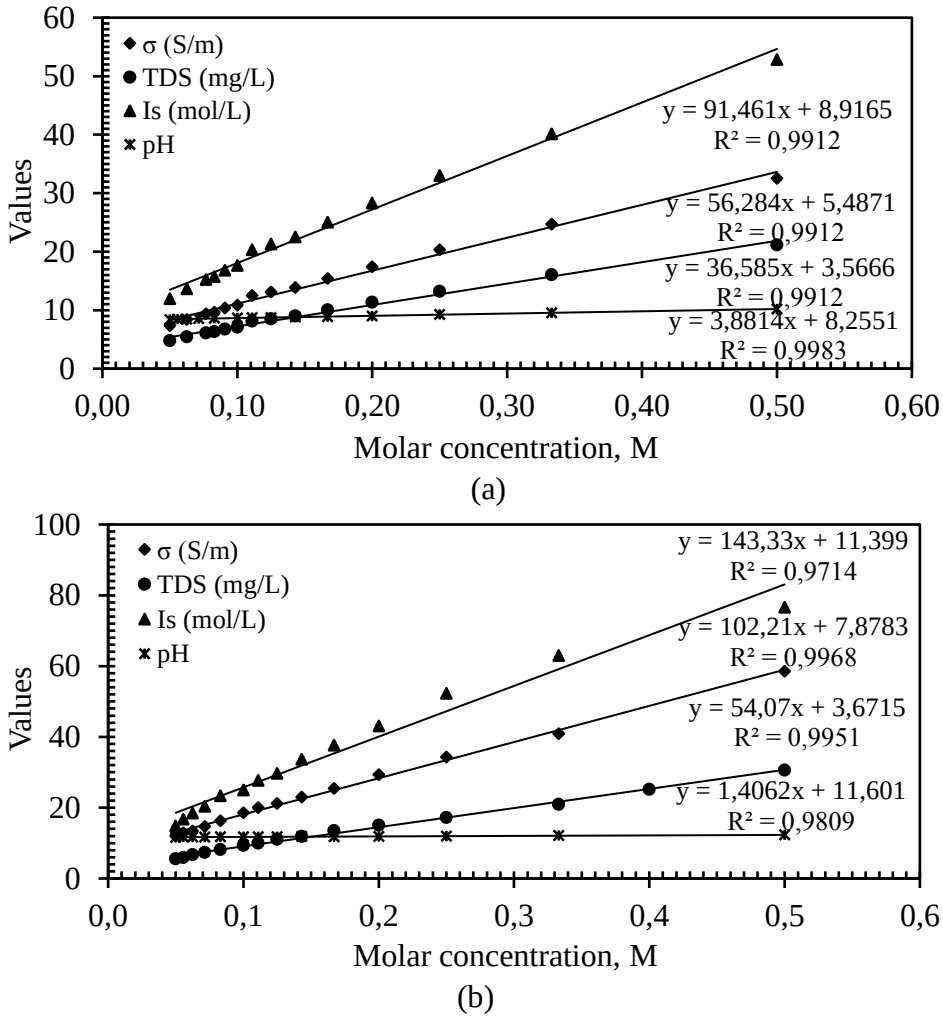

Figure 3.4: The electrical conductivity (σ), total dissolved solids (T_{ds}), ionic strength (I_s*10^{-5}), and pH calibration curves at different molar concentrations for (a) $CaCl_2$ and (b) Na_2CO_3 ionic solutions.

3.4 Experimental setup

In this study, identical soil block samples were used to replicate the in situ soft soil conditions. Figure 3.5 presents the schematic diagrams and dimensions of the test setup of a rectangular glass tank consisting of a soil block chamber, anolyte, and catholyte chambers. The glass test tank is a non-conductor of heat and electricity, non-chemical reactive, and transparent material. Its non-conductive property prevents electrocution and unwanted heat, and its transparency provides easy visual inspection of the level of water and ionic solutions in their reservoirs, to monitor fluid leakage, electroosmotic flow, and alterations in the physicochemical behavior of the EK treated soft soils.

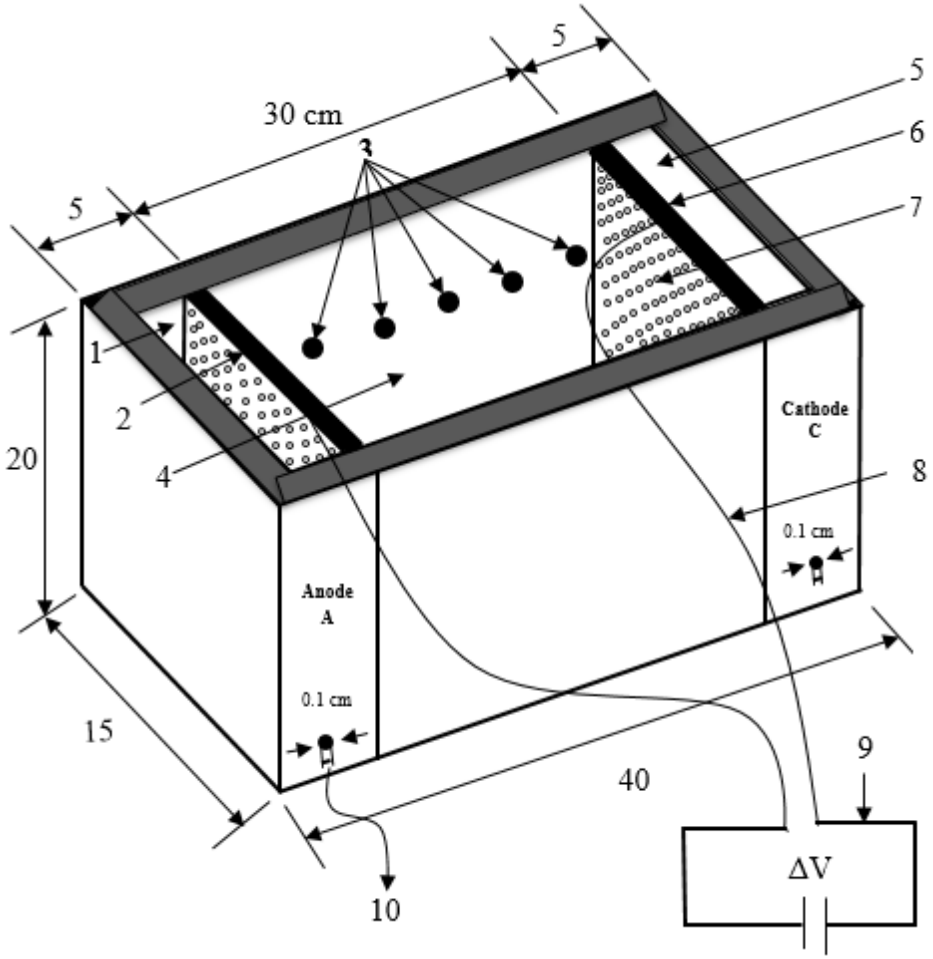

Legends: 1. Anolyte chamber; 2. Anode, A; 3. Soil extraction; 4. Soil chamber; 5. Catholyte chamber; 6. Cathode, C; 7. Perforated electrode plate; 8. Electric wire; 9. Power supply device; 10. Adjustable outlet flow with a control valve. All dimensions of the test tank are in centimeters (cm)

Figure 3.5: Schematic diagram of the EK test tank setup.

The glass test tank components were fixed firmly using a silicone gel sealant at their joints and edges to prevent fluid leakage during the EK treatment of the soil blocks. Finally, a simple leak test was conducted by filling the test tanks with water to be sure that there was no trace of any fluid leakage before the beginning of EK soil treatment.

The central chamber housed the soil block with predetermined dimensions for its index and engineering properties to replicate the field conditions, while the two outside chambers housed the electrodes: anode and cathode, and the ionic solutions: anolyte

and catholyte. Different combinations of ionic solutions such as the $CaCl_2$-DW, Na_2CO_3-DW, and $CaCl_2$-Na_2CO_3 were used in this research study. The location of each ionic solution in the anolyte and catholyte chambers was shown in Table 3.6.

Table 3.6: Locations of ionic solutions in the electrode chambers of the test setups.

Test setups	Combination of ionic solutions	Anolyte solution in anode chamber	Catholyte solution in cathode chamber
1	$CaCl_2$-DW	$CaCl_2$	DW
2	Na_2CO_3-DW	DW	Na_2CO_3
3	$CaCl_2$-Na_2CO_3	$CaCl_2$	Na_2CO_3

In the $CaCl_2$-DW setup, $CaCl_2$ ionic solution and DW were placed in the anolyte and catholyte chambers, respectively. The Na_2CO_3-DW setup consisted of Na_2CO_3 ionic solution in the catholyte and DW in the anolyte chambers, whereas the $CaCl_2$-Na_2CO_3 setup comprised $CaCl_2$ and Na_2CO_3 ionic solutions in the anolyte and catholyte chambers, respectively. A non-reactive strip tape, a hydraulically leak-proof material, was used to hold the contacts tightly between the soil block fitted into the test tank with no sidewall or bottom leakages. The intention was to eliminate the gap between the soil block and test tank and make the ionic solutions to flow only through the soil block placed inside the main chamber of the test tank. The two partitioned walls on both sides of the soil chamber and the cathode and anode plates were perforated with holes, each having a diameter of 0.2 cm and a spacing of 1.5 cm center to center points.

These perforated walls and the perforated electrode plates allowed the free flow of ionic solutions into the soil block. The placing of the filter paper system between the perforated plates and walls and the soil block protected the blocking of the perforated holes with fine soil particles. Also, it prevented the movement of the soil particles from the soil block to contaminate the ionic solution reservoirs. The filter paper served as a

medium to transport the ionic solutions from their reservoirs into the soil blocks in the main compartment. The ionic solutions were supplied continuously into their specific chambers, and the electrodes were connected to an adjustable DC power supply device.

In this study, the EK treatment was conducted on soft soils by using direct current, DC. A DC has been proven to be cost-effective, electrically safe, and efficient for EK treatment of soils (Jayasekera and Hall, 2007; Chien *et al*., 2009). In this study, a constant voltage gradient of 30 $\mathrm{V/m}$ was supplied by the power device at DC of 2 A, and an average power supply of 6.9 $\mathrm{kWh/m^3}$ were applied in the treated soils. The selection of the power supply value was to minimize energy consumption and save cost. The current flow was examined using a digital multimeter device to observe the changes in the electrical energy flow of the treated soils at different time intervals. To initiate the EK process, the soil blocks were subjected to a slow continuous flow of $CaCl_2$ and Na_2CO_3 ionic solutions from anolyte and catholyte reservoirs, respectively.

The electroosmotic flow of the ionic solutions through the soil block was collected via the outlet flow into a gradation tube, and their volumes were measured at different time intervals. Under a constant fluid supply, the experimental setups were under controlled room temperature to prevent moisture loss and superficial cracking of the soil blocks. The exposed electric wires at the fixed contact location with the metallic electrode plates were correctly covered with a sealant of epoxy resin to avoid the corrosion of the electrodes and the electrical wire, which may affect the energy efficiency of the test setups. The test was performed by supplying the constant voltage gradient across the soil blocks for 28 days for the test setups. The electrical energy initiated the EK processes when the power supply device was switched on. The EK processes caused

the flow of different combinations of ionic solutions into the soil block from the anode to the cathode and from the cathode to the anode directions for different EK test setups.

3.4.1 Experimental setup dimensions

In this study, the test setups were in two batches based on their dimensions to study the effect of EK soil treatment for the anode to cathode distances, $d_{A\leftrightarrow E}$ and soil depth, d_s with other testing parameters such as the EK treatment duration, and ionic solutions.

3.4.1.1 Preparation of the first batch-test setup

The first batch-test setup was conducted in a cell comprised of three compartments: soil block chamber, anode, and cathode chambers. The EK cell comprises rectangular glass sheets (0.5 cm thickness), ionic solutions, and conductive electrodes connected to the electrical current device. Table 3.4 provides the dimensions and physical properties of the soil blocks as described in Section 3.3.1, and Table 3.7 summarizes the dimensions of the test tanks, electrodes, and ionic solutions within their chambers, used in the first batch-test setup. Figure 3.6 presents the cross-sectional view of the test tanks in the first batch-test setup to be 40 cm x 15 cm x 20 cm representing the length, width, and height dimensions. The dimension of the middle chambers is 30 cm x 15 cm x 20 cm, to be occupied by soil block, and the two smaller chambers have a dimension of 5 cm x 15 cm x 20 cm, which housed the ionic solutions and electrodes.

Table 3.7: Dimensions of the first batch-test tank setup compartments.

Dimensions	Test tanks (cm)	Electrodes (cm)	Each ionic solution reservoir (cm)
Thickness, T	0.5	0.5	---
Height, H	20.0	---	20.0
Width, W	15.0	15.0	15.0
Length, L	40.0	30.0	5.0

In the first batch-test setups, the index and engineering properties such as Atterberg limits, unconfined compression, swelling, consolidation, and also electrochemical, thermal, and microscopic tests were performed in terms of EK treatment duration, anode-to-cathode distances, $d_{A\leftrightarrow E}$, and different combinations of ionic solutions. Also, the values of electrochemical properties were further analyzed by using an advanced statistical analysis for evaluating and establishing their threshold values required to achieve the better-improved engineering properties during the use of the EK treatment.

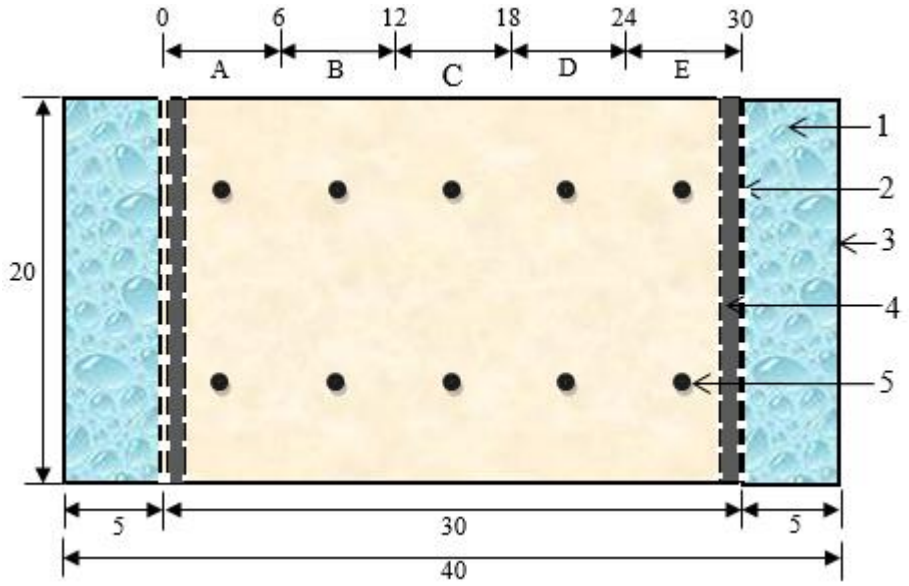

Legends: 1. Ionic solutions; 2. Perforated electrode plate;
3. Test tank; 4. Electrode; 5. Point of soil extraction.
All dimensions are in centimeters (cm).

Figure 3.6: Cross-sectional view of the test tank in the first batch setups.

3.4.1.2 Preparation of the second batch-test setup

The second batch testing was conducted using similar methods in the first batch except for the change in dimensions of the test tanks, soil blocks, electrodes, and the volume of the ionic solutions used. The test was performed in terms of the electrode length, l_e, soil depth, d_s, and the anode to cathode distances, $d_{A\leftrightarrow E}$ using different combinations of ionic solutions. Four different electrode length ratios, l_{ce} of 7.5 cm ($0.25l_{ce}$), 15.0

cm ($0.50l_{ce}$), 22.5 cm ($0.75l_{ce}$) and 30.0 cm ($1.0l_{ce}$) were used in different test tank setups. Table 3.5 summarizes the dimensions and physical properties of the soil block samples, and Table 3.8 presents the internal and external dimensions of the materials used in this test setup. The changing electrode length ratio, l_{ce}, was estimated as shortened electrode length, l_{se}, divided by full electrode length, l_{fe}, that is $l_{ce} = l_{se}/l_{fe}$.

Table 3.8: Dimensions of the second batch-test tank set up compartments.

Dimensions	Test tank (cm)	Electrode (cm)				Ionic solution reservoir (cm)
Thickness, T	0.5	0.5	0.5	0.5	0.5	---
Height, H	40	---	---	---	---	30
Width, W	15	15.0	15.0	15.0	15.0	15
Length, L	40	7.5	15.0	22.5	30.0	5
Length ratio, l_{ce}	---	0.25	0.50	0.75	1.0	---

The effects of ionic solutions on the EK treated soils under changing electrode length, l_e, soil depths, d_s, and anode to cathode distances, $d_{A\leftrightarrow E}$ were considered. Though the soil depth, d_s, and the anode to cathode distances, $d_{A\leftrightarrow E}$ were predetermined and fixed as shown in Figure 3.7, the electrode length ratio, l_{ce} was changing, and the effect of the electrode length, l_e at the predetermined points of soil depth was investigated.

The variation in the plasticity index, PI, and swelling potential, SP values of the EK treated soils were studied at the points of extraction of A, B, C, D, and E, which were at 5 cm distance apart, for determining PI, while points A and E close to the anode and cathode vicinities were considered for determining the SP for the EK treated soils.

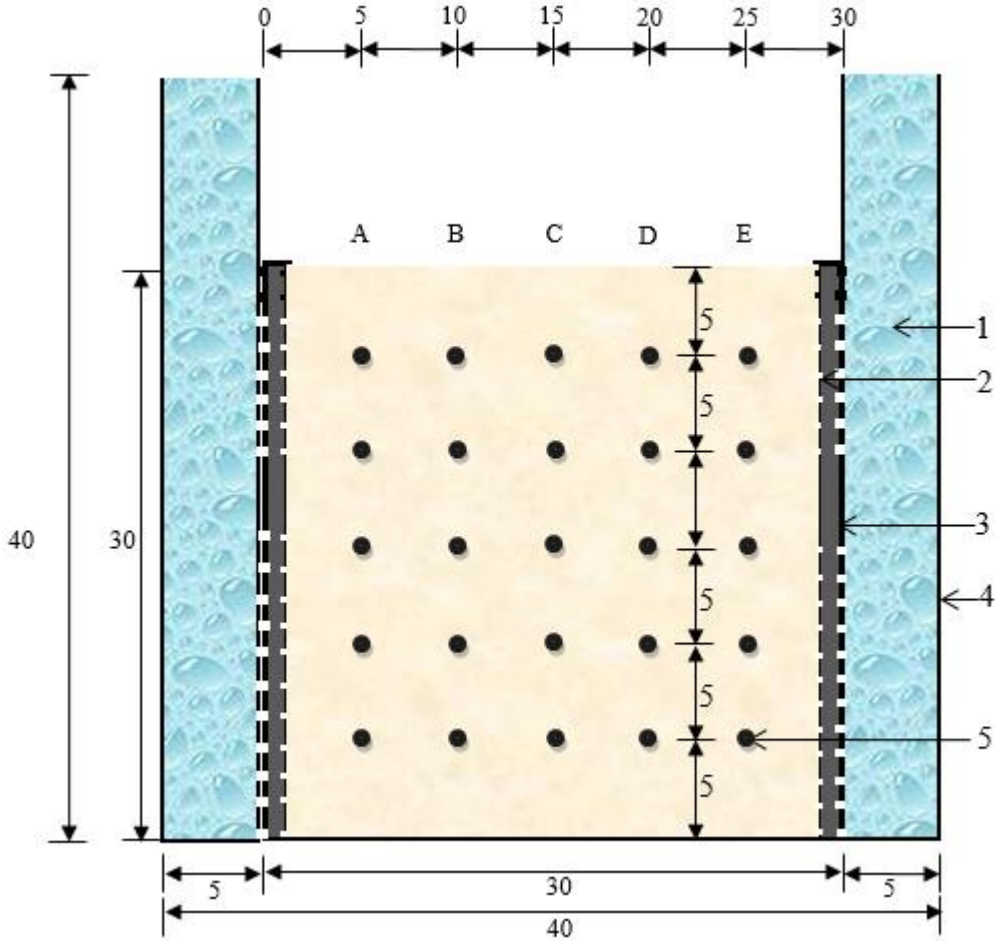

Legends: 1. Electrolyte; 2. Electrode; 3. Perforated electrode plate; 4. Test tank; 5. Point of soil extraction. All dimensions are in centimeters (cm).

Figure 3.7: Cross-sectional view of the test tank in the second batch setups.

After that, the data obtained from the PI and SP values were subjected to advanced statistical modeling for evaluating the most appropriate electrode length to soil depth ratio(s) to achieve the better effective performance for the EK treatment of the soils.

3.4.2 Samples extraction of EK treated soils

The soil samples to be tested were extracted from different locations along points A to E direction within the EK treated soil blocks, as shown in Figure 3.6 and 3.7. The soil sample extraction was conducted using suitable steel molds with internal dimensions of diameter, D of 3.8 cm, and a height H of 7.6 cm for unconfined compression test at points A to E, and diameter, D of 5.0 cm, and a height H of 2.0 cm for one-dimensional

swell and consolidation tests at points A and E. Figures 3.8 and 3.9 present the map view of points of soil extraction of EK treated soils at the edge to edge distances apart.

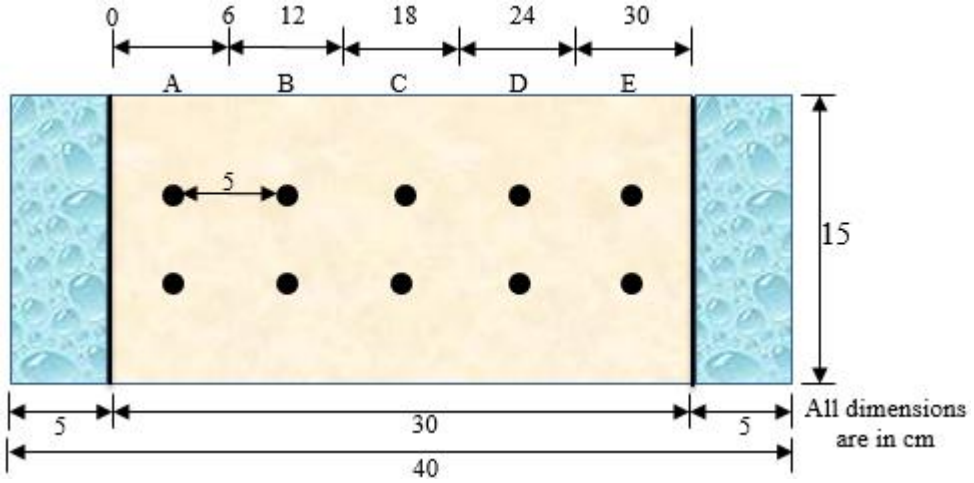

Figure 3.8: Map view of locations for extraction of soil samples from the EK treated soil blocks in the first batch setups.

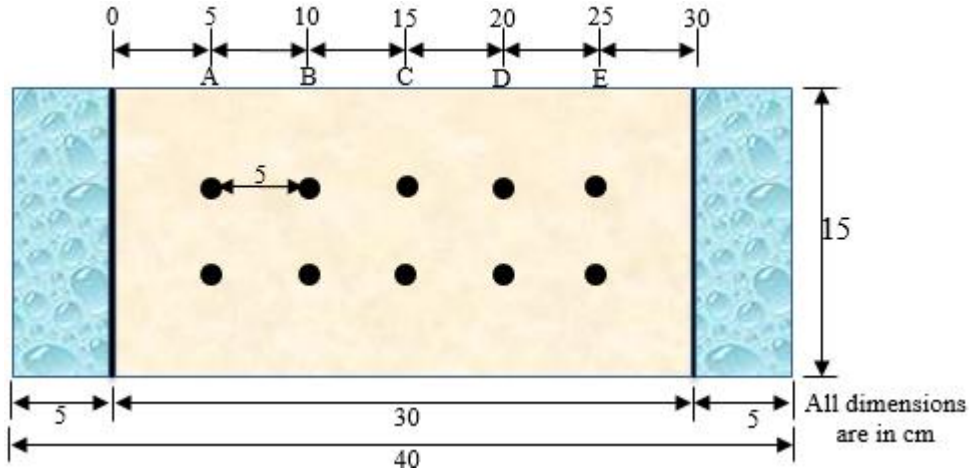

Figure 3.9: Map view of locations for extraction of soil samples from the EK treated soil blocks in the second batch setups.

At each location, two soil samples were obtained along the vertical direction to determine the average outcome of each test result. Table 3.9 presents the number of test setups and samples for the entire EK soil treatment testings for batches 1 and 2.

Table 3.9: Number of test setups and samples for EK soil treatment testing.

Testing Program	EK treatment Duration (days)	Number of samples for electrochemical tests					Number of samples for index and engineering properties							Total soil samples
		pH	σ	T_{ds}	I_s	CEC and S_a	q_{eo}	PI	SP	q_u	CC	C_c C_r C_v m_v t_{90} k	W_{et} d_{ry} C_{ycle}	
Natural soil block	0	2												2
First batch		Number of soil block samples 25												
$CaCl_2$-DW	3	5	5	5	5	1	-	-	-	-	-	-	-	21
$CaCl_2$-DW	7	5	5	5	5	1	-	-	-	5	-	-	-	26
$CaCl_2$-DW	15	5	5	5	5	1	-	-	-	5	-	-	-	26
$CaCl_2$-DW	28	5	5	5	5	1	2	5	5	5	1	3	5	47
DW-Na_2CO_3	3	5	5	5	5	1	-	-	-	-	-	-	-	21
DW-Na_2CO_3	7	5	5	5	5	1	-	-	-	5	-	-	-	26
DW-Na_2CO_3	15	5	5	5	5	1	-	-	-	5	-	-	-	26
DW-Na_2CO_3	28	5	5	5	5	1	2	5	5	5	1	3	5	47
$CaCl_2$-Na_2CO_3	3	5	5	5	3	1	-	-	-	-	-	-	-	21
$CaCl_2$-Na_2CO_3	7	5	5	5	3	1	-	-	-	5	-	-	-	26
$CaCl_2$-Na_2CO_3	15	5	5	5	4	1	-	-	-	5	-	-	-	26
$CaCl_2$-Na_2CO_3	28	5	5	5	4	1	2	5	5	5	1	3	5	46
Thermal														
Second batch		Number of soil block samples 25												
$CaCl_2$-DW	3	5	5	5	5	-	-	-	-	-	-	-	-	20
$CaCl_2$-DW	7	5	5	5	5	-	-	-	-	-	-	-	-	20
$CaCl_2$-DW	15	5	5	5	5	-	-	-	-	-	-	-	-	20
$CaCl_2$-DW	28	5	5	5	5	-	2	5	5	5	1	3	5	46
DW-Na_2CO_3	3	5	5	5	5	-	-	-	-	-	-	-	-	20
DW-Na_2CO_3	7	5	5	5	5	-	-	-	-	-	-	-	-	20
DW-Na_2CO_3	15	5	5	5	5	-	-	-	-	-	-	-	-	20
DW-Na_2CO_3	28	5	5	5	5	-	2	5	5	5	1	3	5	46
$CaCl_2$-Na_2CO_3	3	5	5	5	5	-	-	-	-	-	-	-	-	20
$CaCl_2$-Na_2CO_3	7	5	5	5	5	-	-	-	-	-	-	-	-	20
$CaCl_2$-Na_2CO_3	15	5	5	5	5	-	-	-	-	-	-	-	-	20
$CaCl_2$-Na_2CO_3	28	5	5	5	5	-	2	5	5	5	1	3	5	46
Total duration	**371**	**Total number of samples for all experiments**												**677**

3.5 Experimental methods

3.5.1 Evaluation of electroosmotic flow rate, q_{eo}

The electroosmotic flow rate, q_{eo} values of ionic solutions diffusing into the soil blocks were estimated at every 24-hour interval and were plotted versus time duration.

3.5.2 Evaluation of electrochemical properties

The evaluation of the electrochemical properties of the natural soft soil includes the determination of pH, electrical conductivity, σ, total dissolved solids, T_{ds}, salinity, and ionic strength, I_s. The parameters were measured from the soil samples using a calibrated Multi-parameter (Bante Model 900) device in all the batch testing setups. Also, the monitoring and evaluation of the EK soil treatment were examined for their pore fluid change in concentration due to the variations in the above parameters of the EK treated soils at specific EK treatment duration along the anode to cathode distances.

The pH value of the natural soil was carried out in accordance with ASTM 2976-71 for estimating the range of alkalinity or acidity of the soil pore fluids. In this method, 30 g of each extracted, air-dried soil sample with 75 mL of deionized distilled water was placed in a 150 mL glass bottle, stirred using a handheld mechanical vibrator device for 30 minutes, and then left for curing for approximately one hour. The electrochemical properties of the soil solutions were estimated immediately after properly stirring the soil solution. These properties of the EK treated soils were measured at regular distances of 0-6 cm, 6-12 cm, 12-18 cm, 18-24 cm, and 24-30 cm from the anodic end to cathodic end (point A to E) in Figure 3.9 and 3.10. The test readings were taken every 24 hours intervals for 3, 7, 15, and 28 days. The tests' repetition was conducted to affirm the accuracy and precision of the obtained values.

The total number of soil blocks used was fifty-two, at two soil blocks per test setup (Table 3.9) and all the extracted EK treated soil samples for the electrochemical, index, engineering, thermal, and microscopic tests and analyses were more than six hundred.

A calibrated Multiparameter (Bante 900 model) device was used to measure the pH, total dissolved solids, T_{ds} and electrical conductivity, σ, and each reading was recorded for all soil samples extracted within the treated soil blocks from anode to cathode distances of 0-6 cm, 6-12 cm, 12-18 cm, 18-24 cm, and 24-30 cm in the test for EK treatment duration of 3, 7, 15 and 28 days in the first and second batch-test setups. Thus, the chemical properties of the ionic solution types were calibrated in order to determine their precise and accurate measurements within their specific reservoirs at different changes in molar concentration during the EK treatment of the soft soils.

Also, the changing in the ionic strength, I_s values of the treated soils is a function of the concentration of all ions present after the EK treatment was determined. The T_{ds}, σ, and I_s have empirical linear relationships to determine I_s given in Equations (3.1) - (3.5) (Appelo, 2010; McCleskey *et al*., 2012; Anna, 2017; Aqion, 2018; Rusydi, 2018).

T_{ds} = Σ cations + Σ anions (3.1)

T_{ds} (mg/L) = conversion factor × σ (S/m) (conversion factor = 0.50 to 0.70)

$I_s = \frac{1}{2}\sum_i z_i^2 c_i$ (3.2)

where, c_i and z_i represent the molar concentration and the charge of ion, i.

I_s (mol/L) ≈ 2.5 x 10^{-5} × T_{ds} (mg/L) (conversion factor = 2.5 10^{-5} ± 0.000001) (3.3)

σ (μS/cm) = 6.2 x 10^4 × I_s (mol/L) (3.4)

I_s (mol/L) = 1.6 x 10^{-5} × σ $(\mu S/cm)$ (3.5)

3.5.3 Cation exchange capacity, CEC

The cation exchange capacity (CEC) and specific surface area (S_a) tests were conducted on the EK treated soils after 28 days by using the methylene blue adsorption standard test method (AFNOR, 1993). According to this method, the methylene blue, MB solution was prepared by mixing 10 g dry powder methylene blue with 1 liter of deionized water to attain uniformity. 10 g of oven-dried EK treated powdered soil was mixed with 50 mL deionized water in a 100 mL beaker to form a uniform suspension using an electric stirrer. The ratio of the soil to deionized water was selected, according to Chiappone *et al*. (2004). The prepared methylene blue, MB solution was added into the soil solution with 0.5 mL increments. After each drop of the 0.5 mL addition of methylene blue to the soil solution, it was mixed by a magnetic stirrer for one minute.

Then, a small drop was removed from the solution and dropped carefully on a white filter paper. It produced a dark-colored blue stain circle, with a distinct edge and surrounded by a ring of colorless clearwater area. The doses of the MB solution were increased and mixed with the soil solution, and more drops were obtained on the filter paper until a permanent fuzzy light-blue halo appeared in the blue stain. That reflected the presence of excess doses of MB that was no longer absorbed by the clay mineral.

The normality, N_{MB} of the methylene blue dye, was estimated using Equation (3.6):

Normality, N_{MB} = (weight of methylene blue in g/320) (100-X)/(100) (meq/mL) (3.6)

where X is the moisture content of the methylene blue dye (%).

The methylene blue adsorption, V_{MB} for a given soil is given by using Equation (3.7):

$$V_{MB} = V \times M \times 100/W \text{ (in g/100 g)} \quad (3.7)$$

where,

V is the volume of the methylene blue added to a given soil solution (in cm^3) and;

M is the concentration (in g/cm^3) of the methylene blue solution;

W is the dry weight (in g) of the soil.

The cation exchange capacity (CEC) of a given soil sample can be estimated with the normality, N_{MB} of the methylene blue solution, using Equation (3.8):

$$CEC = (100/W) \times V_{MB} \times N_{MB} \text{ (in meq/100g)} \quad (3.8)$$

3.5.4 Specific surface area, S_a

The specific surface area, S_a of the soil, was determined according to the method proposed by Hequet *et al*. (1998) and Miyoshi *et al*. (2018). The S_a of for a given soil was estimated from the methylene blue (MB) absorption, V_{MB} required to reach the endpoint. The S_a is determined using the empirical formula given in Equation (3.9):

$$S_a = (V_{MB}/100)\,(N/W_{MB})\,(130\times10^{-20}) = 21V_{MB} \text{ (in } m^2/g) \quad (3.9)$$

where,

V_{MB} has been predetermined; a molecule of methylene blue has a S_a of 130 $Å^2$, N is Avogadro's number (6.02×10^{23}), and W_{MB} is the molecular weight of MB. The S_a = $21V_{MB}$ or $24V_{MB}$ if the W_{MB} of methylene blue was 373 g or 320 g, respectively.

3.5.5 Evaluation of engineering and index properties of soils

The basic geotechnical tests were performed to examine the index and engineering properties of the soft soils. The Atterberg limits, compaction characteristics, swelling, unconfined compression, swelling, shrinkage, and consolidation tests were conducted to examine the behavior of the natural soft soil before EK treatment, and then all the aforementioned index and engineering tests were conducted on the EK treated soils.

3.5.5.1 Moisture content determination

The moisture content (*w*) of the in situ untreated soil block and treated soil specimens has been examined by using the ASTM standard of ASTM D2216-19.

3.5.5.2 Atterberg limit tests

The aim of the Atterberg limits tests was to obtain the plastic limit, PL, liquid limit, LL, and calculate the plasticity index, PI values using the ASTM D4118-05 standard.

3.5.5.3 One-dimensional swell tests

The one-dimensional swell tests were performed in line with the standard of ASTM D 4546-08 (method B) standard to examine the swelling behavior of the natural and EK treated soils. The test utilized the mechanism of the one-dimensional oedometer equipment under seven (7) kPa surcharge load. The soil samples were placed into the oedometer test setup, and the obtained data were used to evaluate their swell potentials.

3.5.5.4 One dimensional consolidation test

The one-dimensional consolidation tests were performed by the ASTM D 2435-04 standard to find the compressibility parameters of the natural and treated soils. The soil samples were prepared in rings with a diameter of 7.5 cm and a thickness of 2.0 cm. The soil samples were placed into the odometer test setups, and the readings for consolidation tests were taken to evaluate their compressibility characteristics.

3.5.5.5 Unconfined compression test

The unconfined compressive strength of the natural soft soil and the EK treated soils extracted were measured by the ASTM standard of ASTM D 2166-06 standard.

3.5.5.6 Cyclic wetting-drying tests

The wetting-drying cyclic tests on the untreated and EK treated soil samples were performed using the ASTM standard of ASTM D4843–88. In order to determine the characteristics of swelling-shrinkage cycles of the natural and EK treated soils, the soil

samples were allowed to full swelling and then subjected to drying up to the initial compaction water content, for several cycles until it became stable. Cyclic swelling and drying tests were performed on the extracted EK treated soil samples using an oedometer ring of 5.0 cm and 1.5 cm dimensions in diameter and height, respectively.

When there was no further swelling in the soil samples, they were taken out of the oedometer cells for the drying phase. The samples were then left in a 40^{o}C oven, and changes in diameter, height, and mass were recorded continuously until the readings became steady. The samples were then subjected to swelling again and the same cycling procedures until a steady condition is attained, which was reached after five swell-shrink cycles. The swell-shrink cycles took approximately thirty to forty-five days to complete the five wetting-drying cycles of the EK treated soils.

3.5.6 Thermal analysis

The thermal analyses, TA, which were Differential Thermal Analysis, DTA, and Derivative Thermogravimetric Analysis, DTG, were performed on the untreated, and the EK treated soils of the first batch setups using Q500 Thermogravimetric Analyzer (TA Instruments, USA) under N_2 flow (120 mL/min) with respect to temperature starting from 10^{o}C to 600^{o}C at a heating rate of 10^{o}C/min. The DTA/DTG gives information about the thermal stability of the soft soils after EK treatment.

3.5.7 Microscopic studies

The light optical microscopy, LOM images of 210x magnification were obtained for the natural soft soil, and the EK treated soils of the first batch setups after 28 days by using a Euromex microscope.

Chapter 4

NUMERICAL MODELLING USING DESIGN AND ANALYSIS OF EXPERIMENTS

4.1 Introduction

The previous chapter deals with the research materials and methods used in this study. In this chapter, the numerical modeling of the experimental factors and test results were investigated in detail using the design and analysis of experiments, DOE method.

4.2 Mathematical modeling using DOE

Design of experiment (DOE) is an advanced mathematical method to develop the interactive relationship between a few defined variables that produces a large number of interpretative parameters using a few numbers of experimental data (Montgomery *et al*., 2009). The defined variables are useful in the output of the process with a few numbers of data. The DOE consists of 2-Factorial design, 2FD, Multilevel Categoric design, MCD, and response surface methodology, RSM (Montgomery, 2017). The experimental data showed the effects of the selected input factors on the targeted response of the EK treated soils. The DOE analyzed the performance of ionic solutions in terms of treatment duration, cation exchange capacity, CEC, specific surface area, S_a, pH, electrical conductivity, σ, and ionic strength, I_s, on the unconfined compressive strength, q_u of EK treated soils. The numerical analysis of the data of the selected input factors obtained in the first batch setups is to produce significant threshold values to give a remarkable effective performance in the application of the EK soil treatment.

The second section analyzed the test data obtained from the Atterberg limit and one-dimensional swelling tests at different soil extraction points (Figure 3.10) and the effect of changing electrode length ratio, l_{ce} on the performance of the EK treatment. The performance of the tests, which was with changing electrode length ratios of $0.25l_{ce}$, $0.5l_{ce}$, $0.75l_{ce}$, and $1.0l_{ce}$, with vertical soil depth, (d_s), and lengthwise anode to cathode distances ($d_{A\leftrightarrow E}$) as provided in the second batch-test setups (Figure 3.8).

4.2.1 Mathematical modeling using DOE: first batch setups

In this study, the data obtained from the first batch setups, as provided in Section 3.4.1.1, were used as the input factors, while the q_u was the target response in the numerical model analyses. Table 4.1 shows the factors and their levels using the DOE.

Table 4.1: Factors and their levels using the design of experiment, DOE.

Factors Name	Units	Type	Min.	Med.	Max.
Ionic solutions	---	Categoric	A1	A2	A3
EKT durations	days	Categoric	7	15	28
CEC	meq/100g	Categoric	5.00	9.00	15.00
S_a	m^2/g	Categoric	5.00	11.00	18.00
pH	---	Numeric	8.00	9.50	11.00
σ	S/m	Numeric	4.00	6.00	10.00
I_s	mol/L	Numeric	0.500	1.50	2.00

Each factor was coded in the DOE at three different levels: maximum, medium, and minimum, such as +1, 0, and -1, respectively. The DOE used a multilevel categoric methodology, (MCM), to analyze the selected categoric factors. The factors include ionic solutions, EK treatment durations, CEC, and S_a. The DOE applied a response surface methodology, RSM method, to study the effects of three factors pH, σ, and I_s and their interaction effect on the target response, q_u. There was a replication of q_u

values at the two-factor combinations for three different EK durations of 7, 15, and 28 days, to produce the required numbers of runs in a completely randomized design.

4.2.2 Mathematical modeling using DOE: second batch setups

In this study, the data obtained from the second batch setups in Section 3.4.1.2, which were plasticity index, PI, and swelling potential, SP were the targeted responses in the numerical model analyses. Table 4.2 shows the factors and their levels using the DOE.

Table 4.2: Factors and their levels using the response surface methodology, RSM.

Name	Symbols	Levels of factors (cm)		
Electrode length, l_e	X_1	7.5	15	22.5
Soil depth, d_s	X_2	7.5	15	30
Lateral anode to cathode distances, $d_{A\leftrightarrow E}$	X_3	5	15	25

The data obtained from the PI and SP values were then subjected to advance statistical modeling for evaluating the most appropriate electrode length, l_e configurations to achieve the most effective performance for EK treatment. Modeling and analysis of the experimental results were conducted by response surface methodology (RSM), which was the combination of statistical and mathematical techniques useful for displaying and analyzing different variables (Montgomery *et al*., 2009). Table 4.2 presents the factors and their corresponding low, intermediate, and high-level ranges.

4.2.3 Statistical data analysis (SDA)

The Statease statistical software version 11 trial 2018 (SAS Institute Inc., Cary, NC) provided numerical and statistical analyses. To consider the selected factors as effective and significant factors, and to examine their performance on the outcome of results (target responses), such factors should satisfy specific statistical conditions. The calculated probability values should satisfy probability, P values ≤ 0.0500 or $0.0500 < P < 0.1000$ or ''Prob. > F'' < 0.0500, which indicates that the model term is significant

(Le *et al*., 2003). The P-values > 0.1000 indicate the model terms are not significant. Also, there should be a reasonable agreement in the fit statistics when the observed R-squared (R^2) is high and the difference between the adjusted R^2 and predicted R^2 to be ≤ 0.2 (Le at al., 2003; Wang *et al*., 2008; Montgomery *et al*., 2009).

There should be an adequate precision; a fit statistic tool measures the signal to noise ratio. According to Montgomery *et al*. (2017), an adequate precision ratio > 4 is more desirable in ANOVA analysis. The high F-value indicates that the model is significant statistically (Montgomery *et al*., 2009). The analysis of variance (ANOVA) produced the prediction model, interaction effects, and 3D plots of model terms. The observed values of the output results were obtained from the experimental test, while the ANOVA analysis generated the predicted values from the selected input factors.

4.2.4 Multilevel-categoric methodology (MCM) design

The statistical equations of the MCM design include modified, design model, mean, main effects, and 2 Face interaction, 2FI. The MCM model equations are given in Equation 4.1 and 4.2 (Gelman and Hill, 2006).

$$\text{Mean, M: } \begin{cases} \int_{-\infty}^{\infty} \text{yf (y) dy} & \text{y continuos} \\ \sum_{\text{all y}} \text{yp (y)} & \text{y discrete} \end{cases} \quad (4.1)$$

$$\text{2Face interaction, 2FI: } Y = \beta_o + \sum_{i=1}^{4} \beta_i X_i + \sum_{i=1}^{3} \sum_{j=i+1}^{4} \beta_{ij} X_i X_j \quad (4.2)$$

The MCM is a two-factor factorial using a statistical experimental design to produce a robust response design. In general, if y_{ijk} be the observed response when factor *A* is at the *i*th level (*i* = 1, 2, …, a) and factor *B* is the *j*th level (*j* = 1, 2, … , b) for the *k*th replicate (k = 1, 2, … , n). A model describes the abn factors in a factorial experiment in a completely randomized design. According to Montgomery (2017), the significant effects model on the response given in Equation 4.3, where μ is the entire mean effect:

$$y_{ijk} = \mu + \tau_i + \beta_j + (\tau\beta)_{ij} + \varepsilon_{ijk} \begin{cases} i = 1, 2, \ldots, a \\ j = 1, 2, \ldots, b \\ k = 1, 2, \ldots, n \end{cases} \quad (4.3)$$

τ_i and β_j are the effects of *i*th and *j*th levels for factors A and B. $(\tau\beta)_{ij}$is the interaction effect of τ_i and β_j. ε_{ijk} is a random error function (Montgomery *et al*., 2009).

4.2.5 Response surface methodology, RSM design

Response surface methodology, RSM is an empirical modeling tool of DOE for retrieving large amounts of information from a small number of experiments, evaluating simultaneous interaction effects of variables affecting the response and simultaneous optimization of many factors and responses for optimal conditions (Kamani *et al*., 2018). The RSM unveils the interaction of factors that are not achievable using the conventional experimental methods, a one-factor-at-a-time optimization method. The statistical equations of the RSM design include modified, design model, mean, linear, 2FI, quadratic, cubic, quartic, fifth, and sixth. The sample RSM models are given in Equations 4.4-4.5 (Croarkin *et al*., 2006; Kaur *et al*., 2012):

Linear, L: $Y = b_0 + b_1X_1 + b_2X_2 + \ldots + b_KX_k$ (4.4)

Quadratic, Q: $\hat{y} = b_0 + b_1 b x_1 + b_2 x_2 + b_3 x_3 + b_{12} x_1 x_2 + nb_{13} x_1 x_3 + b_{23} x_2 x_3 + b_{11} x_1^2 + b_{22} x_2^2 + b_{33} x_3^3$ (4.5)

To evaluate the effect of three variables pH, σ, and I_s on the unconfined compressive strength properties of EK treated soils, RSM design was employed by using Design-expert version 11 (Stat-Ease, licensed version) software. The results of the CCF design were analyzed using Equation 4.5 and 4.6 to determine and validate the significant effects and interaction effects of the selected input factors on the output of response.

Chapter 5

RESULTS AND DISCUSSIONS

5.1 Introduction

This chapter presents the results of the effects of the electrokinetic, EK treatment on the electrochemical, thermal, morphological, index, and engineering behavior of soft soil used in this study. Chapter 3 discusses the detailed laboratory testing programs using standard test methods. All the EK soil treatments were performed in glass test tanks. The soil block samples were inundated with distilled water in the test tanks until they reached a maximum degree of saturation at a water content of 48%. Then, followed by the complete electrokinetic (EK) test setup to examine the EK soil treatment at each stage of the study using different combinations of ionic solutions.

The variations of electrochemical properties of EK treated soils were measured within anode to cathode distances of soft soil in the test tank using a Multiparameter (Bante 900 model) device at every 24 hours. The changes in the electroosmotic flow, electrochemical, index, and engineering properties of the EK treated soils were examined. During the EK processing, various Atterberg limits, unconfined compression, one-dimensional consolidation and swelling, wetting-drying cycle tests were carried out on the EK treated soils from different anode to cathode distances.

The cation exchange capacity, CEC, specific surface area, S_a, and thermal analysis were examined and evaluated. The microscopy studies examined the morphological changes of the EK treated soils using a light optical microscope. The recorded data of the testing program were evaluated and analyzed to establish different output results.

Chapter 4 presents the numerical modeling of the selected input factors to establish threshold values of the significant factors. The continuous evaluation of the recorded experimental data over different durations of time during the laboratory testing programs of EK soil treatment was analyzed to study the effects of the ionic solutions on the different electrochemical, index, and engineering behaviors of the treated soils.

This chapter examines the effects of the EK soil treatment on the electroosmotic flow, and various behavioral properties of the EK treated soils. The results of the anode to cathode distance on EK treatment and EK treatment durations, ionic solutions: $CaCl_2$-DW, Na_2CO_3-DW, $CaCl_2$-Na_2CO_3, and the electrode length, l_e configurations during the EK processes have been discussed in detail. The chapter is divided into three main sections to monitor the data of the electrochemical properties at 3, 7, 15, and 28 days, and index and engineering properties of soft soils after 7, 15, and 28 days of the EK treatment for all test setups. The $CaCl_2$-DW setup was conducted to examine the effects of calcium, Ca^{2+} ions on EK testing of soft soils when supplied steadily from the anode chamber, and the Na_2CO_3-DW setup was carried out to investigate the effect of carbonate, CO_2^{3-} ions when continuously supplied from the cathode compartment.

Finally, the paired $CaCl_2$-Na_2CO_3 electrolytes combination was performed to understand the effects of both Ca^{2+} and CO_2^{3-} ions when their ionic solutions are supplied continuously into the soil block from their reservoirs. Finally, the results and

discussion of the aftermath effects of the ionic solutions during the EK treatment technique of soft soils are provided using the experimental and numerical modeling results to explain the overall change in the behavior of the extracted EK treated soils.

5.2 Electroosmotic flow, q_{eo}

Figure 5.1 presents the cumulative electroosmotic flow rate (q_{eo}) of distilled water through the natural soft soil block after 28 days. As can be seen in Figure 5.1, the cumulative electroosmotic flow rate (q_{eo}) was estimated to be 200x10^{-10} m^3/s.

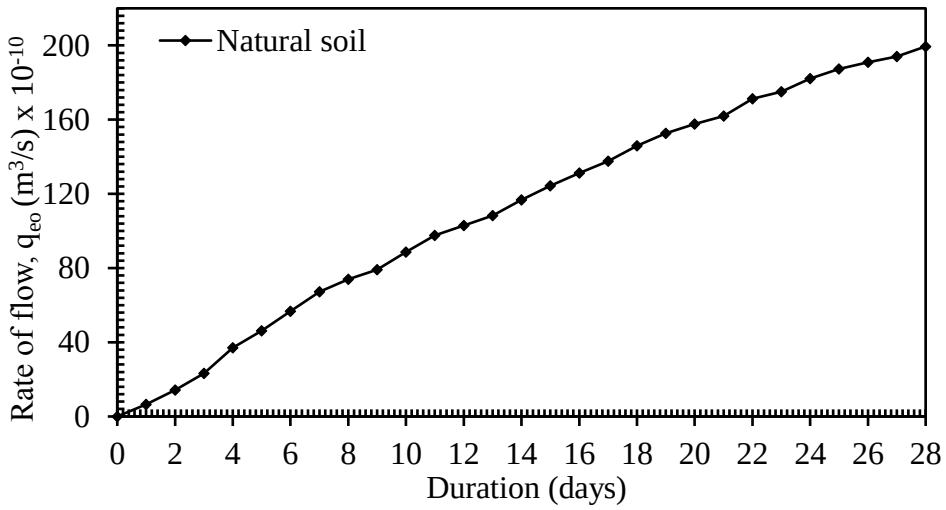

Figure 5.1: The q_{eo} of distilled water in natural soft soil.

5.3 Electrochemical properties of untreated soft soils

In this study, the electrochemical properties of the natural soft soils such as the pH, total dissolved solids (T_{ds}), salinity, electrical conductivity (σ), electrical resistivity (ρ), and ionic strength (I_s), cation exchange capacity (CEC), and specific surface area (S_a) values were determined and presented in Table 5.1. According to the CEC and S_a values obtained, it can be suggested there was a high amount of kaolinite minerals in the natural soft soil (Diamond and Kinter; 1956; Macht *et al*., 2011; Christidis, 2013).

Table 5.1: Electrochemical properties of the natural soft soil.

Properties	Values
pH	8.38
Total dissolved solids, T_{ds} (g/L)	2.06
Salinity (ppt)	2.16
Electrical conductivity, σ (mS/cm)	4.08
Electrical resistivity, ρ (Ω.m)	2.45
Ionic strength, I_s (mol/L)	0.05
Cation exchange capacity, CEC (meq/100g)	14.7
Specific surface area, S_a (m^2/g)	17.5

5.4 Index and engineering properties of the natural soft soil

This section discusses the results of the index and engineering properties of the natural soft soil. In Section 3.2.1, Table 3.1 summarizes the index properties of the soft soil.

5.4.1 Moisture content

The insitu moisture content, *w* of the natural soft soil block, was determined to be 48%.

5.4.2 Hydrometer analysis

Figure 5.2 presents the results of the hydrometer test performed on natural soft soil. From the graph, the soil showed 3% of sand, 36% of silt, and 61% of clay size particles. The test results showed the soil consisted of more than > 50% of fines of clay and silt.

5.4.3 Atterberg limit test

The plastic limit (PL) and liquid limit (LL) of the natural soft soil were estimated to be 33% and 60%, respectively, and the plasticity index (PI) was 27%. Because of its PI and LL, the natural soft soil was located just at the A-line using the Unified Soil Classification System, and it falls in either MH or CH group and the percent clay fines of 61%, the soft soil is predicted to be inorganic clays of high plasticity (Figure 5.3).

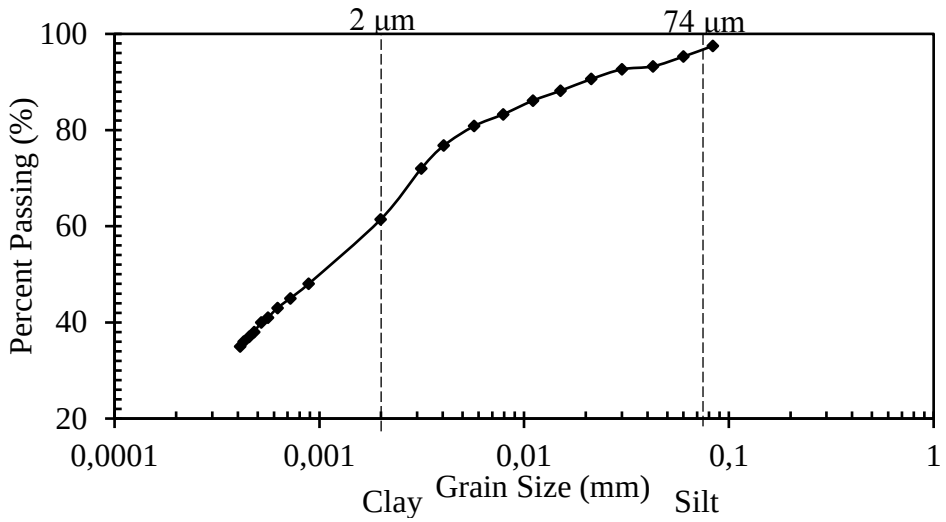

Figure 5.2: Particle size distribution of the natural soft soil.

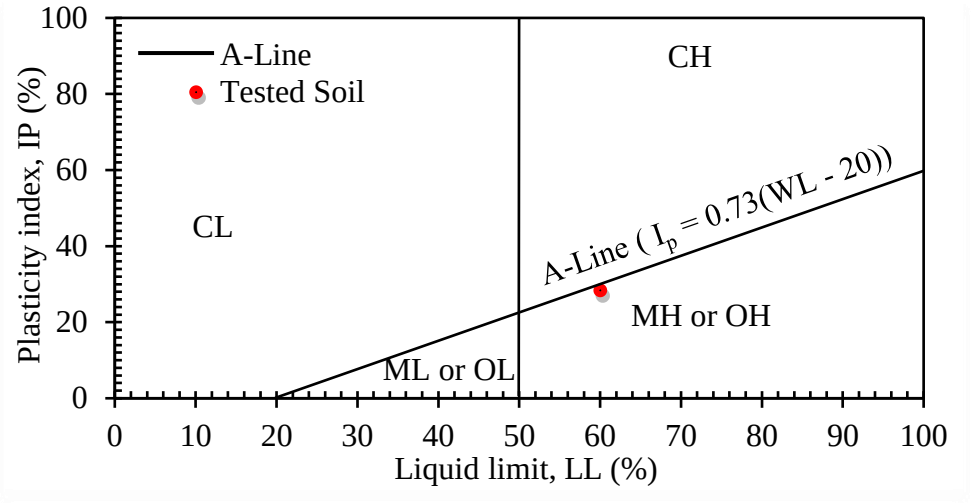

Figure 5.3: Plasticity chart (USCS) of the natural soft soil.

5.4.4 Unconfined compression test

Figure 5.4 presents the stress-strain diagram of natural soft soil. The unconfined compressive strength, q_u of natural soft soil was determined to be 21 kPa.

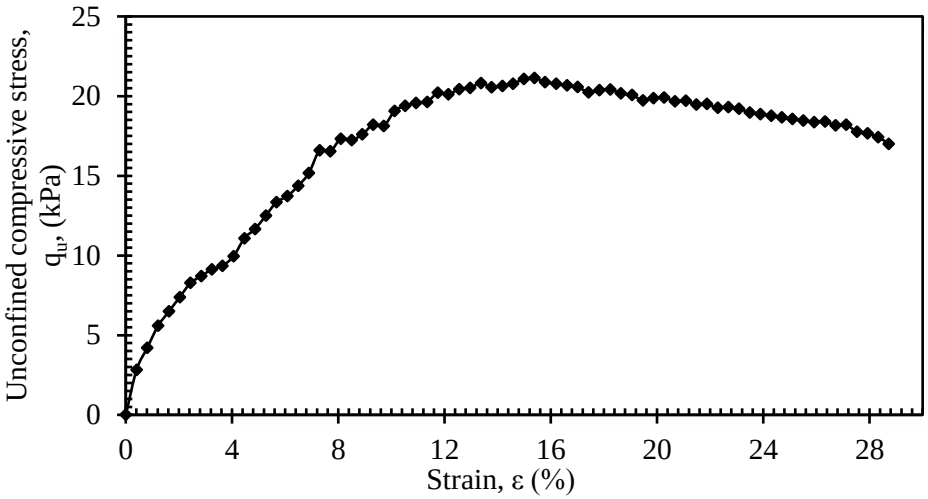

Figure 5.4: Stress-strain diagram for the natural soft soil.

5.4.5 One-dimensional swell test

The percent swelling was estimated by dividing the vertical deformation of soft soil that occurred due to inundation by the initial height of the soil sample in the oedometer apparatus ring. This test was carried out for a minimum of ten (10) days until the steady equilibrium in swelling potential was attained. Figures 5.5 and 5.6 present the swell-time curves for natural soft soil, and the observation was that the maximum vertical swelling potential of the natural soft soil, from both curves, was determined to be 2.4%.

5.4.6 One-dimensional consolidation test

This test was carried out on the natural soft soil to determine the compressibility characteristic of the soft soil. The record values were plotted using a semi-log scale, and the void ratio-log pressure curve was provided. The coefficients of consolidation (C_v), compression index (C_c) rebound index (C_r) and volume changes (m_v) were estimated from the consolidation curve in Figure 5.7. Also, the preconsolidation and swell pressures were determined by using Figure 5.7, and it was found that the swell and preconsolidation pressures were found to be 62 kPa and 80 kPa, respectively. All the determined values from the consolidation curves were presented in Table 5.2.

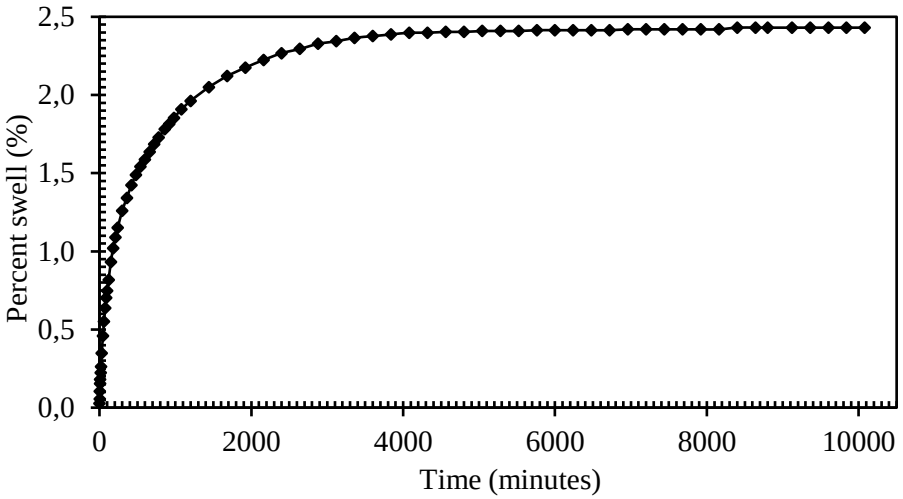

Figure 5.5: Swell-time curve for natural soft soil.

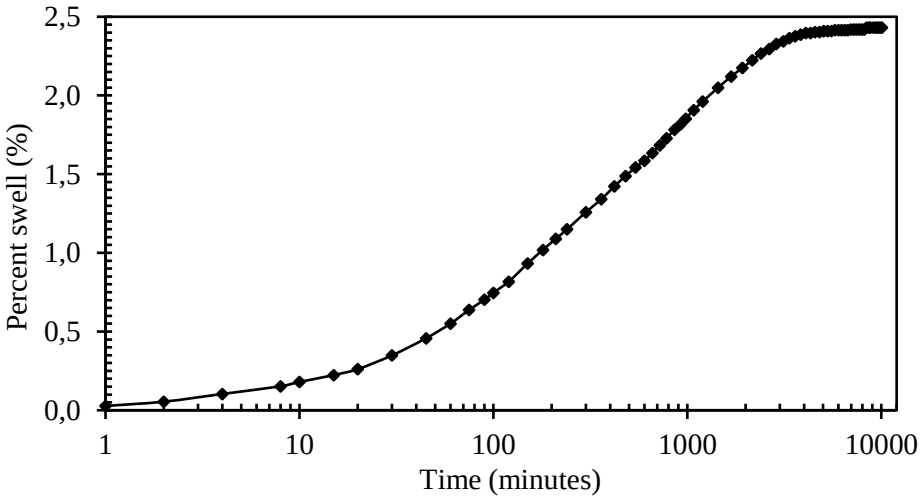

Figure 5.6: Swell-log time curve for natural soft soil.

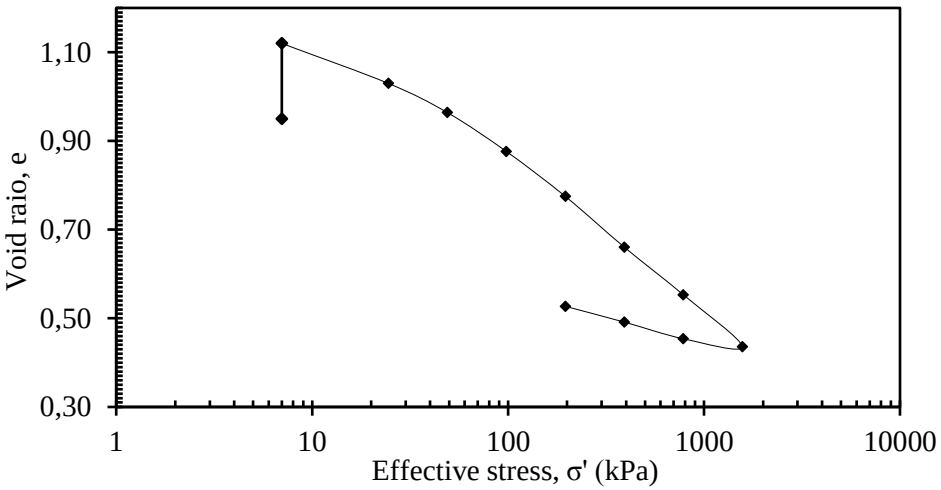

Figure 5.7: Consolidation curve for the natural soft soil.

Table 5.2: Volume-change characteristics of the natural soft soil.

Compressibility characteristics	Values
Compression index, C_c	0.37
Expansion index, C_r	0.13
Coefficient of consolidation, C_v (m^2/s)	$4.25x10^{-6}$
Coefficient of compressibility, m_v (m^2/kN)	$2.56x10^{-4}$
Average degree of consolidation, t_{90} (min)	11.2
Coefficient of permeability, k average (m/s)	$1.07x10^{-8}$
Preconsolidation pressure, σ_p' (kPa)	80
Swell pressure (kPa)	62

5.4.7 Hydraulic conductivity

The hydraulic conductivity was determined by an indirect method using the time-dependent volume change values from the consolidation test. The indirect method uses a one-dimensional consolidation equation because it is easier and quicker to evaluate. The hydraulic conductivity of the natural soft soil was determined to be $1.07x10^{-10}$ m/s**.**

5.4.8 Cyclic Wetting (Swelling) - Drying (Shrinkage) test

Figure 5.8 presents the results of the five repeated wet-dry cycle tests performed on the natural soft soil. The swelling percentage was determined by dividing the change in vertical deformation (ΔH) with the original height of soil (H).

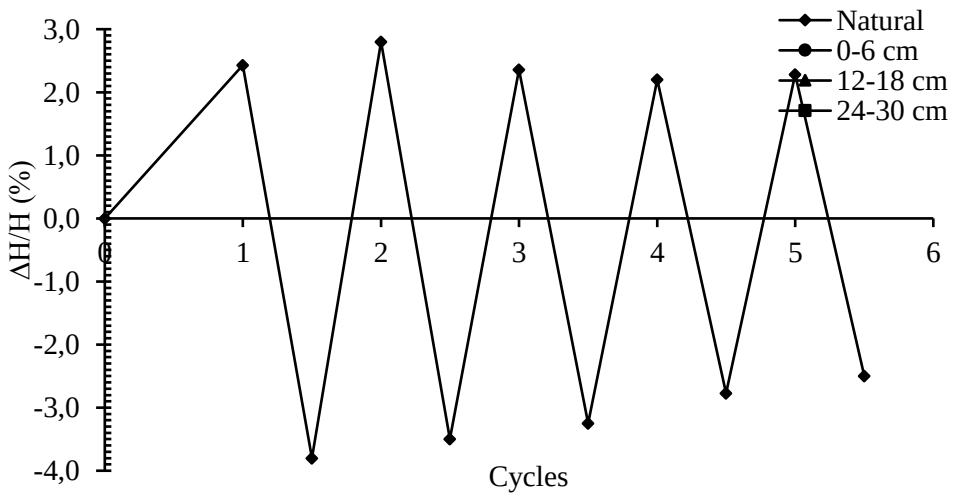

Figure 5.8: Wetting-drying cycles of the natural soft soil.

In the first cycle, the swelling and shrinkage percent obtained were 2.4% and 3.8%, respectively. The equilibrium in swelling and shrinkage occurred after the fourth cycle.

5.4.9 Thermal analysis

Figure 5.9 presents the thermal analyses such as differential thermal analysis (DTA) and derivative thermogravimetric analysis (DTG) curves for the natural soft soil.

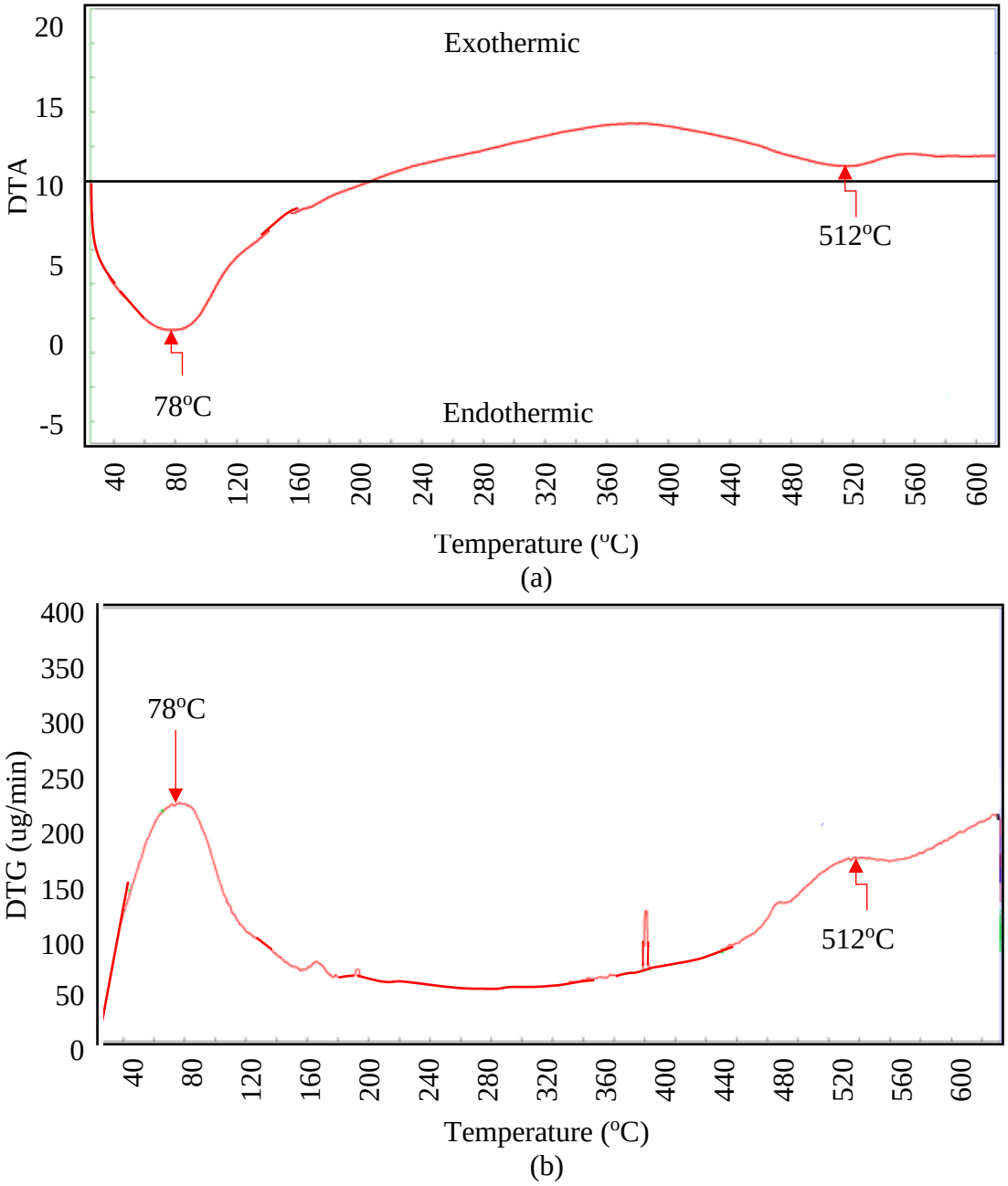

Figure 5.9: (a) DTA and (b) DTG curves of natural soft soil.

From the differential thermal analysis (DTA) and derivative thermogravimetric analysis (DTG) curves in Figures 5.9a and 5.9b respectively, the total weight loss of the natural soft soil was 10%. The first 4.5% weight loss was between 10^{o}C to 105^{o}C, and the second weight loss of 5.5% began from a temperature range of 410^{o}C to 600^{o}C from the curves of differential thermal and derivative thermogravimetric analyses.

The second weight-loss occurrence between 410^{o}C and 600^{o}C was due to the breaking of the clay mineral crystalline structure. The DTA/DTG curves of the natural soft soil showed a well-defined, strong endothermic and exothermic peaks at 512^{o}C and 78^{o}C, respectively, which indicated the presence of kaolinite minerals (Peethamparan *et al*., 2009; Tironi *et al*., 2014; Kapeluszna *et al*., 2017; Khan *et al*., 2017).

5.6 Effect of ionic solutions on the performance of EK treated soils: first batch-test setups

The first batch-test setups comprise the dimensions of the test tanks, electrode length, and ionic solutions' reservoirs described in Section 3.4.1.1 and the dimension of the soil block given in Table 3.4. The testing program was performed based on using different combinations of ionic solutions, along with different lateral anode to cathode distances of the EK treated soils in the test tank, and varying EK testing durations.

5.6.1 Electroosmotic flow rate, q_{eo} of the EK treated soils

Figures 5.10 presents the results of the q_{eo} obtained from the inflow of the ionic solutions of $CaCl_2$-DW, Na_2CO_3-DW, and $CaCl_2$-Na_2CO_3 within the EK treated soil blocks in the first and second batch setups. In Section 3.4.1.1, the ionic solutions were allowed to diffuse through the soil block samples and the rate of flow, q_{eo}, values were measured at every 24-hour interval, and the obtained values were given in Figure 5.10.

The cumulative electroosmotic flow rate (q_{eo}) depends on the ionic solution, surface charge, concentration charge, and soil index properties (Alshawabkeh and Bricka, 2001; Mosavat *et al*., 2013). Table 3.6 shows the location of the reservoirs for different combinations of ionic solutions in the test tanks setups for the EK soil treatment.

Figure 5.10a presents the $CaCl_2$-DW setup, in which $CaCl_2$ ionic solution was supplied from the anolyte reservoir, whereas distilled water was provided from the catholyte reservoir into the soil block. Due to the higher concentration of the $CaCl_2$ ionic solution in the anolyte reservoir, the $CaCl_2$ ionic solution had a higher cumulative flow rate than DW, and the higher flow rate took place from the anode to the cathode direction.

Figure 5.10b presents the Na_2CO_3-DW setup, with Na_2CO_3 was supplied from the catholyte reservoir, and distilled water was supplied from the anolyte reservoir. Due to the higher concentration of Na_2CO_3 ionic solution in the cathode chamber, a higher flow rate was obtained from the cathode to anode direction, $d_{A\leftrightarrow E}$ in the treated soil.

Whereas in the $CaCl_2$-Na_2CO_3 setup (Figure 5.10c), because of the similar molar concentration of $CaCl_2$ and Na_2CO_3 ionic solutions (Table 3.3), the bi-directional flow of the soil pore fluid took place from anode to cathode and cathode to anode directions.

Due to this bi-directional flow of the ionic solutions, the lowest q_{eo} values were obtained in the $CaCl_2$-Na_2CO_3 ionic solution setup, and the flow was from both the cathode to anode, $d_{A\leftrightarrow E}$, and anode to cathode, $d_{A\leftrightarrow E}$ directions in the EK treated soil.

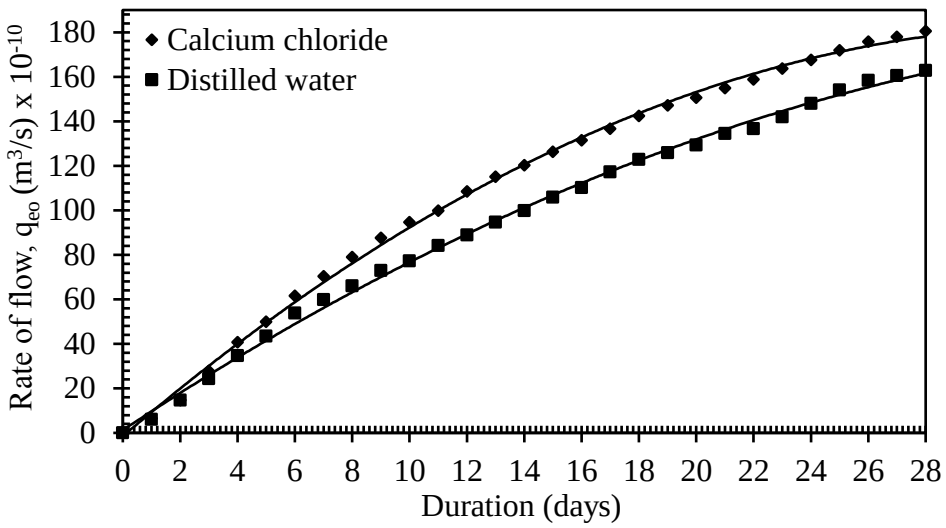

(a)

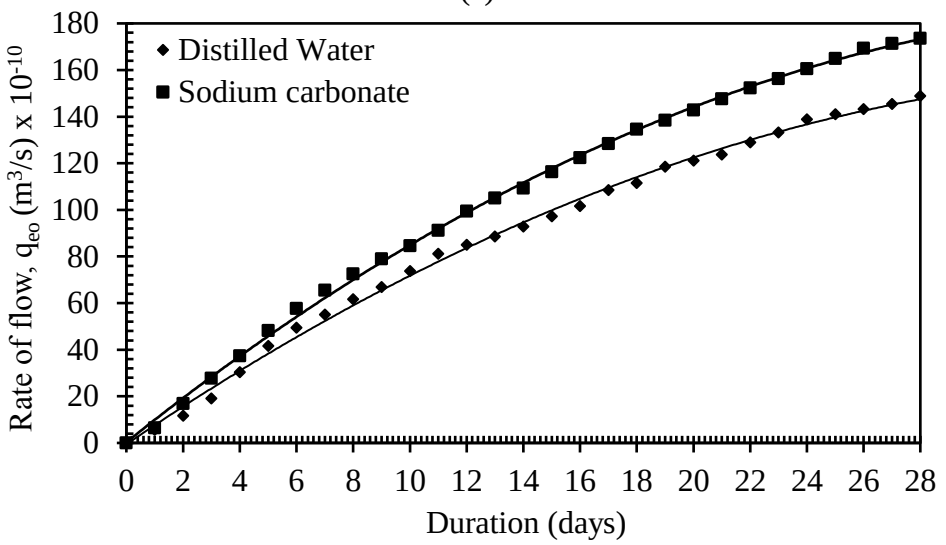

(b)

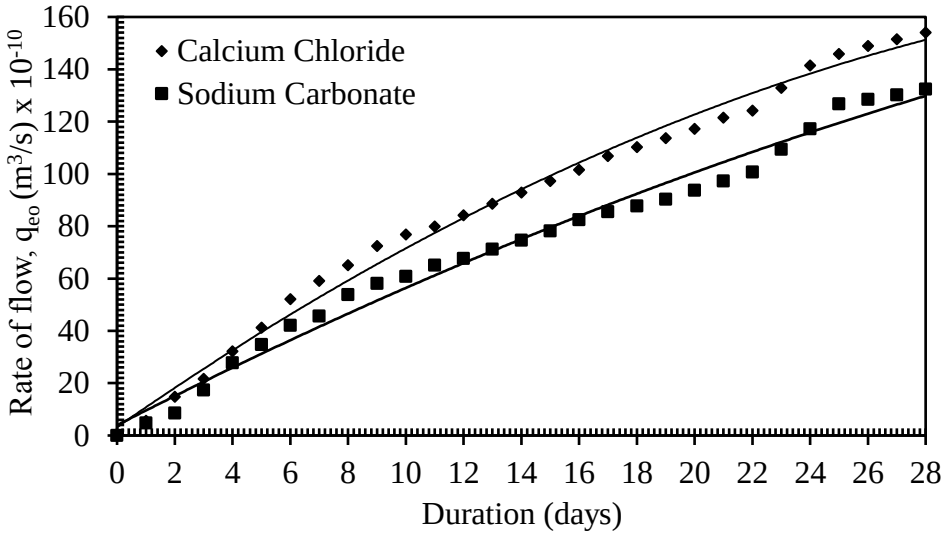

(c)

Figure 5.10: The q_{eo} of ionic solutions of (a) $CaCl_2$-DW (b) Na_2CO_3-DW, and (c) $CaCl_2$-Na_2CO_3 of the EK treated soils in the first batch-test setups.

In Figure 5.10, the highest cumulative rate of flow (q_{eo}) value was obtained for the $CaCl_2$-DW setup from anode to cathode direction could be explained due to the higher valency of Ca^{2+} ions in the $CaCl_2$ ionic solution. The electroosmotic flow caused variations in the index and engineering properties of the EK treated soft soil blocks. The peak rate of flow (q_{eo}) values for the ionic solutions of $CaCl_2$-DW, Na_2CO_3-DW, and $CaCl_2$-Na_2CO_3 were recorded for each test set up and presented in Table 5.3.

Treating soils with $CaCl_2$ ionic solution resulted in a higher rate of flow, q_{eo} values than with Na_2CO_3 ionic solution in this study. The higher rate of flow (q_{eo}) of the ionic solutions within the EK treated soils were in the order of $CaCl_2$ > Na_2CO_3 > DW.

Table 5.3: q_{eo} values of ionic solutions via the EK treated soils in first batch-test setups.

Test setups	Combination of ionic solutions	q_{eo} ionic solution in anode chamber (m^3/s)	q_{eo} ionic solution in cathode chamber (m^3/s)
1	$CaCl_2$-DW	$CaCl_2$: $181x10^{-10}$	DW: $163x10^{-10}$
2	Na_2CO_3-DW	DW: $149x10^{-10}$	Na_2CO_3: $174x10^{-10}$
3	$CaCl_2$-Na_2CO_3	$CaCl_2$: $154x10^{-10}$	Na_2CO_3: $132x10^{-10}$

5.6.2 EK effects on electrochemical properties of soft soils

5.6.2.1 pH

Geochemical reactions such as dissolution, precipitation, cementation, flocculation, aggregation, and particle bonding depend on soil pH (Ou *et al*., 2009; Asadi *et al*., 2013). The electrochemical reaction of clay minerals and ionic solutions initiated EK redox reactions, which generated H_2 and OH^- at the cathodic end to produce base font and formed O_2 and H^+ at the anodic end to produce the acid font (Equations 5.1 to 5.2).

Anode: $2H_2O - 4e^- \rightarrow O_2\uparrow + 4H^+$ $E_o = -1.229$ V (oxidation: loss of electrons) (5.1)

Cathode: $2H_2O + 2e^- \rightarrow H_2\uparrow + 2OH^-$ $E_o = -0.828$ V (reduction: gain of electrons) (5.2)

E_o is the standard reduction electrochemical potential (Baker *et al*., 2004; Mosavat *et al*., 2014).

Figure 5.11 presents the pH values of the EK treated soils measured from the anode to cathode distance in the test setup by using different combinations of ionic solutions and different EK treatment durations. The flow of the charged ions into the soil-initiated variation in the pH values and affected the soil physicochemical behavior.

Figure 5.11a presents the $CaCl_2$-DW setup, the diffusion of $CaCl_2$ ionic solution from the anolyte reservoir into the soil led to the decrease in the pH values of the EK treated soil at the anode end from 8.38 to 8.30. It increased slightly to 8.91 towards the cathode end within three days. The significant reduction in the pH values of the EK treated soil block at the anode end caused the formation of the acidic font at the anode vicinity.

The pH values measured from the EK treated soils in the 7 and 15 days retained almost a similar decreasing trend. The pH value of the EK treated soils in the $CaCl_2$-DW system continued to decrease towards the end of the test, and the lowest pH values were obtained at the 28 days due to the exchange of in cations in the EK treated soils.

Whereas, in the Na_2CO_3-DW setup (Figure 5.11b), the diffusion of the Na_2CO_3 ionic solution from the catholyte reservoir into the soil caused the pH values of the soil pore fluid to increase gradually and caused the EK treated soil to exhibit higher alkaline properties at the cathode end and thus reduced the acidity towards the anode vicinity.

The pH value increased from 8.38 to 9.64 at the cathode vicinity, and 8.71 at the anode vicinity of the EK treated soil within three days of EK treatment duration. However, the pH values from anode to cathode distances decreased steadily at seven days, and a further reduction in the pH values was obtained in 28 days. The decrease in the pH values was more profound at the distances closer to the anode than at the cathode.

Figure 5.11c presents the $CaCl_2$-Na_2CO_3 setup, which produced a significant increase in the pH values of the treated soil ranging from 8.38 to 9.50 and 10.50 at the anode and cathode regions, respectively. It was due to the continuous inflow of $CaCl_2$ and Na_2CO_3 ionic solutions from the anode and cathode reservoirs into the EK treated soil.

The interaction effects of the stabilizing ions from different combinations of ionic solutions with the clay minerals initiated an alkaline environment in the soil block at shorter time intervals between three to seven days. With the increase in the treatment time, the significant reduction in the pH values of the EK treated soils was obtained.

The overall increase in the alkaline nature of the soil block initiated the cementation, aggregation, and flocculation of the soil fines thus improved the properties of the soil blocks. The higher pH values obtained thus minimized the acidic front, which was initially developed at the anode and gradually increased towards the cathode.

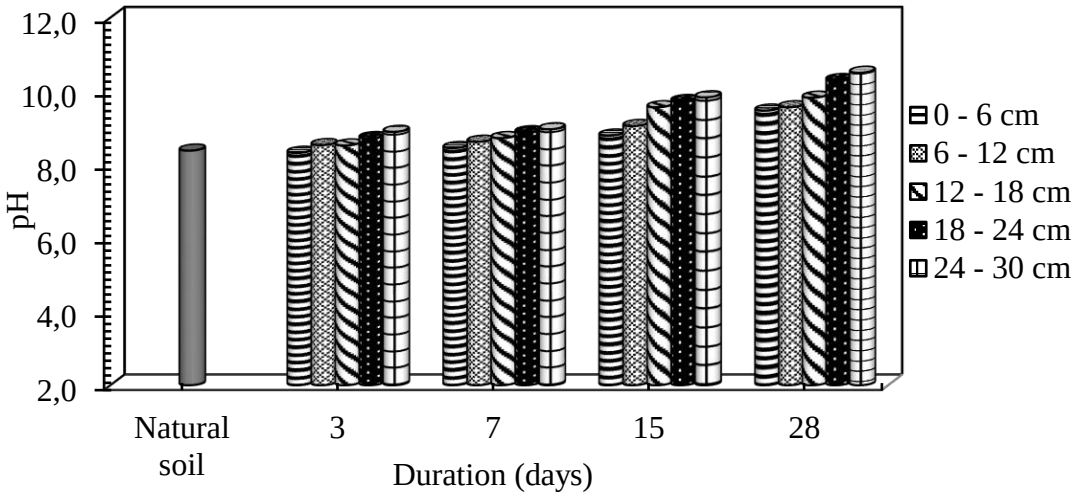

(a)

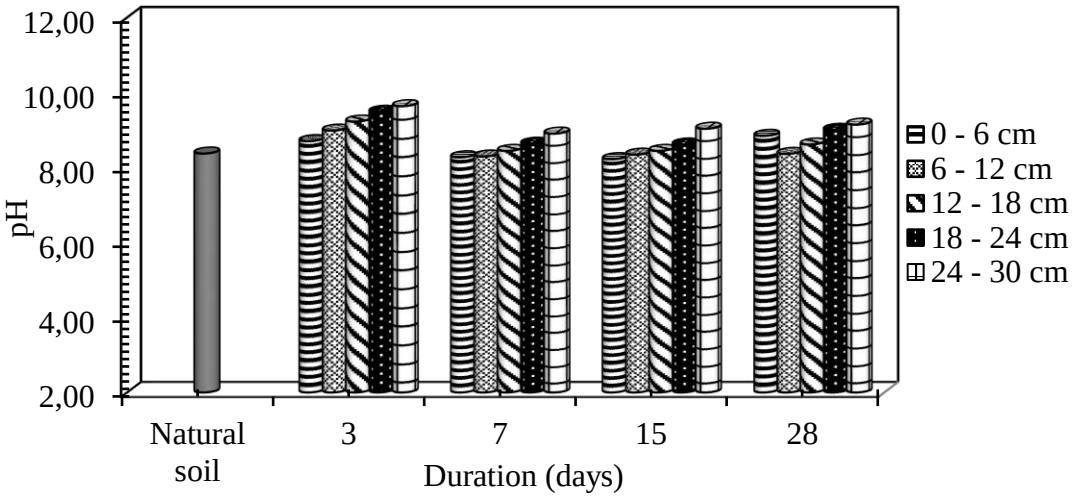

(b)

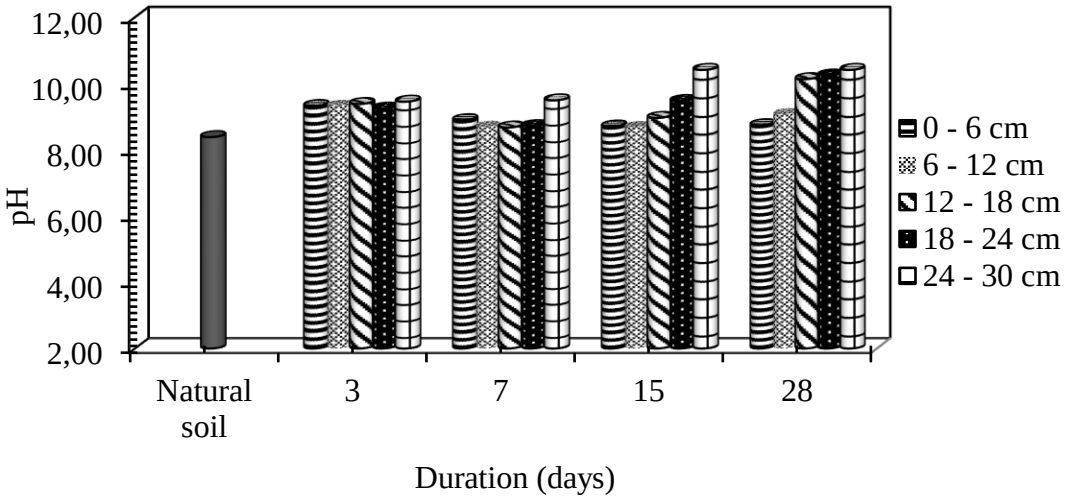

(c)

Figure: 5.11: The variations of pH at the anode to cathode distances using different combinations of ionic solutions of (a) $CaCl_2$-DW, (b) Na_2CO_3-DW, and (c) $CaCl_2$-Na_2CO_3.

5.6.2.2 Total dissolved solids, T_{ds}

The electroosmotic flow of the electrolytes into the soil altered the total dissolved solids, T_{ds} in the treated soil blocks. Figure 5.12 presents the T_{ds} results measured along with the anode to cathode distances within the soil blocks using different ionic solution setups. The initial value of T_{ds} was determined to be 2.06 10^3 mg/L in the untreated soil, and the variations of T_{ds} values were estimated for the EK treated soils.

Figure 5.12a presents the $CaCl_2$-DW setup; the estimated T_{ds} values increased from 2.30 10^3 mg/L to 4.11 10^3 mg/L and 1.34 10^3 mg/L to 3.79 10^3 mg/L at the anode and cathode regions, respectively. The results indicated that the q_{eo} had more influence on the T_{ds} values from lateral anode to cathode distances, $d_{A\leftrightarrow E}$ from the region of the anode to cathode region than from region of the cathode to anode region.

In the Na_2CO_3-DW setup (Figure 5.12b), the estimated T_{ds} values increased from 1.96 10^3 mg/L to 2.24 10^3 mg/L and 1.51 10^3 mg/L to 4.43 10^3 mg/L at the anode and cathode regions, respectively. The results indicated that the q_{eo} had more influence on the T_{ds} values from cathode to anode than from anode to cathode in the treated soil.

Whereas in the $CaCl_2$-Na_2CO_3 setup (Figure 5.12c), the estimated T_{ds} values increased from 2.26 10^3 mg/L to 3.93 10^3 mg/L and 1.65 10^3 mg/L to 5.15 10^3 mg/L at the anode and cathode regions, respectively. The results indicated that the q_{eo} had more influence on the T_{ds} values flow from cathode to anode than from anode to cathode.

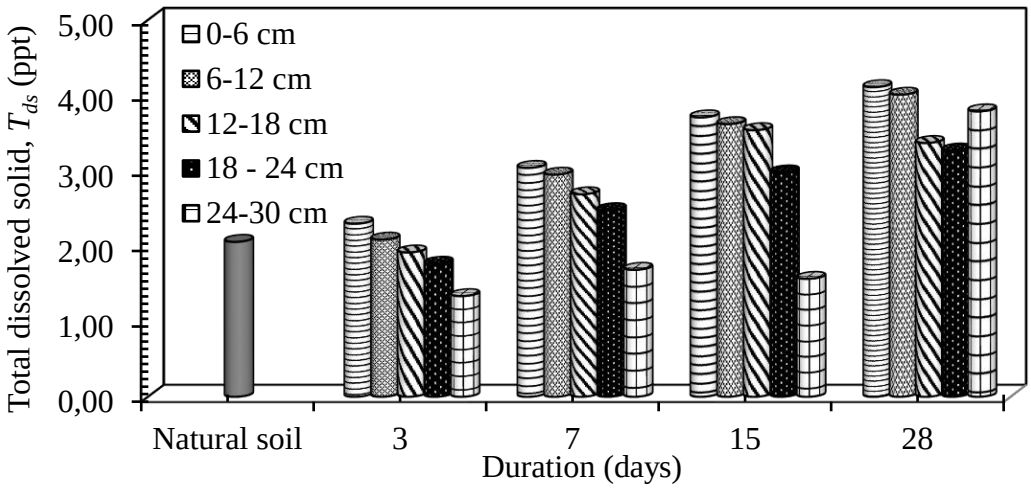

(a)

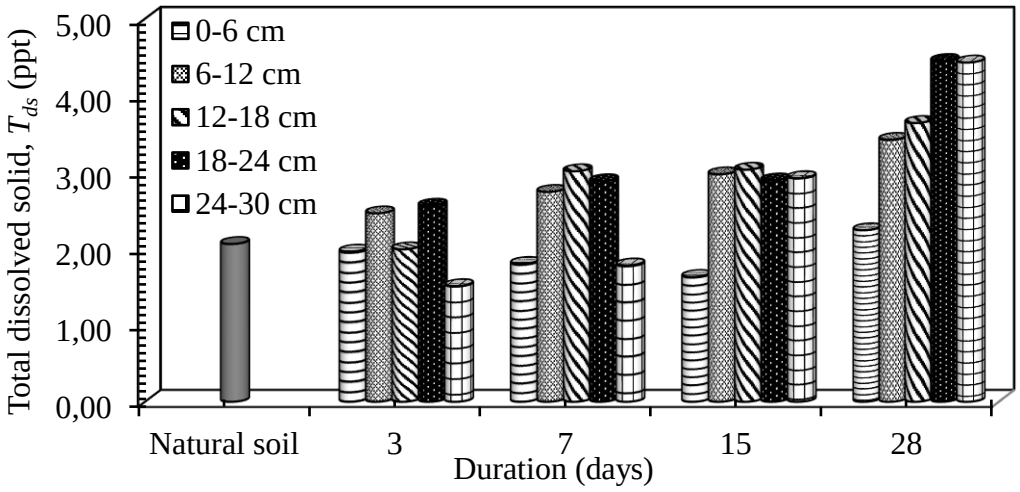

(b)

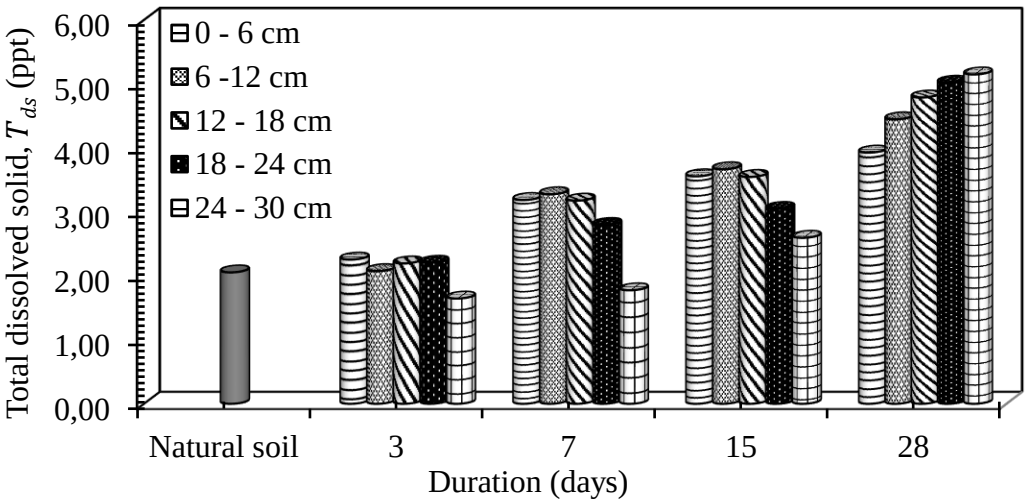

(c)

Figure 5.12: The variations of total dissolved solid, T_{ds} at the anode to cathode distances using different combinations of ionic solutions of (a) $CaCl_2$-DW, (b) Na_2CO_3-DW, and (c) $CaCl_2$-Na_2CO_3.

The most effective zone for Na_2CO_3-DW and $CaCl_2$-DW setups is within the 0-12 cm distance from point A to E and from point E to A, respectively. The effective zone for the $CaCl_2$-Na_2CO_3 setup is 0-18 cm distance. The rate of flow (q_{eo}) of the ionic solutions and DW within the soil blocks is in the order of $CaCl_2$ > Na_2CO_3 > DW.

The order followed the charged ions and electrolytes that produced more effective results in EK treated soil. The diffusion of Ca^{2+} and CO_3^{2-} ions from $CaCl_2$-DW and Na_2CO_3-DW phases, respectively, and diffusion of both ions during the $CaCl_2$-Na_2CO_3 are the main reasons for the increase in the T_{ds} values of the treated soil increased. The high T_{ds} reduced the efficiency of the EK treatment (Rhoades and Ingvalson 1971).

The high salinity reduces the efficiency of the EK treatment and its applications in soils (Rhoades and Ingvalson 1971). Bergado *et al*. (2003) and Jayasekera and Hall (2007) define the optimum limit for soil salinity to be in the range of 6.00 ppt to 10.72 ppt, and that the soil is considered to be extremely saline if T_{ds} exceeds these limits.

In this study, T_{ds} values within a range of 1.34 ppt to 5.15 ppt were achieved, thus making the performance of the EK treatment of soft soils to be very effective in improving the deficient soil properties. The charged ions in the soil pores reacted with the clay minerals salinized the porous soil medium to form cementitious precipitates, which resulted in the aggregation and flocculation of the fine-grained clay particles.

5.6.2.3 Salinity

The electroosmotic flow of the ionic solutions into the soil altered the salinity in the treated soil blocks. Figures 5.13 presents the salinity results, measured along with anode to cathode distances, $d_{A\leftrightarrow E}$ within the soil blocks with different ionic solution phases. The value of salinity was determined to be 2.16 ppt in the untreated soil. Also, the increase in salinity values was estimated carefully for different EK treated soils.

Figure 5.13a presents the $CaCl_2$-DW setup; the estimated S_c increased from 2.47 ppt to 4.51 ppt from point A to E distance. While salinity increased were from 1.32 ppt to 2.75 ppt from point E to A distance. The results indicated that there was a higher electroosmotic flow, q_{eo} from point A to E, $d_{A\leftrightarrow E}$, than from point E to A, $d_{E\leftrightarrow A}$.

Figure 5.13b presents the Na_2CO_3-DW setup; the salinity increased from 2.10 ppt to 2.21 ppt from point A to E distance. While salinity increased from 1.57 ppt to 5.20 ppt from point E to A distance. The results showed that there was a higher electroosmotic flow, q_{eo} from point E to A, cathode to anode than from point A to E, anode to cathode.

Figure 5.13c presents the $CaCl_2$-Na_2CO_3, the significant increase in the salinity from 2.43 ppt to 3.90 ppt from point A to E distance. In comparison, salinity increased from 1.73 ppt to 5.10 ppt from point E to A distance. The estimated results indicated that there was a higher electroosmotic flow from point E to A than from point A to E.

The most effective zone for $CaCl_2$-DW and Na_2CO_3-DW setups is 0-12 cm distance from point A to E and point E to A, respectively. Meanwhile, the overall effective zone for the $CaCl_2$-Na_2CO_3 setup is from the 0-18 cm distance from anode and cathode.

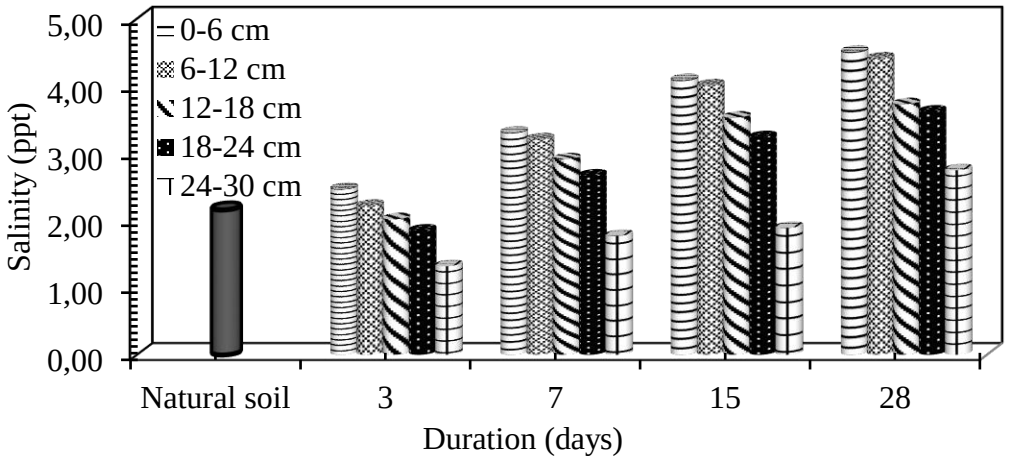

(a)

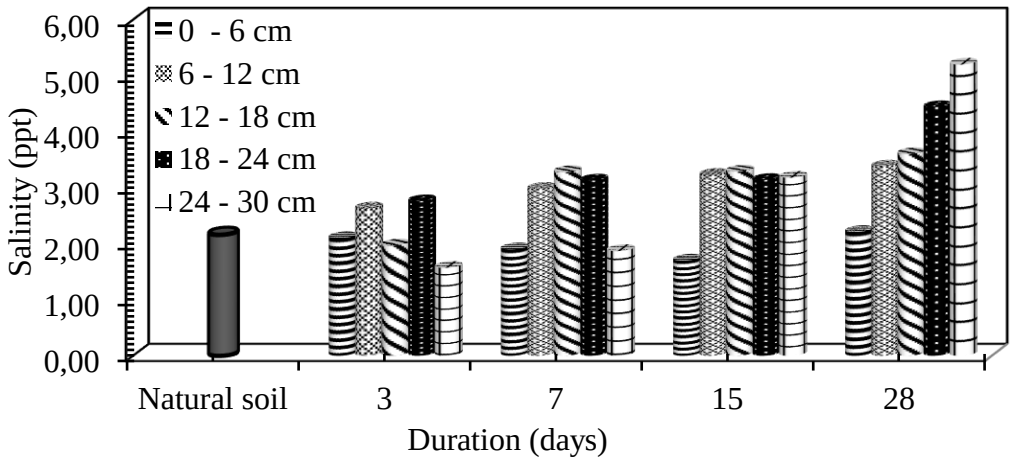

(b)

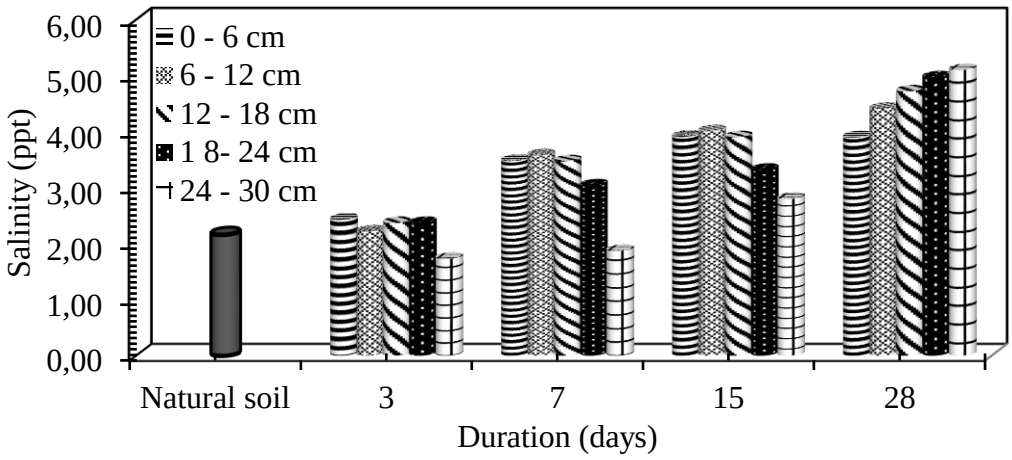

(c)

Figure 5.13: The variations of salinity at the anode to cathode distances using different combinations of ionic solutions of (a) $CaCl_2$-DW, (b) Na_2CO_3-DW, and (c) $CaCl_2$-Na_2CO_3.

5.6.2.4 Electrical conductivity, σ

Electrical conductivity, σ of soils, can be affected by many factors such as pore fluid resistivity, particle shape, and pore size, soil composition, soil porosity, total dissolved solids, temperature, and water content (Yan *et al.*, 2012). During the EK technique, the concentration, electrical and hydraulic gradient developed within the soil pores resulting in changes in soil composition, and as a result, the index and engineering properties of the soil blocks were changed. Figure 5.14 presents the variations of the electrical conductivity, σ of the soil pore fluid measured over EK treatment durations.

Figure 5.14a presents the $CaCl_2$-DW setup; the σ of the treated soils increased as the EK treatment duration time increased from A to E distance. The EK treated soil had a significant increment in σ within the range close to the anolyte ($CaCl_2$) and reduced within the distance towards the catholyte (DW region) during the EK testing durations.

In the Na_2CO_3-DW setup (Figure 5.14b), the σ values obtained increased from the catholyte end and decreased towards the anode end. The result is due to the electroosmotic flow of more concentrated electrolytes during the EK soil treatment.

The q_{eo} of the anolyte and catholyte in the $CaCl_2$-Na_2CO_3 setup (Figure 5.14c) showed that σ values increased more at the cathode end compared to the anode end because of the solubility nature of the electrolytes (Table 3.3). The cumulative rate of flow q_{eo}, adsorption of stabilizing ions, cementitious product formation, and more substantial bonding effect are the factors that necessitated a more effortless flow of electric charges within the soil particles and increased the electrical conductivity, σ values.

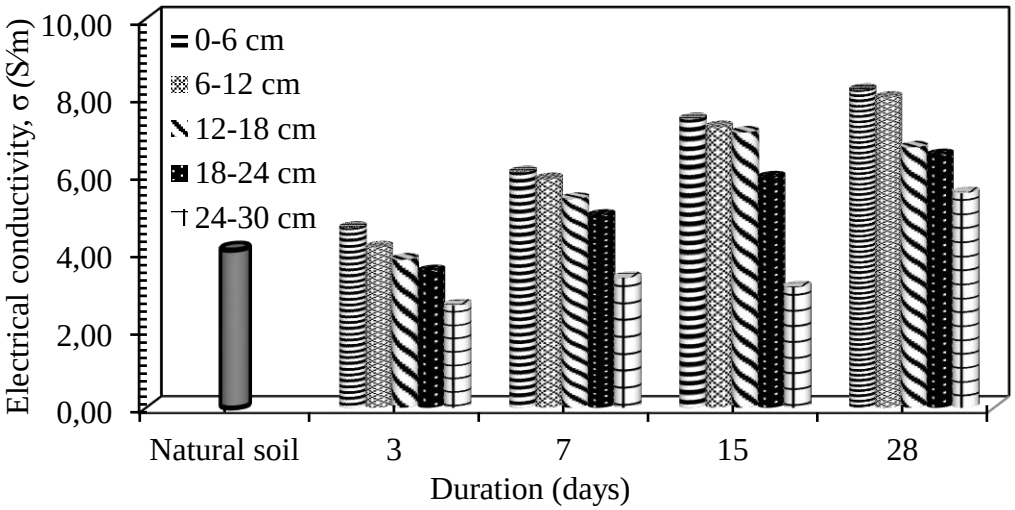

(a)

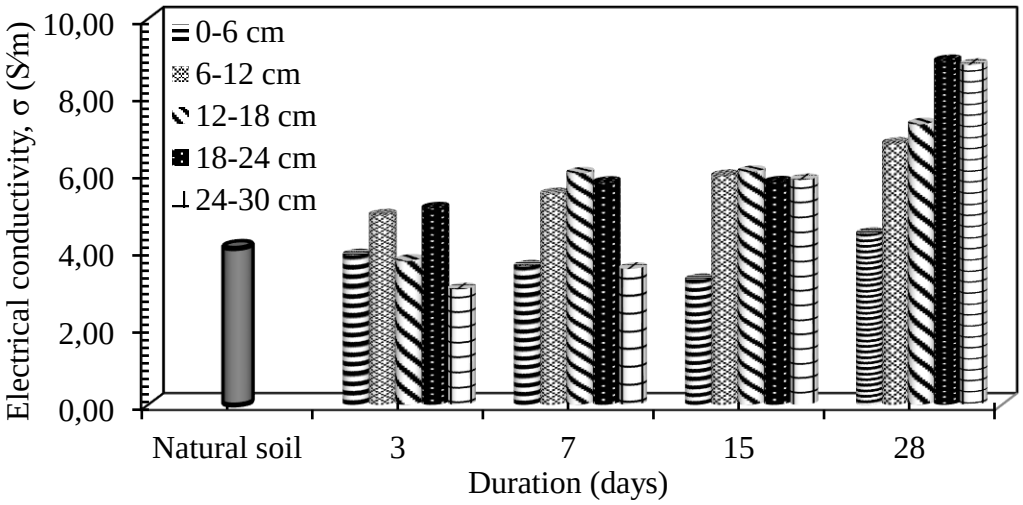

(b)

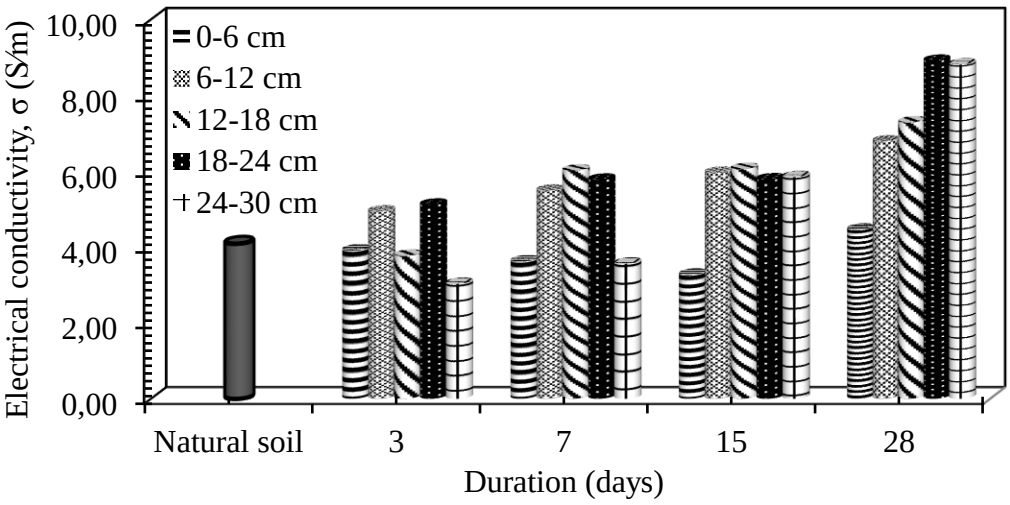

(c)

Figure 5.14: The variations of σ at the anode to cathode distances using different combinations of ionic solutions of (a) $CaCl_2$-DW, (b) Na_2CO_3-DW, and (c) $CaCl_2$-Na_2CO_3.

5.6.2.5 Ionic strength, I_s

The electroosmotic flow of the ionic solutions into the soil altered the ionic strength, I_s of the treated soil blocks. Figures 5.15 presents the I_s results measured along with anode-cathode distances within the soil blocks with different combinations of ionic solutions. The value of I_s was determined to be $0.05\ mol/mL$ in the natural soft soil.

Figure 5.15a presents the $CaCl_2$-DW setup; the estimated I_s values increased from 5.75 mol/mL to 10.28 mol/mL from point A to E, $d_{A\leftrightarrow E}$ distance. While the increased I_s values were from 3.35 mol/mL to 9.48 mol/mL from point E to A, $d_{E\leftrightarrow A}$ distance. The results indicated that there was a higher electroosmotic flow of ionic solutions from point A to E, $d_{A\leftrightarrow E}$ region than from point E to A, $d_{E\leftrightarrow A}$ region (Section 3.4.1.1).

Figure 5.15b presents the Na_2CO_3-DW setup; the I_s values increased from 4.9 mol/mL to 5.6 mol/mL from point A to E distance. While I_s values increased from 3.78 mol/L to 11.08 mol/mL from point E to A distance. The results indicated that there was a higher electroosmotic flow of ionic solution from point E to A than from point A to E.

Figure 5.15c presents the $CaCl_2$-Na_2CO_3, the significant increase in the I_s values from 5.72 mol/mL to 9.83 mol/mL from point A to E distance. While I_s values increased from 4.13 mol/mL to 12.88 mol/mL from point E to A distance. The results indicated that there was a higher electroosmotic flow of ionic solutions from point E to A than from point A to E. The most effective zones for $CaCl_2$-DW and Na_2CO_3-DW setups were 0-6 cm and 0-12 cm distances from point A to E and point E to A, respectively. The effective zones for $CaCl_2$-Na_2CO_3 setup were 0-6 cm, 0-12 cm and 0-18 cm areas.

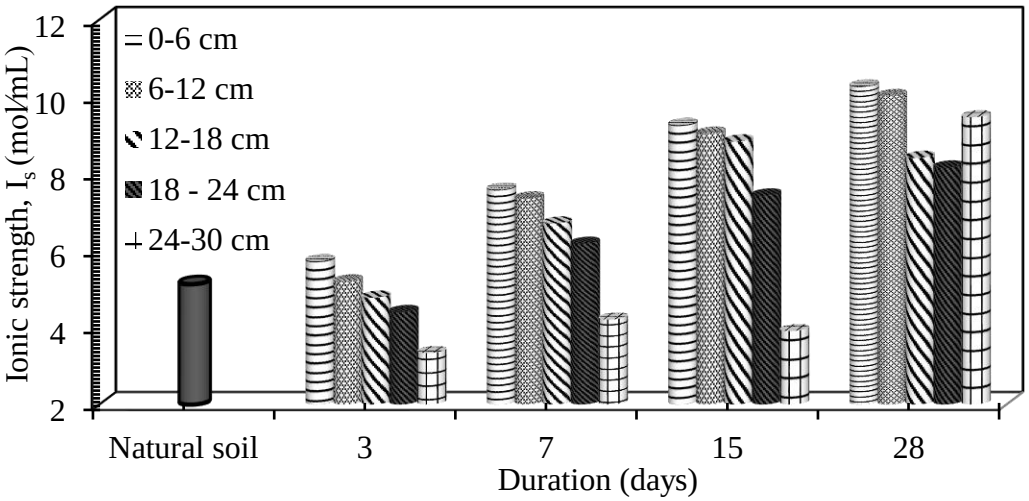

(a)

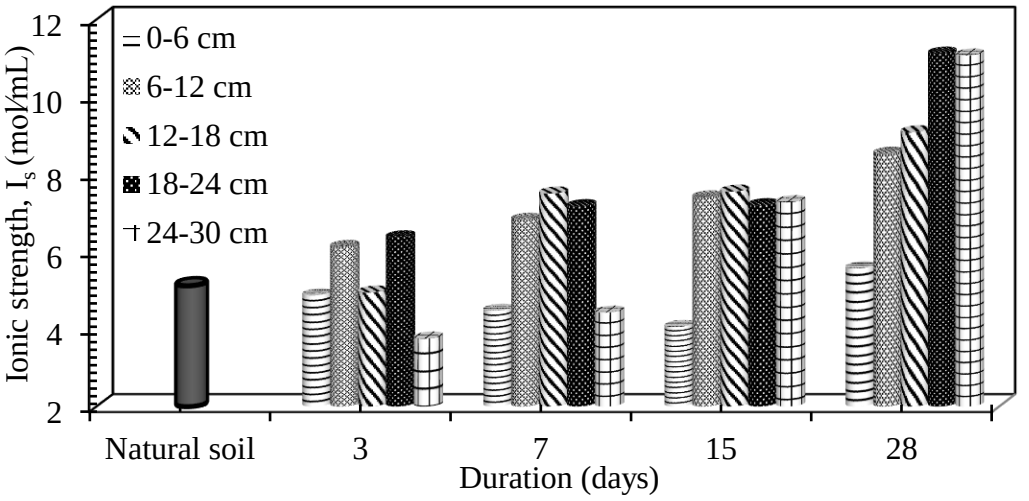

(b)

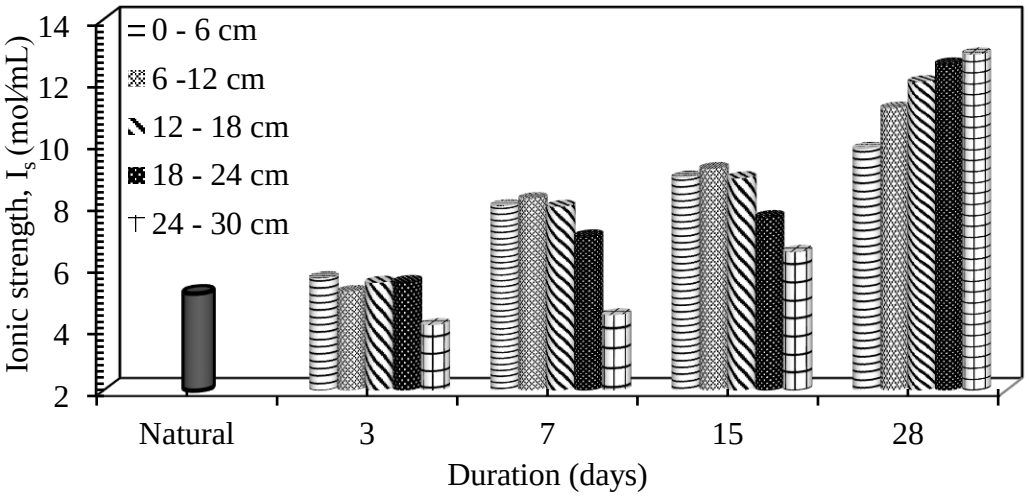

(c)

Figure 5.15: The variations of I_s at the anode to cathode distances using different ionic solutions of (a) $CaCl_2$-DW, (b) Na_2CO_3-DW, and (c) $CaCl_2$-Na_2CO_3.

5.6.2.6 Cation exchange capacity, CEC, and specific surface area, S_a

Table 5.4 presents the measured cation exchange capacity, CEC, and specific surface area, S_a values of EK treated soils at the anode to cathode, $d_{A\leftrightarrow E}$ distances using different combinations of ionic solutions in 28 days. The measured CEC values of the natural soil and EK treated soils at the more active regions for $CaCl_2$-DW (0–6 cm), Na_2CO_3-DW (25–30 cm), and $CaCl_2$-Na_2CO_3 (0–6 cm) setups were 14.7 $meq/100g$, 4.9 $meq/100g$, 9.1 $meq/100g$, and 3.5 $meq/100g$, respectively at 28 days.

Also, the specific surface area, S_a, of the treated soils were determined to be 17.5 m^2/g, 5.3 m^2/g, 10.8 m^2/g, and 4.5 m^2/g for the natural soil, $CaCl_2$-DW, Na_2CO_3-DW, and $CaCl_2$-Na_2CO_3 EK treated soils, respectively, at similar, $d_{A\leftrightarrow E}$ with CEC values.

The test results indicated that the cation exchange capacity and the specific surface area values of the EK treated soils were lower when compared to that of the natural soil due to ions exchange between the ionic solutions and the soil, which resulted in alteration in the physicochemical properties and the mineralogy of the EK treated soils.

The test results showed that pozzolanic, aggregation and cementation of particles occurred in the EK treated soils. The untreated soil has a more considerable amount of clay fines and larger S_a, thus has a higher CEC value. Whereas the EK treated soils became more flocculated and aggregated, with a reduced percentage of clay fines and as such, resulted in a remarkable reduction in the plasticity of the EK treated soils.

Table 5.4: Measured CEC and S_a values of EK treated soils using ionic solutions in 28 days.

Test setups with different phase of ionic solutions	Cation exchange capacity, CEC Anode to cathode distances (cm)					Specific surface area, S_a Anode to cathode distances (cm)				
	5	10	15	20	25	5	10	15	20	25
$CaCl_2$-DW	4.9	5.7	5.8	6.0	6.3	5.3	7.7	7.8	10.8	11.0
Na_2CO_3-DW	13.1	11.9	10.9	9.1	9.1	13.7	13.3	12.6	11.3	10.8
$CaCl_2$-Na_2CO_3	3.5	3.6	3.8	3.7	3.8	4.5	4.5	5.4	6.6	8.7

5.6.3 EK effects on engineering and physical properties of soft soils

5.6.3.1 EK effects on the Atterberg limit of soft soils

The variation of Atterberg limits of EK treated soils within the anode to cathode distances using different combinations of ionic solutions of $CaCl_2$-DW, Na_2CO_3-DW, and $CaCl_2$-Na_2CO_3 in 28 days is given in Figure 5.16. The determined values of treated soils were independently compared with the value obtained for the natural soft soil.

As discussed in Section 3.5.3, the plasticity index, PI, is a function of the physicochemical properties of the clay-ionic solutions and the mineralogy of the soils. The soil minerals have a higher affinity to absorb water to their surface, and within their diffuse double layer, DDL, they can retain more moisture before attaining the liquid limit, LL. Thus, the clay particles with net negative charges have a higher capacity to absorb more moisture and hence, produce higher liquid limit, LL values.

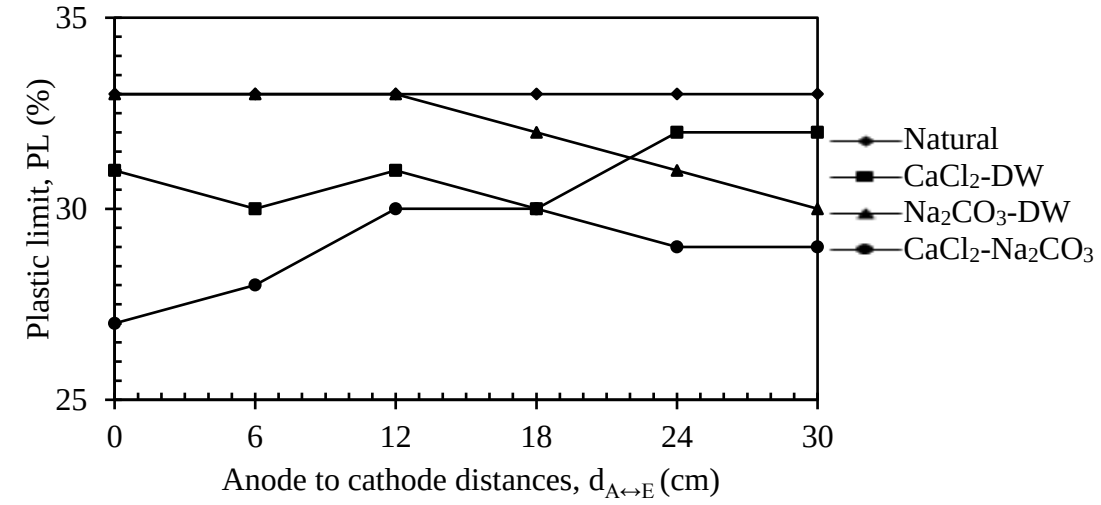

(a)

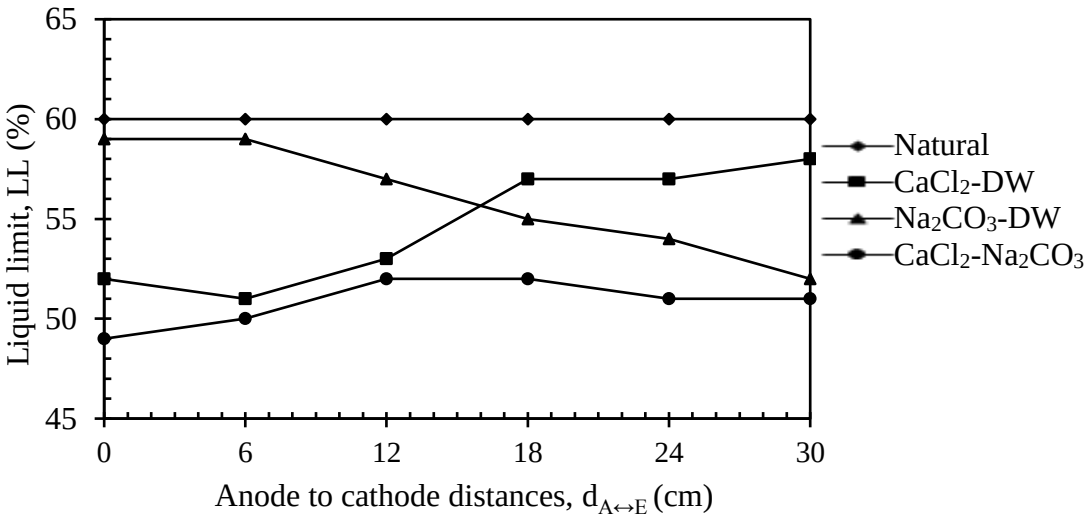

(b)

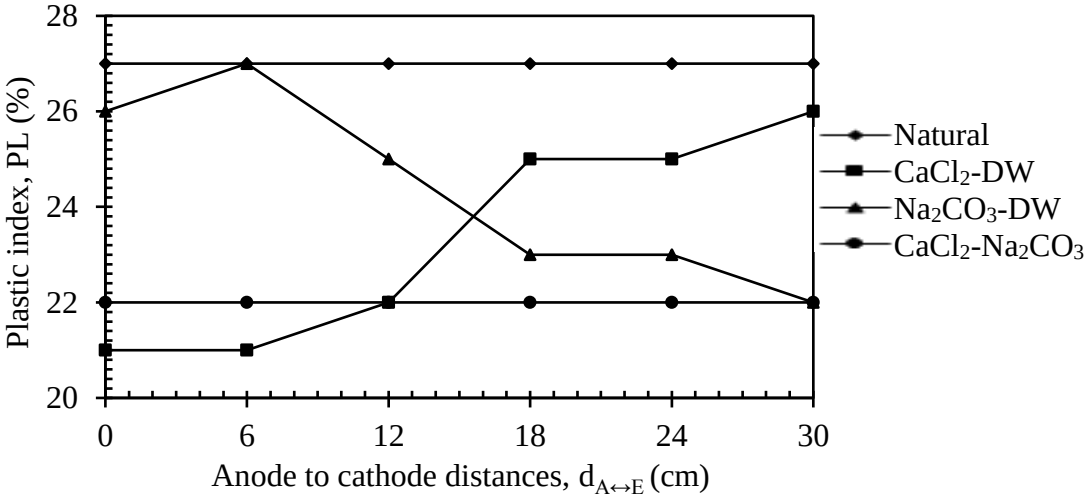

(c)

Figure 5.16: The variations of (a) PL (b) LL and (c) PI of the EK treated soils using a different combination of ionic solutions along the anode to cathode distances.

In the $CaCl_2$-DW setup, the supply of $CaCl_2$ ionic solution into the soil block decreased the soil plasticity of the treated soil, especially in the vicinity close to the anode chamber, whereas in the Na_2CO_3-DW setup, reduction in soil plasticity was observed in the EK treated soil at the cathode chamber, where the Na_2CO_3 ionic solution existed.

On the other hand, in the $CaCl_2$-Na_2CO_3 setup, reduction in the soil plasticity was obtained at both anode and cathode vicinities because of the flow from anode to cathode and cathode to anode directions. Table 5.5 presents the variations in the plasticity index; PI values of the EK treated soft soils. The PI values of the EK treated soils reduced from 27% of the natural soil to 20%, 23%, and 22% for the EK treated soils with ionic solutions: $CaCl_2$-DW, Na_2CO_3-DW, and $CaCl_2$-Na_2CO_3, respectively.

Table 5.5: Variation of plasticity index (PI) of the EK treated soils between the anode to cathode distances.

Ionic solutions	Anolyte solution	Catholyte solution	Plasticity index at different anode to cathode distances (%) Anode to cathode distances of the treated soil (cm)				
			0–6	6–12	12–18	18–24	24–30
$CaCl_2$-DW	$CaCl_2$	DW	20	21	21	24	25
Na_2CO_3-DW	DW	Na_2CO_3	26	24	23	23	22
$CaCl_2$-Na_2CO_3	$CaCl_2$	Na_2CO_3	22	22	22	23	23

5.6.3.2 EK effects on the unconfined compressive strength of soft soils

Figures 5.17 to 5.19 present the stress-strain curves obtained from the unconfined compression tests conducted on the natural soil, and on the EK treated soils. The results obtained indicated that there was a considerable improvement in the unconfined compressive strength, q_u from the samples extracted from the EK treated soil blocks

within the anode to cathode distances, $d_{A\leftrightarrow E}$, at different combinations of ionic solution test setups and different EK treatment durations of 7, 15, and 28 days.

Figures 5.17a and Figure 5.18a present the effect of $CaCl_2$-DW ionic solutions on the q_u values of the EK treated soils within the treatment duration of 7 and 15 days, respectively. In both cases, the $CaCl_2$ ionic solutions in their anode chambers caused an increase in q_u values of the EK treated soil at the anode region; however, the q_u values increased at the cathode end, but the values were lower than at the anode region.

The highest strength was achieved within the anode to cathode distances, $d_{A\leftrightarrow E}$, of 0–6 cm and 6–12 cm at different combinations of ionic solutions for treatment durations of 7 and 15 days. The percent increment in q_u of soil with $CaCl_2$-DW ionic solution within the $d_{A\leftrightarrow E}$ of 0–6 cm and 6–12 cm in 7 days (Figure 5.17a and Table 5.6) were 59% and 51%, respectively. While in 15 days treatment duration, the percent increment in q_u values of soil with $CaCl_2$-DW ionic solution within the $d_{A\leftrightarrow E}$ of 0–6 cm and 6–12 cm ranges were 66% and 58%, respectively (Figure 5.18a and Table 5.7).

Whereas in the Na_2CO_3-DW setup, the Na_2CO_3 ionic solution in the cathode chamber caused a considerable increase in the q_u values of the treated soils at the cathode vicinity, compared to the anode vicinity, as shown in Figure 5.17b and 5.18b. The highest strength was achieved within the $d_{A\leftrightarrow E}$ of 24–30 cm close to the cathode region in the treatment duration of 7 and 15 days (Tables 5.6 and 5.7). For the Na_2CO_3-DW setup, the highest percent increment in q_u values within the $d_{A\leftrightarrow E}$ of 0–6 cm and 6–12 cm distances in treatment durations of 7 and 15 days were 50% and 60%, respectively.

However, in the case of the $CaCl_2$-Na_2CO_3 setup, the q_u values of the EK treated soils increased in the entire EK treated soil block (Figure 5.17c and Figure 5.18c). It can be observed that the gained in strength was within the $d_{A\leftrightarrow E}$ of 0–6 cm, 12–18 cm, and 24–30 cm that is within the entire treated soil block (Tables 5.6 and 5.7). For, $CaCl_2$-Na_2CO_3 setup, the highest percent increment in q_u values within the $d_{A\leftrightarrow E}$ of the treated soils in 7 and 15 days were 49% and 68%, respectively. The highest q_u values were obtained for the soils treated with $CaCl_2$-DW and $CaCl_2$-Na_2CO_3 ionic solutions.

Table 5.6: q_u values of EK treated soils within anode to cathode distances at 7 days.

Ionic solutions	Anolyte solution	Catholyte solution	q_u at different anode to cathode distances (kPa) Anode to cathode distances, $d_{A\leftrightarrow E}$ (cm)				
			0–6	6–12	12–18	18–24	24–30
$CaCl_2$-DW	$CaCl_2$	DW	51	-	43	-	32
Na_2CO_3-DW	DW	Na_2CO_3	25	-	27	-	42
$CaCl_2$-Na_2CO_3	$CaCl_2$	Na_2CO_3	41	-	36	-	35

Table 5.7: q_u values of EK treated soils within anode to cathode distances at 15 days.

Ionic solutions	Anolyte solution	Catholyte solution	q_u at different anode to cathode distances (kPa) Anode to cathode distances, $d_{A\leftrightarrow E}$ (cm)				
			0–6	6–12	12–18	18–24	24–30
$CaCl_2$-DW	$CaCl_2$	DW	61	-	50	-	39
Na_2CO_3-DW	DW	Na_2CO_3	28	-	31	-	53
$CaCl_2$-Na_2CO_3	$CaCl_2$	Na_2CO_3	66	-	55	-	55

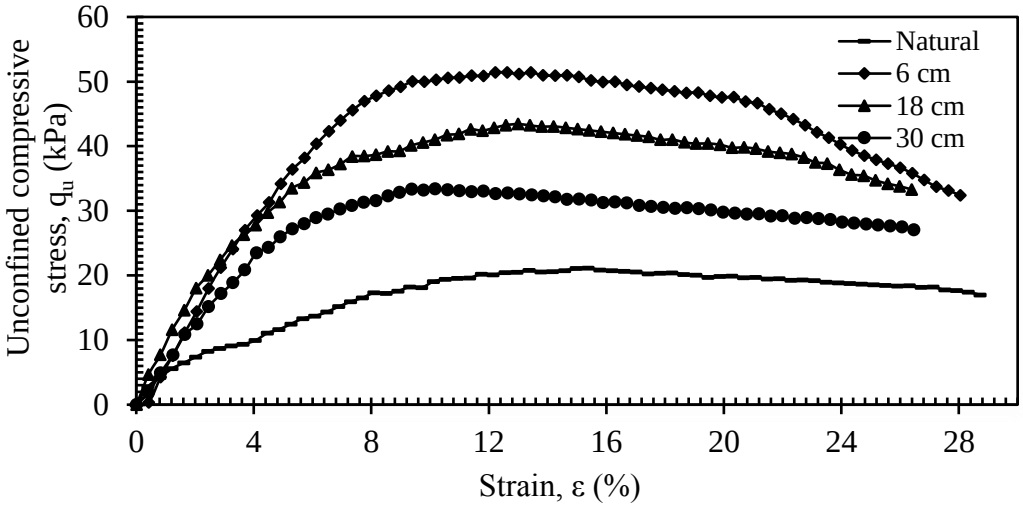

(a)

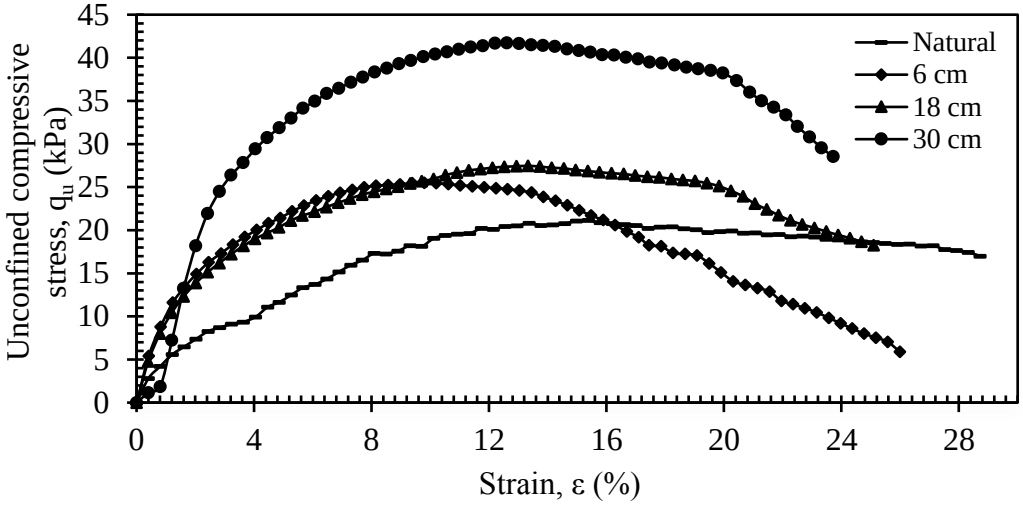

(b)

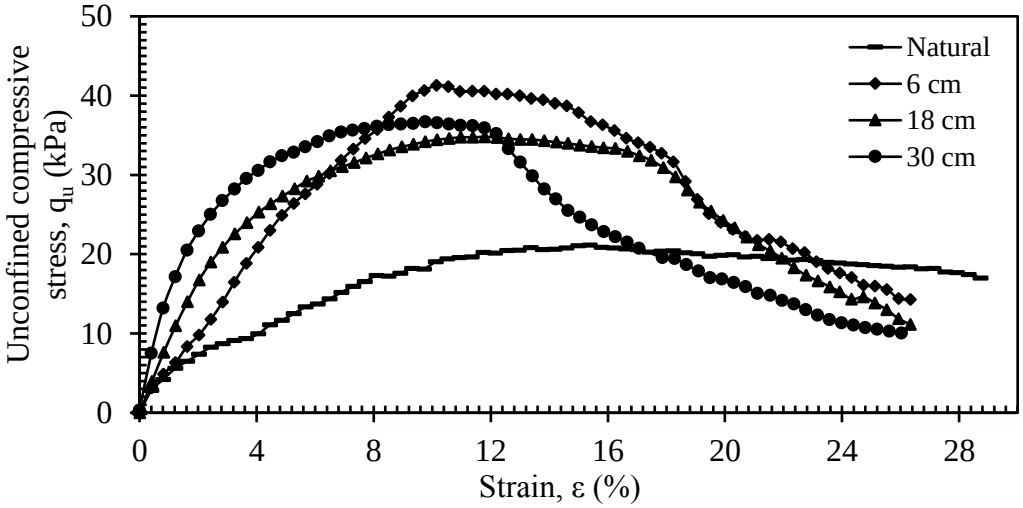

(c)

Figure 5.17: Stress-strain curves of the treated soil samples from anode to cathode distances using different electrolytes phases of (a) $CaCl_2$-DW, (b) Na_2CO_3-DW, and (c) $CaCl_2$-Na_2CO_3 at 7 days.

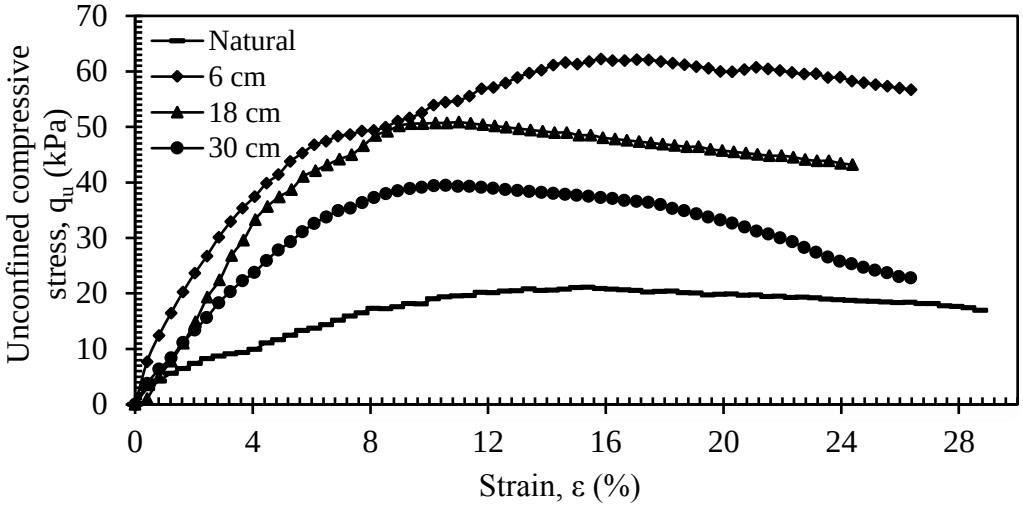

(a)

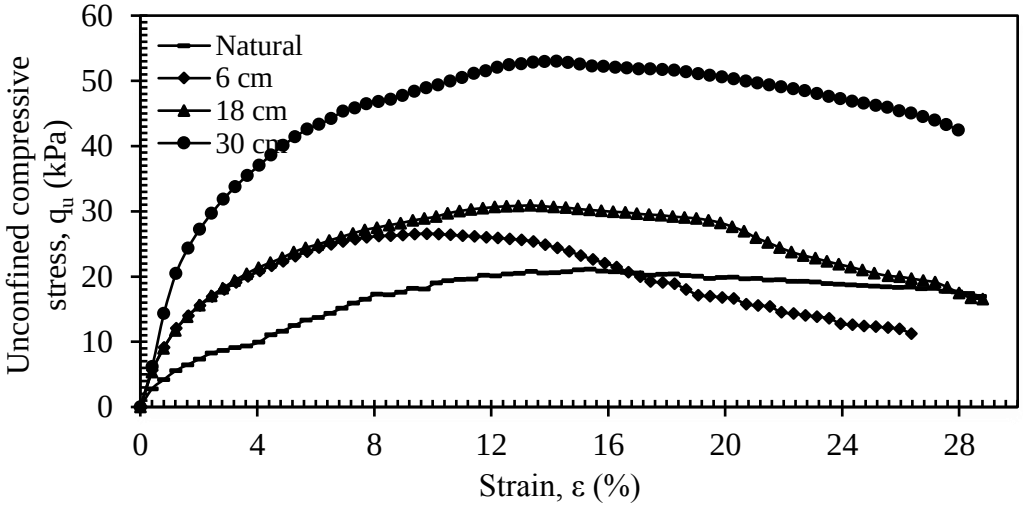

(b)

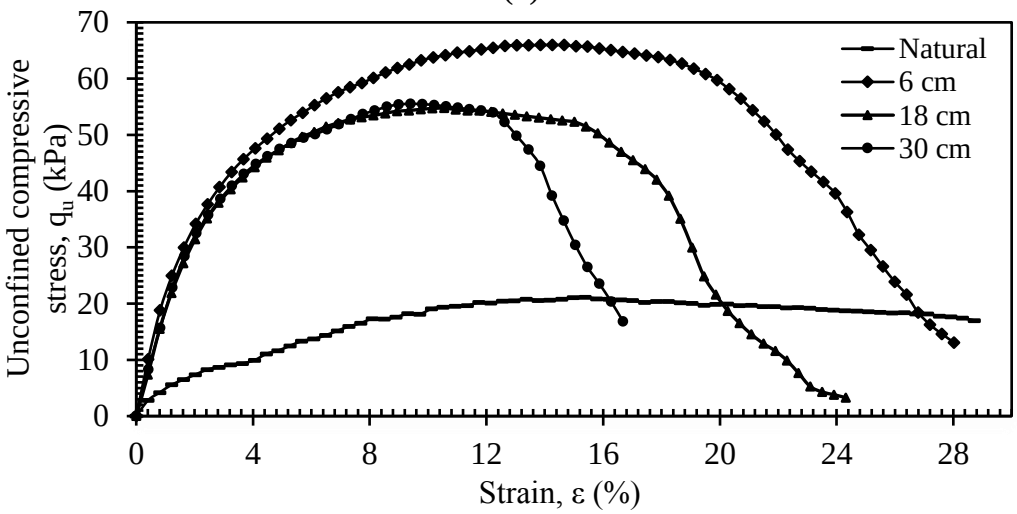

(c)

Figure 5.18: Stress-strain curves of the treated soil samples from anode to cathode distances using different ionic solutions phases of (a) $CaCl_2$-DW, (b) Na_2CO_3-DW, and (c) $CaCl_2$-Na_2CO_3 at 15 days.

The gain in strength in $CaCl_2$ treated soils is an indication that the Ca^{2+} based ionic solutions were considerably more effective in the treated soils when compared to the CO_3^{2-} based ionic solution. This is due to the valency of the Ca^{2+} ions exchange reaction between the Ca^{2+} ions and the clay minerals which caused an alteration in the soil structure and resulted in higher q_u values during the EK treatment of the soft soils.

Figure 5.19 presents the effect of a different combination of ionic solutions on the q_u values of the EK treated soils at a treatment duration of 28 days. Figure 5.19a presents the effect of $CaCl_2$-DW ionic solution on the q_u values of the EK treated soils. The $CaCl_2$ solutions in the anode compartment caused a remarkable increase in q_u values of the EK treated soil at anode vicinity; however, q_u values increased at the cathode end but of lower values than at the anode. In this setup, the highest percent increment of q_u values of the treated soil were in the range of 61% to 76% in 28 days (Table 5.6).

Whereas in the Na_2CO_3-DW setup, the Na_2CO_3 ionic solution in the cathode compartment caused the highest increase in the q_u values at the cathode region, and q_u values increased in the anode region but of lower values at the cathode region, as indicated in Figure 5.19b. In this setup, the highest percent increment of q_u values of the treated soil were in the range of 36% to 67% in 28 days, as provided in Table 5.8.

However, in the case of the $CaCl_2$-Na_2CO_3 setup, the q_u values of the EK treated soils increased throughout the entire EK treated soil block, either close to the anode or the cathode vicinity (Figure 5.19c). The highest q_u value was obtained for the soil block treated with $CaCl_2$-Na_2CO_3 ionic solutions. In this setup, the highest percent increment of q_u values of the EK treated soils were in the range of 72% to 77% in the 28 days.

Table 5.8: q_u values of EK treated soils at anode and cathode distances in 28 days.

Ionic solutions	Anolyte solution	Catholyte solution	q_u at different anode to cathode distances (kPa) Anode to cathode distances, $d_{A\leftrightarrow E}$ (cm)				
			0–6	6–12	12–18	18–24	24–30
$CaCl_2$-DW	$CaCl_2$	DW	90	83	73	60	55
Na_2CO_3-DW	DW	Na_2CO_3	33	37	47	57	63
$CaCl_2$-Na_2CO_3	$CaCl_2$	Na_2CO_3	92	87	84	80	76

The effect of both $CaCl_2$ and Na_2CO_3 ionic solutions contributed to the strength gain of the EK treated soil and resulted in an increase in the q_u values. EK soil treatment with these ionic solutions resulted in changes in the mineralogy and textural properties of the EK treated soil and caused a notable build up in their stability and durability.

The changes in the q_u values of the EK treated soils are due to the dissolution of silica and alumina in a highly alkaline medium, due to the exchangeable ions in clay minerals with Ca^{2+} ions to form cementitious gels. The EK treated soils became flocculated with reduced clay fines due to a reduction in diffused double layer (DDL) thickness and due to the higher bonding force of pozzolanic products with the clay platelets' surface. The coagulation of the clay particles with the binding materials, increased their bond energy and internal friction, leading to a gain in stiffness and strength in treated soils.

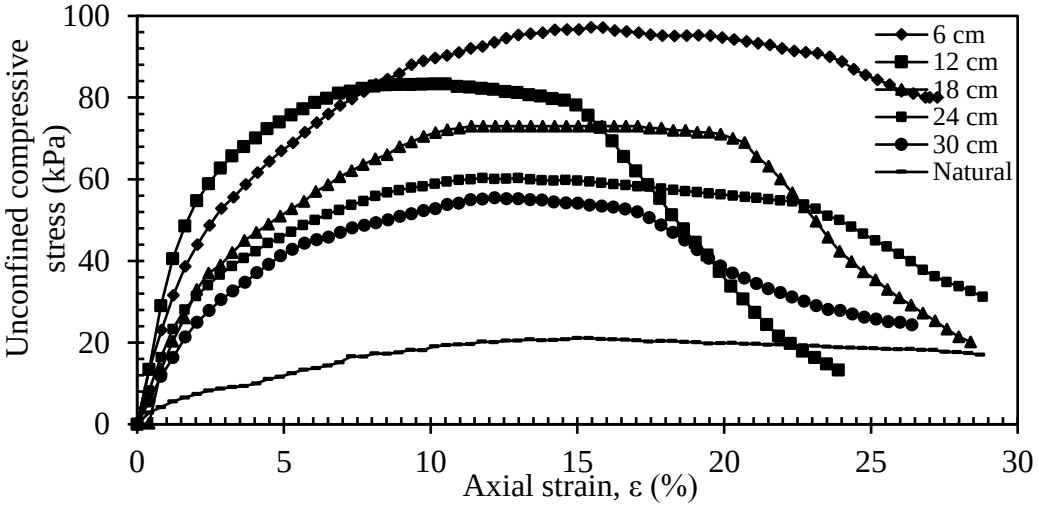

(a)

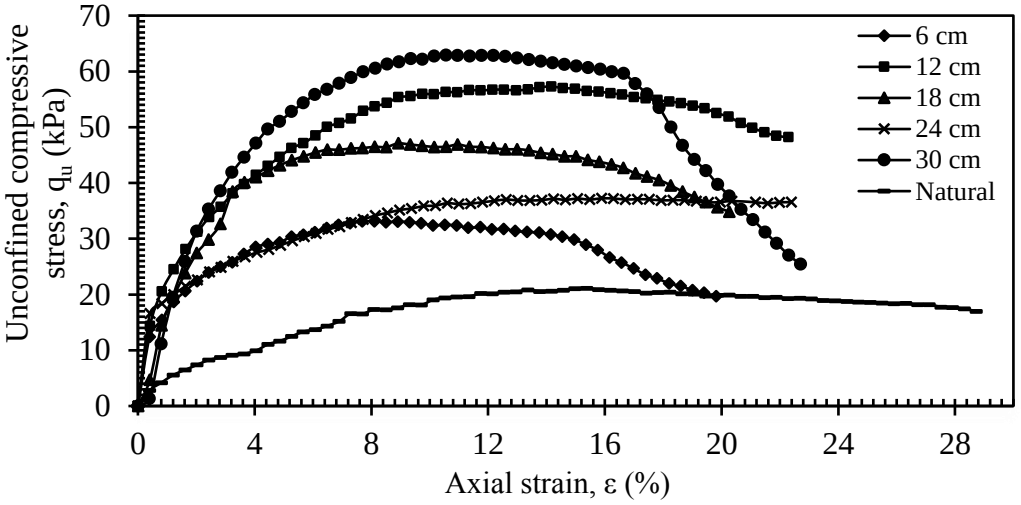

(b)

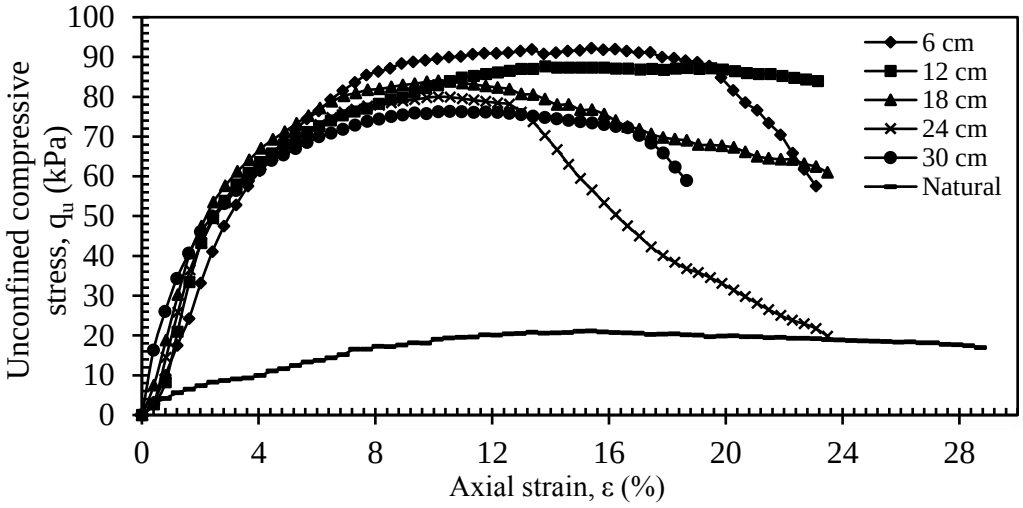

(c)

Figure 5.19: Stress-strain curves of the treated soil samples from the anode to cathode distances using different ionic solutions of (a) $CaCl_2$-DW, (b), Na_2CO_3-DW and (c) $CaCl_2$-Na_2CO_3 at 28 days.

Figure 5.20 presents the combined unconfined compressive strengths, q_u values of EK treated soils at the different lateral anode to cathode distances, at different EK treatment durations of 7, 15, and 28 days using different ionic solution combinations of $CaCl_2$-DW, Na_2CO_3-DW, and $CaCl_2$-Na_2CO_3. It was observed that the q_u values of the EK treated soils increased further as the treatment duration increased to 28 days.

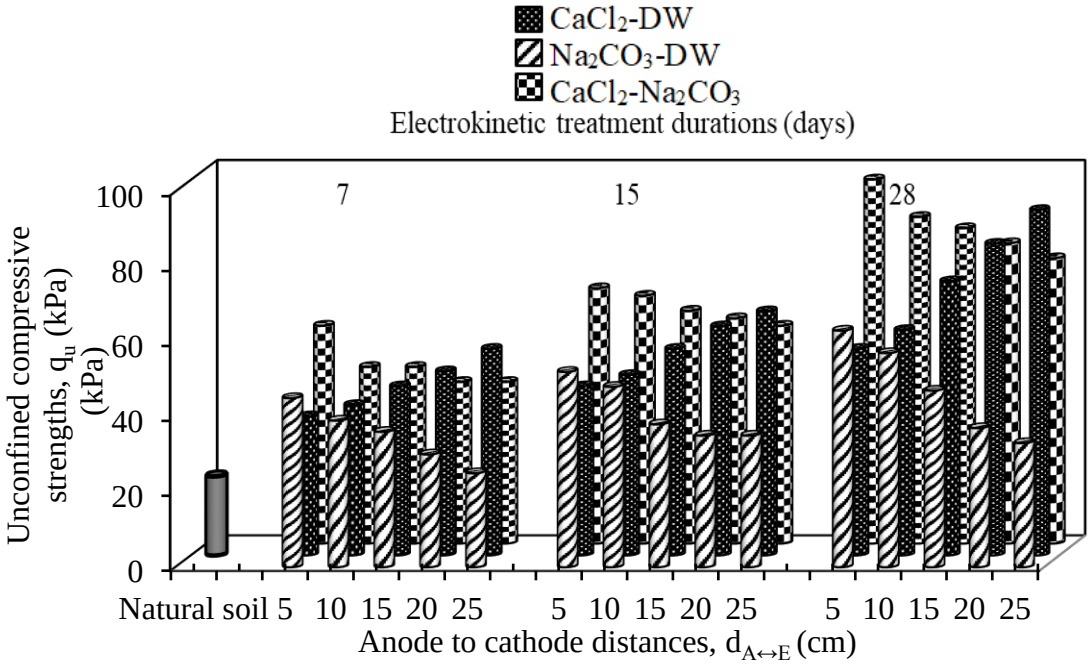

Figure 5.20: Unconfined compressive strengths, q_u values of EK treated soils along different anode to cathode distances, $d_{A\leftrightarrow E}$ at different EK treatment durations using different ionic solution combinations.

5.6.3.3 EK effects on the one-dimensional swell of the EK treated soils

Figures 5.21 presents the swell potential, SP of the EK treated soils after 28 days of the EK treatment subjected to different combinations of ionic solutions. In these curves, the percent vertical swell (VS) was plotted against time in minutes. The figures present the engineering behavior of the swelling characteristics of the EK treated soils extracted from three different locations within the anode to cathode distances of 0–6 cm, 12–18 cm, and 24–30 cm of treated soils in the EK treatment duration of 28 days.

Figure 5.21a presents the effect of $CaCl_2$-DW ionic solution setup on the swelling potential values of the EK treated soils. The $CaCl_2$ solutions in the anode compartment caused a significant reduction in the swelling potential of the EK treated soil at anode vicinity; however, swelling potential values were still high towards the cathode end. In this setup, the highest percent reduction in swelling potential obtained for the EK treated soils in 28 days was 63% at 0–6 cm from the anode end in the EK treated soil.

Whereas in the Na_2CO_3-DW setup, Na_2CO_3 ionic solution in the cathode compartment caused the highest reduction in the swelling potential values at the cathode region, rather than towards the anode region as shown in Figure 5.21b. In this setup, the highest percent reduction in swelling potential obtained for the EK treated soils in 28 days was 48% at 24–30 cm distance from the cathode region in the EK treated soil.

On the other hand, in the case of the $CaCl_2$-Na_2CO_3 setup, the swelling potential values of the EK treated soils decreased within the entire EK treated soil block (Figure 5.21c).

The smallest swelling potential values were obtained for the soil block treated with $CaCl_2$-Na_2CO_3 ionic solutions. In this setup, the highest percent reduction in swelling potential obtained for the EK treated soils in 28 days was approximately 59% at 0–6 cm and 60% at 24–30 cm distances from the anode and cathode region, respectively.

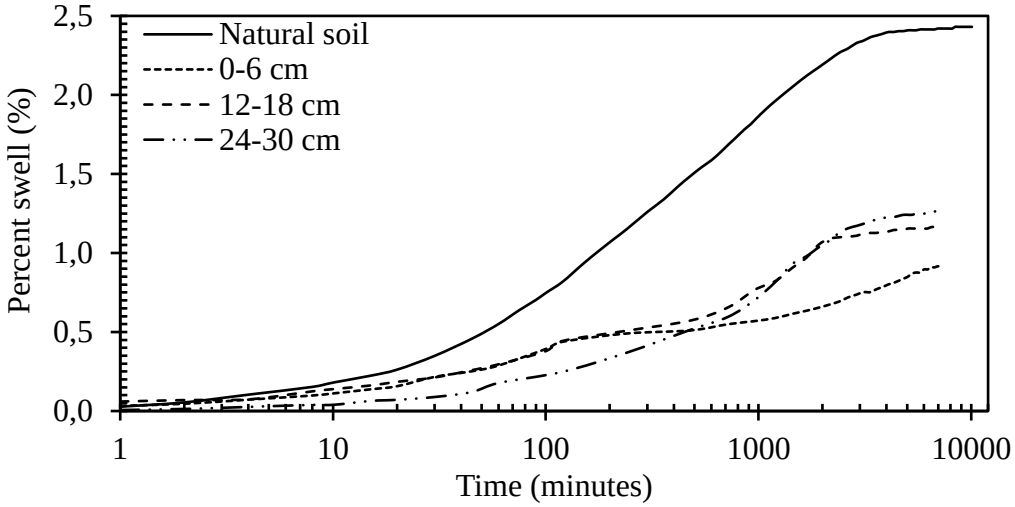

(a)

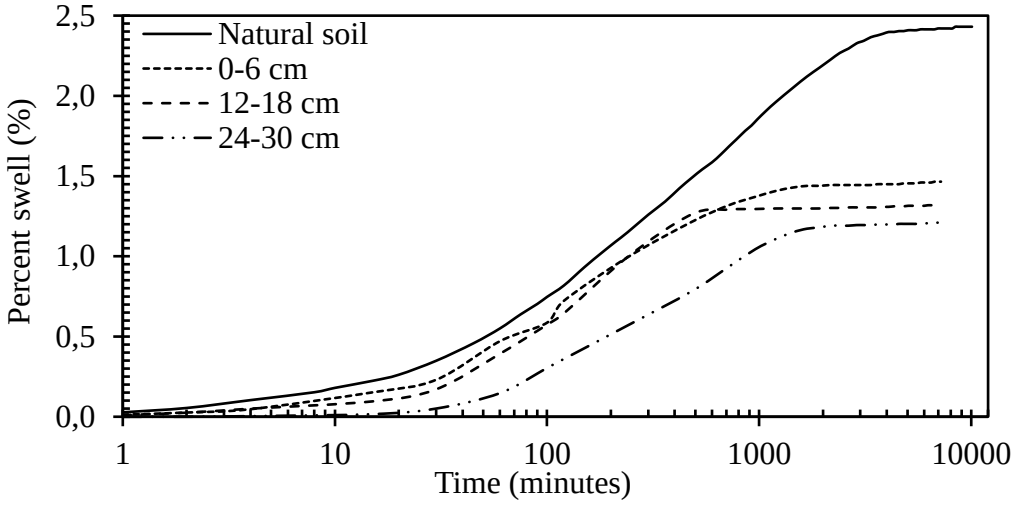

(b)

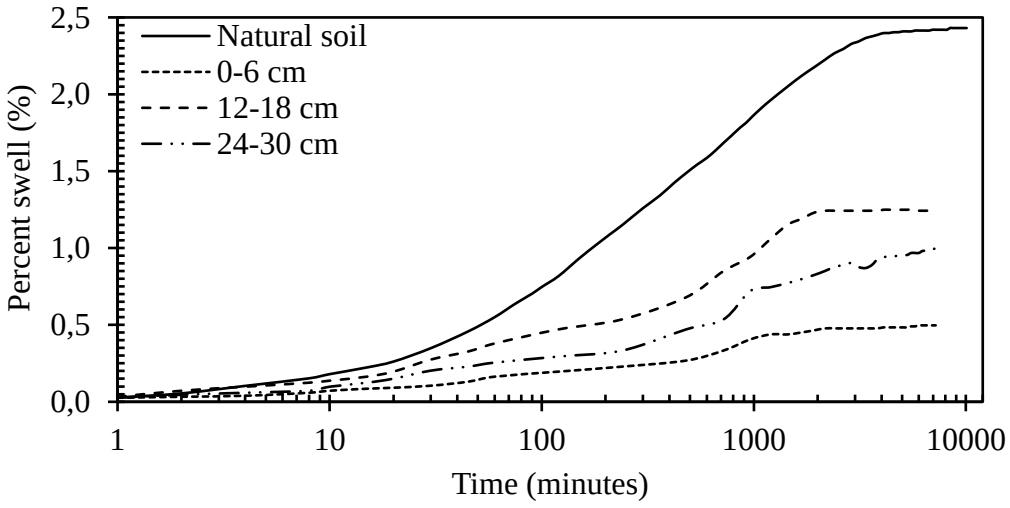

(c)

Figure 5.21: Variation of the EK treated soils from the anode to cathode distances using different ionic solutions of (a) $CaCl_2$-DW, (b) Na_2CO_3-DW, and (c) $CaCl_2$-Na_2CO_3.

Table 5.9 and Figure 5.22 provide the variation in the swelling potential values of the EK treated soils at the anode to cathode distances using different combinations of ionic solutions in 28 days. The smallest swelling potential values were obtained for the EK treated soils using $CaCl_2$-Na_2CO_3 ionic solutions test setup as indicated in Table 5.9.

Table 5.9: Variation of SP of the EK treated soils at the anode to cathode distances.

Ionic solutions	Anolyte solution	Catholyte solution	Swell potential at different anode to cathode distances (%) Anode to cathode distances, $d_{A\leftrightarrow E}$ (cm)		
			0 – 6	12 – 18	24 – 30
$CaCl_2$-DW	$CaCl_2$	DW	0.92	1.25	1.26
Na_2CO_3-DW	DW	Na_2CO_3	1.47	1.32	1.21
$CaCl_2$-Na_2CO_3	$CaCl_2$	Na_2CO_3	0.50	1.24	0.99

Both $CaCl_2$ and Na_2CO_3 ionic solutions contributed to the reduction of SP values of the EK treated soil and resulted in the smaller values of SP. The SP values of the natural soil dropped from 2.4% to 0.89%, 1.2%, and 0.48% with EK treated soils with the ionic solutions of $CaCl_2$-DW, Na_2CO_3-DW, and $CaCl_2$-Na_2CO_3, respectively.

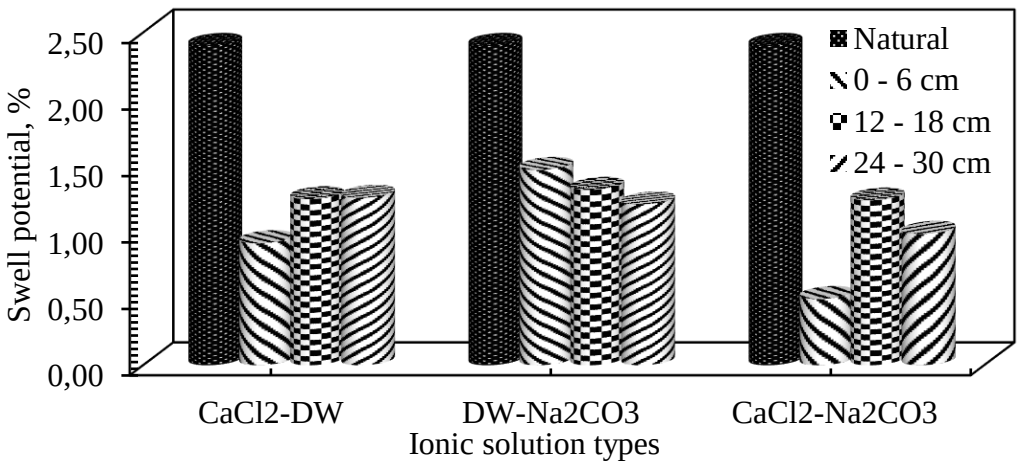

Figure 5.22: Variation of the EK treated soils from the anode to cathode distances, $d_{A\leftrightarrow E}$ using different ionic solutions.

5.6.3.4 EK effects on the one-dimensional consolidation of EK treated soils

The one-dimensional consolidation tests were conducted to investigate the outcomes of ionic solutions on the compressibility behavior of the EK treated soils as an effect of the electroosmotic flow of the ionic solutions from the cathode and anode reservoirs into the soft soil. The variation in the compressibility characteristics, consisting of preconsolidation pressure based on the anode to cathode distances, were studied in detail. Figures 5.23 presents the void ratio, *e* versus log pressure, *p* curves for the treated soils after 28 days of the EK treatment using different ionic solutions setups.

Figure 5.23a presents the effect of $CaCl_2$-DW ionic solution on the compressibility characteristics of the EK treated soils. With the $CaCl_2$ solutions in the anode compartment, it caused a significant reduction in the compression index, C_c, expansion index, C_r and swelling pressure values of the EK treated soil at anode vicinity; however, C_c, C_r, and swelling pressure values were still high towards the cathode end.

In Table 5.10, it can be seen that within 0–6 cm from the anode region, the highest percent reduction in compression index, C_c was 65%, whereas the highest reduction in the expansion index, C_r values were 45%. Also, there was a substantial reduction in the swelling pressure, average degree of consolidation, coefficient of compressibility, and consolidation of the treated soils at 0–6 cm distance from the $CaCl_2$ reservoir.

Whereas in the Na_2CO_3-DW setup, Na_2CO_3 ionic solution in the cathode compartment caused a considerable reduction in the C_c values close to the cathode region, rather than towards the anode region, as shown in Figure 5.23b. As indicated in Table 5.11, the compression index, C_c value reduced significantly by 50% at 24–30 cm and the C_r values decreased considerably by 38% near to the Na_2CO_3 ionic solution chamber.

In the case of the $CaCl_2$-Na_2CO_3 setup, the smallest C_c and C_r values were obtained from the EK treated soils, within the entire EK treated soil block (Figure 5.23c). Tables 5.10 to 5.12 provide the values for the coefficient of compression (m_v), coefficient of consolidation (C_v), the coefficient of permeability (k), the preconsolidation pressure ($\sigma p'$), and the swell pressure of the EK treated soils at 28 days. The m_v, C_v, and the k values were determined for the stress range of 200 kPa to 800 kPa from the curves.

The swell pressure values were determined from the void, *e* versus log pressure, *p* curves by one-dimensional consolidation test. Tables 5.10 to 5.12 showed that there was a considerable reduction in the swell pressure values of the EK treated with $CaCl_2$-DW, Na_2CO_3-DW, and $CaCl_2$-Na_2CO_3 ionic solutions, respectively.

Also, it can be observed that preconsolidation pressure, $\sigma p'$ values increased by 70%, 55%, and 85% for the treated soils with $CaCl_2$-DW, Na_2CO_3-DW, and $CaCl_2$-Na_2CO_3 ionic solutions, respectively. However, the average degree of consolidation, t_{90} increased in all conditions using the different combinations of ionic solutions setups.

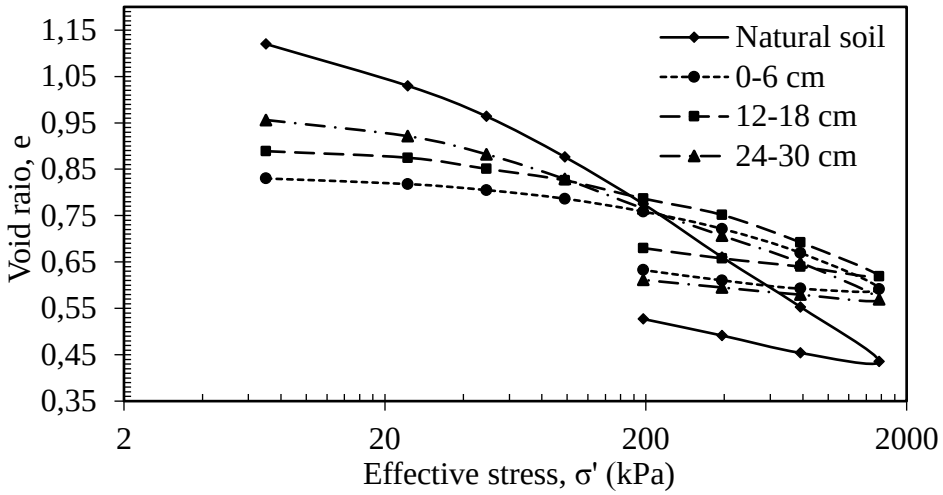

(a)

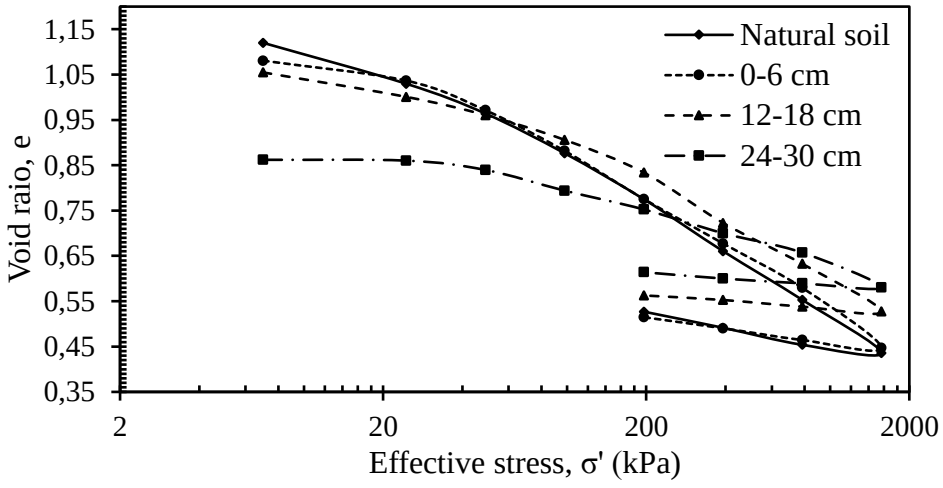

(b)

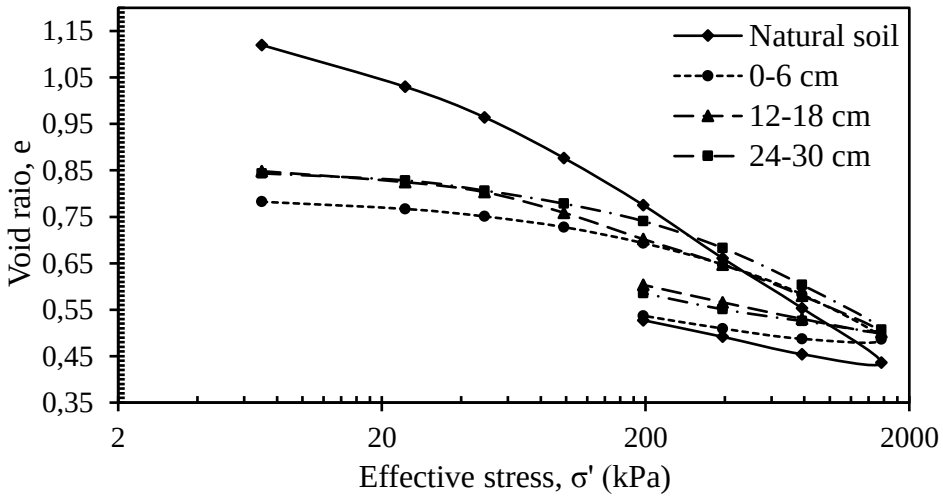

(c)

Figure 5.23: Variation of void ratio versus log pressure curves of the EK treated soils from the anode to cathode distances, $d_{A\leftrightarrow E}$ using different combinations of ionic solutions of (a) $CaCl_2$-DW, (b) Na_2CO_3-DW, and (c) $CaCl_2$-Na_2CO_3.

Table 5.10: Compressibility and swell of natural and EK treated soils extracted at the different anode to cathode distances using $CaCl_2$-DW.

Consolidation parameters	Natural soil	Anode to cathode distances, $d_{A\leftrightarrow E}$ (cm)		
		0–6	12–18	24–30
Compression index, C_c	0.37	0.13	0.18	0.19
Expansion index, C_r	0.13	0.13	0.084	0.084
Coeff. of consolidation, C_v (mm^2/min) 10^{-6}	4.25	8.31	5.75	4.54
Coeff. of compression, m_v (m^2/kN) 10^{-4}	8.22	3.43	3.31	3.27
Average t_{90} (minutes)	11.20	5.70	8.30	10.50
Coefficient of permeability, k (m/s) 10^{-8}	1.07	2.79	1.87	1.46
Preconsolidation Pressure (kPa)	80	160	120	82
Swell pressure (kPa)	62	35	39	57

Table 5.11: Compressibility and swell of natural and EK treated soils extracted at the different anode to cathode distances using Na_2CO_3-DW.

Consolidation parameters	Natural soil	Anode to cathode distances, $d_{A\leftrightarrow E}$ (cm)		
		0–6	12–18	24–30
Compression index, C_c	0.37	0.31	0.25	0.15
Expansion index, C_r	0.13	0.099	0.033	0.013
Coeff. of consolidation, C_v (mm^2/min) 10^{-6}	4.25	4.33	4.68	6.19
Coeff. of compression, m_v (m^2/kN) 10^{-4}	8.22	5.25	4.25	2.92
Average t_{90} (minutes)	11.20	11.00	10.20	7.70
Coefficient of permeability, k (m/s) 10^{-8}	1.07	2.23	1.95	1.77
Preconsolidation Pressure (kPa)	80	80	120	140
Swell pressure (kPa)	62	60	48	40

Table 5.12: Compressibility and swell of natural and EK treated soils extracted at the different anode to cathode distances using $CaCl_2$-Na_2CO_3.

Consolidation parameters	Natural soil	Anode to cathode distances, $d_{A\leftrightarrow E}$ (cm)		
		0–6	12–18	24–30
Compression index, C_c	0.37	0.14	0.19	0.17
Expansion index, C_r (mm^2/min)	0.13	0.073	0.083	0.033
Coeff. of consolidation, C_v (mm^2/min) 10^{-6}	4.25	9.93	5.61	7.57
Coeff. of compression, m_v (m^2/kN) 10^{-4}	8.22	3.10	3.82	3.82
Average t_{90} (minutes)	11.20	4.80	8.50	6.30
Coefficient of permeability, k (m/s) 10^{-8}	1.07	3.02	2.10	2.84
Preconsolidation Pressure (kPa)	80	195	160	160
Swell pressure (kPa)	62	30	42	37

5.6.3.5 EK effect on the wetting-drying cycle of soft soils

Figures 5.24, 5.25, and 5.26 show the wetting and drying cyclic behavior of the EK treated soil with different combinations of ionic solutions of $CaCl_2$-DW, Na_2CO_3-DW, and $CaCl_2$-Na_2CO_3, respectively. To comprehend the effect of the ionic solutions on the wetting-drying cyclic behavior, three types of plots are provided in each figure.

One presents the results of the swelling potential versus the number of cycles, and the other present the results of the shrinkage potential versus the number of cycles obtained from the treated soil samples at the anode to cathode distances. Also, the combined plots for the first two plot the ratio of the axial deformation, ΔH to the initial height of the soil specimen, H for the percent vertical swell/shrink versus the number of cycles.

Figure 5.24 shows the results of cyclic swell and shrinkage potential values versus the number of cycles of the EK treated soils with $CaCl_2$-DW ionic solutions. It was noted that the swelling and shrinkage potentials values of the treated soils decreased with some cycles when compared with the natural soils. The significant reduction in the swelling potential of the treated soils was recorded after the second cycle (Figure 5.24a), and for the shrinkage potential, the reduction was obtained after the first cycle (Figure 5.24b). Equilibrium in swelling/shrinkage was reached in the fourth cycle.

From the forth to the fifth cycle, no further swelling/shrinkage was observed and became constant. It was observed that the most significant reduction in the axial strain deformation was recorded at the anode region due to the $CaCl_2$ solutions in the anode chamber, whereas lesser reduction was recorded towards the cathode end (Figure 5.24c). In this setup, the highest percent reduction in the swelling and shrinkage values were 70% and 85%, respectively, at 0–6 cm from the anode region in the treated soil.

Whereas in the Na_2CO_3-DW setup, Na_2CO_3 ionic solution in the cathode chamber caused the highest reduction in the swelling and shrinkage potentials of the treated soils at the cathode region (Figure 5.25a and 5.25b). For this same ionic solution, the highest percent reduction in the swelling was obtained in 28 days were 58% and 60%, respectively, at 24–30 cm distance from the anode region in the EK treated soil.

The significant reduction in the swelling and shrinkage potentials of the treated soils was recorded after the second cycle (Figure 5.25a), this reduction was obtained after the first cycle (Figure 5.25b). Equilibrium in swelling and shrinkage was reached in the fourth cycle, with no further defined changes observed in the fourth to fifth cycle.

It was observed that the significant reduction in the axial deformation was recorded at the cathode region, as a result of the Na_2CO_3 solutions in the cathode chamber, whereas lesser reduction was obtained towards the anode end (Figure 5.25c). In this setup, the highest percent reduction in swelling and shrinkage values obtained for the treated soils in 28 days was 70% and 85%, respectively, at 0–6 cm from the anode region.

In the case of the $CaCl_2$-Na_2CO_3 setup, the swelling and shrinkage potential values of the EK treated soils decreased within the entire EK treated soil block (Figure 5.26). The smallest swelling and shrinkage potential values were obtained for the soil block treated with $CaCl_2$-Na_2CO_3 ionic solutions. In this setup, the highest percentage reduction in their values obtained for the EK treated soils in 28 days was 75% and 90% at 0–6 cm and 24–30 cm distances from the anode and cathode regions, respectively. The treated soils showed equilibrium from the third to the fifth cycle (Figure 5.26c).

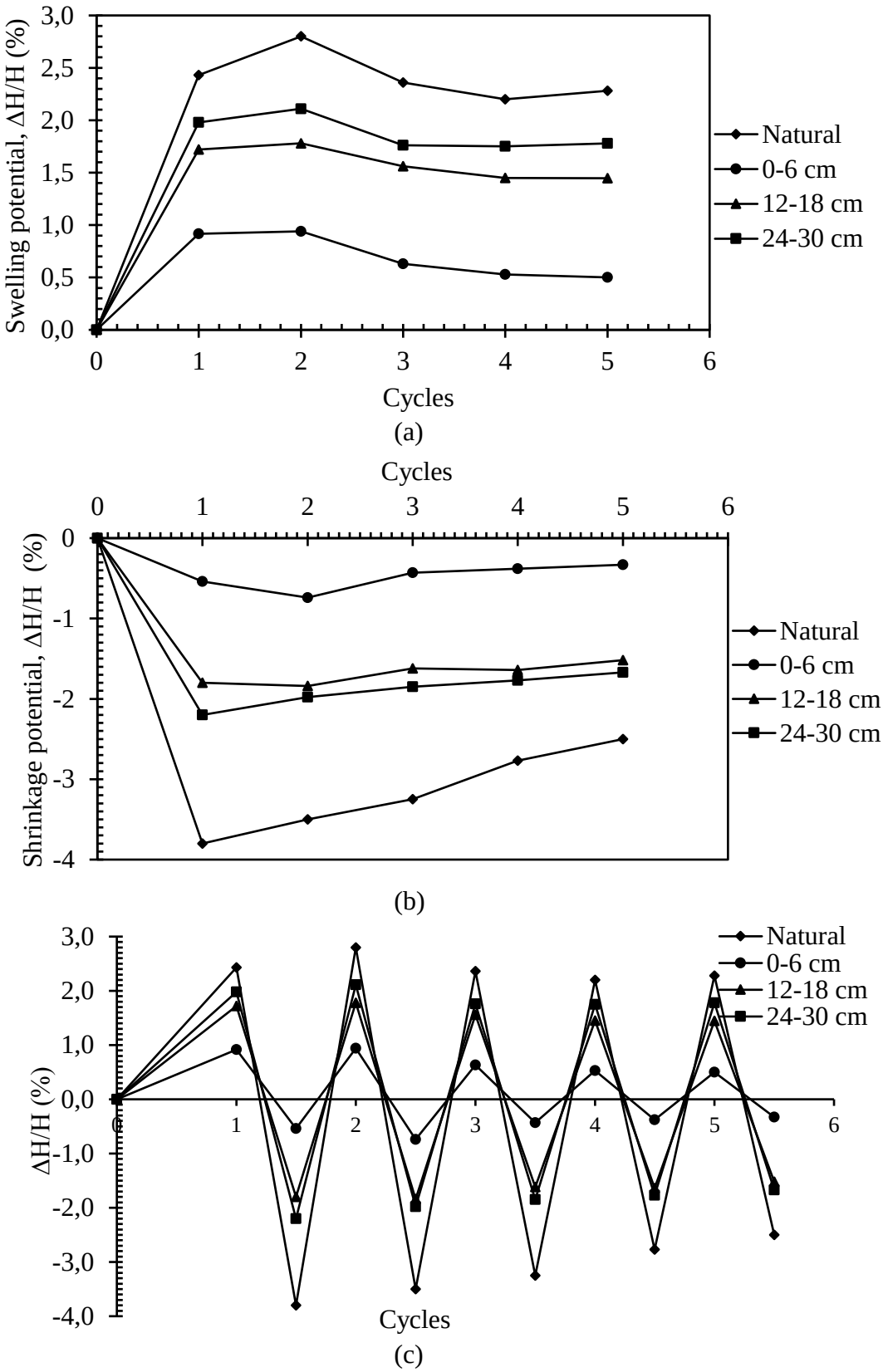

Figure 5.24: Strain variations of EK treated soils using the $CaCl_2$-DW ionic solution along anode to cathode distances (a) Swell potential versus number of cycles, (b) Shrinkage potential versus number of cycles, and (c) Vertical deformation versus number of cycles.

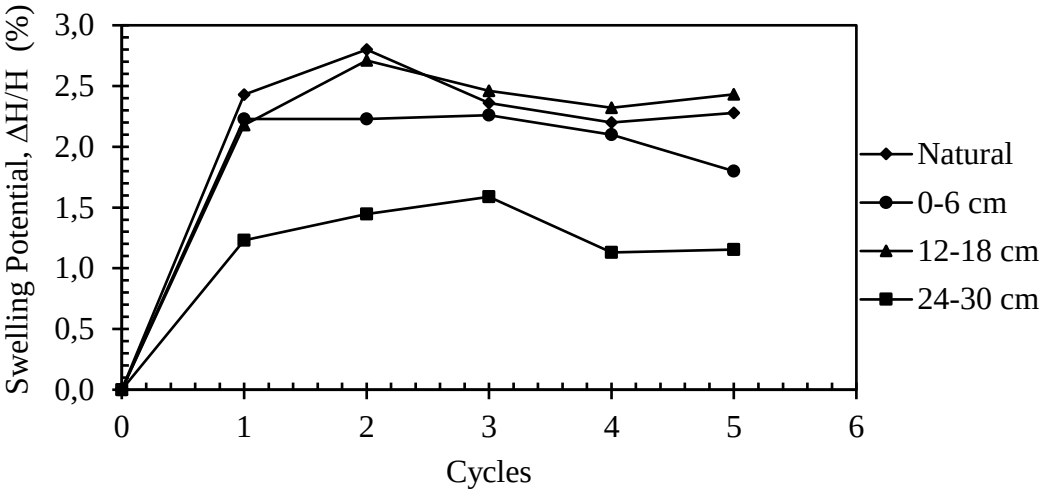

(a)

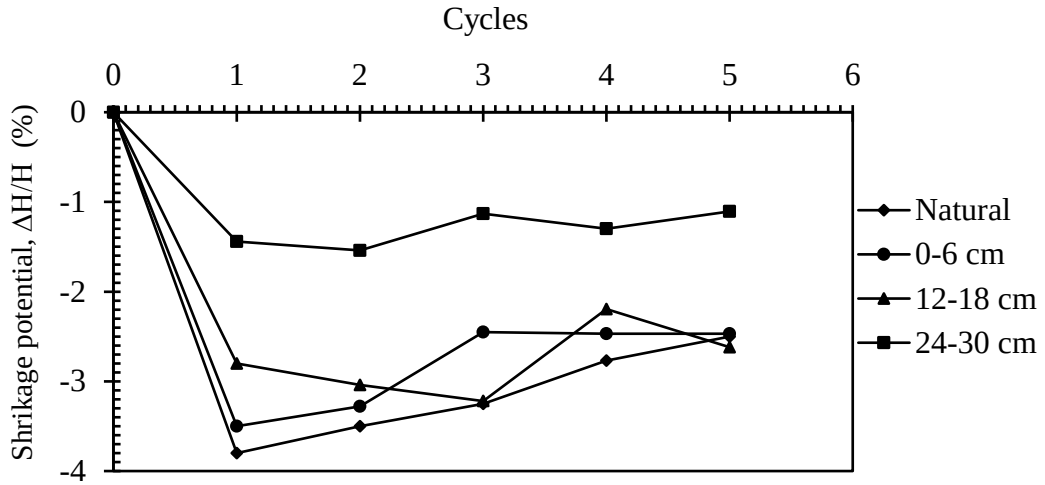

(b)

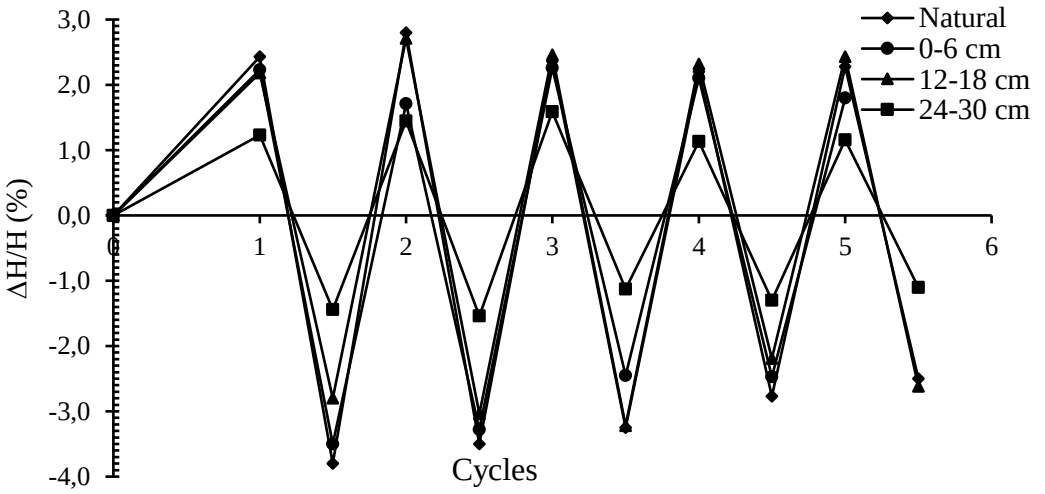

(c)

Figure 5.25: Strain variations of EK treated soils using the Na_2CO_3-DW ionic solution along anode to cathode distances (a) Swell potential versus number of cycles, (b) Shrinkage potential versus number of cycles, and (c) Vertical deformation versus number of cycles.

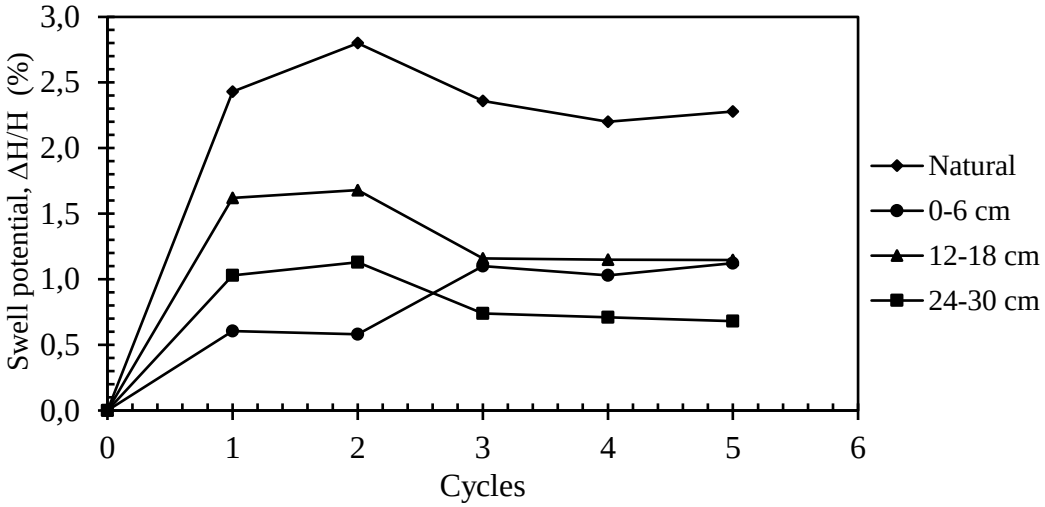

(a)

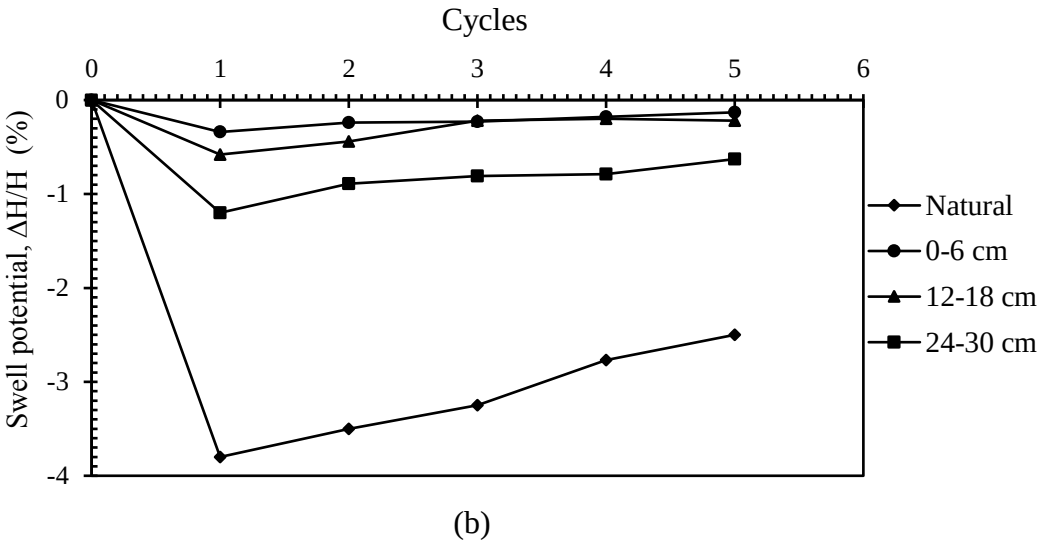

(b)

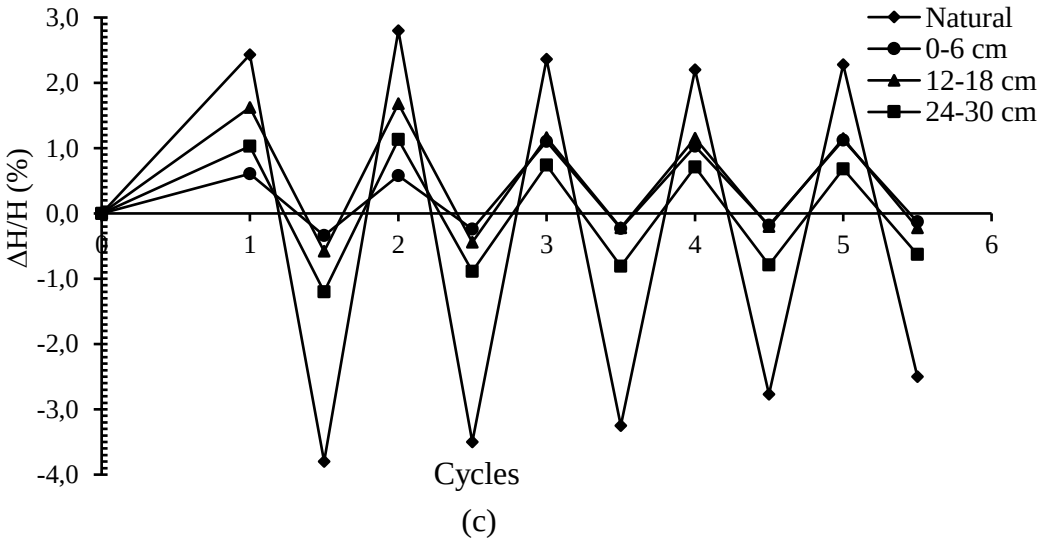

(c)

Figure 5.26: Strain variations of EK treated soils using the $CaCl_2$-Na_2CO_3 ionic solution along anode to cathode distances (a) Swell potential versus number of cycles, (b) Shrinkage potential versus number of cycles, and (c) Vertical deformation versus number of cycles.

5.6.4 EK effects on the thermal properties of soft soils

Figure 5.27 shows the thermal analyses of untreated and EK treated soils. The differential thermal analysis (DTA) curve of the untreated soil showed a well-defined, strong endothermic peak at temperature 512^{o}C, which suggested the breaking down of the crystal lattice layer structure (Peethamparan *et al*., 2008; Kapeluszna *et al*., 2017).

The two endothermic peaks of EK treated soils for both $CaCl_2$-Na_2CO_3, and $CaCl_2$-DW ionic solutions occurred first at 80^{o}C and 90^{o}C and then appeared at 487^{o}C and 521^{o}C, showing the formation of new calcium aluminosilicate hydrates (CASH). The DTA curves of EK treated soil with Na_2CO_3-DW was characterized by one endothermic peak at 76^{o}C, due to loss of water molecules in the dehydration process.

Within the temperature range of 500^{o}C and 700^{o}C, the endothermic peak at 521^{o}C was not as strong as compared to other ionic solutions due to the absence of Ca^{2+} ions in the Na_2CO_3-DW ionic solutions. From the derivative thermogravimetry (DTG) curves provided in Figure 5.27b, the total weight loss of untreated soil was 10%. The first 4.5% weight loss was between 10^{o}C to 105^{o}C and the second weight loss of 5.5% commenced from 410^{o}C to 600^{o}C whereas the total weight loss of the EK treated soils with ionic solutions of $CaCl_2$-DW, Na_2CO_3-DW, and $CaCl_2$-Na_2CO_3 were 4.85%, 6.5%, and 5.69% at the peak temperature of 487^{o}C, 570^{o}C, and 521^{o}C, respectively.

A higher weight loss value at 76^{o}C for Na_2CO_3-DW ionic solution indicates the formation of carbonates, while the lowest weight loss in $CaCl_2$-DW indicates CASH formation in the treated soil. (Miller and Azad, 2000; Solanki and Zaman, 2012).

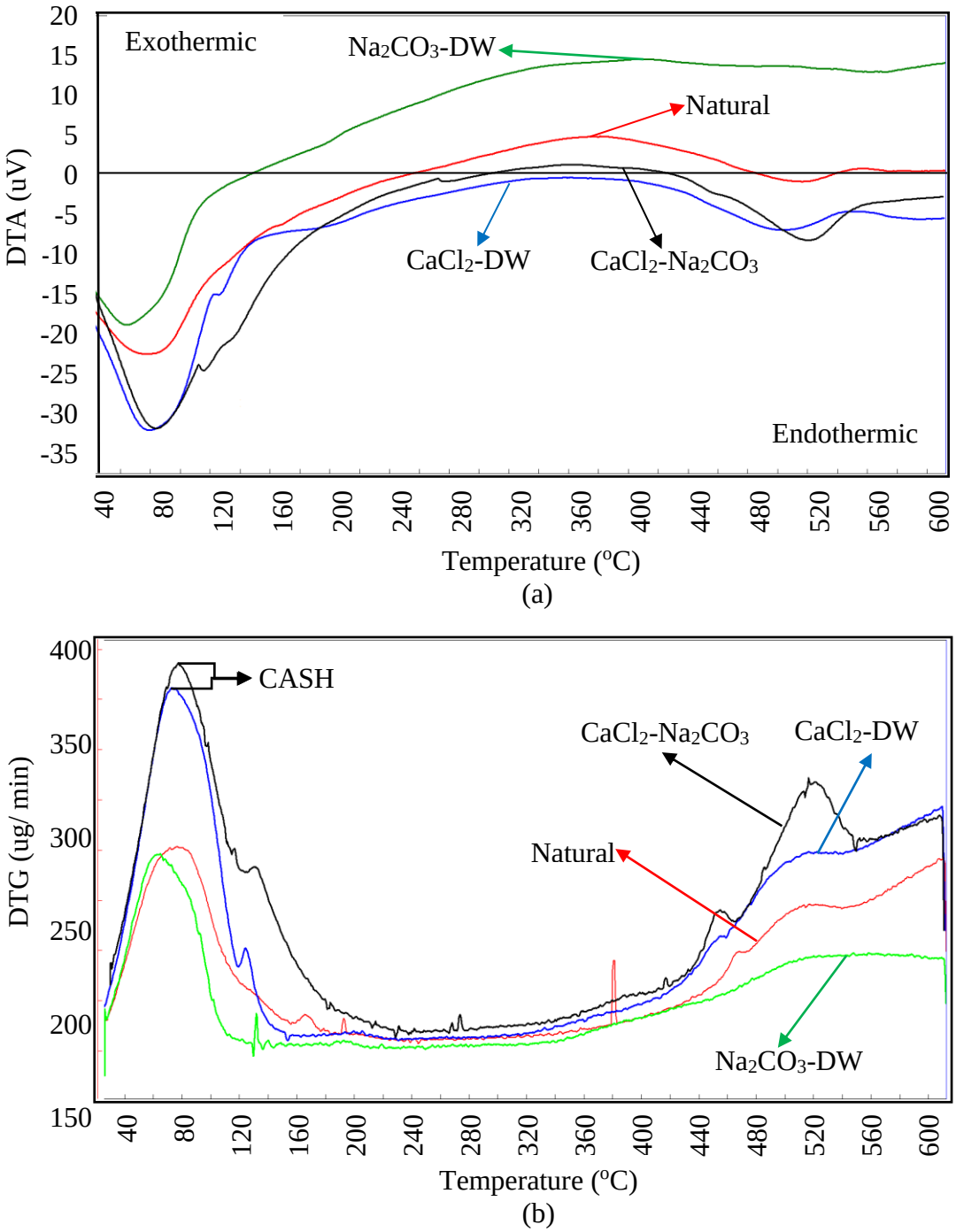

Figure 5.27: (a) DTA curves and (b) DTG curves of the EK treated soils after 28 days from anode to cathode distances using different ionic solution phases of $CaCl_2$-DW, Na_2CO_3-DW, and $CaCl_2$-Na_2CO_3.

As reported in the literature (Coleman *et al*., 2009; Kapeluszna *et al*., 2017), the presence of calcium aluminosilicate hydrates CASH showed a significant endo-effect in the region of 70^{o}C-120^{o}C associated with the formation of CASH cementitious gels. The differential thermal analysis and derivative thermogravimetry studies revealed the formation of CASH gels, which increased the chemical bond strength of the treated soils and resulted in an increase in the unconfined compressive strength, q_u is consistent with the observations reported by Peethamparan *et al*. (2008) and Chaunsali and Peethamparan (2010). Thus, based on the order of total weight loss, the thermal stability is in the order of $CaCl_2$-DW > $CaCl_2$-Na_2CO_3 > Na_2CO_3-DW > natural soil.

5.6.5 EK effects on morphological properties of soft soils

The light-optical microscopic images of the soil samples were used to see the alteration in the morphology of the treated soils under the careful observation of a microscope.

Figure 5.28 presents the microscopic images of the natural and EK treated soils. As aforementioned in Section 5.6.2.1, the initial increase in the pH of the EK treated soils, caused by the soil-ionic solution reactions, initiated the exchange of ions in the porous soil medium and resulted in the aggregation and flocculation of the EK treated soils.

This caused the solid particles of the EK treated soils to become more cemented and have substantially lower plastic character. Figure 5.28 shows the changes in the morphology of the EK treated soils, in terms of their fabric and textural characters.

As reported in the literature (Lav and Lav, 2000; Cristelo *et al*., 2012), the of calcium, Ca^{2+} ions from the ionic solutions in the EK treatment environment resulted in a more flocculated and aggregated structure in the EK treated soils, as shown in the circles in Figure 5.28, and caused a decrease in the plasticity and an increase in the strength.

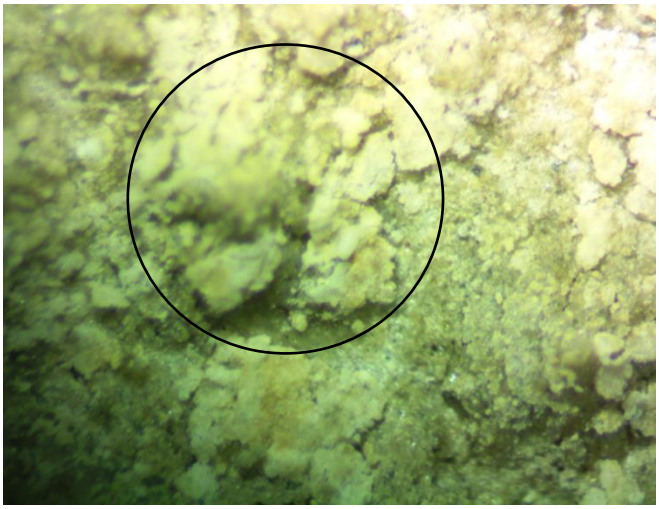

(a)

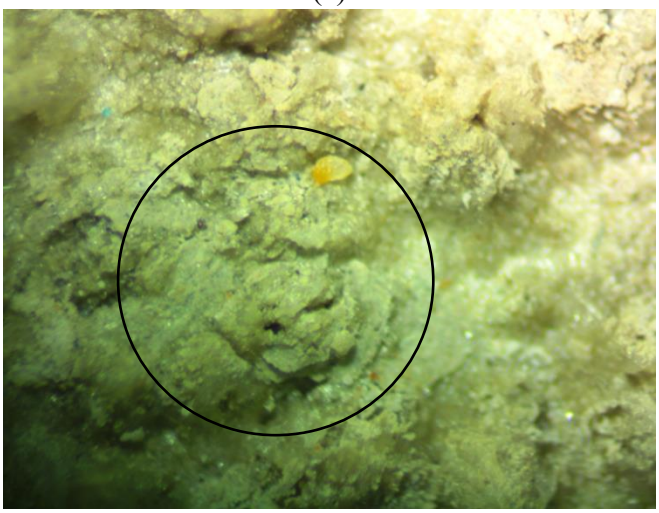

(b)

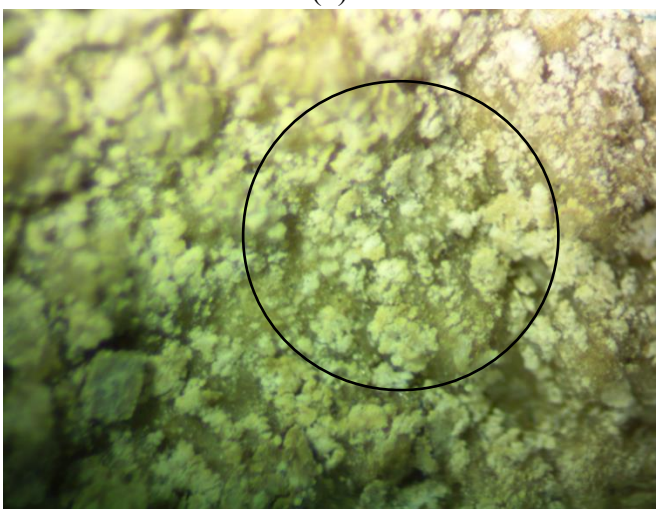

(c)

Figure 5.28: Optical microscopic images showing different morphology for (a) untreated soil, and for EK treated soils using (a) $CaCl_2$-DW, (b) Na_2CO_3-DW and (c) $CaCl_2$-Na_2CO_3 ionic solutions (magnification: 210x).

5.7 Effect of ionic solutions on the performance of EK treated soils: second batch-test setups

The second batch-test setups comprise the dimensions of the test tanks, electrode length, l_e, and ionic solutions' reservoirs, as given in Section 3.4.1.2 and Table 3.5. The testing program was performed based on different combinations of ionic solutions such as $CaCl_2$-DW, Na_2CO_3-DW, and $CaCl_2$-Na_2CO_3, anode to cathode distances, $d_{A\leftrightarrow E}$, electrode lengths, l_e, soil depths, d_s, and EK treatment testing durations.

This part of the study aims to study the effect of changing electrode length, l_e on the performance of the EK treatment on the engineering properties of soft soils. The input factors such as the electrode length, l_e, soil depth, d_s, and anode to cathode distance, $d_{A\leftrightarrow E}$ of the soils in the small-scale laboratory model test tank were considered.

The tests were performed with changing electrode length ratios of $0.25l_{ce}$, $0.50l_{ce}$, $0.75l_{ce}$, and $1.0l_{ce}$, as provided in Table 3.8 in Section 3.4.1.2. The test data obtained from the Atterberg limit and one-dimensional swelling tests at different extraction points from the treated soils (Section 3.4.2 and Figure 3.9) were analyzed, and the effect of changing electrode length, l_e, on the efficacy of the EK treatment was studied.

The main differences between the first and second batch-test setups lie in the dimensions of the test tank setups, soil blocks, electrode lengths, and ionic solutions' reservoirs. However, the soil blocks were subjected to similar EK materials and dimensions such as the anode to cathode distances, $d_{A\leftrightarrow E}$, different combinations of ionic solutions, power supply, test room conditions, such as temperature and humidity.

5.7.1 Electroosmotic flow rate, q_{eo} of the EK treated soils

The q_{eo} values increased due to larger dimensions of the test tank and its components, as provided in Figure 3.3 and Table 3.8, and thus caused a higher inflow of ionic solutions and intense electrochemical reactions in the treated soils. Figure 5.29 presents the results of the q_{eo} obtained from the inflow of the ionic solutions in the EK treated soil blocks in the second batch-test setups. The concept of inflow of ionic solutions in the soil block, the location of the ionic solutions' reservoirs in the test tanks (Table 3.6), and also the treatment duration is similar to the first batch-test setups.

The peak q_{eo} values for the ionic solutions of $CaCl_2$-DW, Na_2CO_3-DW, and $CaCl_2$-Na_2CO_3 were estimated for each test set up and presented in Table 5.13. A similar trend to the first batch-test setups was observed for q_{eo} values such as for $CaCl_2$ > Na_2CO_3 > DW, except that higher q_{eo} values were obtained in all the ionic solution test setups. Thus, the flow rate of ionic solutions was higher via the soil blocks in second batch setups than the first batch and was based only on the anode to cathode distances, $d_{A\leftrightarrow E}$, and not the soil depths, d_s. On the other hand, compared to the remolded soil slurry used in the previous studies (Mosavat *et al*., 2014; Kaniraj *et al*., 2011), because of soil block samples with low hydraulic conductivity used in the present study, lower q_{eo} values were obtained. Also, the obtained q_{eo} values were adequate to initiate soil-ionic solutions reactions to improve the engineering properties of the soft soils.

Table 5.13: q_{eo} values of ionic solutions via the EK treated soils in second test setups.

Test setups	Combination of ionic solutions	q_{eo} of ionic solution from anode chamber (m^3/s)	q_{eo} ionic solution from cathode chamber (m^3/s)
1	$CaCl_2$-DW	$CaCl_2$: $361x10^{-10}$	DW: $250x10^{-10}$
2	Na_2CO_3-DW	DW: $163x10^{-10}$	Na_2CO_3: $181x10^{-10}$
3	$CaCl_2$-Na_2CO_3	$CaCl_2$: $383x10^{-10}$	Na_2CO_3: $237x10^{-10}$

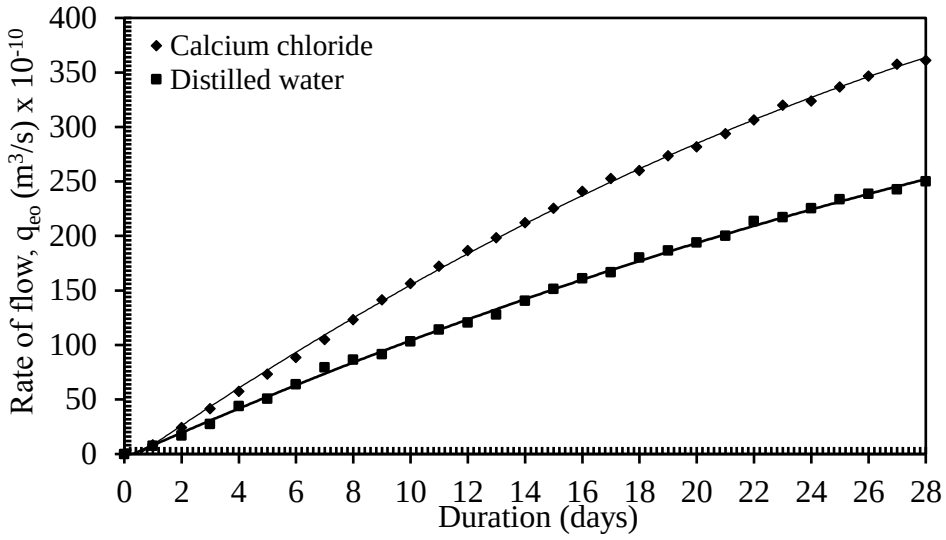

(a)

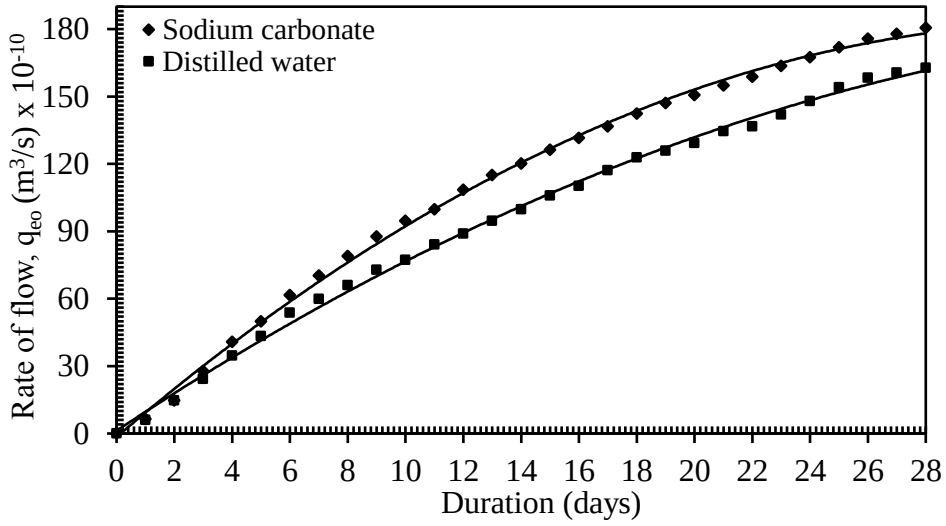

(b)

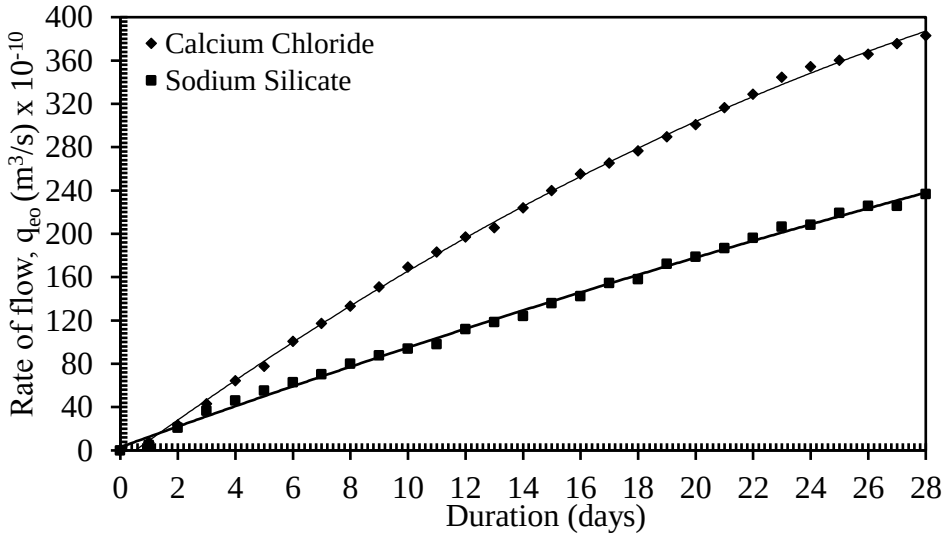

(c)

Figure 5.29: The rate of electroosmotic flow, q_{eo} of ionic solutions of (a) Na_2CO_3-DW, (b) $CaCl_2$-DW, and (c) $CaCl_2$-Na_2CO_3 during the EK treatment.

5.7.2 EK effect on the plasticity index of soft soils

This section presents the variation of Atterberg limits: liquid limit, LL, plastic limit, PL and plasticity index, PI of the EK treated soils under different electrode lengths, l_e in the 28 days of EK treatment using only the $CaCl_2$-Na_2CO_3 ionic solutions test setup.

The changes in plasticity of the EK treated soils at different soil depths, d_s, and at different electrode lengths, l_e along anode to cathode distances, $d_{A\leftrightarrow E}$ were examined (Section 3.4.1.2). Figure 5.30 showed the PL, LL, and PI values obtained from the EK treated soils at points of extraction of A, B, C, D, and E measured at different soil depths, d_s by using a full electrode length, l_e of 30 cm, and its changing electrode length ratio is one ($1.0l_{ce}$). The electrode length ratios were $0.75l_{ce}$, $0.50l_{ce}$ and $0.25l_{ce}$ were for the electrode lengths, l_e, of 22.5 cm, 15.0 cm, and 7.50 cm, respectively.

For the analysis of electrode length, l_e to soil depth, d_s ratio, the ionic solutions used were $CaCl_2$ and Na_2CO_3 at the anode and cathode ends, respectively. Figure 5.30 showed a reduction in the plasticity index, PI of the treated soils, which were recorded at points of extraction A and E, due to their proximity to the ionic solution cells.

Whereas points B and D had a lower reduction. The least reduction in the plasticity index (PI) values were obtained at point C, which was at the midpoint of the EK treated soil block samples. The findings indicated that EK treatment was effective along the electrode length proximity and decreased the PI of the soil block in a downward direction. The $1.0l_{ce}$ has an effective reduction in the PI values of the treated soils due to the provision of a larger surface area of the soil-electrodes contact in their chambers.

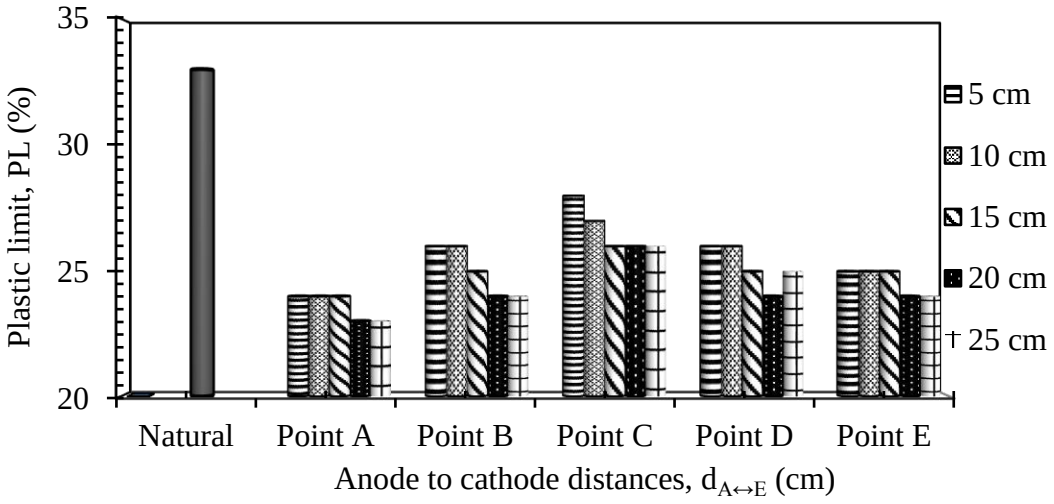

(a)

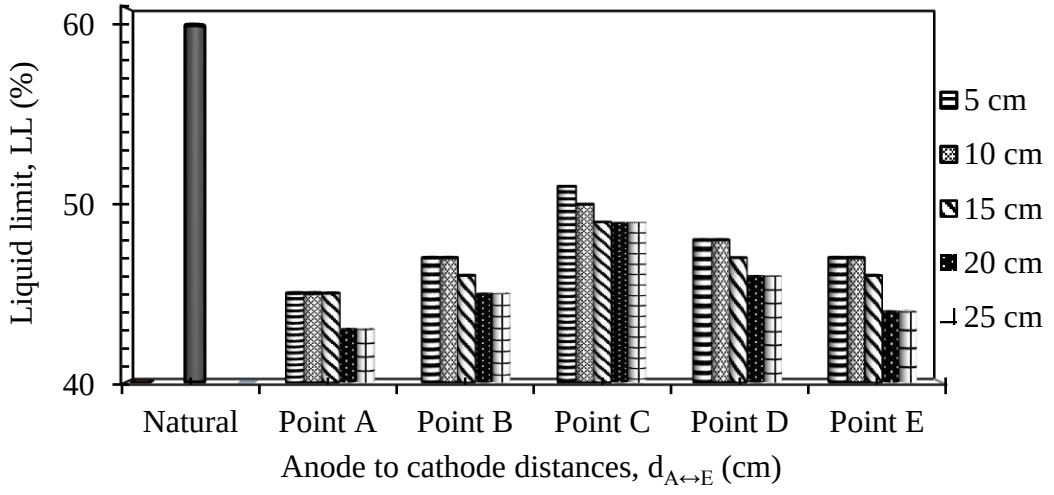

(b)

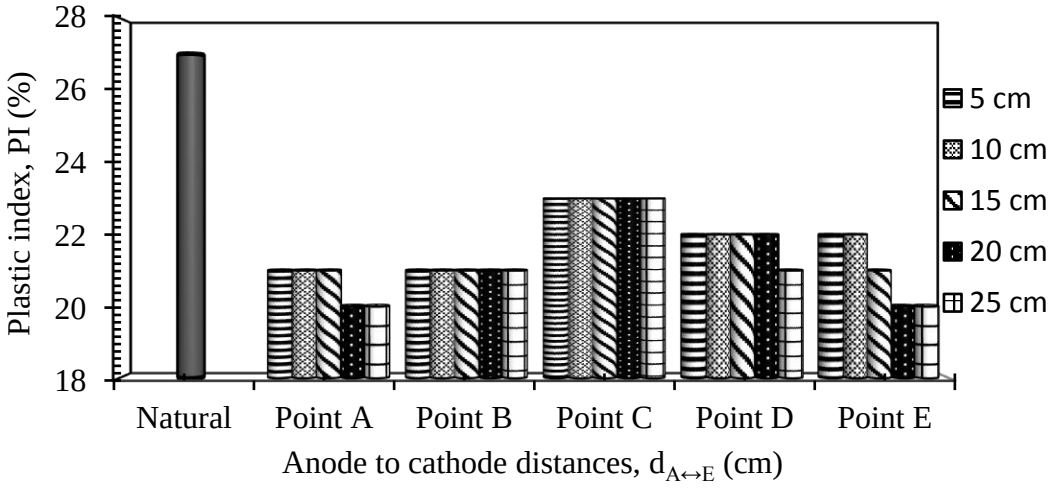

(c)

Figure 5.30: The variations of (a) PL and (b) LL and (c) PI of the EK treated soils at different points A, B, C, D, and E using total electrode length, l_e of 30 cm (l_{ce} = 1.0) and the $CaCl_2$-Na_2CO_3 ionic solutions combination.

Figure 5.31 provides the plastic limit (PL), liquid limit (LL), and plasticity index (PI) values obtained for changing electrode length ratio of $0.75l_{ce}$ at different soil depths (d_s). The figure indicated that the plasticity index (PI) values obtained at points of extraction of A and E are less than the values obtained at points of extraction of B and D. The changing electrode length ratio of $0.75l_{ce}$ resulted in a similar efficacy in the performance of EK treatment at different soil depths when compared to that of $1.0l_{ce}$.

The percent reduction in the PI values for points of extraction of A, B, C, D, and E using electrode length ratio $0.75l_{ce}$ was 26%, 22%, 11%, 19%, and 25%, respectively, at 25 cm soil depth (d_s), while the percent reduction in the plasticity index (PI) values obtained at 5 cm soil depth (d_s) were 22%, 14%, 7%, 15%, and 19%, respectively.

Thus, the effective depth, Z_e, in terms of EK treatment for $1.0l_{ce}$, is approximately equal to $0.75l_{ce}$. The average percent significant reduction in the plasticity index (PI) values recorded for points A, B, C, D, and E respectively, were 39%, 36%, 33%, and 39%, at 25 cm soil depth, d_s while the lowest plasticity index (PI) value was obtained at 5 cm soil depth, d_s as 33% for all the points of extraction of A, B, C, D, and E.

Thus, the effective depth, Z_e of $0.75l_{ce}$, is as significant as $1.0l_{ce}$ (Figure 5.31). Therefore, it is economical to use an electrode length of 22.5 cm of corresponding changing electrode length ratio of $0.75l_{ce}$ in order to attain effective result in EK soil treatment at a corresponding predetermined soil depth (d_s) by the way of shortening or changing the dimensional length of the conductive electrodes used in this study.

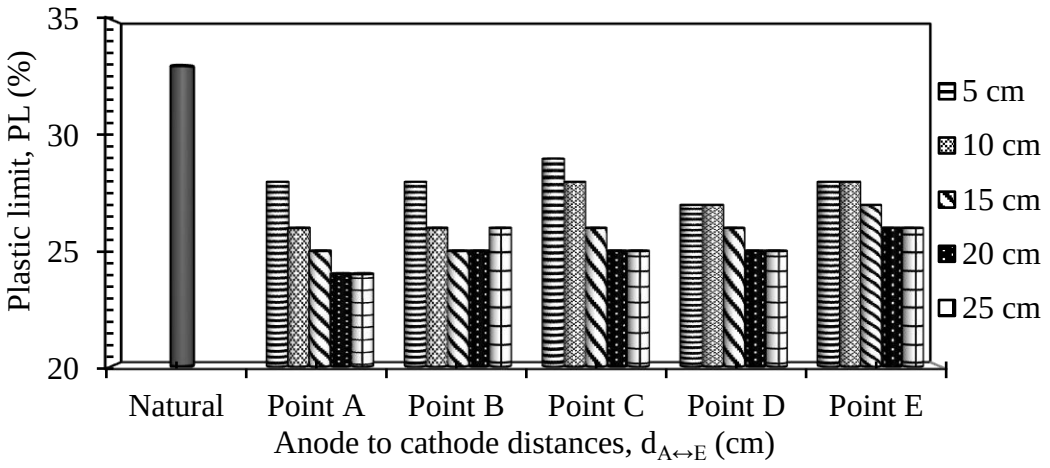

(a)

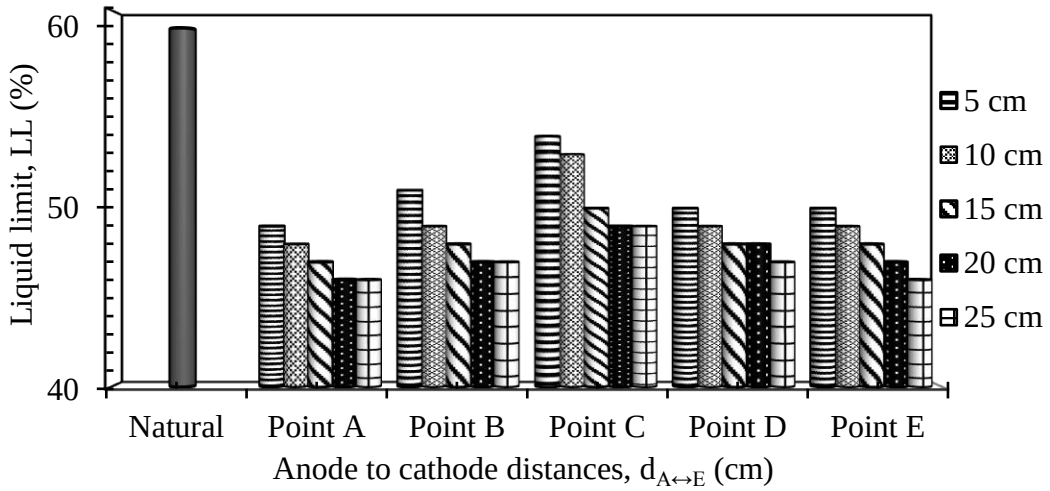

(b)

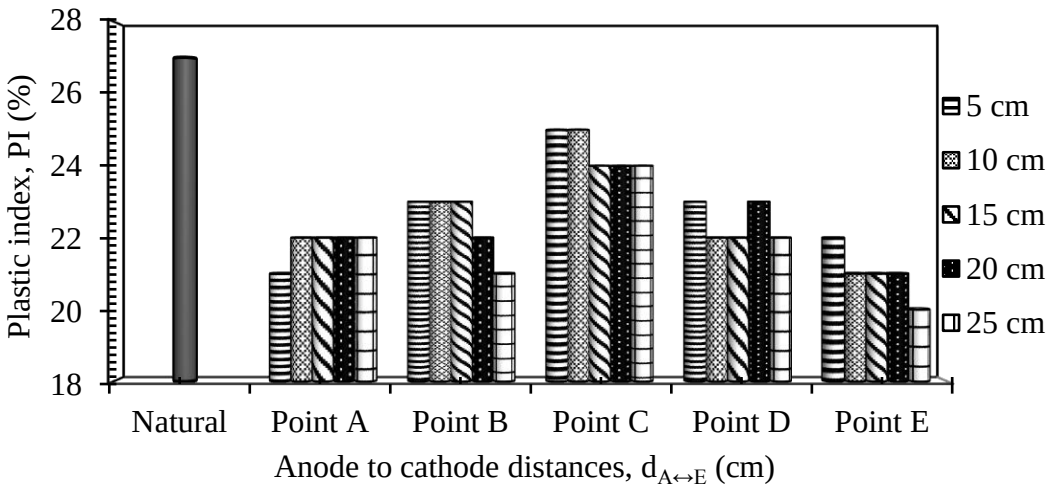

(c)

Figure 5.31: The variations of (a) PL and (b) LL and (c) PI of the EK treated soils at different points A, B, C, D, and E using total electrode length, l_e of 22.5 cm (l_{ce} = 0.75) and the $CaCl_2$-Na_2CO_3 ionic solutions combination.

For $0.50l_{ce}$, the PL, LL, and PI values at different d_s are provided in Figure 5.32. The PI values of the treated soils at points A and E were less than the PI values of the treated soils at points B and D, but point C had the least reduction in the PI values.

The plasticity index (PI) values of the treated obtained for electrode length ratio of $0.50l_{ce}$ was lesser at different soil depth (d_s) layers when compared to the plasticity index (PI) values of the treated for electrode length ratios of $1.0l_{ce}$ and $0.75l_{ce}$. The trend in the reduction of plasticity index (PI) values of the treated soils for electrode length ratio of $0.50l_{ce}$ along with the soil depths (d_s) of 5cm to 10 cm were similar to the plasticity index (PI) values of the EK treated soils obtained for $1.0l_{ce}$ and $0.75l_{ce}$.

The percent reduction in the PI values of the treated soils for points of extraction of A, B, C, D, and E using electrode length ratio of $0.50l_{ce}$ was 36%, 30%, 21%, and 36%, respectively, at 25 cm soil depth (d_s), while the lesser percent reduction PI values of the treated soils were obtained at 5 cm soil depth d_s, as 33%, 24%, 18%, and 30%.

Thus, the effective depth, Z_e in terms of EK treatment for changing electrode length ratio of $0.50l_{ce}$, was approximately equal ≈ to changing electrode length ratio of $0.75l_{ce}$ at 5 cm soil depth (d_s), but less effective at 25 cm soil depth (d_s), indicating that the changing electrode length ratio of $0.50l_{ce}$ was not effective for the corresponding full d_s range. The effective depth, Z_e for changing electrode length ratio of $0.50l_{ce}$, is effective up to 25 cm soil depth (d_s), but not up to the total soil depth (d_s) (Figure 5.32). Thus, due to these findings, it could be suggested that it is economical to use the $0.50l_{ce}$ in order to achieve EK treatment up to 25 cm d_s, hence reducing the cost and the dimensional length of electrode materials used for EK soil treatment.

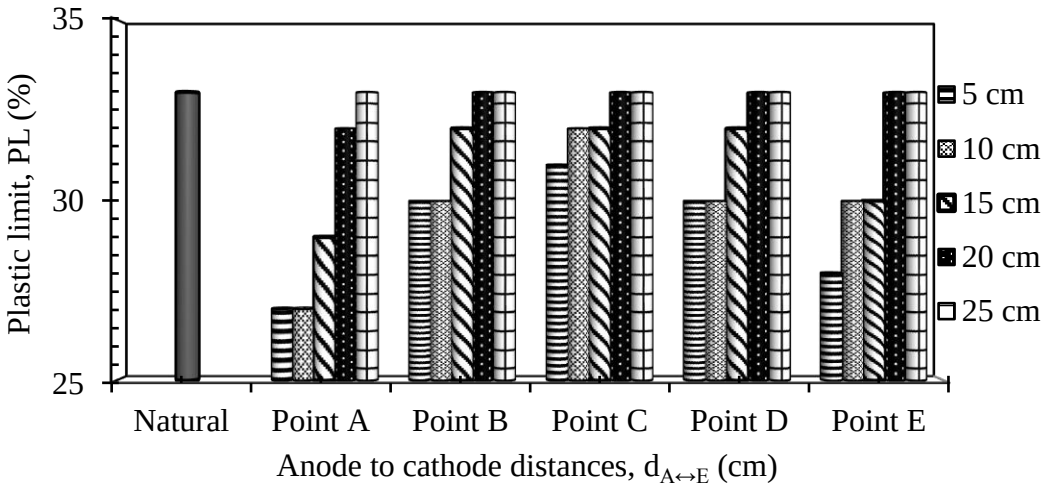

(a)

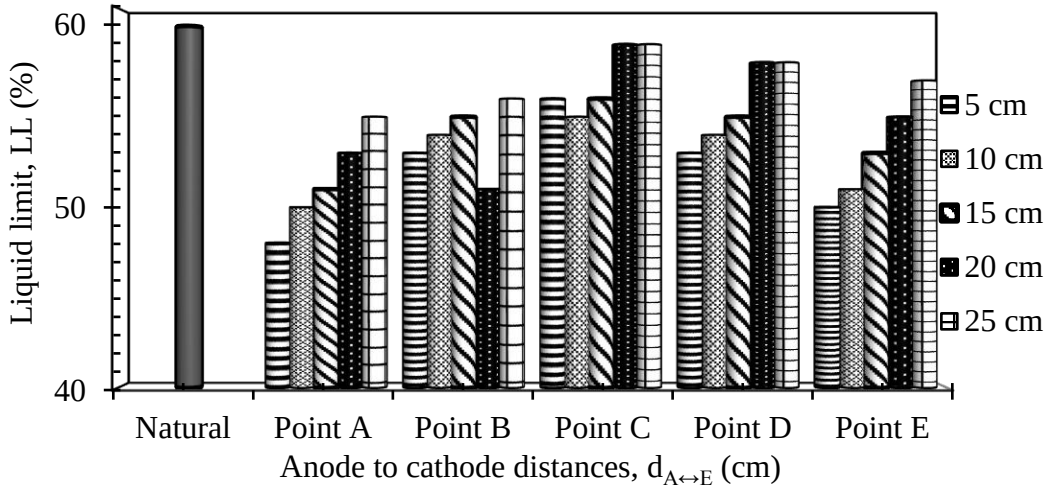

(b)

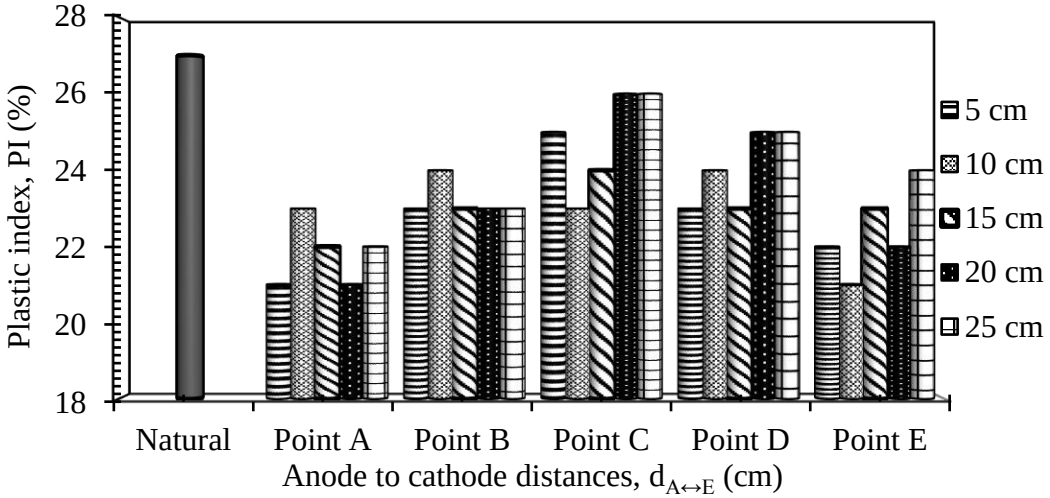

(c)

Figure 5.32: The variations of (a) PL and (b) LL and (c) PI of the EK treated soils at different points A, B, C, D, and E using total electrode length, l_e of 15 cm (l_{ce} = 0.50) and the $CaCl_2$-Na_2CO_3 ionic solutions combination.

For $0.25l_{ce}$, the PL, LL, and PI values at different d_s are provided in Tables 5.24 to 5.26. Also, the PI values at points of extraction of A and D reduced greatly > points B and C. The percent reduction of PI values for $0.25l_{ce}$ are lesser at different d_s layers when compared to $1.0l_{ce}$ and $0.75l_{ce}$, but are closely related to PI values for $0.25l_{ce}$.

The percent reduction in the PI values for points of extraction of A, B, C, and D using $0.25l_{ce}$ are 24%, 18%, 18%, and 21%, respectively at 25 cm d_s, while the least PI values were obtained at 5 cm d_s at a percent reduction of 30%, 18%, 21%, and 30%.

Thus, the effective depth, Z_e, in terms of EK soil treatment for $0.25l_{ce}$, is approximately equal to changing electrode length ratio of $0.50l_{ce}$ at soil depth, d_s of 5 cm but less effective at soil depth, d_s of 25 cm indicated that the changing electrode length ratio of $0.25l_{ce}$ was not effective for the corresponding soil depth, d_s of 25 cm.

The effective depth, Z_e for changing electrode length ratio of $0.25l_{ce}$, is effective up to soil depth (d_s) of 15 cm but not up to soil depth (d_s) of 22.5 cm (Figure 5.33). Thus, it is not effective to use the changing electrode length ratio of $0.25l_{ce}$ for the EK soil treatment since no economic value or efficient EK soil treatment was achieved.

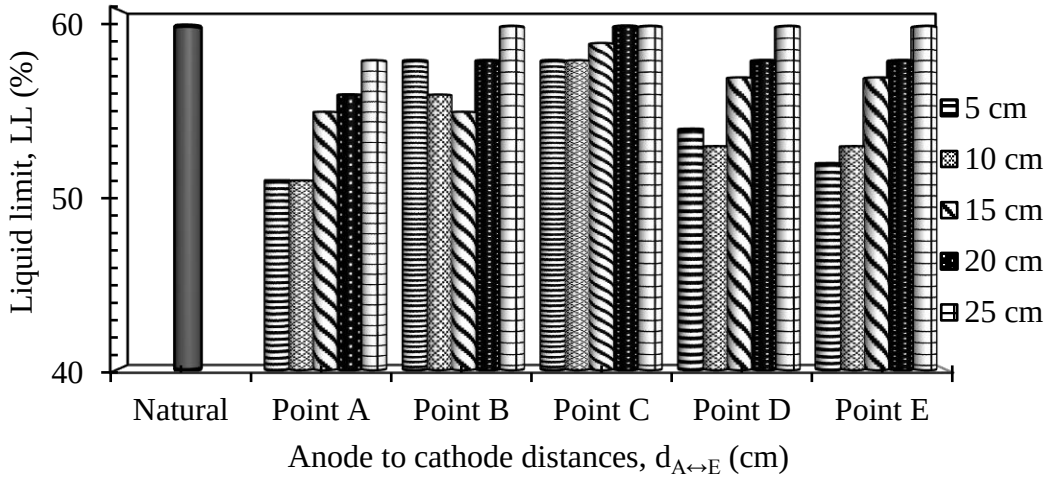

(a)

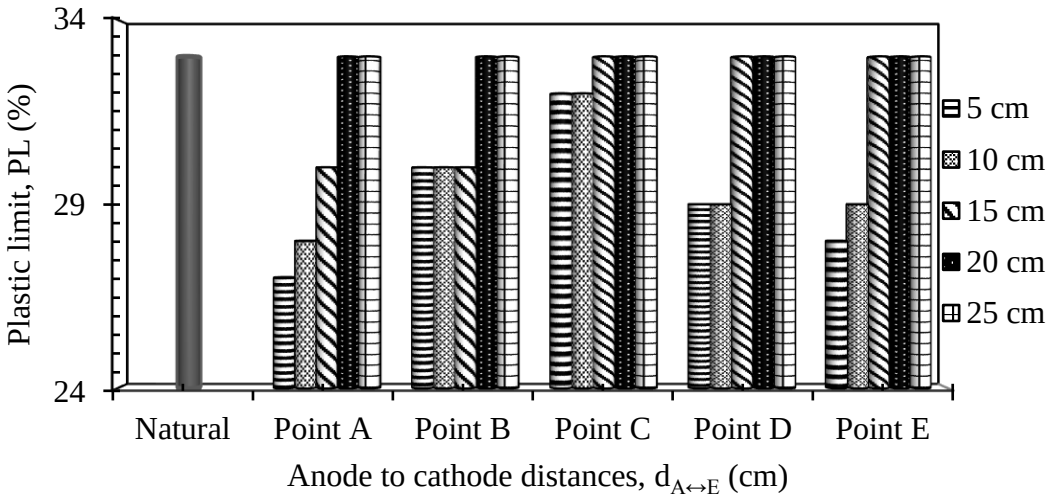

(b)

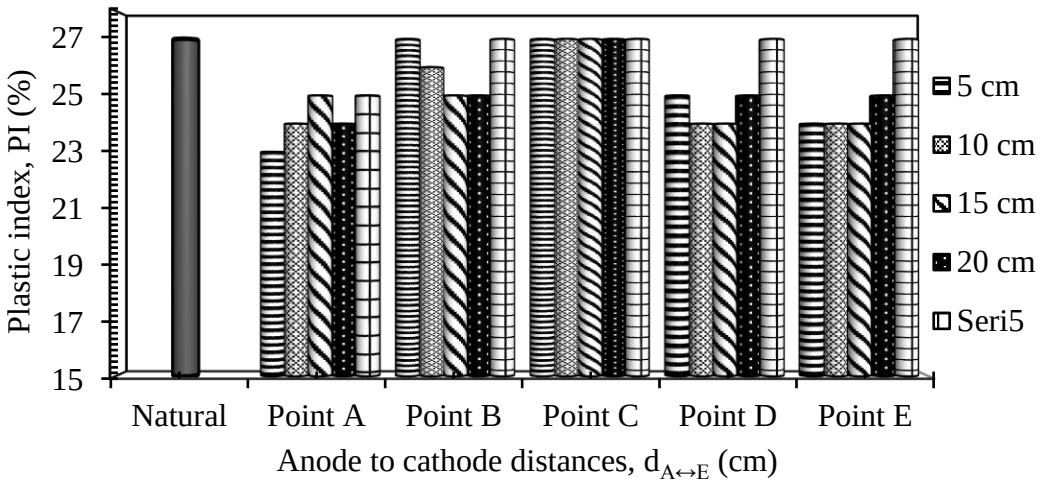

(c)

Figure 5:33: The variations of (a) PL and (b) LL and (c) PI of the EK treated soils at different points A, B, C, D, and E using total electrode length, l_e of 7.5 cm (l_{ce} = 0.25) and the $CaCl_2$-Na_2CO_3 ionic solutions combination.

5.7.3 EK effects on the swell potential of soft soils

In this section, Figure 5.34 presents the changes in the swelling potential of EK treated soils under varied electrode lengths, l_e and soil depths, d_s in 28 days using $CaCl_2$-Na_2CO_3 ionic solutions at points of A, C, and E, at the anode to cathode distances.

Figure 5.34a presents the effect of $CaCl_2$-Na_2CO_3 ionic solution setup on the SP values of the EK treated soils at different electrode lengths, l_e at point A. The $CaCl_2$ solutions from the anode chamber and in combination with the full electrode length, l_e of 30 cm, which is at an electrode length ratio of $1.0 l_{ce}$ caused a reduction in the SP values of the treated soils at the soil depth, d_s from the 5cm up to the 25 cm at the anode region.

Whereas, the electrode length to depth ratio of $0.75 l_{ce}$ and $0.50 l_{ce}$ had a significant reduction of swelling potential values of the treated up to the soil depth (d_s) of 15 cm. Also, the electrode length ratio of $0.25 l_{ce}$ had the least reduction of swelling potential values of EK treated soils at point A, even with the proximity to the anode chamber.

Figure 5.34b presents the effect of $CaCl_2$-Na_2CO_3 ionic solution setup on the SP values of the EK treated soils at different electrode lengths, l_e at point C in the middle section of the test setup. The $CaCl_2$ solutions, in combination with different electrode lengths, had a much lower reduction in the swelling potential (SP) values of the treated soils along with the soil depth, d_s from 5cm up to 25 cm. However, for changing electrode length ratios of $1.0 l_{ce}$ and $0.75 l_{ce}$, a moderate reduction of the SP values of the treated soils was achieved, whereas for the $0.50 l_{ce}$ and $0.25 l_{ce}$, a much smaller reduction of SP values was gained. Figure 5.34c presents the effect of $CaCl_2$-Na_2CO_3 ionic solution on the SP values of the treated soils at different electrode length ratios, l_{ce}, at point C.

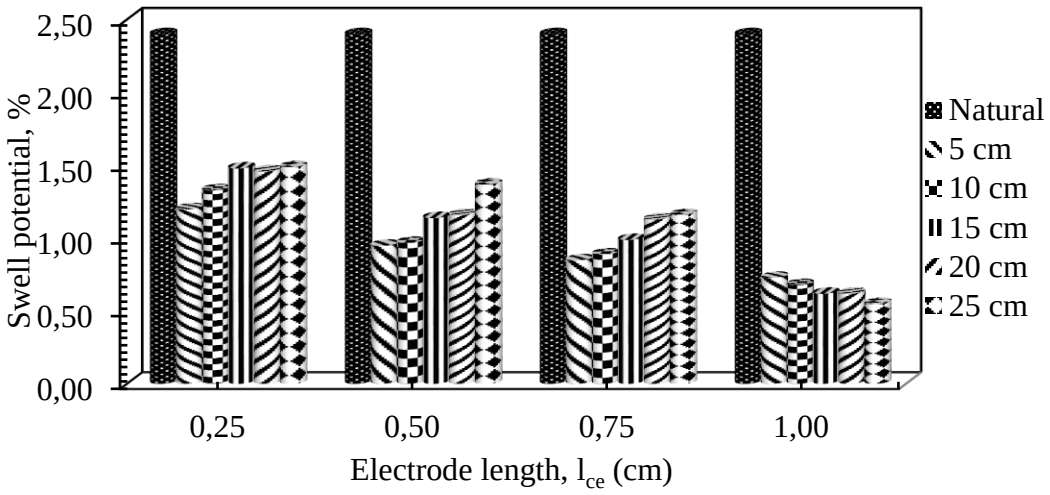

(a)

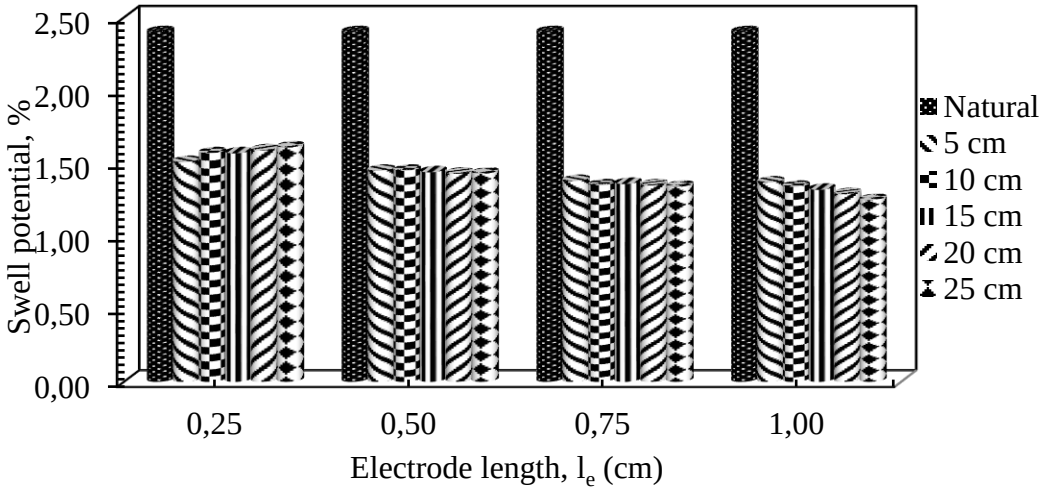

(b)

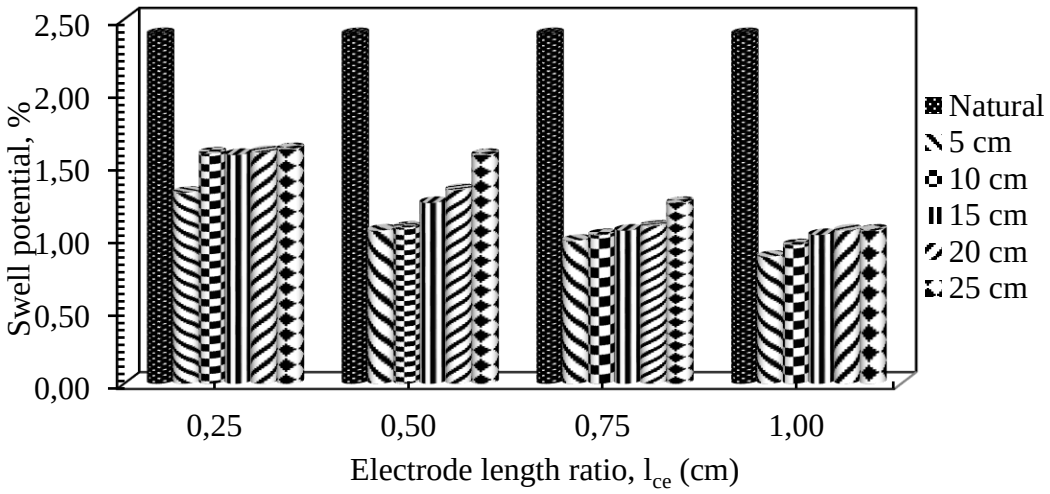

(c)

Figure 5:34: The variations of SP of the EK treated soils using the $CaCl_2$-Na_2CO_3 ionic solutions combination, different electrode length, l_e and soil depth, d_s at points (a) A, (b) C, and (c) E along anode to cathode distance, $d_{A\leftrightarrow E}$.

The Na_2CO_3 ionic solutions from the cathode chamber and with $1.0l_{ce}$ caused a reduction in the SP values of the treated soils up to d_s of 15 cm at the cathode region. Whereas $0.75l_{ce}$ and $0.50l_{ce}$ had a reduction in SP values of the treated up to the d_s of 10 cm. The $0.25l_{ce}$ had the least reduction of SP values of the treated soil at d_s of 5 cm, even with the proximity to the cathode chamber that housed the Na_2CO_3 solutions.

5.8 Evaluation of EK treatment of soft soils using a numerical model

In this section, the effect of ionic solutions, treatment duration, cation exchange capacity (CEC), specific surface area (S_a), pH, electrical conductivity (σ), and ionic strength (I_s) on the unconfined compressive strength, q_u of the treated soils was examined using a numerical model designed by design and analysis of experiment.

5.8.1 Numerical modeling of unconfined compressive strength of EK treated soils

Figure 5.35 presents the unconfined compressive strengths, q_u values of the EK treated soils measured at different EK treatment durations using different ionic solutions. The values obtained for the q_u values in the treated soils were in the range of 25 to 92 kPa.

The observation was that the q_u values of the treated soils increased as the treatment duration increased using the different ionic solutions in the anode to cathode distances.

To indicate the effect of the ionic solutions on the cation exchange capacity (CEC), specific surface area (S_a), pH, electrical conductivity (σ), and ionic strength (I_s) values for the natural soil and EK treated soils at 28 days, all the measured values were given in Table 5.14, and they were analyzed using the design and analysis of experiment.

The findings in Table 5.14 indicated that EK treatment caused a reduction in the cation exchange capacity, CEC, and specific surface area, S_a of the EK treated soils because the soil particles were subjected to flocculation and aggregation in the EK treated soils.

In this study, the design of experiment, DOE, analyzed the input factors, and the q_u values of EK treated soils. Table 5.15a presents the analysis of variance (ANOVA) for input factors of different ionic solutions and treatment duration to evaluate their effects on the measured unconfined compressive strength, q_u values of the EK treated soils.

Table 5.14: Measured values of EK treated soils using ionic solutions in 28 days.

Test set up	EK duration (days)	Anode to cathode distances, $d_{A\leftrightarrow E}$ (cm)	Measured soil factors				
			CEC meq/100g	S_a m^2/g	pH ---	σ S/m	I_s (10^{-4}) mol/L
Natural soil	-	-	14.7	17.5	8.38	4.08	0.65
$CaCl_2$-DW ionic solution	28	5	4.90	5.31	8.37	8.18	1.31
		10	5.71	7.70	8.85	7.78	1.25
		15	5.83	7.80	8.97	6.71	1.07
		20	5.99	10.80	9.01	6.51	1.04
		25	6.27	11.00	9.15	5.54	8.86
Na_2CO_3-DW ionic solution	28	5	13.10	13.70	8.74	4.45	0.71
		10	11.90	13.30	9.08	6.78	1.09
		15	10.87	12.60	10.13	7.28	1.17
		20	9.11	11.30	10.24	8.91	1.43
		25	9.12	10.78	10.41	8.91	1.43
$CaCl_2$-Na_2CO_3 ionic solution	28	5	3.52	4.51	9.91	9.85	1.58
		10	3.62	4.50	10.18	9.38	1.50
		15	3.80	4.54	10.52	8.99	1.44
		20	3.70	6.60	10.88	9.41	1.51
		25	3.80	8.70	10.97	9.62	1.50

Table 5.15a: ANOVA model fit for q_u in terms of ionic solutions and EK treatment duration.

Source	Sum of Squares	df	Mean Square	F-value	P-value	
Model	9686.00	8	1210.75	12.24	< 0.0001	significant
A: Ionic solutions	3242.17	2	1621.08	16.39	< 0.0001	significant
B: Treatment duration	5703.17	2	2851.58	28.83	< 0.0001	significant
AB	740.67	4	185.17	1.87	0.1444	insignificant
Pure Error	2670.75	27	98.92			
Cor Total	12356.75	35				
Std. Dev.	9.95			R^2	0.7839	
Mean	51.58			Adjusted R^2	0.7198	
CV %	19.28			Predicted R^2	0.6158	
				Adeq. Precision	10.4568	

The Model F-value of 12.24 implies the model is significant. There is only a 0.01% chance that a "Model F-value" this large could occur due to noise. Values of P-value less than 0.0500 indicates model terms are significant. In this case, A and B are significant model terms. df represents the degree of freedom in the ANOVA.

Table 5.15b: ANOVA model fit for q_u in terms of ionic solutions and CEC.

Source	Sum of Squares	df	Mean Square	F-value	P-value	
Model	2361.78	4	590.44	149.69	0.0001	significant
A: Ionic solutions	1761.56	2	880.78	223.30	< 0.0001	significant
B: CEC	600.22	2	300.11	76.08	0.0007	significant
C-S_a	600.22	2	300.11	76.08	0.0007	significant
Residual	15.78	4	3.94			
Cor Total	2377.56	8				
Std. Dev.	1.99			R^2	0.9934	
Mean	71.78			Adjusted R^2	0.9867	
CV %	2.77			Predicted R^2	0.9664	
				Adeq. Precision	35.3526	

The Model F-value of 149.69 implies the model is significant. There is only a 0.01% chance that a "Model F-value" this large could occur due to noise. Values of P-value less than 0.0500 indicates model terms are significant. In this case, A and B are significant model terms. df represents the degree of freedom in the ANOVA.

The observed and predicted R^2 values were in reasonable agreement with the adjusted R^2 values. The adequate precision ratio indicated an adequate signal. Thus, the P-value and F-value implied that the model term was significant. The statistical analysis suggested that the different ionic solutions and treatment duration were substantial factors, which had a notable effect on the performance of the treatment of the soft soil.

However, the interaction effect of the ionic solutions and treatment duration was insignificant. Figure 5.35 presents the plots for the prediction model and 3D graphical plots of the ionic solutions and treatment duration. The prediction model is in support of ANOVA, which showed the observed and predicted R^2 values were in agreement.

According to the statistical interpretation of the 3D plots, the different combinations of ionic solutions had a significant effect on the treated soils in the order of $CaCl_2$-Na_2CO_3 > $CaCl_2$-DW > Na_2CO_3-DW and produced better strength at longer treatment duration. It showed that the electrochemical reaction between $CaCl_2$-Na_2CO_3 and clay particles had produced a significant result, which supported the idea of the formation of cementitious gels within the tiny pores of the soft clay soils and thus increased the soil strength. The effect of the factors on unconfined compressive strength, q_u of the treated soils is in the order of treatment duration > different combinations of ionic solutions > interaction effect of different combinations of ionic solutions and treatment duration.

In this case, different combinations of ionic solutions and treatment duration factors were significant model terms. Therefore, the analysis showed that the strength properties of the treated soils were significantly affected by different combinations of ionic solutions and treatment duration than the interaction effect between these factors.

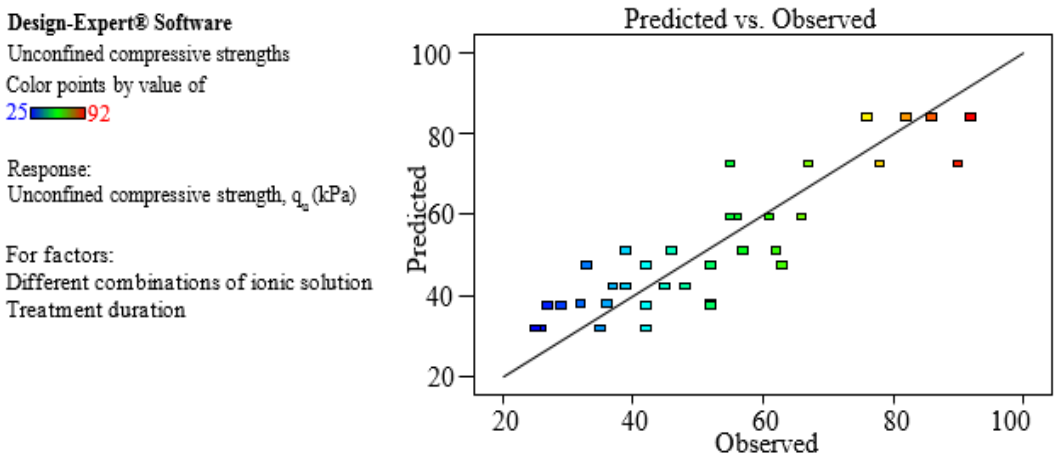

(a)

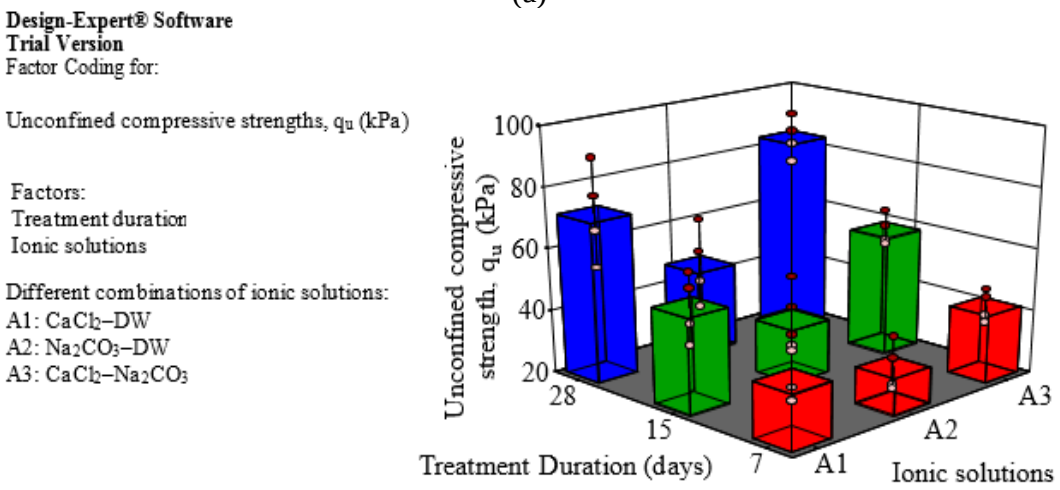

(b)

Figure 5.35: (a) Prediction model and (b) 3D plots for different combinations of ionic solutions and EK treatment duration with respect to q_u response.

Table 5.15b shows the ANOVA analysis for the input factors combination of ionic solutions, CEC, and S_a. The P-value and F-value indicated that the model was significant. The observed and predicted R^2 values were in a strong agreement with the adjusted R^2. The adequate precision ratio showed a sufficient signal. The model terms were significant. The analysis showed that each factor had a considerable effect on the performance of the ionic solutions on the EK treated soft soils. The prediction model validated the R^2 values generated with the analysis of variance (ANOVA) of the DOE.

Figures 5.36 and 5.37 showed the prediction model and 3D plots between the factors: ionic solutions and CEC, and ionic solutions and S_a to ascertain their effects on q_u, respectively. The analysis showed that the factors of ionic solutions, cation exchange capacity, CEC, and specific surface area, S_a had a significant effect on the strength properties of the treated soils, but the interactions of the factors were insignificant.

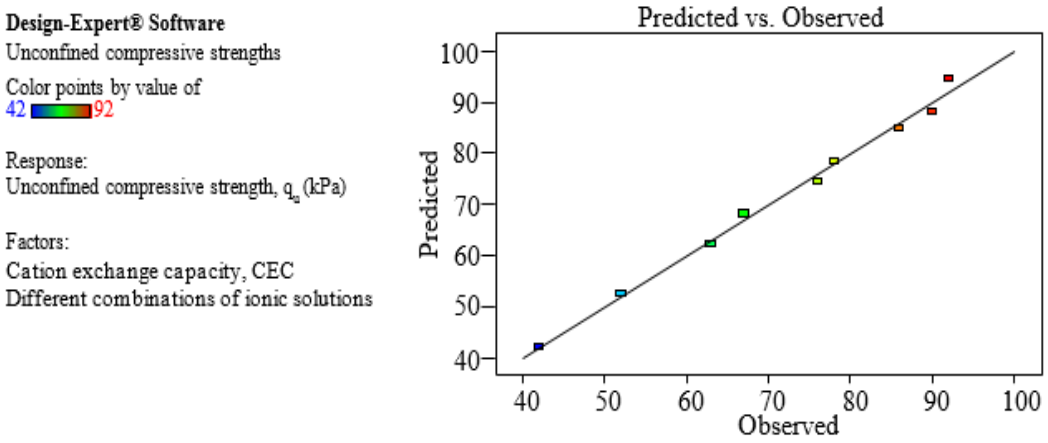

(a)

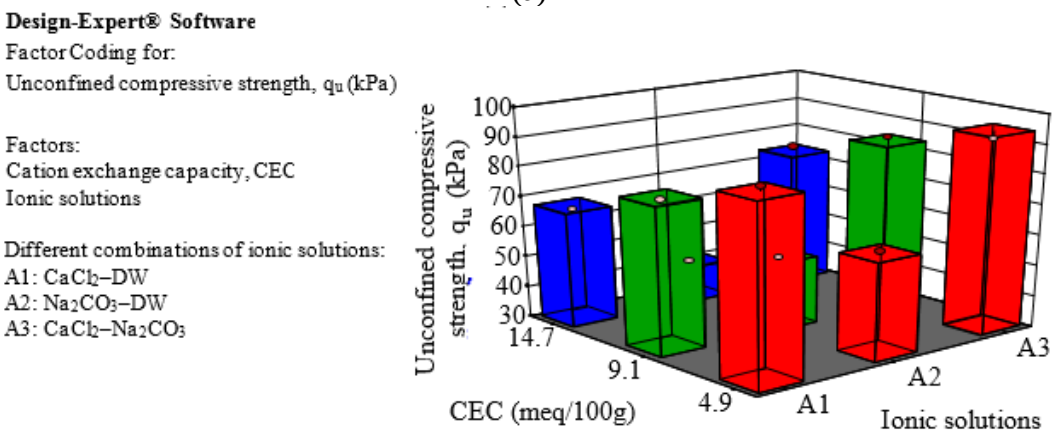

(b)

Figure 5.36: (a) Prediction model and (b) 3D plots of electrolyte type and CEC variables with respect to q_u response.

The observation was that the EK treated soils at the lowest CEC, (4.9 meq/100g), and S_a, (4.5 m^2/g) had a considerable effect on the performance of the EK treated soils. An indication that the EK treated soil became more effectively strengthened at low CEC and S_a values. The 3D plots indicated that the different combinations of ionic solutions

had a more significant effect in the order of $CaCl_2$-Na_2CO_3 > $CaCl_2$-DW > Na_2CO_3-DW, respectively. The significant factors were in the order of ionic solutions > CEC > S_a > interaction effects of ionic solutions, CEC and S_a, validated by the ANOVA.

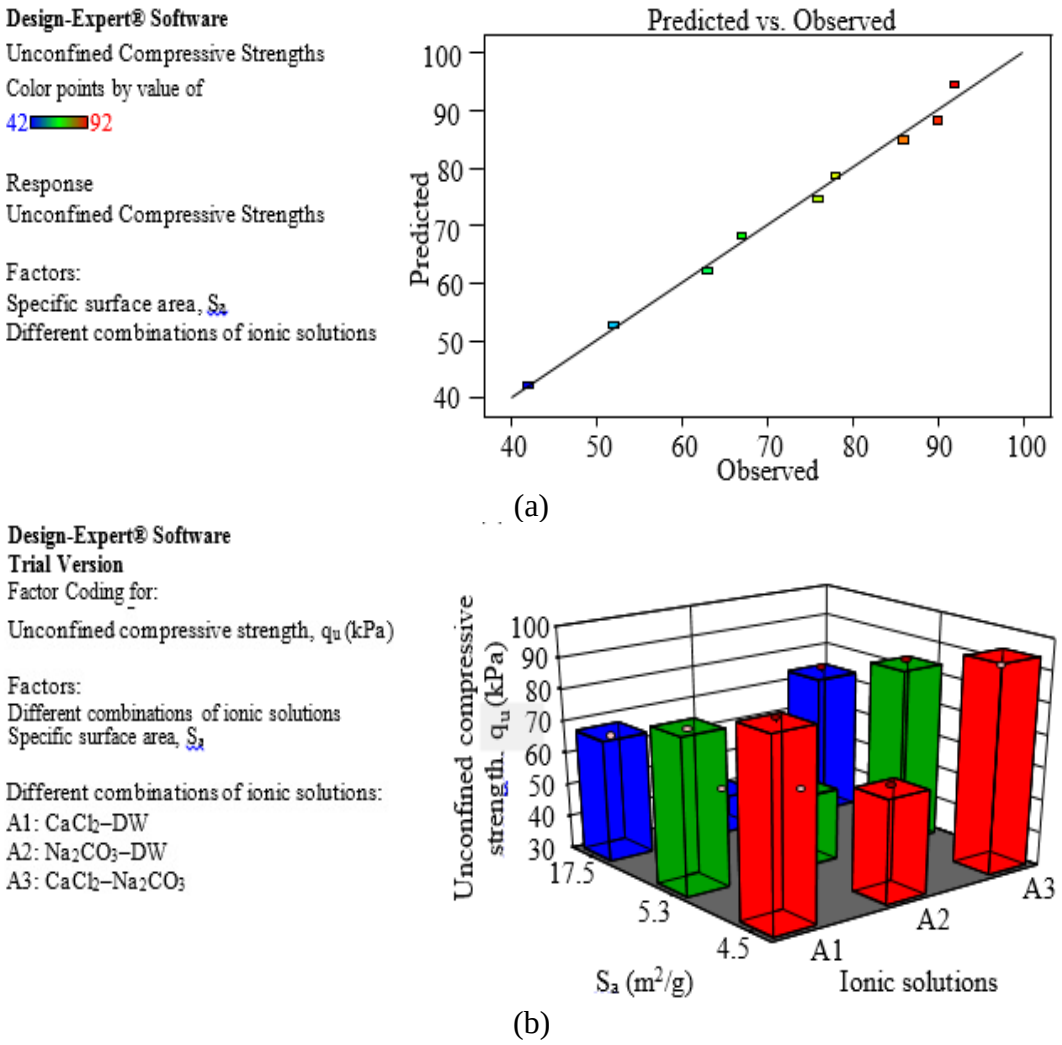

Figure 5.37: (a) Prediction model and (b) 3D plots of different combinations of ionic solutions and S_a variables on q_u response.

Table 5.16 provided the analysis of variance employed by the response surface methodology, RSM. The input factors considered were the pH, electrical conductivity (σ), and ionic strength (I_s). The probability P-values and F-values indicated that the model terms for electrical conductivity (σ) and ionic strength (I_s) were significant.

Table 5.16: Summary of ANOVA for q_u values of treated soils model fit with pH, σ, and I_s.

Source	Sum of Squares	df	Mean Square	F-value	P-value	
Model	8187.88	9	909.76	5.67	0.0002	significant
A: pH	9.85	1	9.85	0.0614	0.8062	insignificant
B: Electrical conductivity, σ	775.54	1	775.54	4.84	0.0370	significant
C: Ionic strength, I_s	4984.62	1	4984.62	31.09	< 0.0001	significant
AB	1335.04	1	1335.04	8.33	0.0078	significant
AC	40.04	1	40.04	0.2497	0.6215	insignificant
BC	0.3750	1	0.3750	0.0023	0.9618	insignificant
A^2	162.13	1	162.13	1.01	0.3239	insignificant
B^2	316.42	1	316.42	1.97	0.1719	insignificant
C^2	157.31	1	157.31	0.9811	0.3311	insignificant
Residual	4168.87	26	160.34			
Lack of Fit	529.37	5	105.87	0.6109	0.6926	
Pure Error	3639.50	21	173.31			
Cor Total	12356.75	35				
Std. Dev.	12.66			R^2	0.6626	
Mean	51.58			Adjusted R^2	0.5458	
CV %	24.55			Predicted R^2	0.3655	
				Adeq. Precision	8.5324	

The Model F-value of 5.67 implies the model is significant. There is only a 0.01% chance that a "Model F-value" this large could occur due to noise. Values of "Prob. > F" less than 0.0500 indicates model terms are significant. In this case, B, C, and AB are significant model terms.

Thus, the model term for pH and σ interaction had a significant effect. The prediction model for the observed and predicted R^2 was in reasonable agreement with the adjusted R^2. The adequate precision ratio indicated an appropriate analysis. The interaction effect showed that the interaction of factors pH and σ had a more significant effect on q_u than the interaction of factors pH and I_s, or σ and I_s as indicated in Table 5.16.

Figure 5.38 shows the contour and 3D plots showing the effect of the interaction of factors of pH, σ, and I_s on q_u response. Figures 5.40a, 5.40b, and 5.40c showed that high pH alkaline font at high σ and high I_s produced a higher effect on q_u in the EK treated soils, while the acidic pH font at low σ and low I_s had a less remarkable effect on the q_u.

The contour plots validated the significant effect of the model terms. In Figure 5.41a, the contour lines for the interaction factors pH and σ were curved, which indicated that the model term was significant on the performance of the EK treatment of the soft soil.

Whereas the model terms of interaction factors in Figures 5.40b and 5.40c, for the interaction factors of pH and ionic strength (I_s); and electrical conductivity (σ) and ionic strength (I_s) had semi curves and parallel lines, respectively. Thus, the factors had individual substantial effects, but the interaction of the factors had no significance.

The considerable effect of the factors analyzed in this section was in the order of I_s > σ > interaction effect of pH and σ > pH > σ and ionic strength, I_s > interaction effect of pH and ionic strength, I_s. The DOE produced the threshold values obtained for pH = 9.5, ionic strength, I_s = 1.55 10^{-4} mol/L, and electrical conductivity, σ = 6.0 m/S with a substantial performance for the effective strengthening of the EK treated soils.

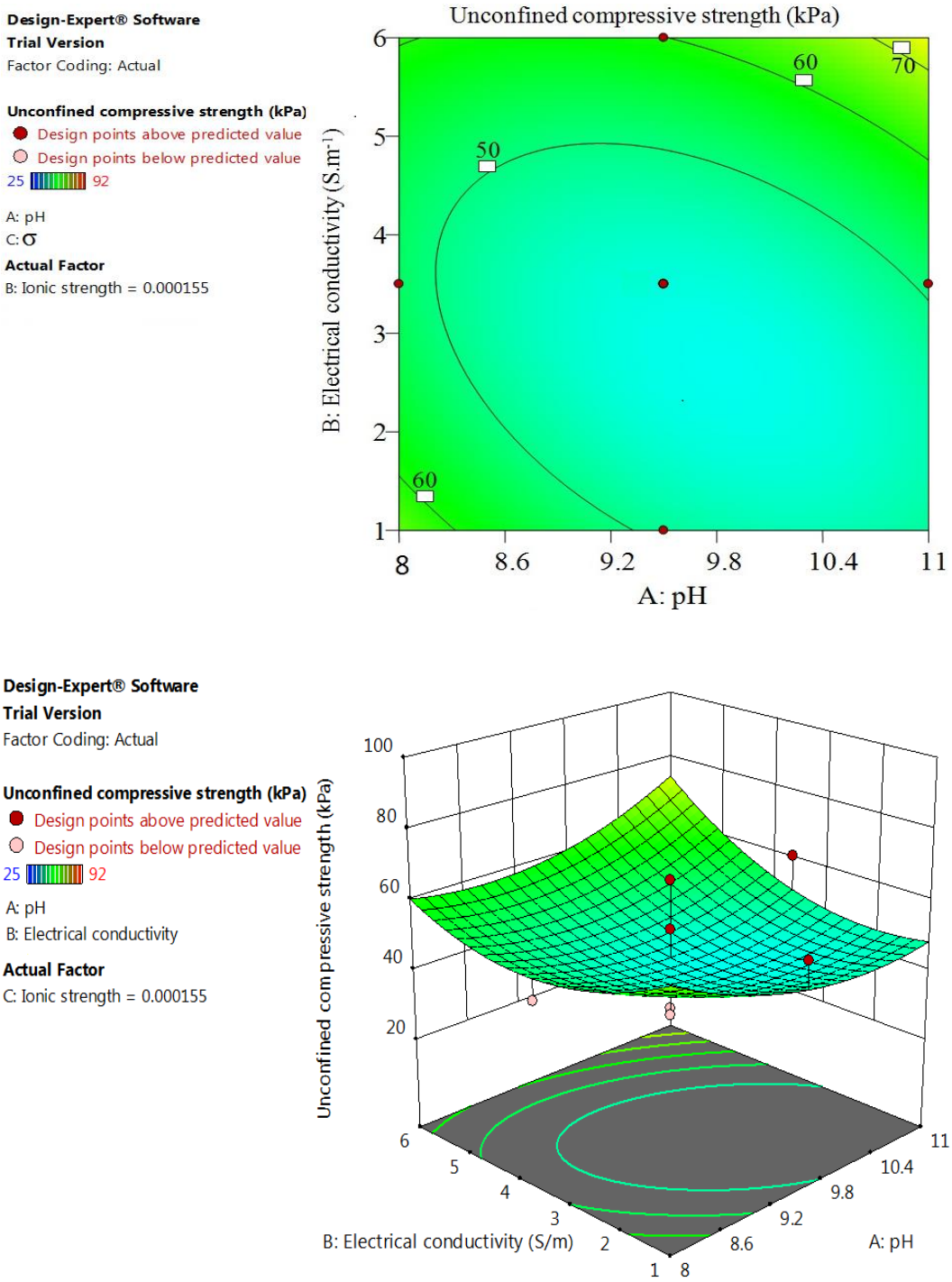

(a) Effect of A: pH, and B: electrical conductivity, σ on q_u response.

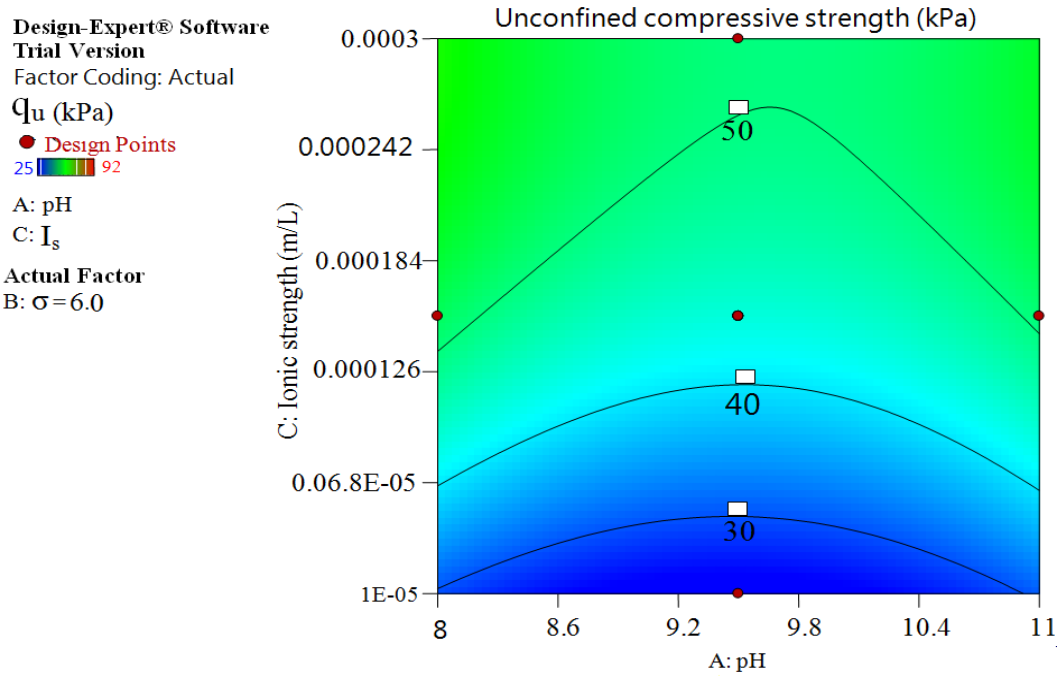

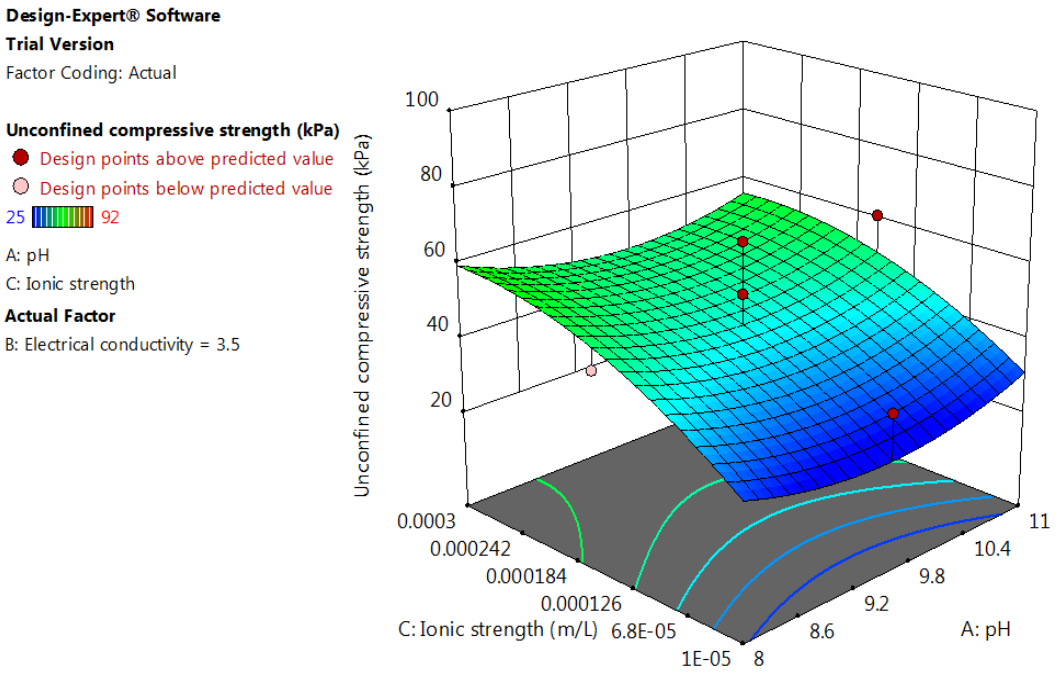

(b) Effect of A: pH, and C: ionic strength, I_s factors on q_u response.

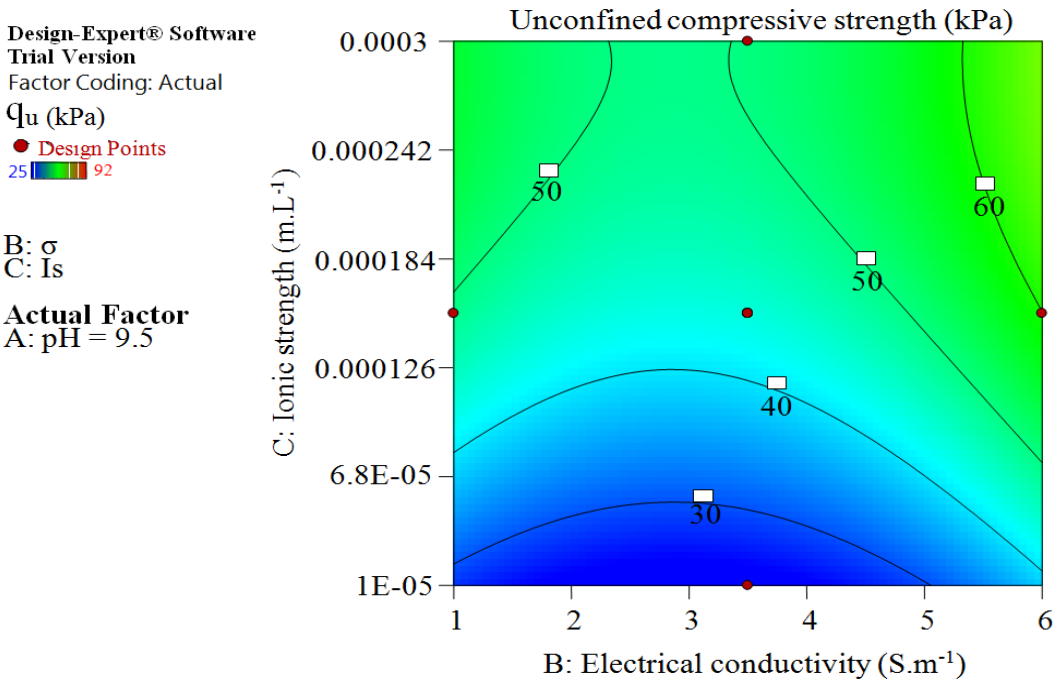

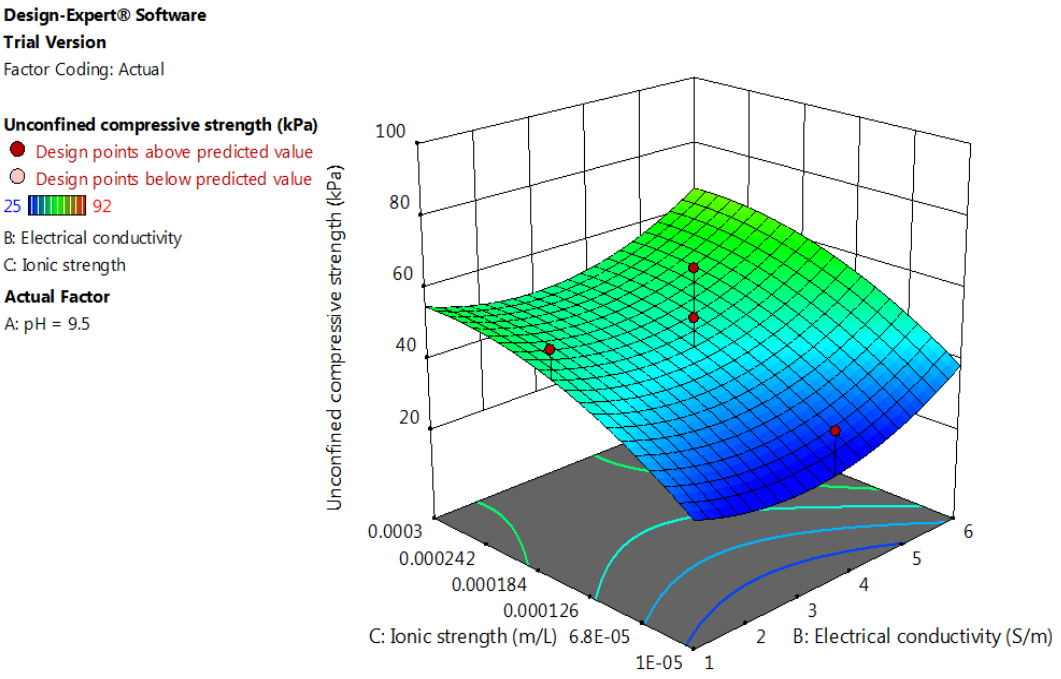

(c) Effect of B: electrical conductivity, σ, and C: ionic strength, I_s on q_u response.

Figure 5.38: Contour and 3D plots showing effects of the interaction of factors A: pH, B: electrical conductivity, σ, and C: ionic strength, I_s factors for (a) AB, (b) AC and (c) BC on q_u response.

5.8.2 Effect of changing electrode length ratio, $l_{ce,}$ and soil depth, d_s on the performance of EK treatment of soft soil: numerical models

The performance of the EK treatment at changing electrode length, l_e, soil depth, $d_{s,}$ and along lateral anode to cathode distances, $d_{A\leftrightarrow E}$, was examined using numerical models. Based on the findings, the changing electrode length, l_e had significant effects on the performance of EK treatment on soft soils at different soil depths, $d_{s,}$ and anode to cathode distances, $d_{A\leftrightarrow E}$ directions. Thus, depending on the specific soil depth, d_s, the suitable electrode length, l_e can be accurately modeled, designed, and configured to efficiently improve the deficient soils using the design of experiment, DOE methods.

5.8.2.1 Analytical study of plasticity index, PI of EK treated soils at changing electrode length, $l_{ce,}$ and soil depth, d_s at different points of soil extraction

In the present study, the obtained PI and SP values of the EK treated soils with electrode length ratio, l_{ce} and at different soil depths, d_s measured at different points A, B, C, D, and E, shown in Figure 5.39 along anode to cathode distances, $d_{A\leftrightarrow E}$ were examined and analyzed. Table 5.17 presents the PI values of the EK treated soils at electrode length ratio, l_{ce}, soil depths, d_s, and anode to cathode distances, $d_{A\leftrightarrow E}$.

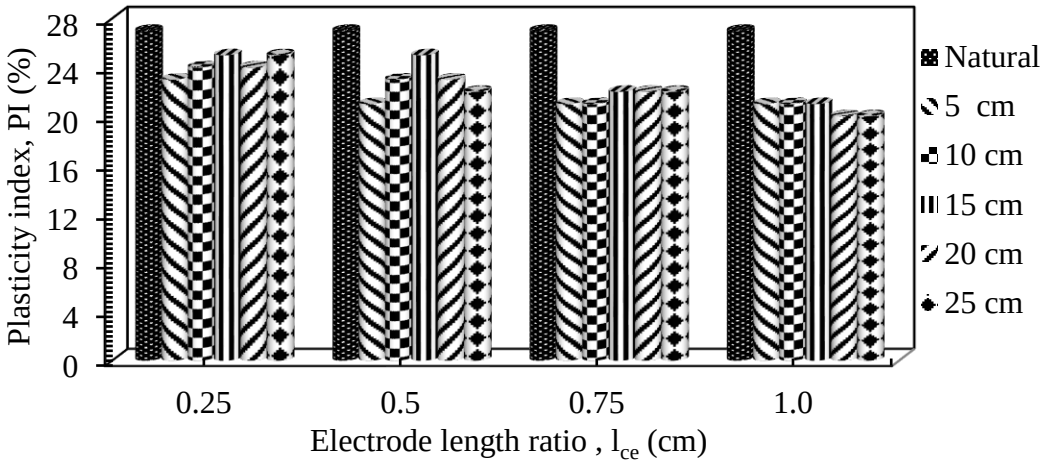

Figure 5.39: Plasticity index, PI of EK treated soils for changing electrode length ratios, l_{ce} to soil depth, d_s at point A.

Table 5.17: Plasticity index (PI) values of EK treated soils at different l_e, d_s and $d_{A\leftrightarrow E}$.

Anode to cathode distances, $d_{A\leftrightarrow E}$ (cm)	Soil depth, d_s (cm)	Electrode length, l_e (cm)			
		7.50	15.0	22.5	30.0
		Plasticity index, PI (%)			
Natural soil	-	27	27	27	27
Point A (5 cm distance from anode)	5	23	21	21	21
	10	24	23	22	21
	15	25	25	22	21
	20	24	23	22	20
	25	25	22	22	20
Point B (10 cm distance from anode)	5	27	23	23	21
	10	26	24	23	21
	15	25	23	23	21
	20	25	23	24	21
	25	27	23	24	21
Point C (15 cm distance from anode)	5	27	25	25	23
	10	27	25	25	23
	15	27	26	24	23
	20	27	26	24	23
	25	27	26	24	23
Point D (20 cm distance from anode)	5	25	24	23	22
	10	24	23	22	22
	15	24	23	22	22
	20	25	25	23	22
	25	27	25	22	21
Point E (25 cm distance from anode)	5	24	22	23	22
	10	24	21	21	22
	15	24	23	21	21
	20	25	22	21	20
	25	27	24	20	20

*circle represents the critical point, C_p

Figure 5.39 summarizes the effects of the electrode length, l_e on soils plasticity at different soil depths, d_s at point A. At point A, the effects of $1.0l_{ce}$ (electrode length of 30cm) and $0.75l_{ce}$ on the PI values of the EK treated soils were approximately similar. Also, the effects of $0.25l_{ce}$ and $0.50l_{ce}$ PI values of the EK treated soils were

identical to each other. At point A, the efficiency of EK treatment was in the order of changing electrode length rations of $1.0l_{ce} > 0.75l_{ce} > 0.50l_{ce} > 0.25l_{ce,}$ along with the soil depth, d_s. The EK treatment is effective on the EK treated soils at point A due to proximity to the electrolyte chamber housing the ionic solution and the anode plate.

At point B, the effects of the electrode length, l_e on PI at different soil depths, d_s are provided in Figure 5.40. At point B, the effects of the changing l_e on the PI values of the EK treated soils at different d_s was less effective when compared to point A. The efficiency of varying l_{ce} reduced due to an increasing distance from the anode/ionic solution chamber. Thus, at point B, the efficacy of the EK soil treatment was in the order of $1.0l_{ce} \approx 0.75l_{ce} > 0.50l_{ce} \approx 0.25l_{ce}$ along with the different soil depths, d_s.

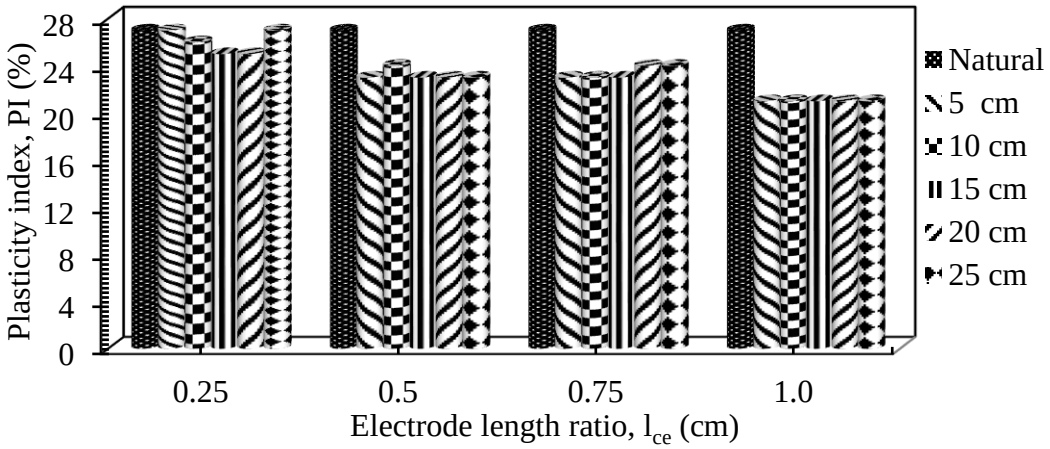

Figure 5.40: PI of EK treated soils for changing electrode length ratios, l_{ce} to soil depth, d_s at point B.

At point C, the effects of the electrode depth, d_e on plasticity index (PI) at different soil depths, d_s are provided in Figure 5.41. At point C, the effects of the changing l_{ce} on PI values of the EK treated soils at different d_s showed that the efficiency of changing l_{ce} reduced significantly due to a distance from the ionic solution chambers.

Hence, at point C, the efficacy of the EK treatment was in the order of $1.0l_{ce} \approx 0.75l_{ce} \approx 0.50l_{ce} \approx 0.25l_{ce}$ along with the soil depth, d_s direction. The least performance of EK treatment was achieved at point C due to the distance to both the anode and cathode ends and the ionic solutions chambers and therefore made it the most critical zone.

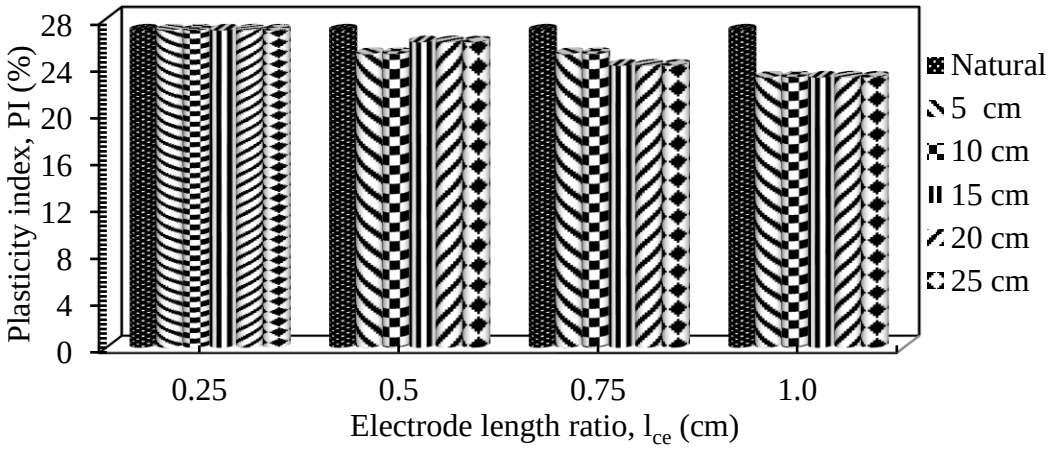

Figure 5.41: PI of EK treated soils for changing electrode length ratios, l_{ce} to soil depth, d_s at point C.

At point D, the effects of the electrode length ratio, l_{ce} on plasticity index (PI) values at different soil depths, d_s are provided in Figure 5.42. At the point of extraction at D, the effects of the changing l_{ce} on the PI values of the EK treated soils at different d_s was in the order of changing electrode ratios of $1.0l_{ce} \approx 0.75l_{ce} > 0.50l_{ce} \approx 0.25l_{ce}$.

The EK treatment is less effective on the treated soils at the point of extraction point at D than at points of extraction at A and E due to distant proximity to the chamber housing the different combinations of the ionic solutions and the cathode plate.

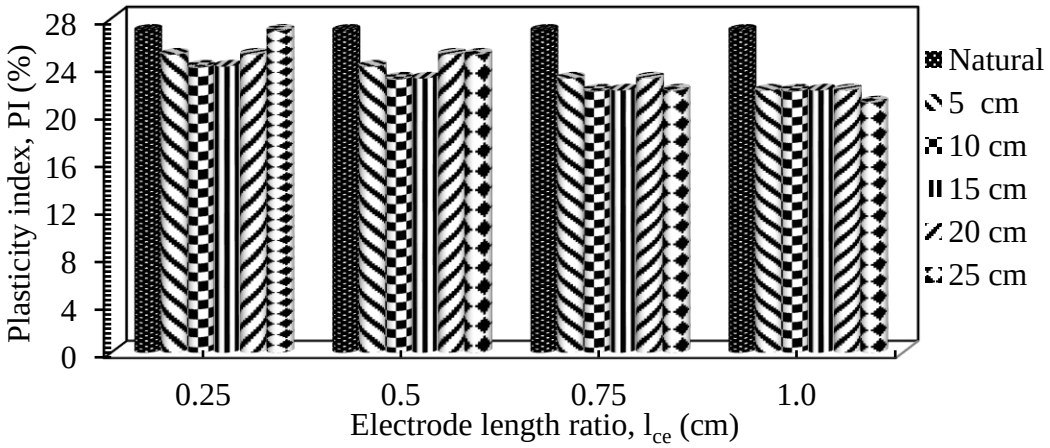

Figure 5.42: Plasticity index, PI of EK treated soils for changing electrode length ratios, l_{ce} to soil depth, d_s at point D.

At point E, the efficiency of EK treatment was found to be in the order of $1.0l_{ce} \approx 0.75l_{ce} > 0.50l_{ce} > 0.25l_{ce}$ along with the soil depth, d_s. Figure 5.43 presents the plasticity index, PI values at different electrode length ratio, l_{ce}, soil depths, d_s and lateral anode to cathode distances, $d_{A\leftrightarrow E}$. At the point of extraction at E, the effects of $1.0l_{ce}$ and $0.75l_{ce}$ were similar but more significant than the effects of $0.25l_{ce}$ and $0.50l_{ce}$ and high efficiency was observed, due to proximity to the ionic solution cell.

The results of the Atterberg limit values of the EK treated soils extracted at different points of extraction of A, B, C, D, and E were remarkably consistent, showing that the PI values significantly reduced in the vicinity of the electrodes for the electrode length ratio, l_{ce}. At the same time, the central portion was slightly affected by the varying l_{ce} to the d_s. Also, it can be observed that the different dimensions of the l_{ce} are significant and consistent both from the anode to cathode distances at different soil depths, d_s.

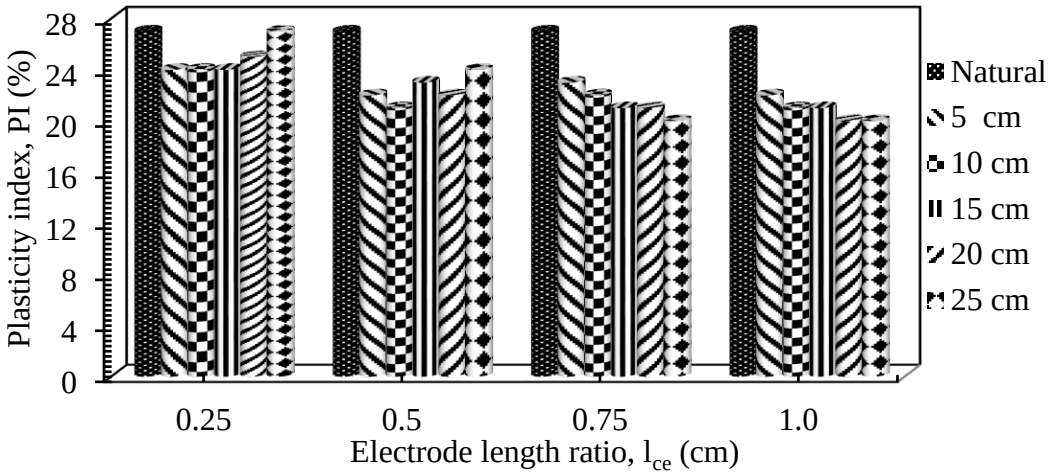

Figure 5.43: PI of EK treated soils for electrode length, l_{ce} to soil depth, d_s at point E.

However, $1.0l_{ce} \approx 0.75l_{ce} > 0.5l_{ce} > 0.25l_{ce}$ along with the d_s. Therefore, based on the findings, the l_{ce} affects the d_s significantly. Thus, depending on the target d_s, a suitable l_{ce} can be designed to efficiently improve or stabilize the soft soil using the EK treatment method.

5.8.2.2 Analytical study of swelling potential, SP of EK treated soils at changing electrode length ratios, l_{ce}, to soil depth, d_s, at different points of soil extraction

Table 5.18 and Figure 5.44 present the SP of the EK treated soils, at points A and E, the effects of changing electrode length ratio, l_{ce} at different soil depths, d_s can be observed to decrease along the soil depths, d_s. In a general term, for the PI and the SP of the EK treated soils, the efficiency of changing electrode length ratios, l_{ce} was in the order of changing electrode length ratios of $1.0l_{ce} > 0.75l_{ce} > 0.50l_{ce} > 0.25l_{ce}$.

Thus, it was observed that the experimental results depend on the surface area contact of the electrode plates with the EK treated soils, and the proximity and the electroosmotic driving flow of ionic solutions along with both the soil depth, d_s and lateral anode to cathode distance, $d_{A\leftrightarrow E}$ directions.

Table 5.18: Swelling potential (SP) values of EK treated soils at different l_e, d_s, and $d_{A\leftrightarrow E}$.

Anode to cathode distances, $d_{A\leftrightarrow E}$ (cm)		Soil depth, d_s (cm)	Electrode length, l_e (cm)			
			7.5	15.0	22.5	30.0
			Swell potential, SP (%)			
Natural soil		-	2.40	2.40	2.40	2.40
Treated soils						
Point A	5 cm distance from the anode	5 cm	1.20	0.95	0.85	0.73
		10 cm	1.33	0.97	0.89	0.68
		15 cm	1.48	1.14	0.99	0.62
		20 cm	1.46	1.16	1.13	0.62
		25 cm	1.49	1.37	1.16	0.55
Point C	15 cm distance from the anode	5 cm	1.51	1.45	1.38	1.37
		10 cm	1.58	1.45	1.36	1.35
		15 cm	1.57	1.44	1.36	1.32
		20 cm	1.59	1.43	1.35	1.29
		25 cm	1.51	1.43	1.34	1.25
Point E	25 cm distance from the anode	5 cm	1.31	1.05	0.98	0.87
		10 cm	1.58	1.07	1.02	0.95
		15 cm	1.57	1.24	1.05	1.02
		20 cm	1.59	1.33	1.08	1.05
		25 cm	1.61	1.57	1.24	1.05

5.8.2.3 Critical points, C_p for plasticity index, PI and swelling potential, SP data

Tables 5.17 and 5.18 present the experimental data of the PI, and the SP values of the EK treated soils. The critical point, C_p, was defined at the predetermined locations of extraction in the test tanks for given input factors. The C_p is the least effective region where the obtained data of the PI values in the EK treated soils were close to the PI values of the insitu soil, as shown by the oval icon in Tables 5.17 and 5.18.

The critical point (C_p) was used to analyze the effect of experimental factors on the PI, and the SP of the EK treated soils. The C_p was used as a reference point in the RSM to examine the input factors, and their interactive effects at the worst engineering conditions on the PI and the SP values of the EK treated soils using the ionic solutions.

The significant input factors at the C_p maybe deemed suitable and enable geotechnical engineers to navigate a design space for the large scale in situ application of ground improvement. The C_p for the PI and the SP at different electrode lengths, l_e, soil depths, d_s, and lateral anode to cathode distances, $d_{A\leftrightarrow E}$ were given in the relationships provided below as:

d_s versus $d_{A\leftrightarrow E}$ at critical electrode length, l_e of 15 cm

l_e versus $d_{A\leftrightarrow E}$ at critical soil depth, d_s of 15 cm

d_s versus l_e at critical lateral distances, $d_{A\leftrightarrow E}$ of 15 cm

5.8.2.4 Statistical interpretations of plasticity index, PI data

Table 5.19 presents the ANOVA analysis for the plasticity index (PI) values obtained from the EK treated soils. The probability, p-value less than 0.05, indicated that the factors, X_1: electrode length, l_e, X_3: lateral anode to cathode distances, $d_{A\leftrightarrow E}$, and X_1: electrode length, l_e and X_2: soil depth, d_s combination were significant model terms. The plasticity index (PI) values changed significantly along the fixed factor X_2: soil depth, d_s, which on its own, was not a significant model term. In this case, X_1, X_3, X_1X_2, X_1^2, X_3^2 were significant model terms and had a significant effect on the PI values of the EK treated soils. The interactive effect of factors X_2, X_1X_3, and X_2X_3 model terms was negligible on the plasticity index (PI) of the EK treated soils. The model F-value of the ANOVA analysis implied that the model term was significant.

Figure 5.44a presents the predicted PI versus actual PI values. The actual R^2 value predicted R^2 value, and adjusted R^2 were 0.8175, 0.7992, and 0.7783, respectively. The high actual R^2, the predicted R^2, and the adjusted R^2 values indicated a substantial agreement between the experimental and the model values obtained. The adequate precision ratio of 26.81 was greater than > 4 and showed there was an adequate signal.

Table 5.19: ANOVA for PI of EK treated soils at changing l_e at different d_s and $d_{A\leftrightarrow E}$.

Source	Sum of Squares	df	Mean Square	F-value	p-value	
Model	335.92	9	37.32	44.79	< 0.0001	significant
X_1: Electrode length, l_e	137.64	1	137.64	165.18	< 0.0001	significant
X_2: Soil depth, d_s	0.2160	1	0.2160	0.2592	0.6119	insignificant
X_3: Anode to cathode, $d_{A\leftrightarrow E}$	6.02	1	6.02	7.22	0.0086	significant
X_1X_2	6.56	1	6.56	7.87	0.0061	significant
X_1X_3	0.4000	1	0.4000	0.4801	0.4902	insignificant
X_2X_3	1.56	1	1.56	1.88	0.1743	insignificant
X_1^2	13.69	1	13.69	16.43	0.0001	significant
X_2^2	0.0893	1	0.0893	0.1072	0.7442	insignificant
X_3^2	126.23	1	126.23	151.49	< 0.0001	significant
Residual	74.99	90	0.8332			
Cor Total	410.91	99				

The Model F-value of 44.79 implies the model is significant. There is only a 0.01% chance that a "Model F-value" this large could occur due to noise. Values of P-value less than 0.0500 indicates model terms are significant. In this case, X_1 and X_2 are significant model terms. df represents the degree of freedom in the ANOVA.

5.8.2.5 Statistical interpretations of swelling potential, SP analysis

Table 5.20 presents the ANOVA analysis for the SP values of the EK treated soils. The obtained probability, a p-value less than 0.05, showed that the factors, X_1: electrode length, l_e , X_2: soil depth, d_s, and X_1: X_3: electrode length, l_e, and anode to cathode distances, $d_{A\leftrightarrow E}$ is significant model terms. In this case, X_1, X_2, X_3, X_1X_3 were substantial model terms and appeared to have a significant effect on the SP response. The p-values of factors greater than > 0.10 showed they are not significant.

The interactive effect of factors X_1X_2 and X_2X_3 model terms were negligible on the EK treated soils. The model F-value was 56.54, which implies that the model term was significant. Figure 5:44b gives the predictive model for the SP values. The actual R^2 value was 0.9137. The predicted R^2 value and the adjusted R^2 were 0.8980 and 0.8782, respectively, and their difference < 0.2. The high actual R^2, the predicted R^2, and the adjusted R^2 values showed firm correlations between the experiment and model values. The adequate precision ratio of 29.01 was greater than > 4 showed a sufficient signal.

Table 5.20: ANOVA for SP of EK treated soils at changing l_e at different d_s and $d_{A\leftrightarrow E}$.

Source	Sum of Squares	df	Mean Square	F-value	p-value	
Model	3.01	6	0.5019	58.26	< 0.0001	significant
X_1: Electrode length, l_e	2.06	1	2.06	239.60	< 0.0001	significant
X_2: Soil depth, d_s	0.4947	1	0.4947	57.41	< 0.0001	significant
X_3: Anode to cathode, $d_{A\leftrightarrow E}$	0.1814	1	0.1814	21.05	< 0.0001	significant
X_1X_2	0.0041	1	0.0041	0.4758	0.4951	insignificant
X_1X_3	0.0464	1	0.0464	5.38	0.0267	significant
X_2X_3	0.0009	1	0.0009	0.1058	0.7471	insignificant
Residual	0.2843	33	0.0086			
Cor Total	3.30	39				

The Model F-value of 58.26 implies the model is significant. There is only a 0.01% chance that a "Model F-value" this large could occur due to noise. Values of P-value less than 0.0500 indicates model terms are significant. In this case, X1 and X2 are significant model terms. df represents the degree of freedom in the ANOVA.

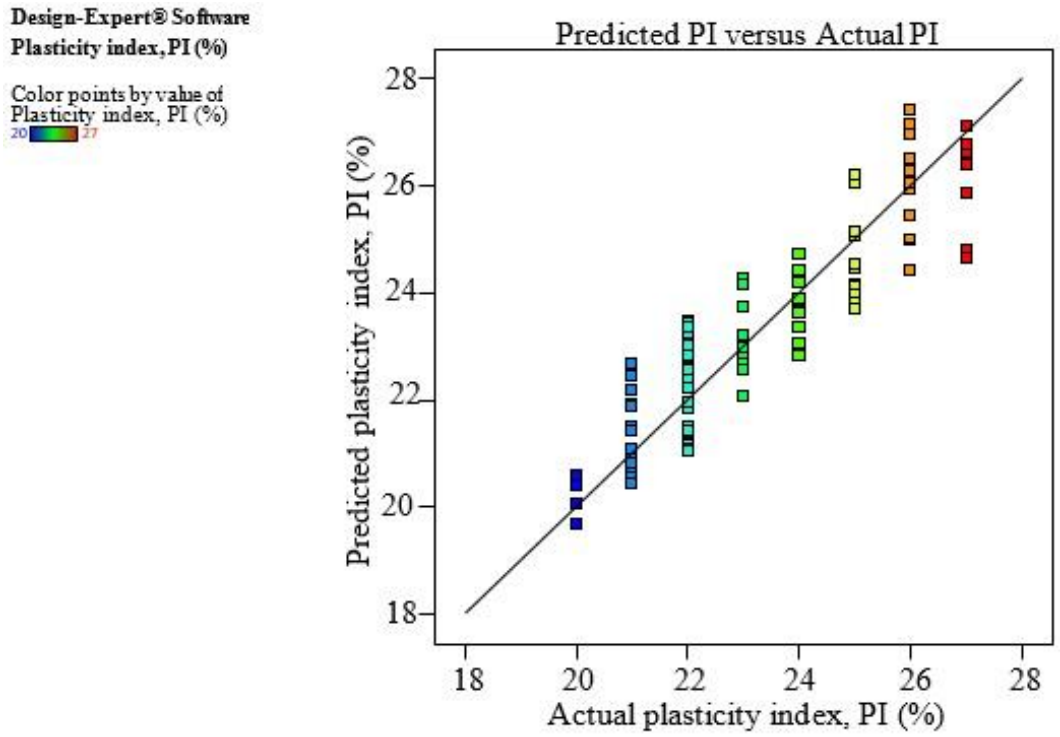

(a)

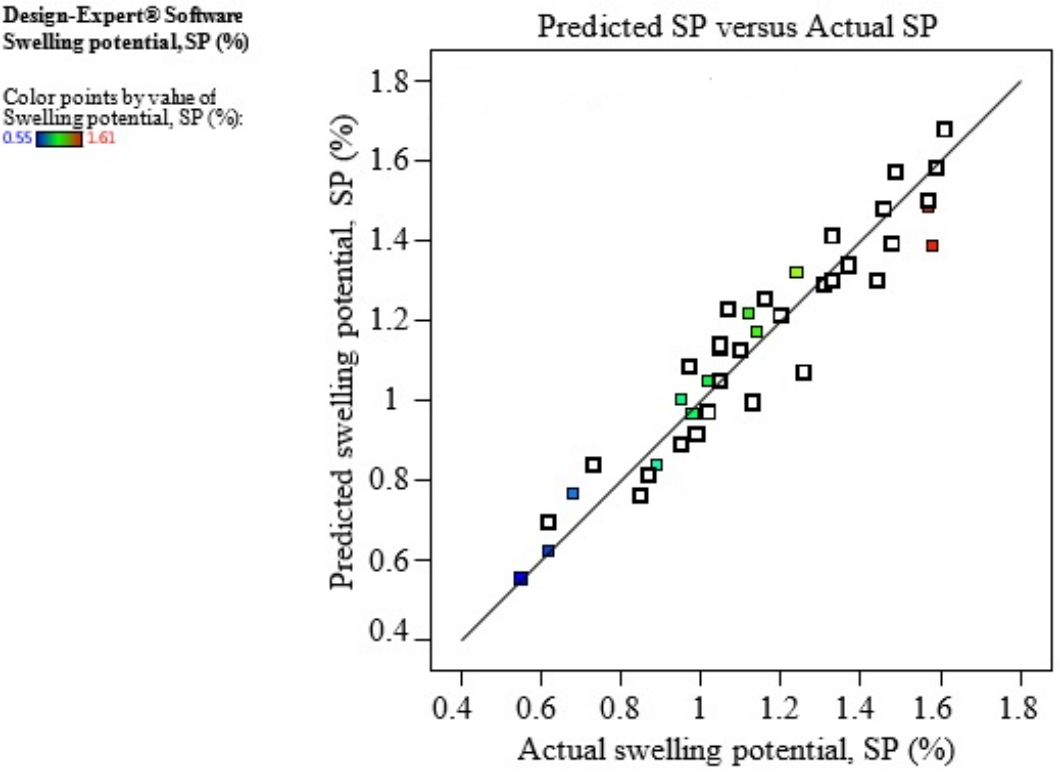

(b)

Figure 5.44: A predictive model for (a) plasticity index, PI (b) swelling potential, SP of the EK treated soils.

5.8.2.6 Effects of electrode length, l_e versus soil depth, d_s on PI

Figure 5.45 presents the response surface plots for electrode length, l_e, and soil depth, d_s, to examine their significant effects on PI values of the EK treated soils.

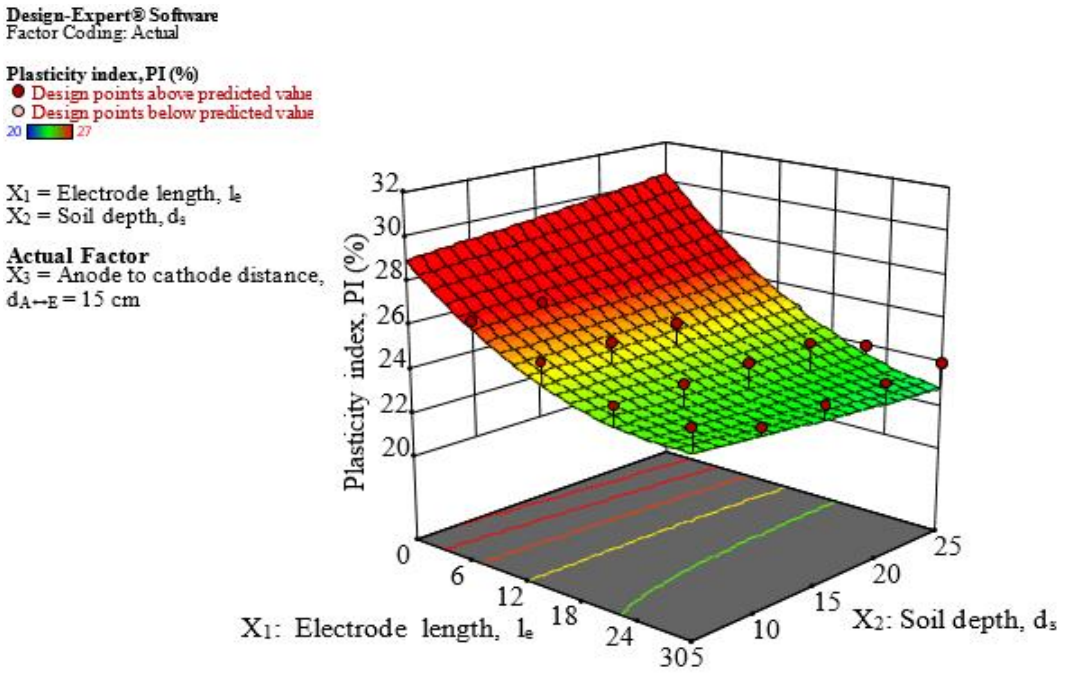

Figure 5.45: Effects of electrode length, l_e versus soil depth, d_s on plasticity index, PI of EK treated soils.

It was observed that EK treated soils exhibited its lowest plasticity index (PI) values at the higher electrode length, l_e, and the highest PI values at the shortest electrode length along with the changing deeper soil layers. At the C_p, the effects of the changing electrode length ratios, $1.0l_{ce}$, $0.75l_{ce}$, and $0.50l_{ce}$, were significant for the total soil depth, d_s of 30 cm, whereas the effect of changing electrode length ratio of $0.25l_{ce}$ was not significant for the entire soil depth, d_s. An indication that the performance of the EK treatment on the soil blocks depends on the surface area contact of the electrodes, their interaction with the ionic solutions, and their potential to discharge electrical energy needed to initiate electrochemical gradients along with the soil depth, d_s.

It was observed that the changing electrode length, l_e, significantly affected the performance of the EK treated soils. The changing electrode length, l_e aided changes in the clay-ionic solutions reactions, thus altering the PI values of the EK treated soils. In terms of electrode length ratio, l_{ce} and soil depth, d_s, the $0.50l_{ce}$, and $0.75l_{ce}$ were suitable enough to achieve high efficiency in the EK treatment for a given soil depth.

5.8.2.7 Effects of electrode length, l_e versus anode to cathode distances, $d_{A\leftrightarrow E}$ on PI

Figure 5.46 presents the 3D response surface model and interactive effect plots between the electrode length, l_e, and lengthwise anode to cathode distances: $d_{A\leftrightarrow E}$ to examine their effects on the plasticity index (PI) values of the EK treated soils.

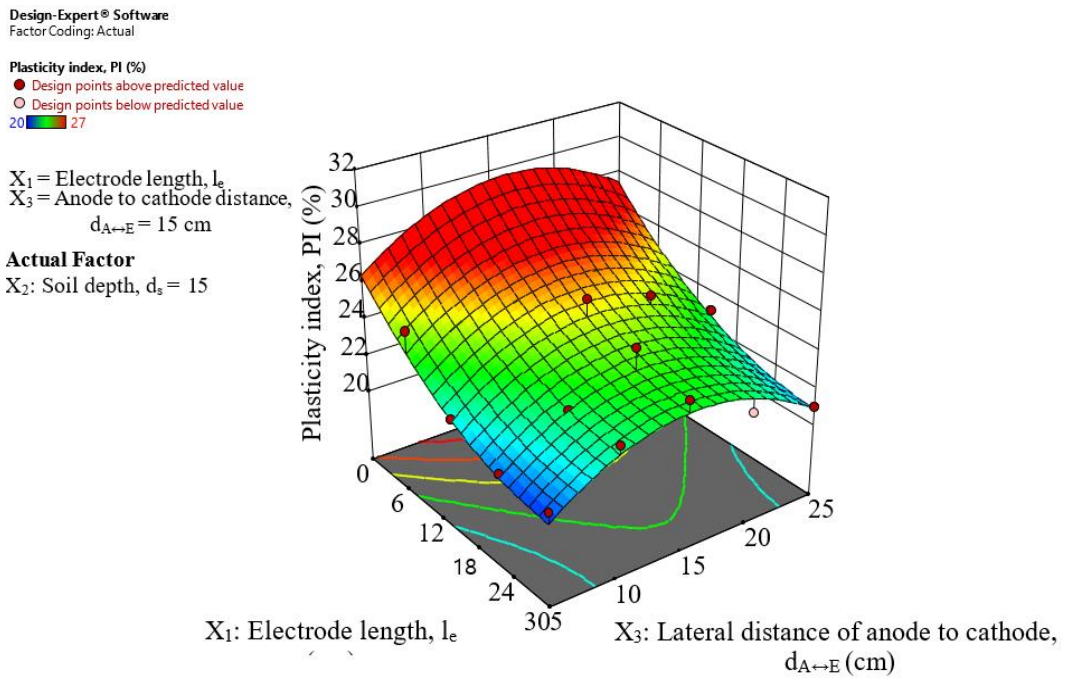

Figure 5.46: Effects electrode length, l_e versus lateral anode to cathode distances, $d_{A\leftrightarrow E}$ on plasticity index, PI of EK treated soils.

The EK treated soils were observed to display their lowest PI values at the higher electrode length, l_e, especially at the points of extraction with the closest proximity to the anode and cathode plates in the ionic solution chambers. The changing electrode

length, l_e had a significant effect on PI values of the EK treated soil along the anode to cathode distances, $d_{A\leftrightarrow E}$ at the selected critical point, C_p for soil depth, d_s, 15 cm.

It was observed that at higher electrode length, l_e, the EK treated soils exhibited its lowest PI values at the anode to cathode distances, $d_{A\leftrightarrow E}$ at points A and E in both the lateral and the depth directions. An indication that the performance of the EK soil treatment depends on the surface area contact and proximity of the electrodes with the treated soils.

The longer the electrode length, l_e the higher surface area it covers within a soil system; thus, the higher the clay-ionic solution reactions, alteration of the soil chemistry, and effective improvement of the EK treated soils. The response surface plots indicated that the PI values of the treated soils were lowest at higher electrode length, l_e and the points of extraction of A and E, close to the anodic and cathodic ends, respectively.

5.8.2.8 Effects of soil depth, d_s versus lateral anode to cathode distances, $d_{A\leftrightarrow E}$ on PI

Figure 5.47 presents the response surface plots to ascertain how significant the different ionic solutions setups were effectively changing the plasticity index (PI) values of the EK treated soils along with soil depth, d_s, and anode to cathode distances.

The performance of EK treatment is more active along the lateral anode to cathode distances, $d_{A\leftrightarrow E}$ when compared with the corresponding soil depths, d_s at the same points of extraction. It was observed that the EK treated soils exhibited its significant reduction of plasticity index (PI) values at the points of extraction of A and E in both

the lateral and depth directions. The nearer the proximity, the higher the clay-ionic solutions reactions, altered the soil chemistry and improved the treated soils effectively. The response surface plots indicated that the plasticity index (PI) values in the EK treated soils were at the lower values, near to the anodic and cathodic ends, but high plasticity index (PI) values were obtained at the predetermined critical point, C_p.

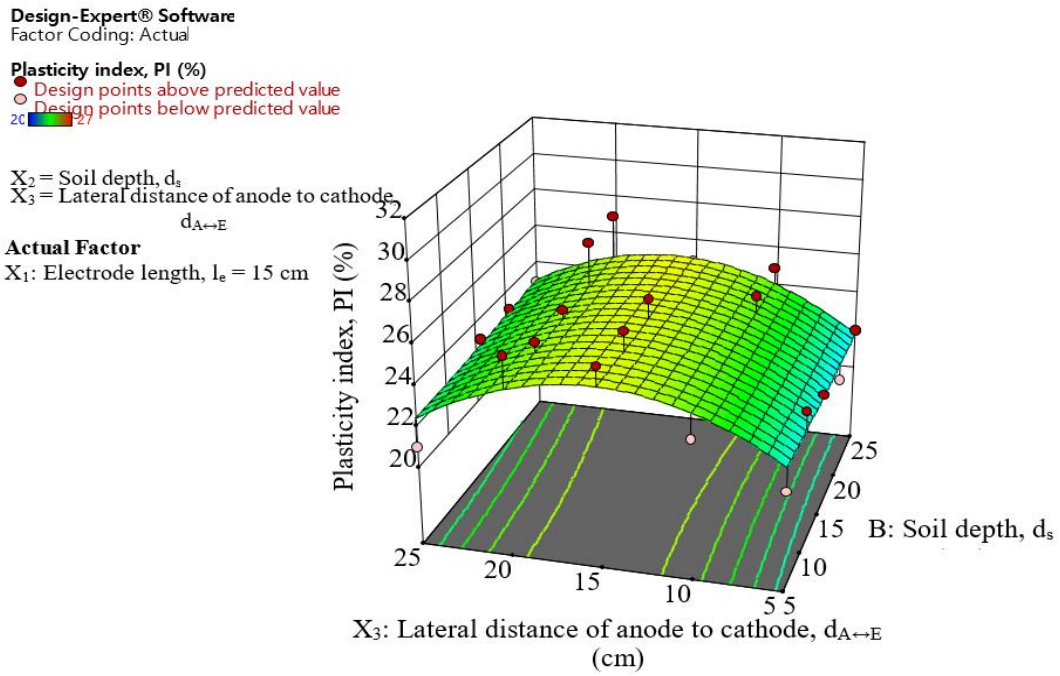

Figure 5.47: Effects of soil depth, d_s versus anode to cathode distances, $d_{A\leftrightarrow E}$ on plasticity index, PI of EK treated soils.

5.8.2.9 Effects of electrode length, l_e versus soil depth, d_s on SP values

It was observed in the response surface plots, that the changes in electrode length, l_e caused different combinations of ionic solutions to have different changing effects on the swelling potential values of the EK treated soils along different soil depths, d_s (Figure 5.48).

5.8.2.10 Effects of electrode length, l_e versus anode to cathode distances, $d_{A\leftrightarrow E}$ on SP

Figure 5.49 presents the response surface plots of electrode length, l_e versus anode to cathode distances, $d_{A\leftrightarrow E}$. In consideration of the changes in electrode length, l_e, it caused a significant reduction in swelling potential values of the EK treated soils, even at the critical point, C_p of soil depth, d_s, 15 cm. The flow of the ionic solutions along anode to cathode distances: $d_{A\leftrightarrow E}$, specifically at points of extraction of A and E, at the anode to cathode ends, significantly altered the swelling potential (SP) values at those points. The high electrode length, l_e had a significant reduction effect on (SP), while the reduced electrode length, l_e had little effect on the (SP) of the treated soils.

5.8.2.11 Effects of soil depth, d_s versus anode to cathode distances, $d_{A\leftrightarrow E}$ on SP

Figure 5.50 presents the soil depth, d_s correlation with the anode to cathode distances, $d_{A\leftrightarrow E}$, specifically at points of extraction of A and E, at the anode to cathode ends, respectively. To define the effect of the ionic solutions as a result of the changes in the electrode length, l_e at the critical point, C_p, showed that the swelling potential values of the EK treated soils had a significant reduction at points of extraction of A and E.

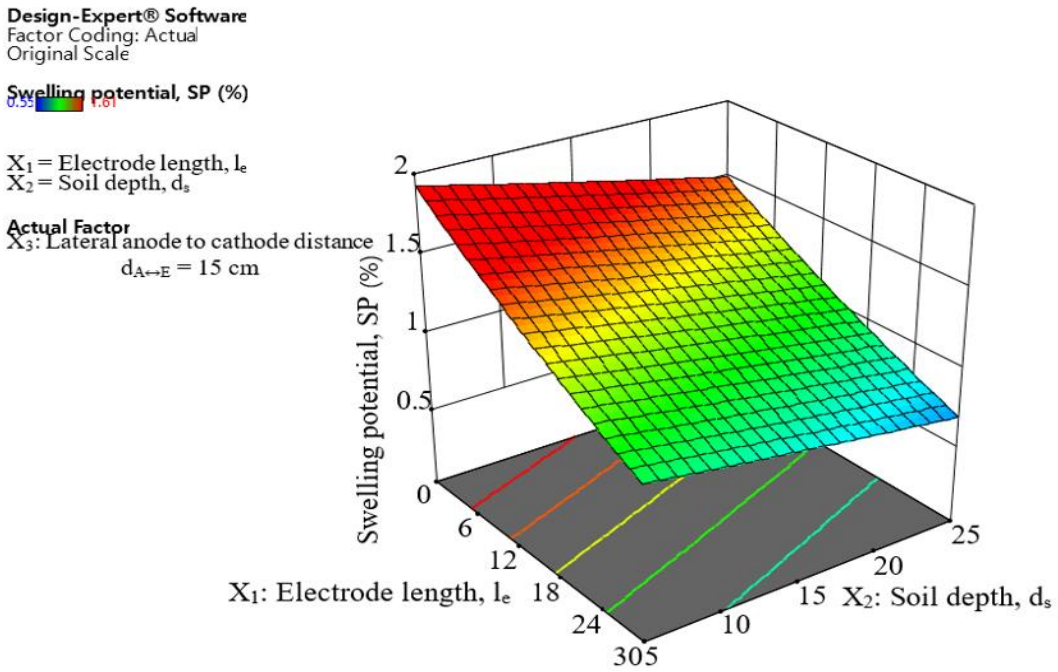

Figure 5.48: Effects of electrode length, l_e versus soil depth, d_s on swelling potential, SP of EK treated soils.

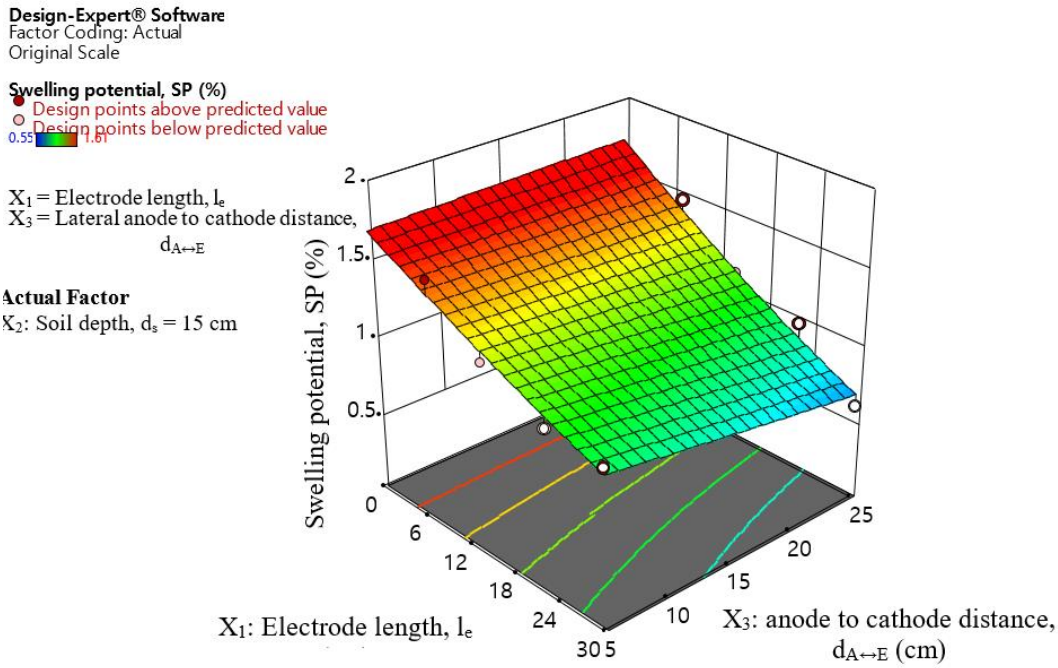

Figure 5.49: Effects of soil depth, l_e versus anode to cathode distances, $d_{A\leftrightarrow E}$ on swelling potential, SP of EK treated soils.

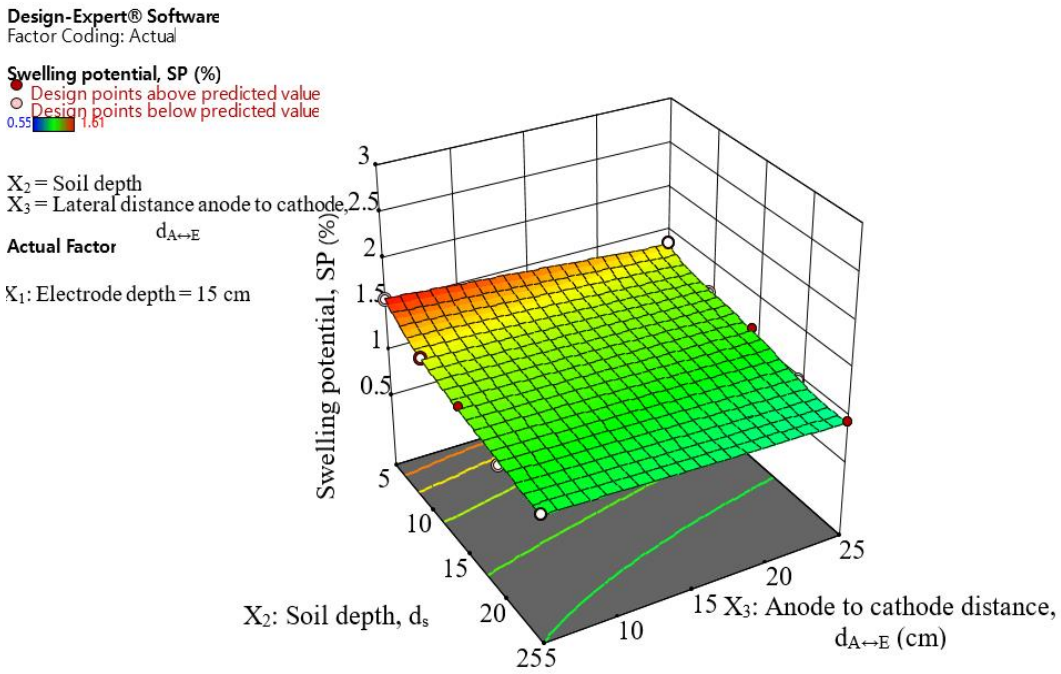

Figure 5.50: Effects of soil depth, d_s versus anode to cathode distances, $d_{A\leftrightarrow E}$ on swelling potential, SP of EK treated soils.

5.8.2.12 Building the plasticity index, PI and swelling potential, SP formulas

The following equations for the plasticity index and swelling potential of the EK treated soils were obtained through statistical analysis using the Statease software program. The equations were developed to build a relationship between the plasticity index and swelling potential with the selected input factors, the different combination of ionic solutions, electrode length, l_e, soil depth, d_s, and anode to cathode distances, $d_{A\leftrightarrow E}$.

$$PI = 23.29625 + 0.043214d_s - 0.375000l_e + 0.676500d_{A\leftrightarrow E} - 0.005667d_s*l_e + 0.002500d_s*d_{A\leftrightarrow E} - 0.001067l_e*d_{A\leftrightarrow E} + 0.000893d_s^2 + 0.008000l_e^2 - 0.022000d_{A\leftrightarrow E}^2 \quad 5.3$$

$$SP = 1.99205 - 0.021074d_s - 0.023874l_e - 0.002323d_{A\leftrightarrow E} + 0.0000173d_s*l_e + 0.000067d_s*d_{A\leftrightarrow E} - 0.0000411l_e*d_{A\leftrightarrow E} \quad 5.4$$

Thus, obtaining such equations derived from a numerical model can be used to estimate the required electrode length, l_e for a given soil depth, d_s and anode to cathode distances, $d_{A\leftrightarrow E}$ to achieve a specific plasticity index and swelling potential values in the EK soil treatment for a wide range of problematic soils in large field applications.

Chapter 6

CONCLUSIONS AND RECOMMENDATIONS

6.1 Conclusions

Based on the obtained experimental and numerical model results of the EK treated soils in the study, the preliminary conclusions can be drawn for the soft soil used:

- The effect of different combinations of ionic solutions on the performance of electrokinetic treatment of soft soils was considered based on the electrokinetic, EK treatment duration, anode to cathode distances, changing electrode lengths, and soil depths. It was observed that the selected factors had significant effects on the efficacy of the index, engineering, thermal, and morphological properties of the treated soils.

- The cumulative electroosmotic rate of flow q_{eo} was obtained from the flow of the different combinations of ionic solutions of $CaCl_2$-DW, $CaCl_2$-Na_2CO_3, and Na_2CO_3-DW, from their respective anode and cathode compartment, and, diffused into and absorbed by the EK treated soils. The result of the cumulative electroosmotic rate of flow, q_{eo} of the ionic solutions within the EK treated soils, are in the order of $CaCl_2$ > Na_2CO_3 > DW. The Ca^{2+} ions diffused into the soft soil and reacted with, and absorbed by this soil faster than the CO_3^{2-} ions. The q_{eo} showed the evidence of diffusion, migration, and absorption of ionic solution within the EK treated soil system. The use of $CaCl_2$ and Na_2CO_3 ionic solutions

induced an adequate EK flow in the treated soils with promising results for large scale applications.

- EK treatment caused an increment in the values of the electrochemical properties of the treated soils such as the pH, electrical conductivity, σ, total dissolved solids, T_{ds}, and ionic strength, I_s. The increment in the values was significant at the anode and cathode vicinity where there were efficient electrokinetic reactions and processes between the soil and the ionic solutions due to the initial inflow and proximity of both the ionic solutions and electro-conductive electrodes.

- There was an overall decrease in the cation exchange capacity, CEC, and the specific surface area, S_a values of the treated soils, due to the exchange of ions between the ionic solutions and clay minerals within the soil set up system, which resulted in the precipitation of new ions and as such aided the cementation, flocculation, and aggregation of clay fines, and altered the physicochemical, mineralogical, index, engineering, morphological and thermal properties of the treated soils along both the anode to cathode distances and soil depths.

- The combinations of ionic solutions were effective and efficient to reduce the plasticity behavior of the treated soils at different treatment durations along the anode to cathode distances, changing electrode lengths, and the soil depths. This is due to the modification of the physicochemical properties of the clay-ionic solutions and moisture content of the treated soil. As such, the changes in the soil chemistry affected the moisture absorption of the treated soils during the EK process and resulted in a considerable reduction in the liquid limit, plastic limit,

and plasticity index values of the EK treated soils. Also, the drastic decrease in the cation exchange capacity, and the specific surface area values of the treated soils caused a significant reduction in the plasticity of the EK treated soils. Also, there was a considerable reduction and improvement in the compressibility characteristics of the treated soils.

- The thermal and microscopy studies suggested the formation of CASH gels, which aided the flocculation and aggregation of the soil fines, most notably the treated soils with the $CaCl_2$-DW and $CaCl_2$-Na_2CO_3 ionic solutions, because of the presence of Ca^{2+} ions in the ionic solutions. Thus, stronger interparticle chemical bond strength was achieved in the EK treated soils.

- The different combinations of ionic solutions were effective and efficient to increase the unconfined compressive strength, q_u of the treated soils. The $CaCl_2$ ionic solution provided a better gain in strength than the Na_2CO_3 ionic solution. However, the combination of $CaCl_2$-Na_2CO_3 ionic solutions resulted in the best increase in the strength of the EK treated soils. The gain in strength was attributed to the flocculated and aggregated texture of the treated soil, due to the formation of the cementitious CASH gels, which were detected by DTA and DTG. The increase in the chemical bond strength of the soil particles caused better soil strengthening, stiffness, and stability.

- The effect of ionic solutions on the performance of the EK treatment was considered in terms of the changing electrode lengths and soils depths. It was observed that the variations in electrode length considerably affected the index and

engineering properties of the treated soils along different soil depths. This was due to the contact interactions between the conductive electrodes and ionic solutions, and surface area covered by the electrode to the treated soil along with both the lateral and vertical directions. As such, the longer electrode length, that is, the more surface contact area the anode and cathode had with the ionic solutions, and their proximity to EK treated soils. The better was the performance of EK treatment on soft soils, such as a reduction in the plasticity and increment in q_u of the EK treated soils in all the test setups.

- A design of experiment methodology for examining the significant factors in the electrokinetic application for strengthening soft soils has been proposed in this study. The results presented in this study have highlighted the significant performance of the controlling input factors on the unconfined compressive strength, q_u values obtained from the EK treatment of soft soils used in this study. The threshold values of the EK treated soil were developed for all the electrochemical properties considered in the study. The relative significant effects of the selected factors used in the design of the experiment in their order of importance on the soil strengthening were in the order of the EK treatment duration > ionic solutions > ionic strength, I_s > cation exchange capacity, CEC or specific surface area, S_a > electrical conductivity, σ > interaction effect of pH and electrical conductivity, σ > pH. The longer the EK treatment duration, with the right choice of ionic solutions, are considered to yield an excellent unconfined compressive strength for the soft soil.

- The longer EK treatment duration and ionic solution in the order of $CaCl_2$-Na_2CO_3**,** $CaCl_2$-DW**,** Na_2CO_3-DW, were recommended for greater efficiency of EK treatment.

- This study showed the significant factors in the EK treatment of soft soils through the design of experiment, DOE. The design model can be used to navigate a robust design space for a wide range of problematic soils for in situ geotechnical EK applications. The prediction models and ANOVA analyses validated the substantial agreement between the observed and predicted R^2 values obtained for the DOE of the factors and result outputs. Also, DOE analyzed the significant effects of changing electrode length on the determined plasticity index, and swelling potential of the EK treated soils along with the soil depth, and lateral anode to cathode distances.

- The design and analyses of experiments, DOE indicated that the changing electrode length had a significant effect on the performance of the EK treatment of the soils. The changing electrode length was changing the plasticity index, and swelling potential values of the EK treated soils adjacent or beneath the electrodes, along the soil depths and the anode to cathode distances. The efficiency of the electrode length ratio during the EK treatment was in the order of $1.0l_{ce} > 0.75l_{ce} > 0.50l_{ce} > 0.25l_{ce}$ along with the soil depth and anode to cathode distances for the plasticity index and the swelling potential of the EK treated soils.

- The efficiency of EK treatment at different points of extraction within the treated soil block samples was in the order of A ≈ E > B ≈ D > C for the plasticity index

values, and A ≈ E > C for the swelling potential values of the EK treated soils. The full electrode length ratio ($1.0l_{ce}$) produced the highest efficiency in the performance of ionic solutions on the properties of the treated soils; however, the electrode length ratio of $0.50l_{ce}$ to $0.75l_{ce}$ was suitable enough to improve the properties of the soft soil.

- A statistical equation was developed to estimate the sufficient electrode length suitable for specific soil depth and anode to cathode distances for the problematic fine-grained soil used in this study. The equations generated by the DOE adopted in this study can guide the practicing engineers to navigate accurate design models to choose the most suitable and significant input factors for different combinations of ionic solutions and the electrode length, which can be used to navigate a design model for a large scale in situ applications of EK treatment to improve a wide range of problematic soils. This study has shown that the combination of Na_2CO_3 and $CaCl_2$ ionic solutions, which are a rare combination in the electrokinetic studies, are effective enough to stabilize soft soils for in situ geotechnical applications.

6.2 Recommendations

In this study, a few recommendations to further study the effect of different combinations of ionic solutions on the performance of EK treatment of soft soils have been proposed.

- The variety of soil types with different chemical concentrations of the same ionic solutions should be performed so that more general results could be made for the use of practicing engineers. The use of non-toxic agro-industrial liquid wastes for

EK soil treatment should be considered for the management and recycling of liquid wastes.

- The use of new corrosion prevented methods should be considered in order to avoid degradation of conductive metallic electrodes, which reduces the efficiency of EK soil treatment. Also, further studies should consider examining, evaluating, and analyzing the spatial and depth effects of EK soil treatment and their effect on adjacent structures.

- The long-term stability of the EK treated soils concerning climate changes, and the influence of environmental factors such as wetting-drying and freezing-thawing cycles should be studied as future research topics so that the long-term behavior of the EK treated soils could be further understood.

- Further studies should also consider the standardization of EK materials, methods, and setups and more statistical and numerical model for EK soil treatment to optimize the dependent factors and output of results, and more detail discussion of the energy efficiency and cost of EK treatment of soils should be considered to maximize its cost-time efficiency.

REFERENCES

Abiodun, A. A., & Nalbantoglu, Z. (2020). Effect of ionic solutions on the performance of electrokinetic treatment of soft soils. *European Journal of Environmental and Civil Engineering*, 1-18.

Abiodun, A. A., & Nalbantoglu, Z. (2018). Sacrificial Anode Protection for Electrodes in Electrokinetic Treatment of Soils. In *Proceedings of China-Europe Conference on Geotechnical Engineering* (pp. 773-777). Springer, Cham.

Abiodun, A. A., & Nalbantoglu, Z. (2017). A Laboratory model study on the performance of lime pile application for marine soils. *Marine Georesources & Geotechnology*, *35*(3), 397-405.

Abiodun, A. A., & Nalbantoglu, Z. (2016). An overview of electrokinetic for soil treatment. *4th International Conference on New Developments in Soil Mechanics and Geotechnical Engineering, 02-04 June 2016, Near East University, Nicosia, North Cyprus.*

Abiodun, A. A., & Nalbantoglu, Z. (2015). Lime pile techniques for the improvement of clay soils. *Canadian Geotechnical Journal*, *52*(6), 760-768.

Abdullah, W. S., & Al-Abadi, A. M. (2010). Cationic–electrokinetic improvement of an expansive soil. *Applied Clay Science*, *47*(3-4), 343-350.

Acar, Y. B., & Alshawabkeh, A. N. (1993). Principles of electrokinetic remediation. *Environmental science & technology*, *27*(13), 2638-2647.

Ahmad, K. A. K., Kassim, K. A. K. K. A., & Taha, M. R. T. M. R. (2006). Electroosmotic flows and electromigrations during electrokinetic processing of tropical residual soil. *Malaysian Journal of Civil Engineering*, *18*(2).

Ahmad, K. B., Taha, M. R., & Kassim, K. A. (2011). Electrokinetic treatment on a tropical residual soil. *Proceedings of the Institution of Civil Engineers-Ground Improvement*, *164*(1), 3-13.

Ahmad Tajudin, S. A., Jefferson, I., Madun, A., Abidin, M. H. Z., Baharuddin, M. F. T., & Mohammad Razi, M. A. (2015). Monitoring of electric current during electrokinetic stabilisation test for soft clay using EKG electrode. In *Applied Mechanics and Materials* (Vol. 773, pp. 1560-1564). Trans Tech Publications Ltd.

Airoldi, F., Jommi, C., Musso, G., & Paglino, E. (2009). Influence of calcite on the electrokinetic treatment of a natural clay. *Journal of Applied Electrochemistry*, *39*(11), 2227.

Alshawabkeh, A. N. (2009). Electrokinetic soil remediation: challenges and opportunities. *Separation Science and Technology*, *44*(10), 2171-2187.

Alshawabkeh, A. N. (2001). Basics and application of electrokinetic remediation. Handouts prepared for a short course. *Handouts Prepared for a Short Course*, 95.

Alshawabkeh, A. N., & Bricka, R. M. (2001). Heavy metals extraction by electric fields. *Environmental restoration of metals-contaminated soils*, 167-186.

Alshawabkeh, A. N., & Sheahan, T. C. (2003). Soft soil stabilisation by ionic injection under electric fields. *Proceedings of the Institution of Civil Engineers-Ground Improvement*, *7*(4), 177-185.

Appelo, C. A. J. (2010). Specific conductance-how to calculate the specific conductance with PHREEQC.

Aqion (2020). Electrical conductivity, ionic strength and total dissolved solids. Retrieved from https://www.aqion.de/site/133.

Arutselvam, A. (2014). An improved technique for soft clay stabilization using electrokinetic process. *International Journal On Engineering Technology and Sciences*, *3*(1), 349-3976.

Asadi, A., Huat, B. B., Nahazanan, H., & Keykhah, H. A. (2013). Theory of electroosmosis in soil. *International Journal of Electrochemical Science*, *8*(1), 1016-1025.

Asadollahfardi, G., & Rezaee, M. (2019). Electrokinetic remediation of diesel-contaminated silty sand under continuous and periodic voltage application. *Environmental Engineering Research*, *24*(3), 456-462.

Asavadorndeja, P., & Glawe, U. (2005). Electrokinetic strengthening of soft clay using the anode depolarization method. *Bulletin of engineering geology and the environment*, *64*(3), 237.

Askin, T., & Turer, D. (2016). Effect of electrode configuration on electrokinetic stabilization of soft clays. *Quarterly Journal of Engineering Geology and Hydrogeology*, *49*(4), 322-326.

Association Française de Normalization. (AFNOR). (1993). Measurement of the amount and activity of the clay fraction (Norme Française NF P, 94–068).

ASTM. (2007). ASTM D422-63: Standard Test Method for Particle-Size Analysis of Soils.

ASTM, D. (2008). Standard test methods for one-dimensional swell or collapse of cohesive soils. *D4546-08*.

ASTM, D. (2011). Standard test methods for one-dimensional consolidation properties of soils using incremental loading. *D2435/D2435M-11*.

ASTM, D. 2166/D 2166M (2013) Standard test method for unconfined compressive strength of cohesive soil. *ASTM International, West Conshohocken*.

ASTM, D. (2010). Standard test methods for liquid limit, plastic limit, and plasticity index of soils. *D4318-10*.

Azhar, A. T. S., Azim, M. A. M., Syakeera, N. N., Jefferson, I. F., & Rogers, C. D. F. (2017, August). Application of Electrokinetic Stabilisation (EKS) Method for Soft Soil: A Review. In *IOP Conf. Ser. Mater. Sci. Eng* (Vol. 226).

Azhar, A. T. S., Nordin, N. S., Azmi, M. A. M., Embong, Z., Sunar, N., Hazreek, Z. A. M., & Aziman, M. (2018, April). The Physical Behavior of Stabilised Soft Clay by Electrokinetic Stabilisation Technology. In *J. Phys. Conf. Ser* (Vol. 995, pp. 1-10).

Azzam, R., & Oey, W. (2001). The utilization of electrokinetics in geotechnical and environmental engineering. *Transport in Porous Media*, *42*(3), 293-314.

Badv, K., & Mohammadzadeh, K. (2015). Laboratory assessment of the electro-osmotic consolidation technique for Urmia lake sediments. *Iranian Journal of Science and Technology Transactions of Civil Engineering*, *39*(C2+), 485-496.

Barker, J. E., Rogers, C. D. F., Boardman, D. I., & Peterson, J. (2004). Electrokinetic stabilisation: an overview and case study. *Proceedings of the Institution of Civil Engineers-Ground Improvement*, *8*(2), 47-58.

Bergado, D. T., Sasanakul, I., & Horpibulsuk, S. (2003). Electro-osmotic consolidation of soft Bangkok clay using copper and carbon electrodes with PVD. *Geotechnical Testing Journal*, *26*(3), 277-288.

Burnotte, F., Lefebvre, G., & Grondin, G. (2004). A case record of electroosmotic consolidation of soft clay with improved soil electrode contact. *Canadian Geotechnical Journal*, *41*(6), 1038-1053.

Cai, Y., Qiao, H., Wang, J., Geng, X., Wang, P., & Cai, Y. (2017). Experimental tests on effect of deformed prefabricated vertical drains in dredged soil on consolidation via vacuum preloading. *Engineering Geology*, *222*, 10-19.

Cameselle, C., Gouveia, S., Akretche, D. E., & Belhadj, B. (2013). Advances in electrokinetic remediation for the removal of organic contaminants in soils. *Organic Pollutants-Monitoring, Risk and Treatment*, 209-229.

Casagrande, A. (1952). Electro-osmotic stabilization of soils. *Boston Society Civil Engineers Journal*.

Charles, J. A., & Watts, K. S. (2002). *Treated ground: engineering properties and performance; CIRIA C572*. CIRIA.

Chaunsali, P., & Peethamparan, S. (2010). Microstructural and mineralogical characterization of cement kiln dust–Activated fly ash binder. *Transportation research record*, *2164*(1), 36-45.

Chew, S. H., Karunaratne, G. P., Kuma, V. M., Lim, L. H., Toh, M. L., & Hee, A. M. (2004). A field trial for soft clay consolidation using electric vertical drains. *Geotextiles and Geomembranes*, *22*(1-2), 17-35.

Chien, S. C., Teng, F. C., & Ou, C. Y. (2015). Soil improvement of electroosmosis with the chemical treatment using the suitable operation process. *Acta Geotechnica*, *10*(6), 813-820.

Chien, S. C., Ou, C. Y., & Lee, Y. C. (2010). A novel electroosmotic chemical treatment technique for soil improvement. *Applied clay science*, *50*(4), 481-492.

Chien, S. C., Ou, C. Y., & Wang, M. K. (2009). Injection of saline solutions to improve the electro-osmotic pressure and consolidation of foundation soil. *Applied clay science*, *44*(3-4), 218-224.

Choi, Y. S., & Lui, R. (1995). A mathematical model for the electrokinetic remediation of contaminated soil. *Journal of hazardous materials*, *44*(1), 61-75.

Coleman, N. J., Awosanya, K., & Nicholson, J. W. (2009). Aspects of the in vitro bioactivity of hydraulic calcium (alumino) silicate cement. *Journal of Biomedical Materials Research Part A: An Official Journal of The Society for Biomaterials, The Japanese Society for Biomaterials, and The Australian Society for Biomaterials and the Korean Society for Biomaterials*, *90*(1), 166-174.

Croarkin, C., Tobias, P., Filliben, J. J., Hembree, B., & Guthrie, W. (2006). NIST/SEMATECH e-handbook of statistical methods. *NIST/SEMATECH, July. Available online: http://www. itl. nist. gov/div898/handbook*.

Cristelo, N., Glendinning, S., Fernandes, L., & Pinto, A. T. (2012). Effect of calcium content on soil stabilisation with alkaline activation. *Construction and Building Materials*, *29*, 167-174.

Christidis, G. E. (2013). Assessment of industrial clays. In *Developments in clay science* (Vol. 5, pp. 425-449). Elsevier.

Darcy, H. (1856). The public fountains of the city of Dijon. *Dalmont, Paris*, *647*.

da Silva, E. B. S., de Lima, M. D., Oliveira, M. M., Costa, E. C. T. D. A., da Silva, D. R., & Martínez-Huitle, C. A. (2017). Electrokinetic treatment of polluted soil with petroleum coupled to an advanced oxidation process for remediation of its effluent. *Int. J. Electrochem. Sci*, *12*, 1247-1262.

Deriszadeh, M., & Wong, R. C. K. (2014). One-dimensional swelling behavior of clay and shale under electrical potential gradient. *Transport in porous media*, *101*(1), 35-52.

Diamond, S., & Kinter, E. B. (1956). Surface areas of clay minerals as derived from measurements of glycerol retention. *Clays and clay minerals*, *5*(1), 334-347.

Esmaeily, A., Elektorowicz, M., Habibi, S., & Oleszkiewicz, J. (2006). Dewatering and coliform inactivation in biosolids using electrokinetic phenomena. *Journal of Environmental Engineering and Science*, *5*(3), 197-202.

Estabragh, A. R., Moghadas, M., Javadi, A. A., & Abdollahi, J. (2019). Stabilisation of clay soil with polymers through electrokinetic technique. *European Journal of Environmental and Civil Engineering*, 1-19.

Expert, D. (2011). Version 11.0.3 by Stat-Ease. *INC, MN, USA*.

Fick, A. (1855). Ueber diffusion. *Annalen der Physik*, *170*(1), 59-86.

Fourie, A. B., Johns, D. G., & Jones, C. F. (2007). Dewatering of mine tailings using electrokinetic geosynthetics. *Canadian Geotechnical Journal*, *44*(2), 160-172.

Fu, H., Fang, Z., Wang, J., Chai, J., Cai, Y., Geng, X., ... & Jin, F. (2018). Experimental comparison of electroosmotic consolidation of Wenzhou dredged clay sediment using intermittent current and polarity reversal. *Marine Georesources & Geotechnology*, *36*(1), 131-138.

Gaafer, M., Bassioni, H., & Mostafa, T. (2015). Soil improvement techniques. *International Journal of Scientific & Engineering Research*, *6*(12), 217-222.

Gingine, V., Shah, R., Koteshwar, R., & Harikrishna, P. (2013). A review on study of electrokinetic stabilization of expansive soil. *Int J Earth Sci Eng*, *6*, 176-181.

Glendinning, S., Lamont-Black, J., Jones, C. J. F. P., & Hall, J. (2008). Treatment of lagooned sewage sludge in situ using electrokinetic geosynthetics. *Geosynthetics International*, *15*(3), 192-204.

Glendinning, S., Lamont-Black, J., & Jones, C. J. (2007). Treatment of sewage sludge using electrokinetic geosynthetics. *Journal of Hazardous Materials*, *139*(3), 491-499.

Hamir, R. B., Jones, C. J. F. P., & Clarke, B. G. (2001). Electrically conductive geosynthetics for consolidation and reinforced soil. *Geotextiles and Geomembranes*, *19*(8), 455-482.

Harris, A., Nosrati, A., & Addai-Mensah, J. (2018). The influence of pulp and interfacial chemistry and mode of electrical power input on electroosmotic dewatering of Na-exchanged smectite dispersions. *Applied Clay Science*, *162*, 214-222.

Hassan, I., Mohamedelhassan, E., Yanful, E., & Bo, M. W. (2016). Enhanced electrokinetic bioremediation by pH stabilisation. *Environmental Geotechnics*, *5*(4), 222-233.

Hequet, E., Abidi, N., & Gourlot, J. P. (1998). Application of methylene blue adsorption to cotton fiber specific surface area measurement: Part I. Methodology. *J. Cotton Sci*, *2*, 164-173.

Islam, T., Chik, Z., Mustafa, M. M., & Sanusi, H. (2012). Modeling of electrical resistivity and maximum dry density in soil compaction measurement. *Environmental Earth Sciences*, *67*(5), 1299-1305.

Ivliev, E. A. (2008). Electro-osmotic drainage and stabilization of soils. *Soil Mechanics and Foundation Engineering*, *45*(6), 211-218.

Iyer, R. (2001). Electrokinetic remediation. *Particulate Science and Technology*, *19*(3), 219-228.

James, J., James, A., Kumar, A., Gomthi, E., & Prasath, K. K. (2019). Plasticity and swell-shrink behaviour of electrokinetically stabilized virgin expansive soil using calcium hydroxide and calcium chloride solutions as cationic fluids. *Civil and Environmental Engineering Reports*, *29*(1), 128-146.

Jayasekera, S. (2015). Electrokinetics to modify strength characteristics of soft clayey soils: a laboratory based investigation. *Electrochimica Acta*, *181*, 39-47.

Jayasekera, S. (2008). *An investigation into modification of the engineering properties of salt affected soils using electrokinetics* (Doctoral dissertation, University of Ballarat).

Jayasekera, S. (2007). Stabilizing volume change characteristics of expansive soils using electrokinetics: a laboratory based investigation. In *International Conference in Geotechnical Engineering: Colombo, Sri Lanka*.

Jayasekera, S. (2004). Electroosmotic and hydraulic flow rates through kaolinite and bentonite clays. *Australian Geomechanics*, *39*(2), 79-86.

Jayasekera, S., & Hall, S. (2007). Modification of the properties of salt affected soils using electrochemical treatments. *Geotechnical and Geological Engineering*, *25*(1), 1.

Jensen, W. G. (2003). *Geotechnical policy and procedures manual*. Nebraska Department of Roads.

Jeyakanthan, V., Gnanendran, C. T., & Lo, S. C. (2011). Laboratory assessment of electro-osmotic stabilization of soft clay. *Canadian Geotechnical Journal*, *48*(12), 1788-1802.

Jones, C. J., Lamont-Black, J., & Glendinning, S. (2011). Electrokinetic geosynthetics in hydraulic applications. *Geotextiles and Geomembranes*, *29*(4), 381-390.

Jones, C. J. F. P., Glendinning, S., Huntley, D. T., & Lamont-Black, J. (2006). Soil consolidation and strengthening using electrokinetic geosynthetics—concepts and analysis. *Geosynthetics. Millpress, Rotterdam*, *1*, 411-414.

Kamani, H., Safari, G. H., Asgari, G., & Ashrafi, S. D. (2018). Data on modeling of enzymatic elimination of direct red 81 using response surface methodology. *Data in brief*, *18*, 80-86.

Kaniraj, S. R., Huong, H. L., & Yee, J. H. S. (2011). Electro-osmotic consolidation studies on peat and clayey silt using electric vertical drain. *Geotechnical and Geological Engineering*, *29*(3), 277-295.

Kaniraj, S. R., Huong, H. L., & Yee, J. H. S. (2011). Electro-osmotic consolidation studies on peat and clayey silt using electric vertical drain. *Geotechnical and Geological Engineering*, *29*(3), 277-295.

Kaniraj, S. R., & Yee, J. H. S. (2011). Electro-osmotic consolidation experiments on an organic soil. *Geotechnical and Geological Engineering*, *29*(4), 505-518.

Kapeluszna, E., Kotwica, Ł., Różycka, A., & Gołek, Ł. (2017). Incorporation of Al in CASH gels with various Ca/Si and Al/Si ratio: Microstructural and structural characteristics with DTA/TG, XRD, FTIR and TEM analysis. *Construction and Building Materials*, *155*, 643-653.

Karunaratne, G. P., Jong, H. K., & Chew, S. H. (2004). New electrically conductive geosynthetics for soft clay consolidation. In *Proceeding of the 3rd Asian Regional Conference on Geo-synthetics* (pp. 277-284).

Kaur, G., Rath, G., Heer, H., & Goyal, A. K. (2012). Optimization of protocell of silica nanoparticles using 3 2 factorial designs. *AAPS PharmSciTech*, *13*(1), 167-173.

Keykha, H. A., Huat, B. B., & Asadi, A. (2014). Electrokinetic stabilization of soft soil using carbonate-producing bacteria. *Geotechnical and Geological Engineering*, *32*(4), 739-747.

Khan, M. I., Khan, H. U., Azizli, K., Sufian, S., Man, Z., Siyal, A. A., ... & ur Rehman, M. F. (2017). The pyrolysis kinetics of the conversion of Malaysian kaolin to metakaolin. *Applied Clay Science*, *146*, 152-161.

Kim, B. K., Baek, K., Ko, S. H., & Yang, J. W. (2011a). Research and field experiences on electrokinetic remediation in South Korea. *Separation and purification technology*, *79*(2), 116-123.

Kim, K. J., Kim, D. H., Yoo, J. C., & Baek, K. (2011b). Electrokinetic extraction of heavy metals from dredged marine sediment. *Separation and Purification Technology*, *79*(2), 164-169.

Kollannur, N. J., & Arnepalli, D. N. (2019). Electrochemical treatment and associated chemical modifications of clayey soils: a review. *International Journal of Geotechnical Engineering*, 1-10.

Lambe, T. W., & Whitman, R. V. (1969). Soil mechanics. John Willey & Sons. *Inc., New York*, *553*.

Lamont-Black, J., Hall, J. A., Glendinning, S., White, C. P., & Jones, C. J. (2012). Stabilization of a railway embankment using electrokinetic geosynthetics. *Geological Society, London, Engineering Geology Special Publications*, *26*(1), 125-139.

Lav, A. H., & Lav, M. A. (2000). Microstructural development of stabilized fly ash as pavement base material. *Journal of Materials in Civil Engineering*, *12*(2), 157-163.

Lefebvre, G., & Burnotte, F. (2002). Improvements of electroosmotic consolidation of soft clays by minimizing power loss at electrodes. *Canadian Geotechnical Journal*, *39*(2), 399-408.

Liaki, C., Rogers, C. D. F., & Boardman, D. I. (2010). Physico-chemical effects on clay due to electromigration using stainless steel electrodes. *Journal of Applied Electrochemistry*, *40*(6), 1225-1237.

Liaki, C. (2006). *Physicochemical study of electrokinetically treated clay using carbon and steel electrodes* (Doctoral dissertation, University of Birmingham).

Li, Y., Gong, X., Lu, M., & Tao, Y. (2012). Non-mechanical behaviors of soft clay in two-dimensional electro-osmotic consolidation. *Journal of Rock Mechanics and Geotechnical Engineering*, *4*(3), 282-288.

Liu, L., Zhou, A., Deng, Y., Cui, Y., Yu, Z., & Yu, C. (2019). Strength performance of cement/slag-based stabilized soft clays. *Construction and Building Materials*, *211*, 909-918.

Liu, P., & Shang, J. Q. (2014). Improvement of marine sediment by combined electrokinetic and chemical treatment. *International Journal of Offshore and Polar Engineering*, *24*(03), 232-240.

Loch, J. G., Lima, A. T., & Kleingeld, P. J. (2010). Geochemical effects of electro-osmosis in clays. *Journal of applied Electrochemistry*, *40*(6), 1249-1254.

Malekzadeh, M., & Sivakugan, N. (2017). One-dimensional electrokinetic stabilization of dredged mud. *Marine Georesources & Geotechnology*, *35*(5), 603-609.

Malekzadeh, M., Lovisa, J., & Sivakugan, N. (2016). An overview of electrokinetic consolidation of soils. *Geotechnical and Geological Engineering*, *34*(3), 759-776.

Mandal, T., Tinjum, J. M., & Edil, T. B. (2016). Non-destructive testing of cementitiously stabilized materials using ultrasonic pulse velocity test. *Transportation Geotechnics*, *6*, 97-107.

Masi, M., & Losito, G. (2015). Spectral induced polarization for monitoring electrokinetic remediation processes. *Journal of Applied Geophysics*, *123*, 284-294.

McCleskey, R. B., Nordstrom, D. K., & Ryan, J. N. (2012). Comparison of electrical conductivity calculation methods for natural waters. *Limnology and Oceanography: Methods*, *10*(11), 952-967.

Meegoda, N. J., & Ratnaweera, P. (1994). Compressibility of contaminated fine-grained soils. *Geotechnical Testing Journal*, *17*(1), 101-112.

Megur, G. A., & Rakaraddi, P. G. (2014). A Study on Stabilization of soil by electro kinetic Method. *IJRET: International Journal of Research in Engineering and Technology*.

Micic, S., Shang, J. Q., Lo, K. Y., Lee, Y. N., & Lee, S. W. (2001). Electrokinetic strengthening of a marine sediment using intermittent current. *Canadian Geotechnical Journal*, *38*(2), 287-302.

Miller, G. A., & Azad, S. (2000). Influence of soil type on stabilization with cement kiln dust. *Construction and building materials*, *14*(2), 89-97.

Milligan, V. (1994). First application of electro-osmosis to improve friction pile capacity-three decades later. In *International conference on soil mechanics and foundation engineering* (pp. 1-5).

Mitchell, J. K., & Soga, K. (2005). *Fundamentals of soil behavior* (Vol. 3). New York: John Wiley & Sons.

Mitchell, J. K., & Soga, K. (1993). Fundamentals of Soil Behavior, John Wiley&Sons. *Inc., New York, 422*. Muraoka

Mitchell, J. K. Fundamentals of Soil Behavior., 1993. *NY: John Wiley&Sons*, *437*.

Mitchell, J. K. (1991). Conduction phenomena: from theory to geotechnical practice. *Geotechnique*, *41*(3), 299-340.

Miyoshi, Y., Tsukimura, K., Morimoto, K., Suzuki, M., & Takagi, T. (2018). Comparison of methylene blue adsorption on bentonite measured using the spot and colorimetric methods. *Applied Clay Science, 151*, 140-147.

Moayedi, H., & Mosallanezhad, M. (2017). Physico-chemical and shrinkage properties of highly organic soil treated with non-traditional additives. *Geotechnical and Geological Engineering, 35*(4), 1409-1419.

Moayedi, H., Nazir, R., Kazemian, S., & Huat, B. K. (2014a). Microstructure analysis of electrokinetically stabilized peat. *Measurement, 48*, 187-194.

Moayedi, H., Nazir, R., Kassim, K. A., & Huat, B. K. (2014b). Measurement of the electrokinetic properties of peats treated with chemical solutions. *Measurement, 49*, 289-295.

Moayedi, H., Kassim, K. A., Kazemian, S., Raftari, M., & Mokhberi, M. (2014c). Improvement of peat using Portland cement and electrokinetic injection technique. *Arabian Journal for Science and Engineering, 39*(10), 6851-6862.

Mohamedelhassan, E., Curtain, K., Fenos, M., Girard, K., Provenzano, A., & Tabaczuk, W. (2012). Electrokinetic Treatment for Model Caissons with Increasing Dimensions. *Advances in Civil Engineering, 2012*.

Mohamedelhassan, E. (2011). Laboratory model test on improving the properties of soft clay by electrokinetics. *International Scholarly Research Notices, 2011*.

Mohamedelhassan, E., & Shang, J. Q. (2002). Feasibility assessment of electro-osmotic consolidation on marine sediment. *Proceedings of the Institution of Civil Engineers-Ground Improvement*, *6*(4), 145-152.

Mohamedelhassan, E., & Shang, J. Q. (2001). Analysis of electrokinetic sedimentation of dredged Welland River sediment. *Journal of hazardous materials*, *85*(1-2), 91-109.

Montgomery, D. C. (2017). *Design and analysis of experiments*. John Wiley & sons.

Montgomery, D.C., Runger, G.C., Hubele, N.F. 2009. Engineering Statistics, John Wiley and Sons, USA.

Mosavat, N., Oh, E., & Chai, G. (2014). Laboratory evaluation of physico-chemical variations in bentonite under electrokinetic enhancement. *International journal of GEOMATE: geotechnique, construction materials and environment*, *6*(1), 817-823.

Mosavat, N., Oh, E., & Chai, G. (2013). Laboratory assessment of kaolinite and bentonite under chemical electrokinetic treatment. *Journal of Civil & Environmental Engineering*, *3*(01), 1-7.

Mosavat, N., Oh, E., & Chai, G. (2012). A review of electrokinetic treatment technique for improving the engineering characteristics of low permeable problematic soils. *International journal of GEOMATE*, *2*(2), 266-272.

Morefield, S. W., Mclnerney, M. K., Hock, V. F., Marshall Jr, O. S., Malone, P. G., Weiss Jr, C. A., & Sanchez, J. (2006). Rapid Soil Stabilization and Strengthening Using Electrokinetic Techniques. In *Transformational Science And Technology For The Current And Future Force: (With CD-ROM)* (pp. 529-533).

Nalbantoğlu, Z. (2004). Effectiveness of class C fly ash as an expansive soil stabilizer. *Construction and Building Materials*, *18*(6), 377-381.

Nalbantoğlu, Z., & Gucbilmez, E. (2002). Utilization of an industrial waste in calcareous expansive clay stabilization. *Geotechnical Testing Journal*, *25*(1), 78-84.

Nalbantoğlu, Z., & Gucbilmez, E. (2001). Improvement of calcareous expansive soils in semi-arid environments. *Journal of arid environments*, *47*(4), 453-463.

Ng, Y. S., Gupta, B. S., & Hashim, M. A. (2014). Stability and performance enhancements of Electrokinetic-Fenton soil remediation. *Reviews in Environmental Science and Bio/Technology*, *13*(3), 251-263.

Nordin, N. S. (2015). *Physicochemical properties of batu pahat clay using electrokinetic stabilisation method* (Doctoral dissertation, Universiti Tun Hussein Onn Malaysia).

Nordin, N. S., Tajudin, S. A., & Kadir, A. A. (2013). Stabilization of soft soil using electrokinetic stabilisation method. *International Journal of Zero Waste Generation*, *1*(1), 5-12.

Olphen, H. V. (1977). *An introduction to clay colloid chemistry, for clay technologists, geologists, and soil scientists* (No. 2nd edition).

Ou, C. Y., Chien, S. C., & Liu, R. H. (2015). A study of the effects of electrode spacing on the cementation region for electro-osmotic chemical treatment. *Applied Clay Science*, *104*, 168-181.

Ou, C. Y., Chien, S. C., & Lee, T. Y. (2013). Development of a suitable operation procedure for electroosmotic chemical soil improvement. *Journal of geotechnical and geoenvironmental engineering*, *139*(6), 993-1000.

Ou, C. Y., Chien, S. C., & Chang, H. H. (2009). Soil improvement using electroosmosis with the injection of chemical solutions: field tests. *Canadian geotechnical journal*, *46*(6), 727-733.

Ozkan, S., Gale, R. J., & Seals, R. K. (1999). Electrokinetic stabilization of kaolinite by injection of Al and PO43− ions. *Proceedings of the Institution of Civil Engineers-Ground Improvement*, *3*(4), 135-144.

Paz-Garcia, J. M., Baek, K., Alshawabkeh, I. D., & Alshawabkeh, A. N. (2012). A generalized model for transport of contaminants in soil by electric fields. *Journal of Environmental Science and Health, Part A*, *47*(2), 308-318.

Peethamparan, S., Olek, J., & Diamond, S. (2009). Mechanism of stabilization of Na-montmorillonite clay with cement kiln dust. *Cement and Concrete research*, *39*(7), 580-589.

Peethamparan, S., Olek, J., & Diamond, S. (2008). Physicochemical behavior of cement kiln dust–treated kaolinite clay. *Transportation Research Record*, *2059*(1), 80-88.

Pérez-Corona, M., Ochoa, B., Cárdenas, J., Hernández, G., Solís, S., Fernández, R., ... & Bustos, E. (2013). Comparison of different arrangements of electrodes during the electrokinetic treatment of polluted soil with hydrocarbons and its final application in situ. In *Recent Research Development in Electrochemistry* (Vol. 9, p. 59). Transworld Research Network Kerala.

Ranjitha, K., & Blessing, B. M. (2017). Soil Stabilization by Electrokinetic Method. *Int. J. Sci. Res*, *6*, 1316-1320.

Ramadan, B. S., Effendi, A. J., & Helmy, Q. (2018). Integrating Electrokinetic and Bioremediation Process for Treating Oil Contaminated Low Permeability Soil. In *E3S Web of Conferences* (Vol. 31, p. 03005). EDP Sciences.

Reddy, K. R., Urbanek, A., & Khodadoust, A. P. (2006). Electroosmotic dewatering of dredged sediments: Bench-scale investigation. *Journal of Environmental Management*, *78*(2), 200-208.

Rittirong, A., Shang, J. Q., Mohamedelhassan, E., Ismail, M. A., & Randolph, M. F. (2008). Effects of electrode configuration on electrokinetic stabilization for caisson anchors in calcareous sand. *Journal of geotechnical and geoenvironmental engineering*, *134*(3), 352-365.

Rogers, C. D. F., Liaki, C., & Boardman, D. I. (2003). Advances in the engineering of lime stabilized clay soils. In *International conference on problematic soils, Nottingham, UK*.

Rogers, C. D. F., Barker, J. E., Boardman, D. I., & Peterson, J. (2002). Electro-kinetic stabilisation of a silty clay soil. In *Proc., 4th Int. Conf. on Ground Improvement Techniques* (Vol. 2, pp. 621-628).

Rojo, A., Hansen, H. K., & Monárdez, O. (2014). Electrokinetic remediation of mine tailings by applying a pulsed variable electric field. *Minerals Engineering*, 55, 52-56.

Rozas, F., & Castellote, M. (2012). Electrokinetic remediation of dredged sediments polluted with heavy metals with different enhancing electrolytes. *Electrochimica Acta*, *86*, 102-109.

Rusydi, A. F. (2018, February). Correlation between conductivity and total dissolved solid in various type of water: A review. In *IOP Conference Series: Earth and Environmental Science* (Vol. 118, No. 1, p. 012019). IOP Publishing.

Samidurai, V., Jeevanandan, K., & Ragul, R. (2017). Soil stabilization by electro kinetic technique. *International Journal of Advanced Research in Civil, Structural, Environmental and Infrastructure Engineering and Developing, 3(1).*

Schmidt, C. A. B., de Almeida, M. D. S. S., & Barbosa, M. C. (2006). Electrokinetic behavior of two clayey soils based on laboratory experiments. In *5th ICEG Environmental Geotechnics: Opportunities, Challenges and Responsibilities for Environmental Geotechnics: Proceedings of the ISSMGE's fifth international congress organized by the Geoenvironmental Research Centre, Cardiff University and held at Cardiff City Hall on 26–30th June 2006* (pp. 279-286). Thomas Telford Publishing.

Segall, B. A., Matthias, J. A., & O'Bannon, C. E. (1980). Electro-osmosis chemistry and water quality. *Journal of the Geotechnical Engineering Division*, *106*(10), 1148-1152.

Shackelford, C. D., & Daniel, D. E. (1991). Diffusion in saturated soil. I: Background. *Journal of Geotechnical Engineering*, *117*(3), 467-484.

Shang, J. Q., Mohamedelhassan, E., & Ismail, M. (2004). Electrochemical cementation of offshore calcareous soil. *Canadian Geotechnical Journal*, *41*(5), 877-893.

Shang, J. Q. (1997). Electrokinetic sedimentation: a theoretical and experimental study. *Canadian geotechnical journal*, *34*(2), 305-314.

Shin, J. Y., Thompson, D. J., & Zervos, A. (2017). The influence of soil nonlinear properties on the track/ground vibration induced by trains running on soft ground. *Transportation Geotechnics*, *11*, 1-16.

Shrestha, R. A., Pham, T. D., & Sillanpää, M. (2009). Remediation of chrysene from contaminated soil by enhanced electrokinetics. *Int. J. Electrochem. Sci*, *4*, 1387-1394.

Solanki, P., & Zaman, M. (2012). Microstructural and mineralogical characterization of clay stabilized using calcium-based stabilizers. In *Scanning electron microscopy*. IntechOpen.

Sondi, I., Bišćan, J., Vdović, N., & Škapin, S. D. (2009). The electrokinetic properties of carbonates in aqueous media revisited. *Colloids and Surfaces A: Physicochemical and Engineering Aspects*, *342*(1-3), 84-91.

Suied, A. A., Ahmad Tajudin, S. A., Zakaria, M. N., & Madun, A. (2018). Potential electrokinetic remediation technologies of laboratory scale into field application-methodology overview.

Sumbarda-Ramos, E. G., Guerrero-Gutierrez, O. X., Murillo-Rivera, B., González, I., & Oropeza-Guzman, M. T. (2010). Electrokinetic treatment for clayed and sandy soils. *Journal of applied electrochemistry*, *40*(6), 1255-1261.

Thuy, T. T. T., Putra, D. P. E., Budianta, W., & Hazarika, H. (2013). Improvement of expansive soil by electro-kinetic method. *Journal of Applied Geology*, *5*(1).

Tironi, A., Trezza, M. A., Scian, A. N., & Irassar, E. F. (2014). Thermal analysis to assess pozzolanic activity of calcined kaolinitic clays. *Journal of Thermal Analysis and Calorimetry*, *117*(2), 547-556.

Tran, K. Q., Satomi, T., & Takahashi, H. (2018). Effect of waste cornsilk fiber reinforcement on mechanical properties of soft soils. *Transportation Geotechnics*, *16*, 76-84.

Virkutyte, J., Sillanpää, M., & Latostenmaa, P. (2002). Electrokinetic soil remediation—critical overview. *Science of the Total Environment*, *289*(1-3), 97-121.

Wahab, A., Embong, Z., Naseem, A. A., Madun, A., Zainorabidin, A., & Kumar, V. (2018). The Effect of Electrokinetic Stabilization (EKS) on Peat Soil Properties at Parit Botak area, Batu Pahat, Johor, Malaysia. *Indian Journal of Science and Technology*, *11*, 44.

Wang, Z. F., Shen, J. S., & Cheng, W. C. (2018). Simple method to predict ground displacements caused by installing horizontal jet-grouting columns. *Mathematical Problems in Engineering*, *2018*.

Wang, D., Kang, T., Han, W., & Liu, Z. (2011). Electrochemical modification of tensile strength and pore structure in mudstone. *International journal of rock mechanics and mining sciences (1997)*, *48*(4), 687-692.

Wu, M. Z., Reynolds, D. A., Fourie, A., & Thomas, D. G. (2013). Optimal field approaches for electrokinetic in situ oxidation remediation. *Groundwater Monitoring & Remediation*, *33*(1), 62-74.

Yan, M., Sun, C., Dong, J., Xu, J., & Ke, W. (2015). Electrochemical investigation on steel corrosion in iron-rich clay. *Corrosion Science*, *97*, 62-73.

Yan, S., Singh, A. N., Fu, S., Liao, C., Wang, S., Li, Y., ... & Hu, L. (2012). A soil fauna index for assessing soil quality. *Soil Biology and Biochemistry*, *47*, 158-165.

Yeung, A. T. (2011). Milestone developments, myths, and future directions of electrokinetic remediation. *Separation and Purification Technology*, *79*(2), 124-132.

Yeung, A. T. (2006). Contaminant extractability by electrokinetics. *Environmental engineering science*, 23(1), 202-224.

Yeung, A. T., & Datla, S. (1995). Fundamental formulation of electrokinetic extraction of contaminants from soil. *Canadian Geotechnical Journal*, *32*(4), 569-583.

Yuan, J., & Hicks, M. A. (2016). Numerical simulation of elasto-plastic electro-osmosis consolidation at large strain. *Acta Geotechnica*, *11*(1), 127-143.

Yuan, S., Long, H., Xie, W., Liao, P., & Tong, M. (2012). Electrokinetic transport of CMC-stabilized Pd/Fe nanoparticles for the remediation of PCP-contaminated soil. *Geoderma*, *185*, 18-25.

Zhang, L., Wang, N. W., Jing, L. P., Fang, C., Shan, Z. D., & Li, Y. Q. (2017). Electro-osmotic chemical treatment for marine clayey soils: a laboratory experiment and a field study. *Geotechnical Testing Journal*, *40*(1), 72-83.

Zhang, D., Cao, Z., Fan, L., Liu, S., & Liu, W. (2014). Evaluation of the influence of salt concentration on cement stabilized clay by electrical resistivity measurement method. *Engineering Geology*, *170*, 80-88.

Zhou, J., Tao, Y. L., Xu, C. J., Gong, X. N., & Hu, P. C. (2015). Electro-osmotic strengthening of silts based on selected electrode materials. *Soils and Foundations*, *55*(5), 1171-1180.